Understanding the Quark-Gluon Plasma with ALICE at the LHC

Marco van Leeuwen, Nikhef and CERN

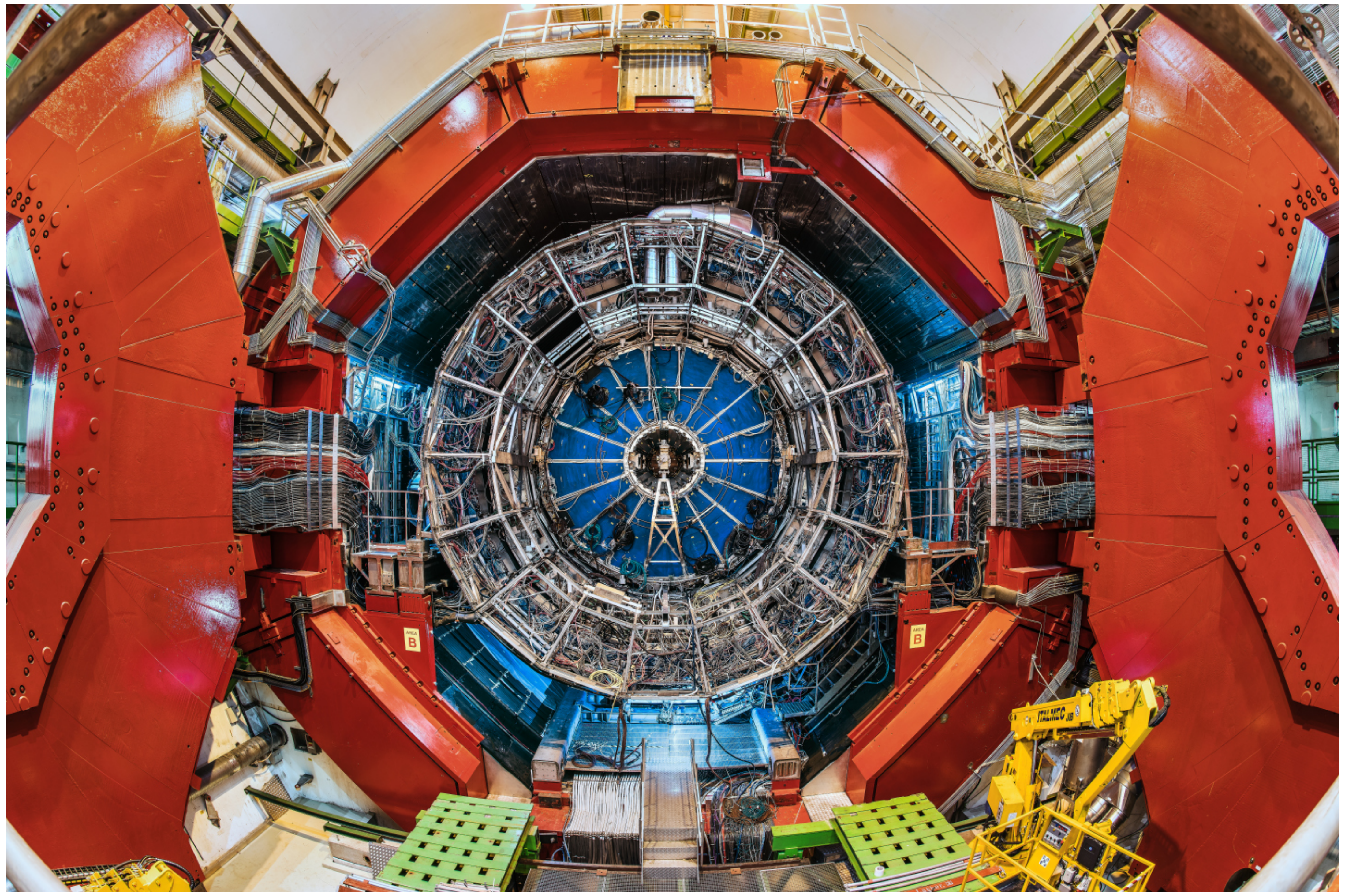

Wigner 121 Symposium, 18-20 September 2023, Budapest

Particles and interactions

Atomic scale: electromagnetic interactions

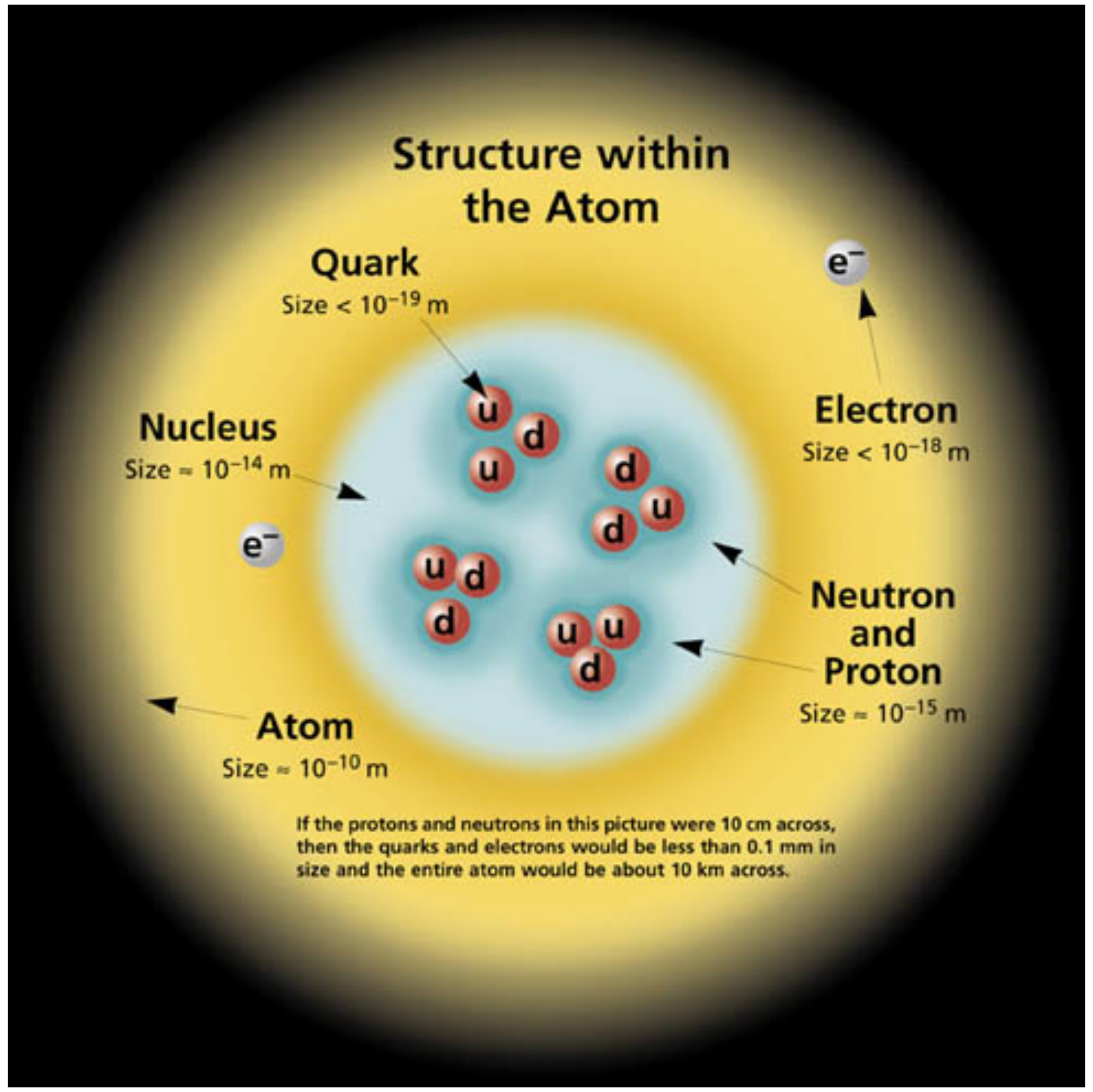

Electrons, protons carry 1 unit of electric charge

Standard Model: quantum field theory of fundamental particles

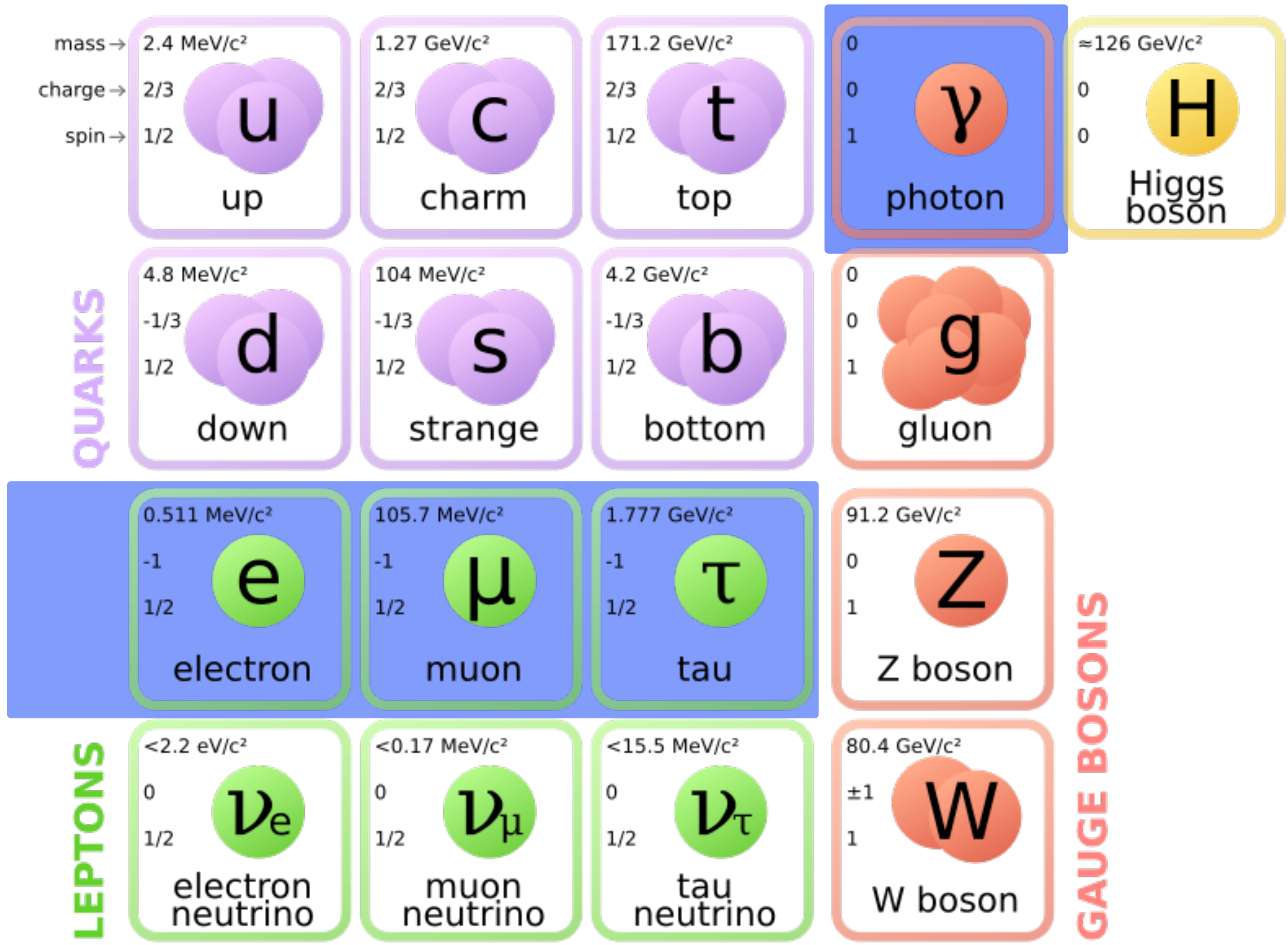

Leptons (e, μ, 𝒯) and photon are the fundamental particles of the electromagnetic interactions

Particles and interactions

Atomic scale: electromagnetic interactions

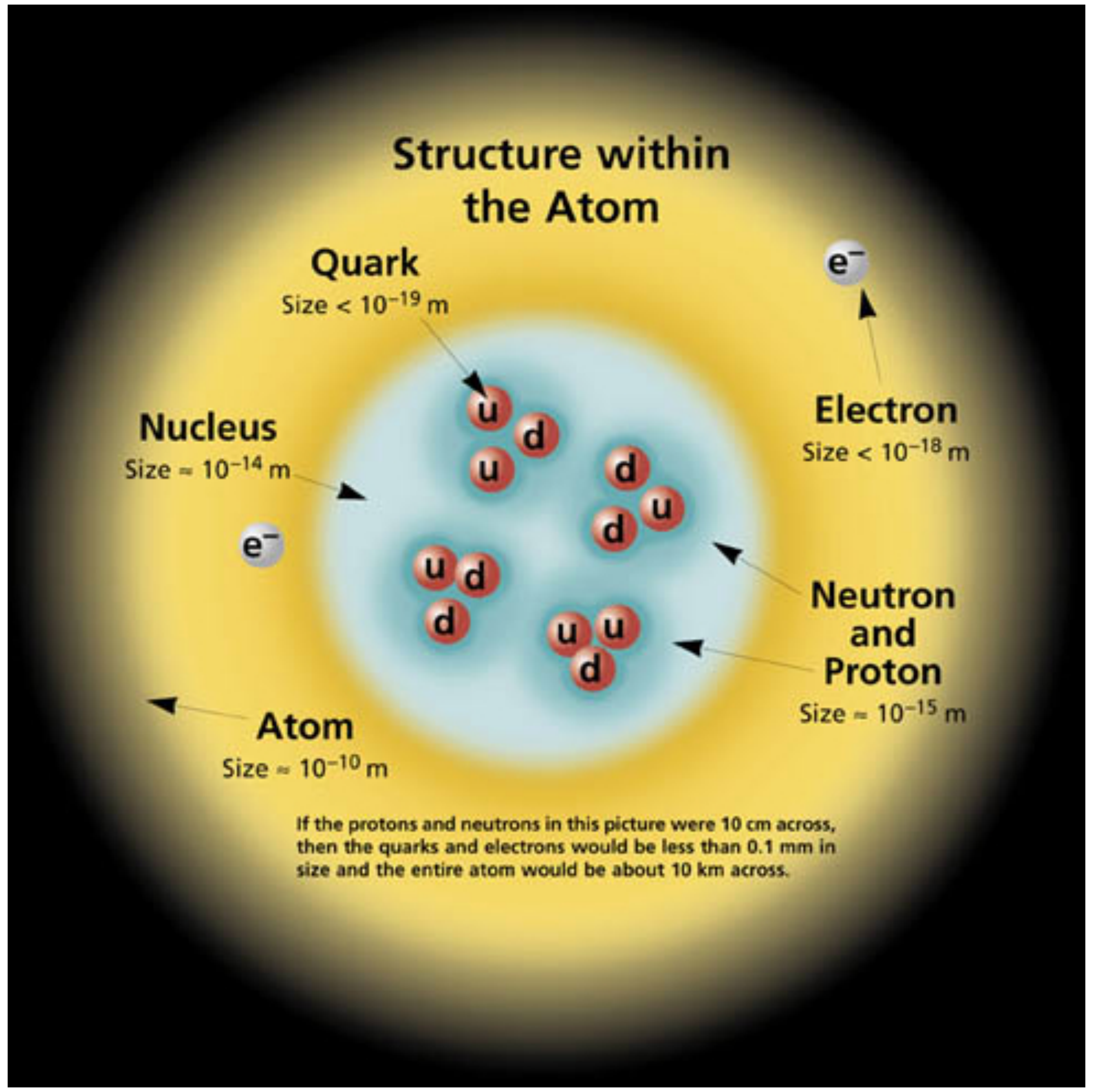

Electrons, protons carry 1 unit of electric charge

Standard Model: quantum field theory of fundamental particles

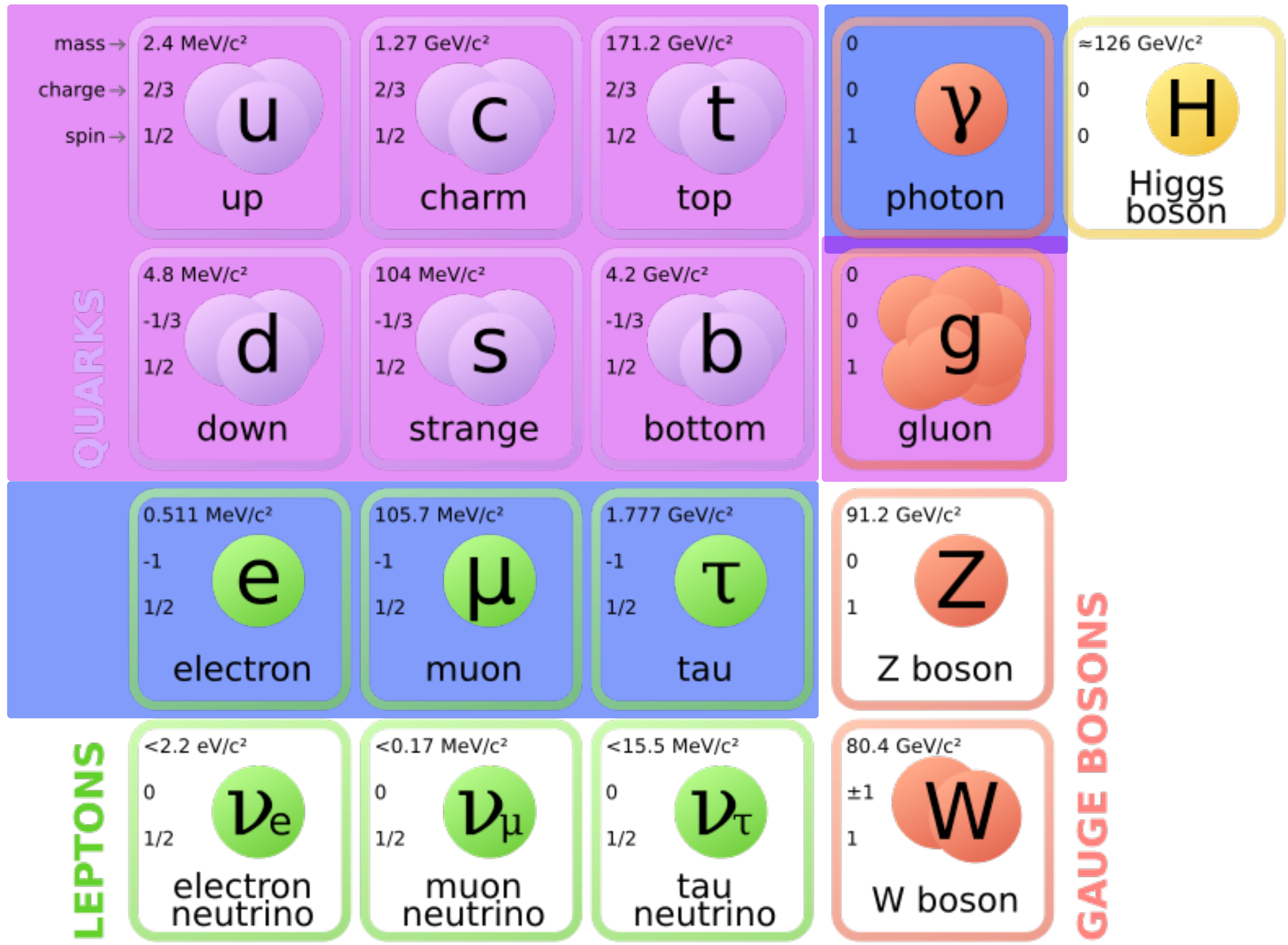

Leptons (e, μ, $\mathcal{T}$) and photon are the fundamental particles of the electromagnetic interactions

Quarks and gluons at the fundamental particles of the strong interaction

Dominant interaction on the subatomic scale (> MeV, < 1 fm)

Experimental signatures of quarks and gluons: three-jet events

TASSO experiment @ PETRA @ DESY

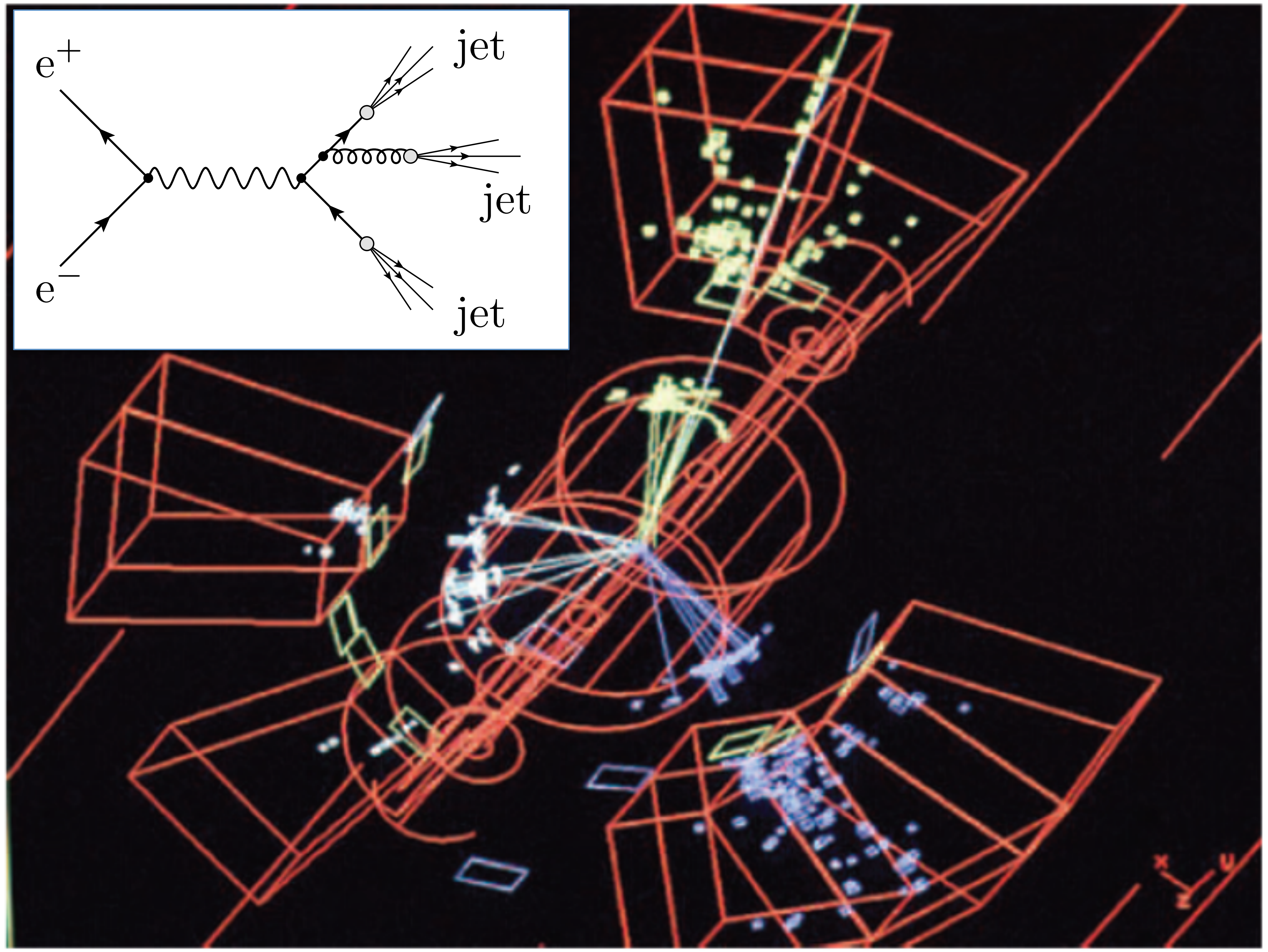

collision energy: $\sqrt{s}$ = 13-31 GeV

ALEPH @ LEP (CERN)

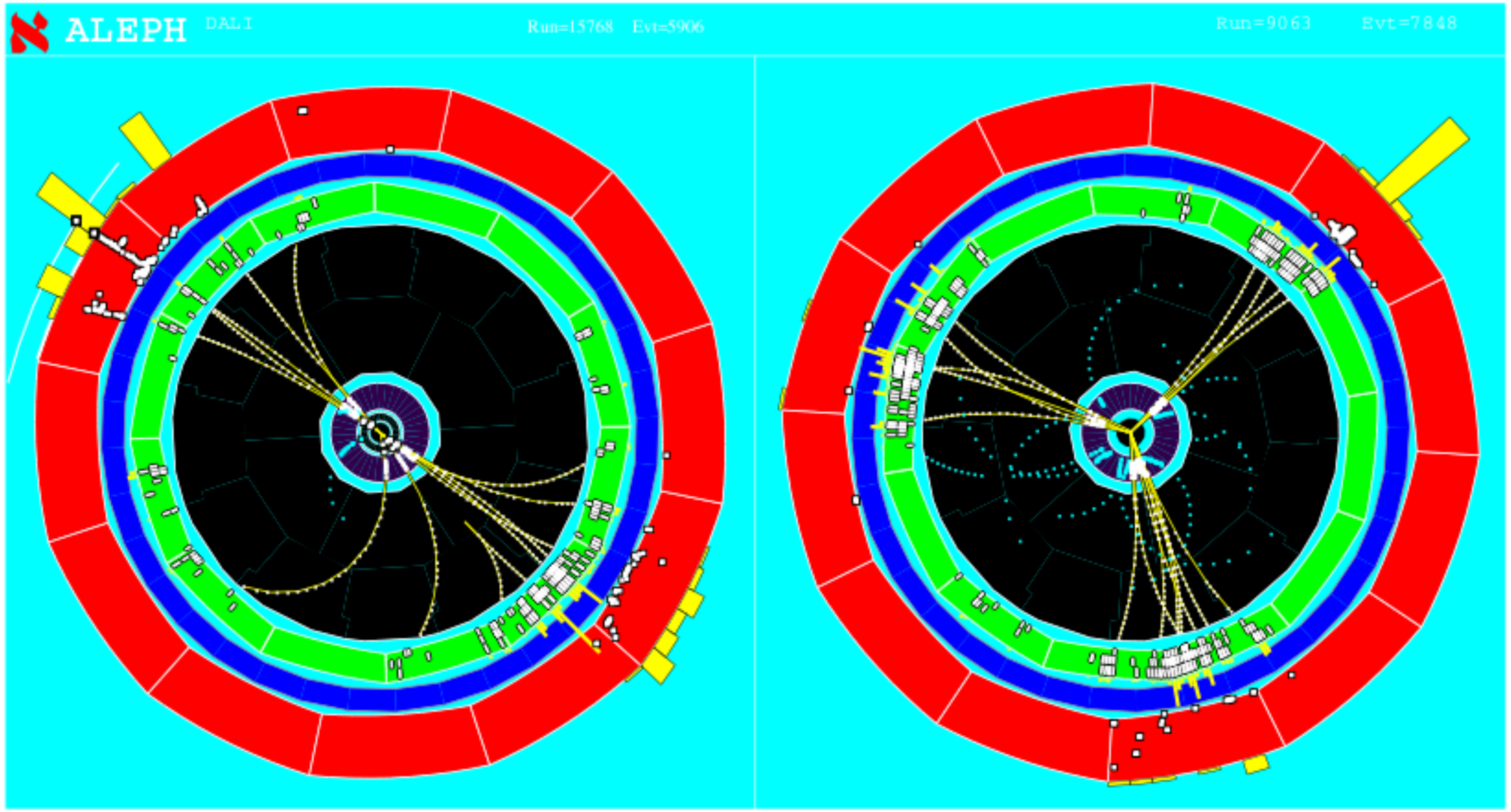

collision energy: $\sqrt{s}$ = 90-209 GeV

NB: quarks and gluons are not detected individually — parton shower and hadronisation

The running coupling of QCD

QCD potential (lattice QCD)

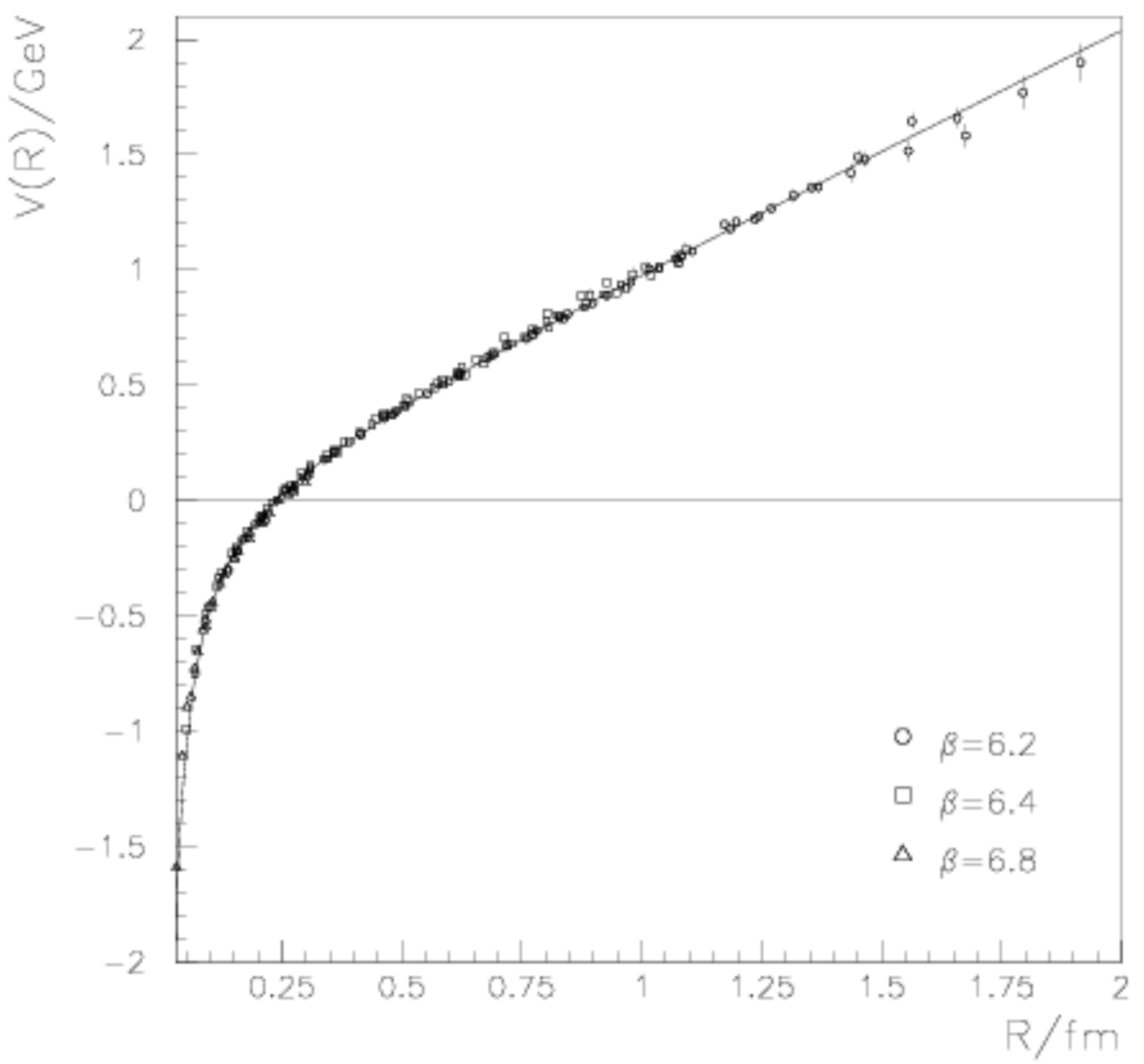

Bali, hep-lat/9311009

Low-energy, large distances: quarks are bound into hadrons

QCD coupling constant

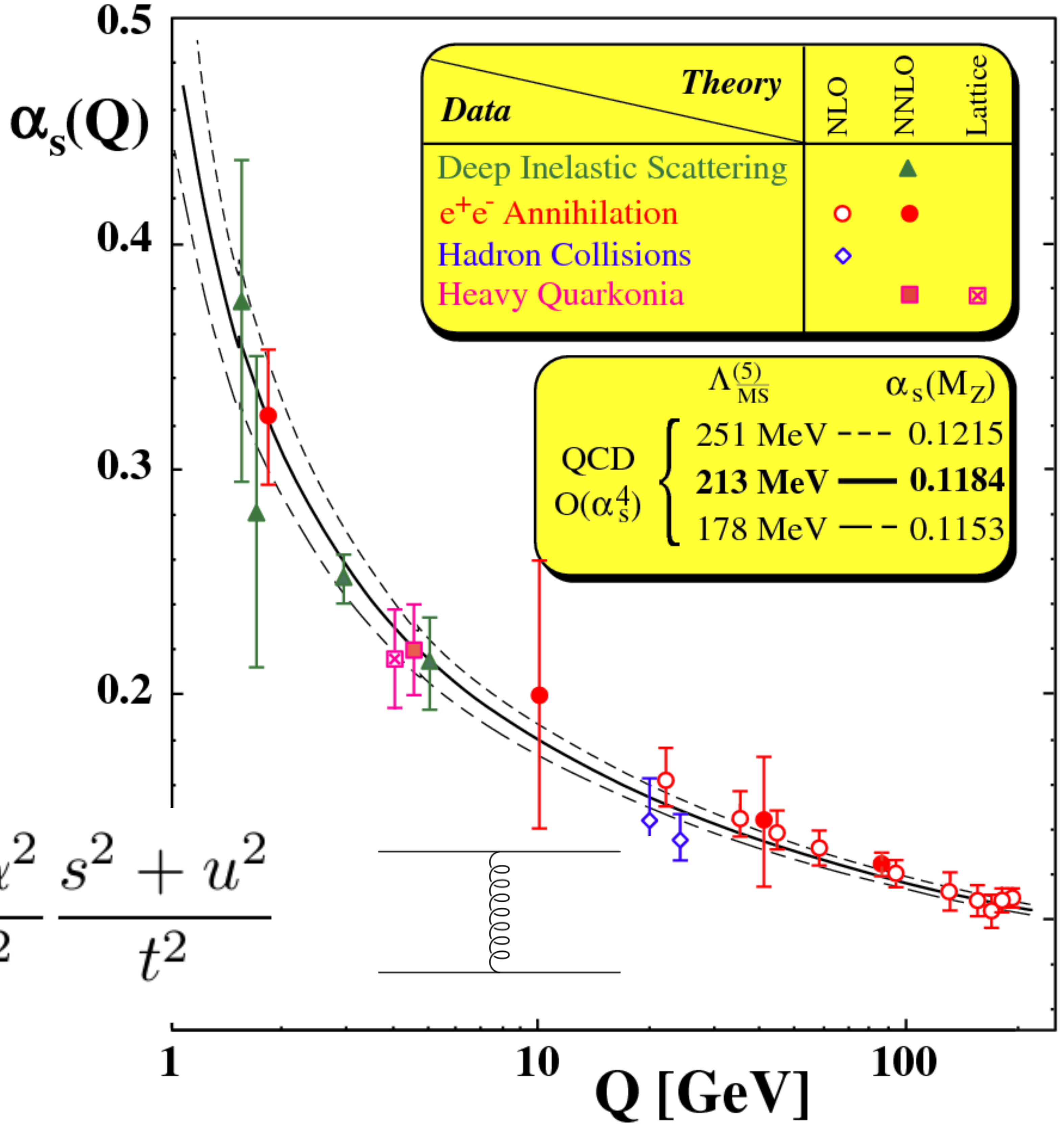

$$\frac{4\pi\alpha^2}{9s^2}\,\frac{s^2+u^2}{t^2}$$

$e^+\,e^- \rightarrow q\,\bar{q}\,g$

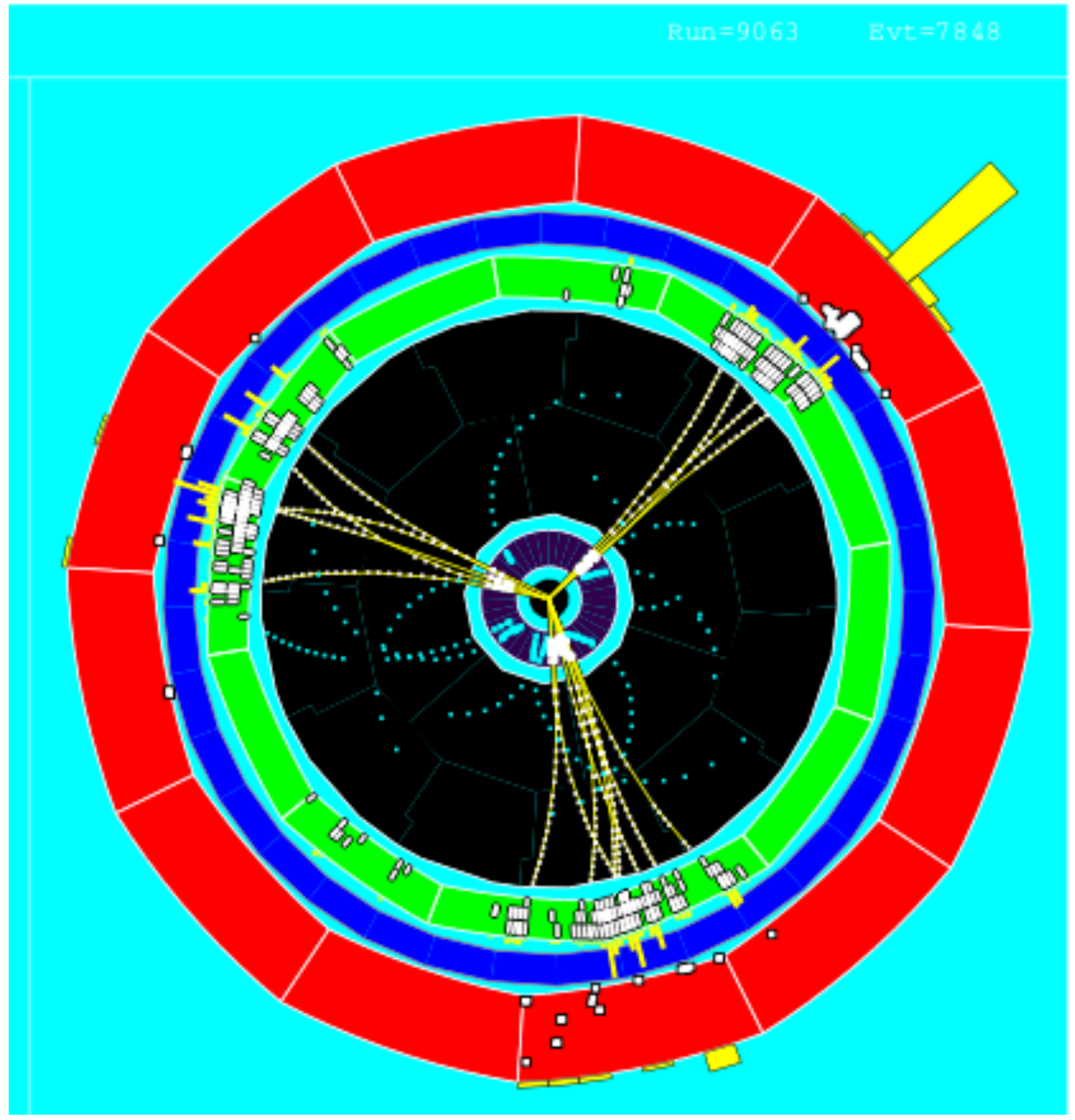

High energy, short distances: quarks and gluons interact as quasi-free particles

At large distance, small energy: perturbative calculations do not converge
Static QCD potential does not capture full dynamics

Understanding the interactions

Three regimes giving rise to subfields of physics:

	Electromagnetism	Strong interaction
Free particles	Two-body scattering	
Bound states	Atomic physics	Hadronic, nuclear physics
Many-body physics	Condensed matter: thermal, electrical properties, superconductivity, etc	Heavy-ion physics: quark-gluon plasma

Heavy-ion collisions are used to study ‘condensed matter physics’ of QCD
Unique form of ‘quantum condensed matter’

Condensed matter of QCD: the quark-gluon plasma

Lattice QCD calculations: energy density vs temperature

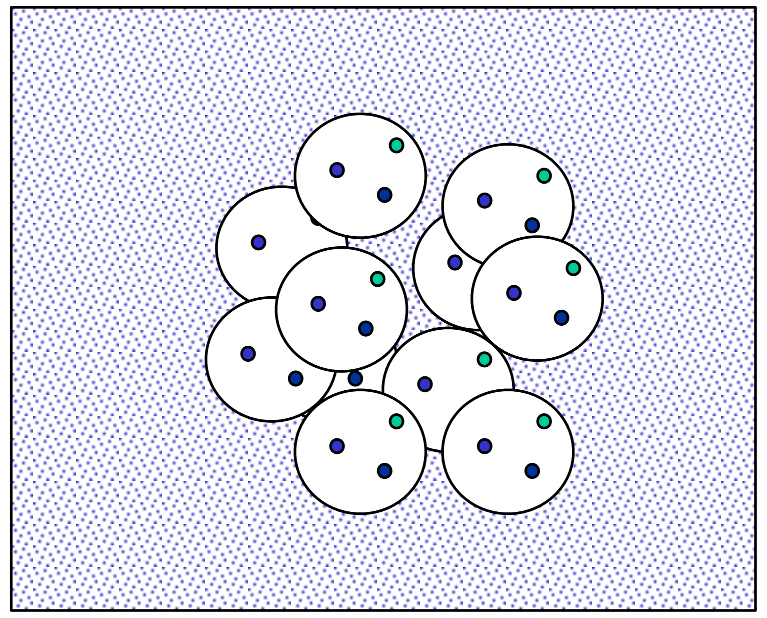

Low temperature:
quarks and gluons confined in hadrons

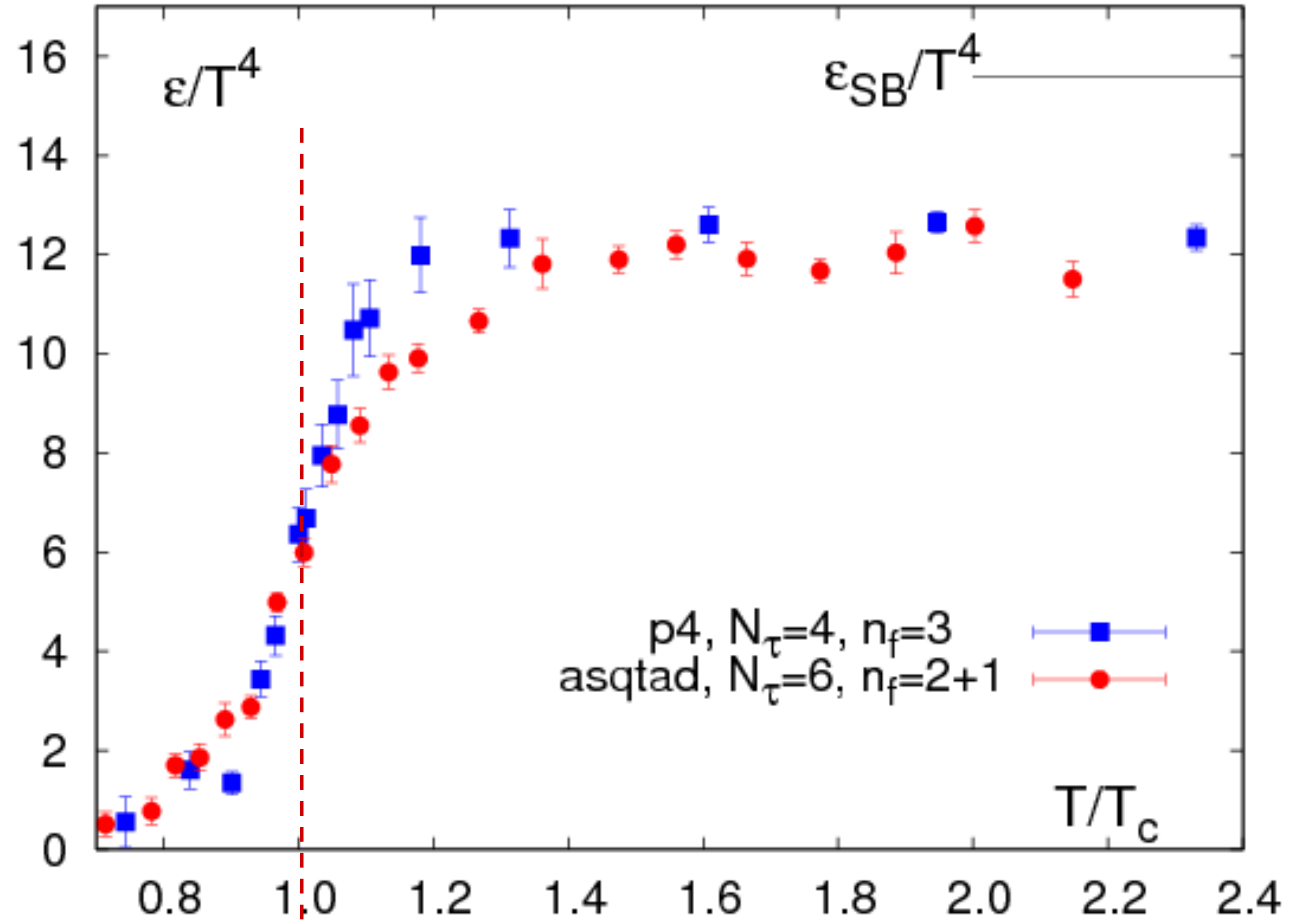

T_c ~ 155 MeV
ε_c ~ 1 GeV/fm^3

Bernard et al. hep-lat/0610017

ALICE

Condensed matter of QCD: the quark-gluon plasma

Lattice QCD calculations: energy density vs temperature

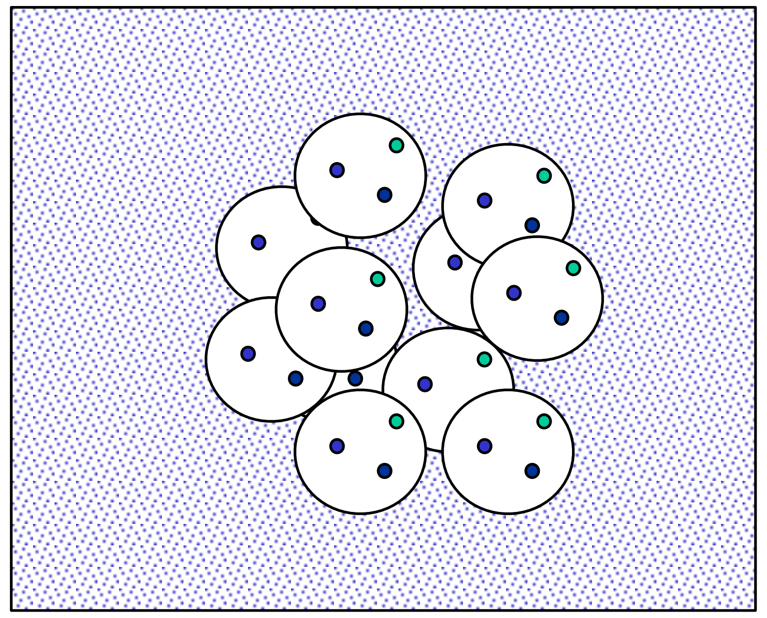

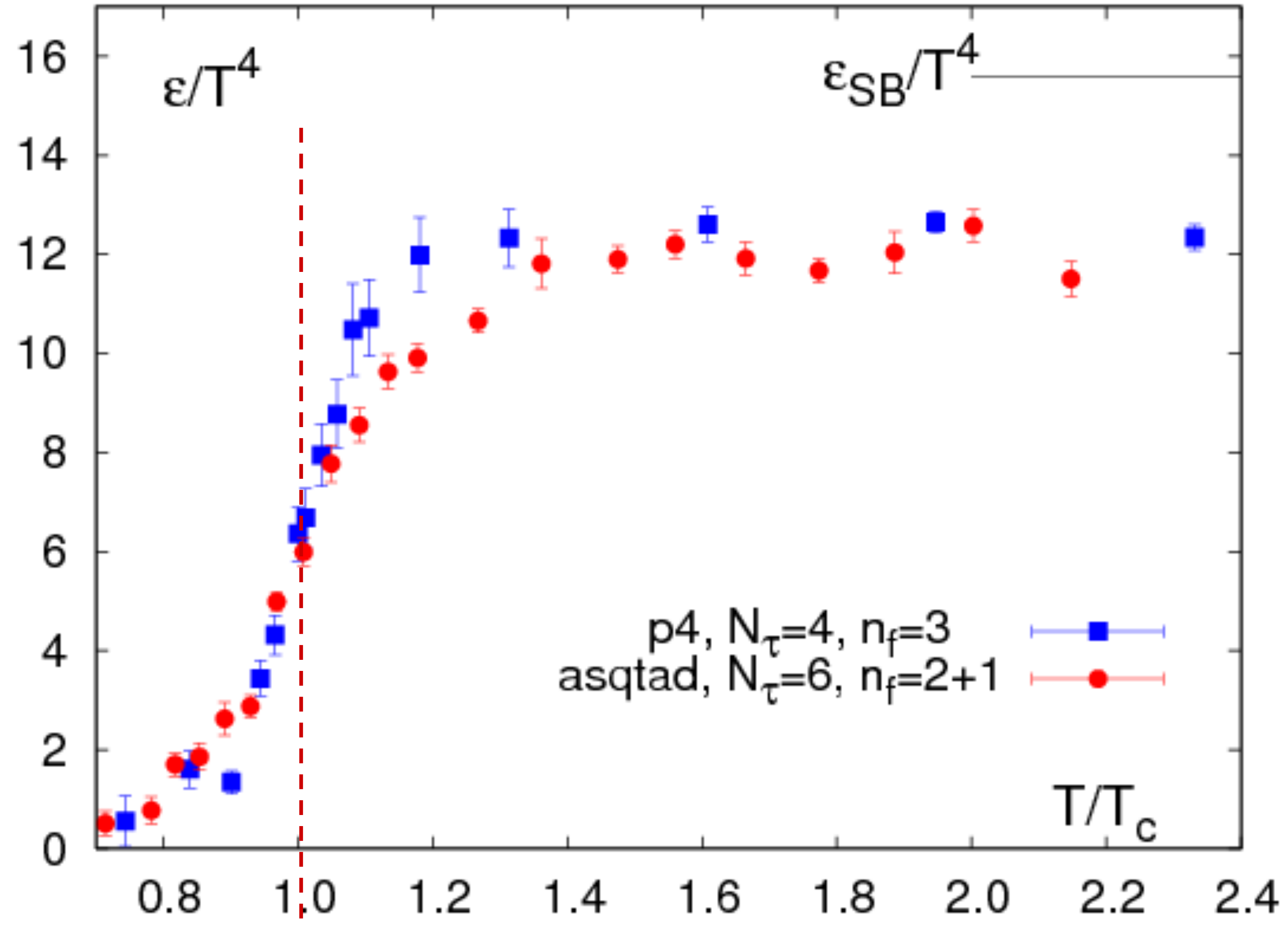

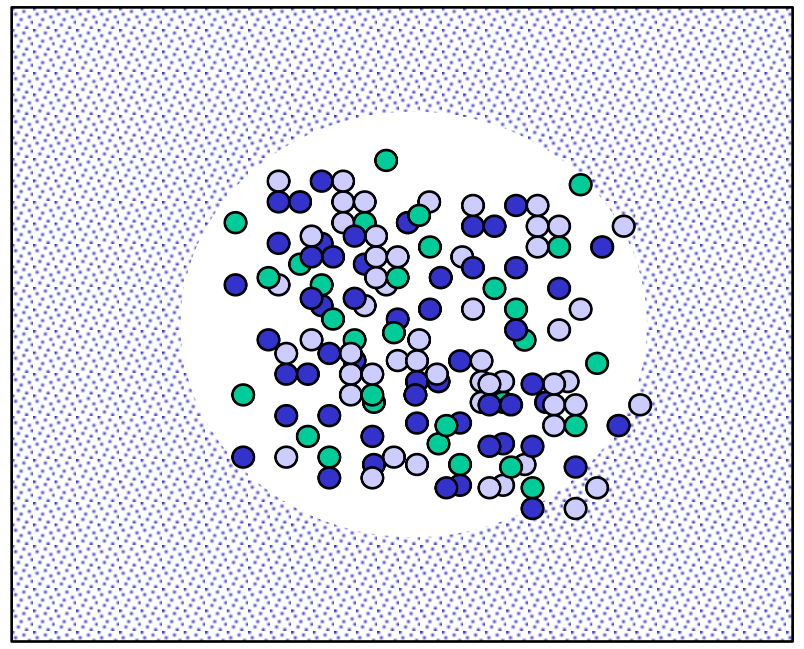

T_c ~ 155 MeV

ε_c ~ 1 GeV/fm³

Bernard et al. hep-lat/0610017

Low temperature:
quarks and gluons confined in hadrons

High temperature:
deconfined quark-gluon plasma

Phase transition at critical temperature $T_c \approx$ 155 MeV ≈ 10^{12} K

Condensed matter of QCD: the quark-gluon plasma

Lattice QCD calculations: energy density vs temperature

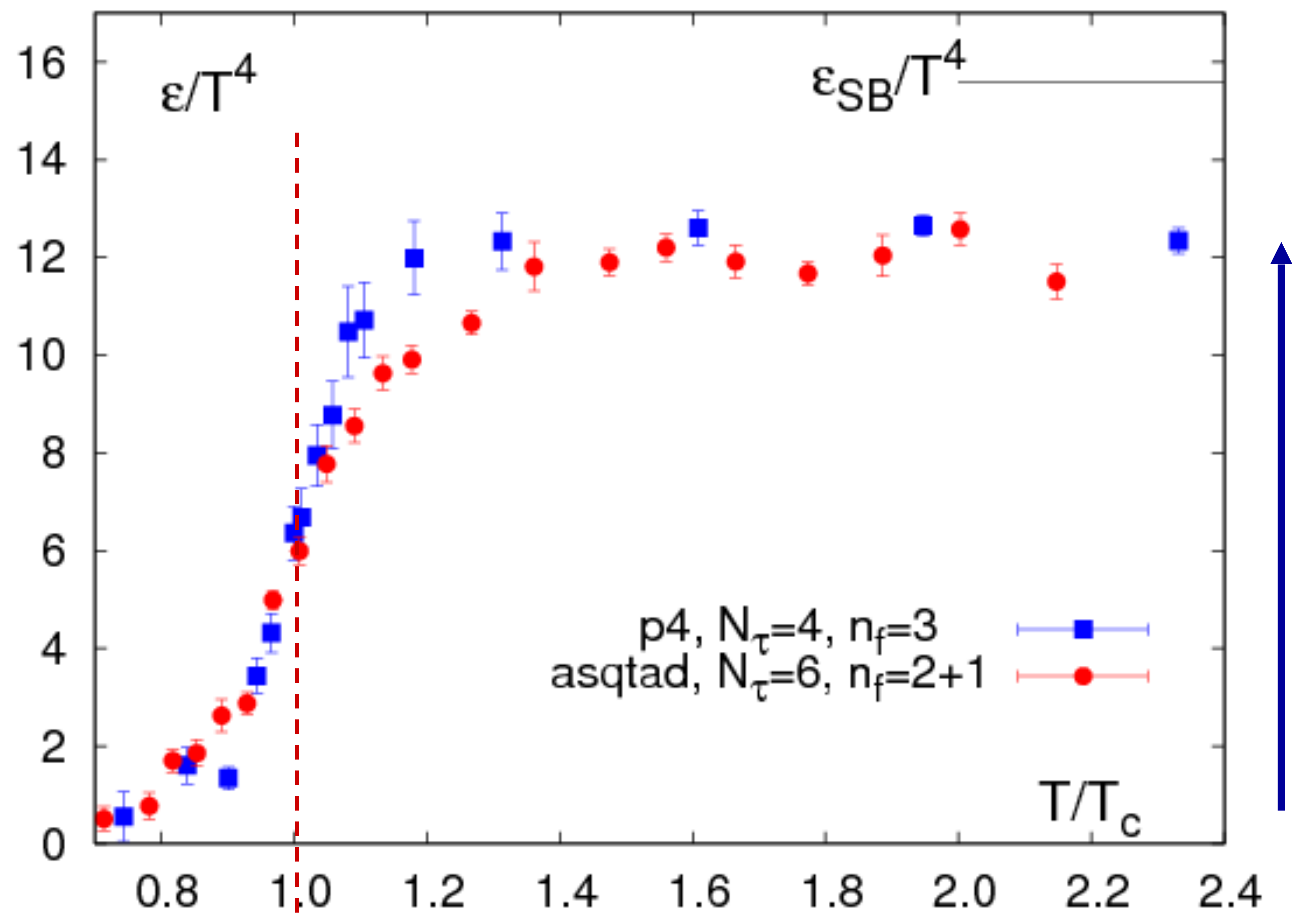

T_c ~ 155 MeV
ε_c ~ 1 GeV/fm³

Bernard et al. hep-lat/0610017

$$\varepsilon \propto gT^4$$

g: degrees of freedom

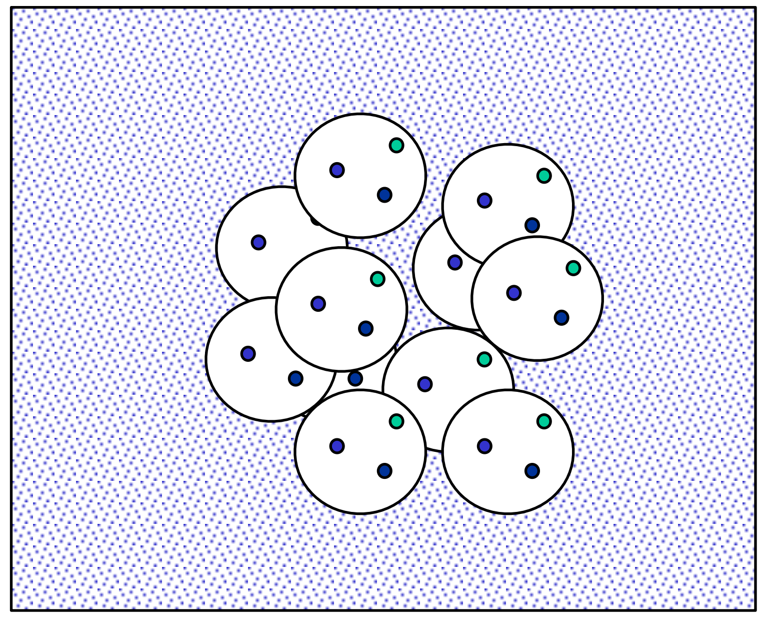

Low temperature:
quarks and gluons confined in hadrons

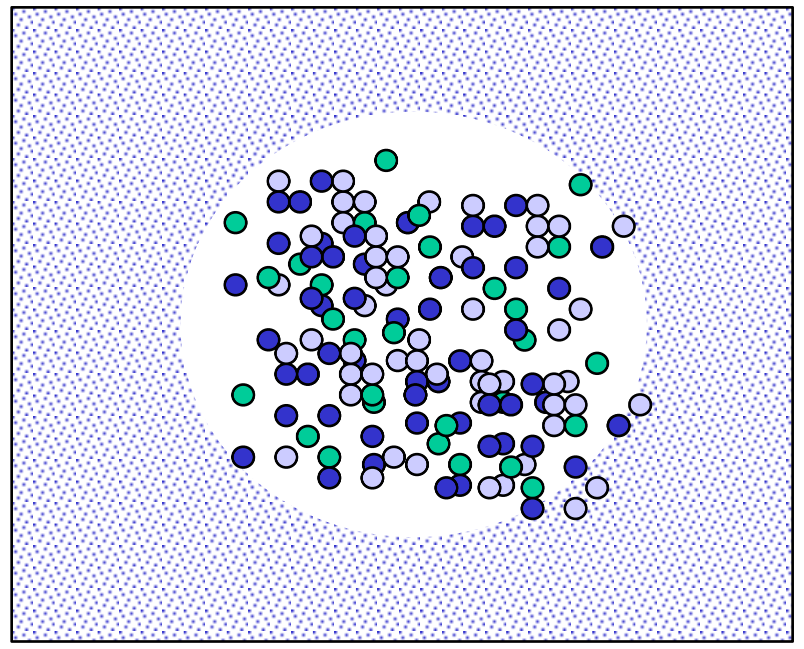

High temperature:
deconfined quark-gluon plasma

Phase transition at critical temperature $T_c \approx$ 155 MeV ≈ 10^{12} K

Increase of number of degrees of freedom: hadrons (3 pions) → quarks+gluons (37)

The Large Hadron Collider and ALICE

The Large Hadron Collider

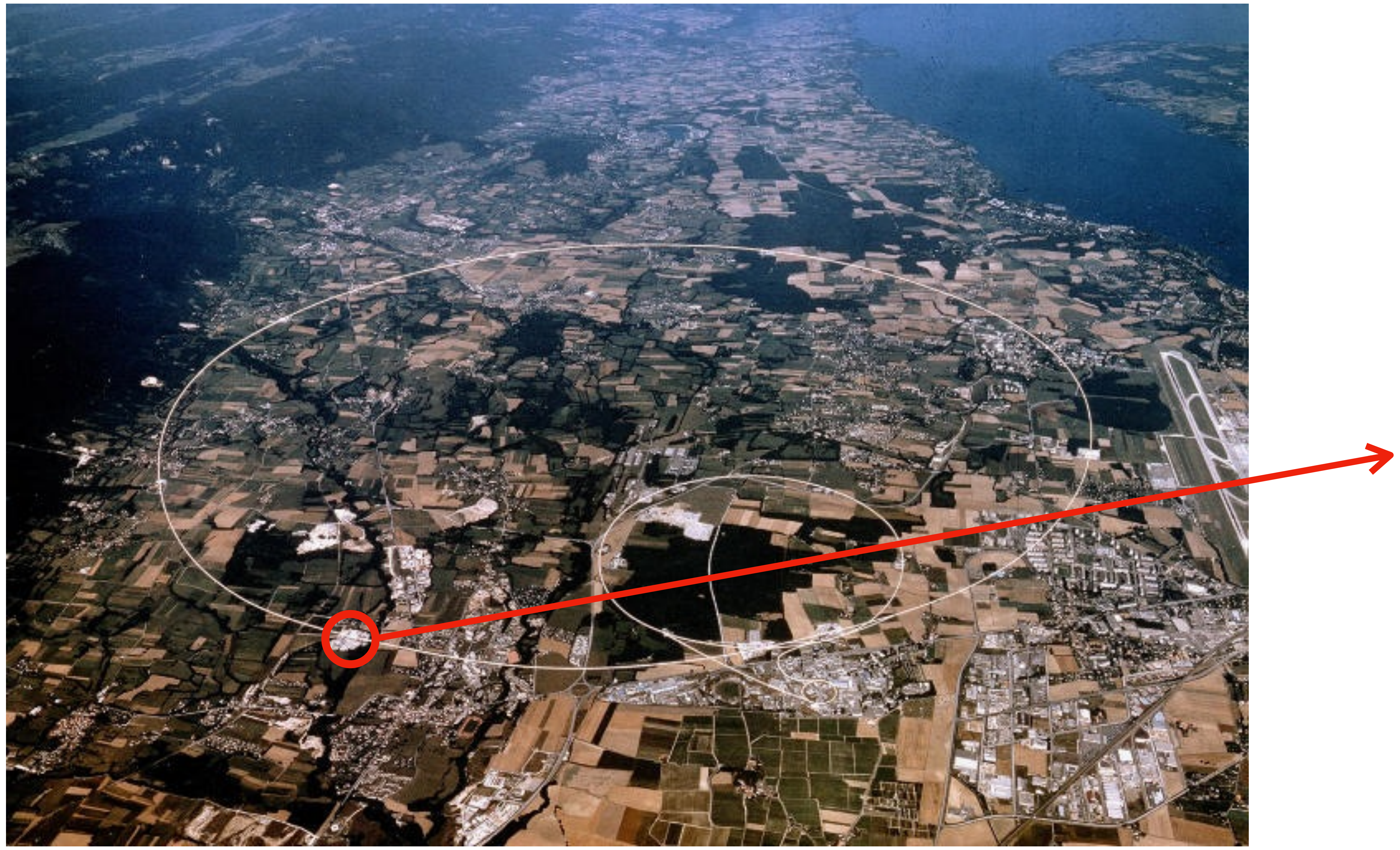

A Large Ion Collider Experiment

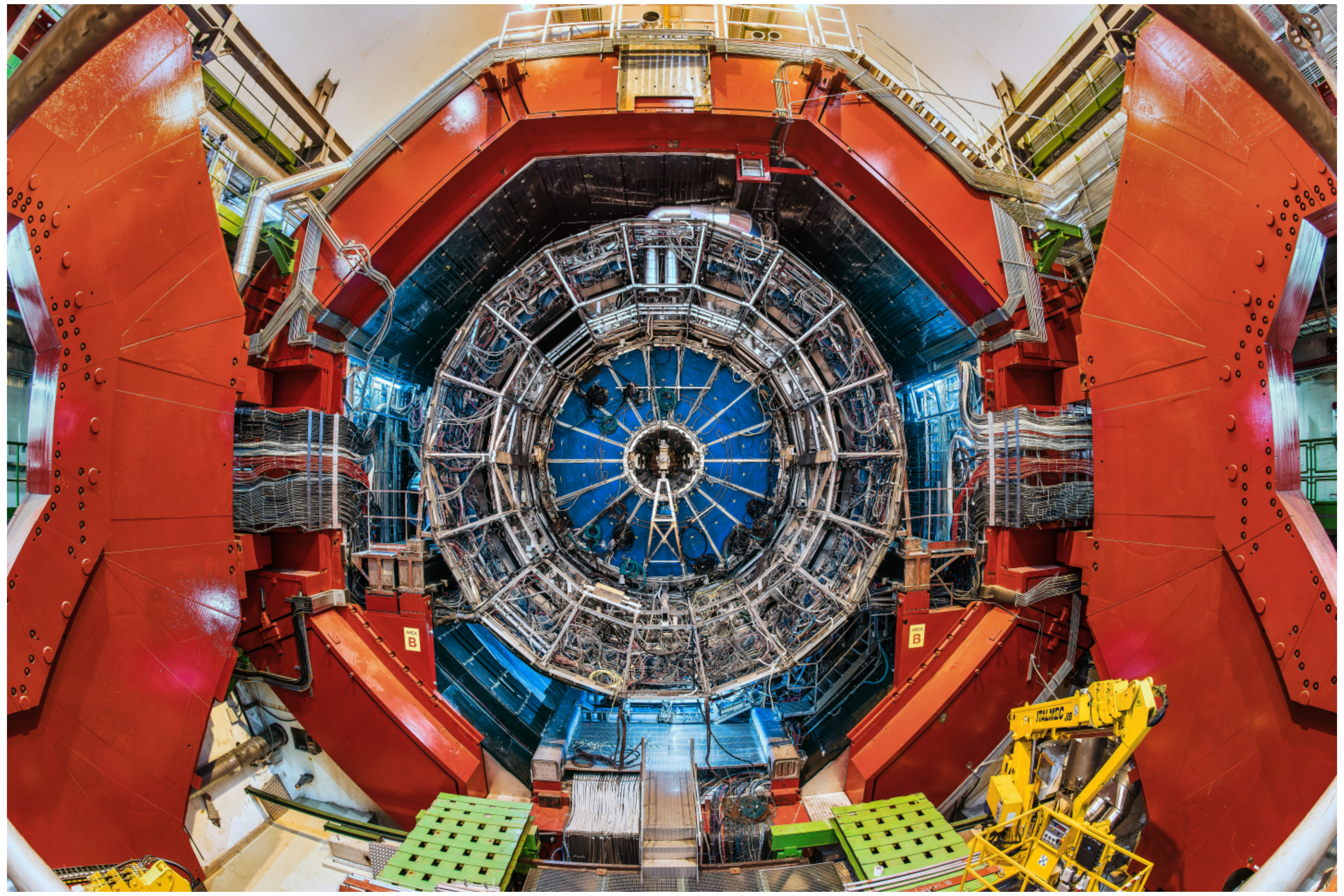

LHC: most powerful particle accelerator-collider in the world
pp collision: 13.6 TeV
Pb-Pb collisions: 5.36 TeV per nucleon pair

ALICE: one of the four large LHC experiments
Focus on strong interaction, heavy-ion collisions

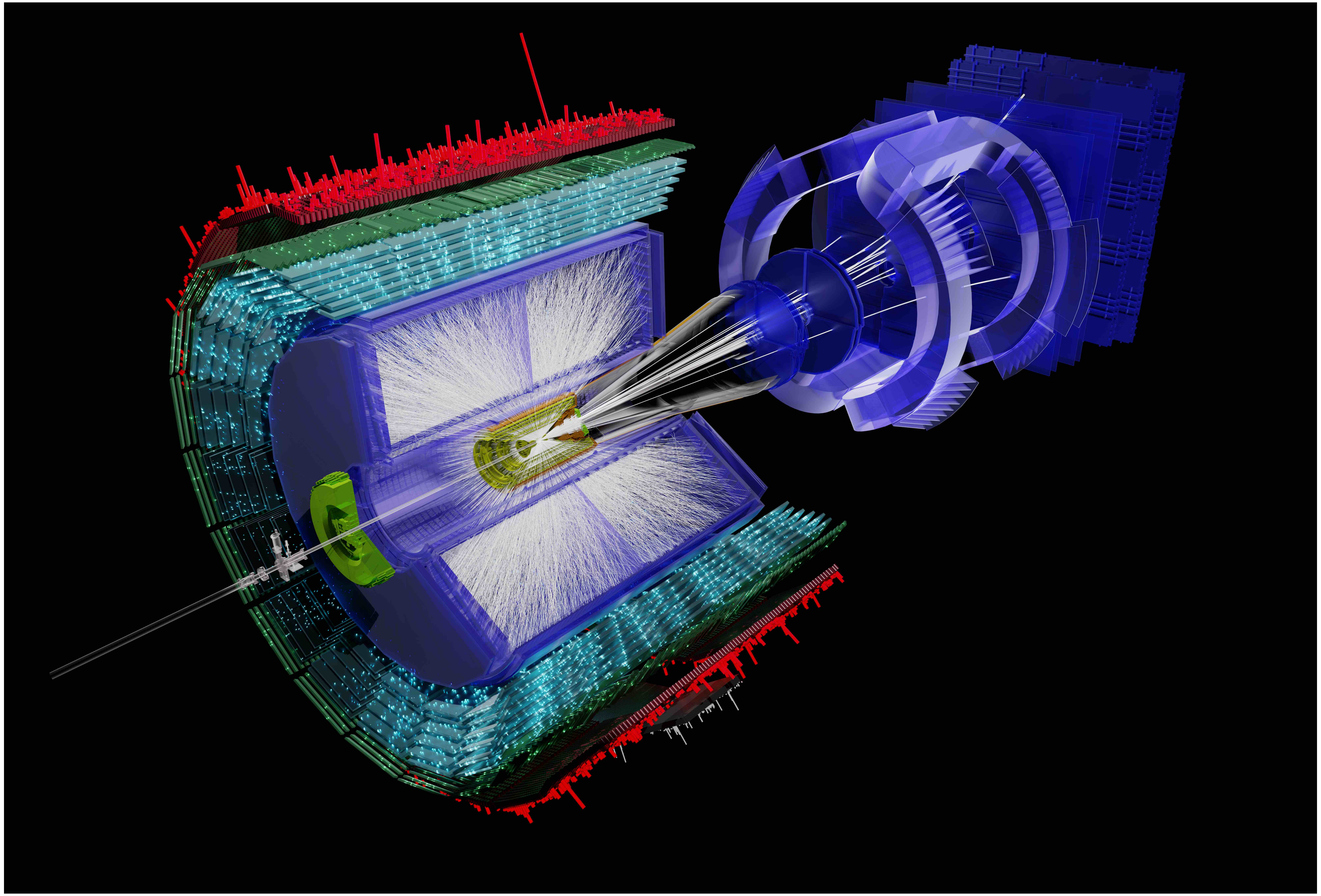

Thousands of particles are produced in each lead ion collision
— study momentum distributions, correlations, types of particles

Heavy ion collisions: Little Bangs

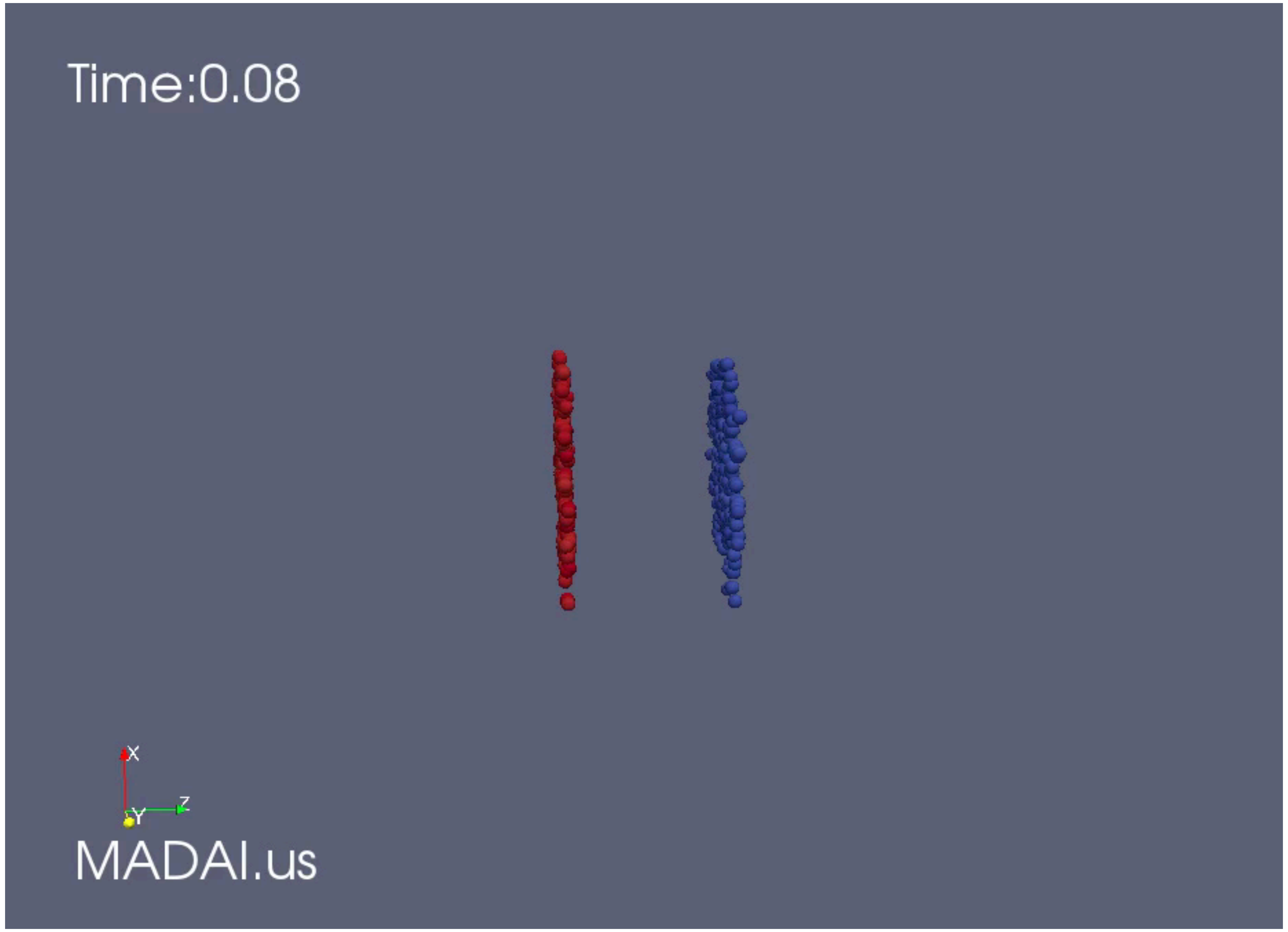

MADAI

Stages of the collision: initial stages — QGP/fluid stage — hadron formation (freeze out)

'Little Bang': recreate primordial matter in the laboratory

Heavy ion collisions: Little Bangs

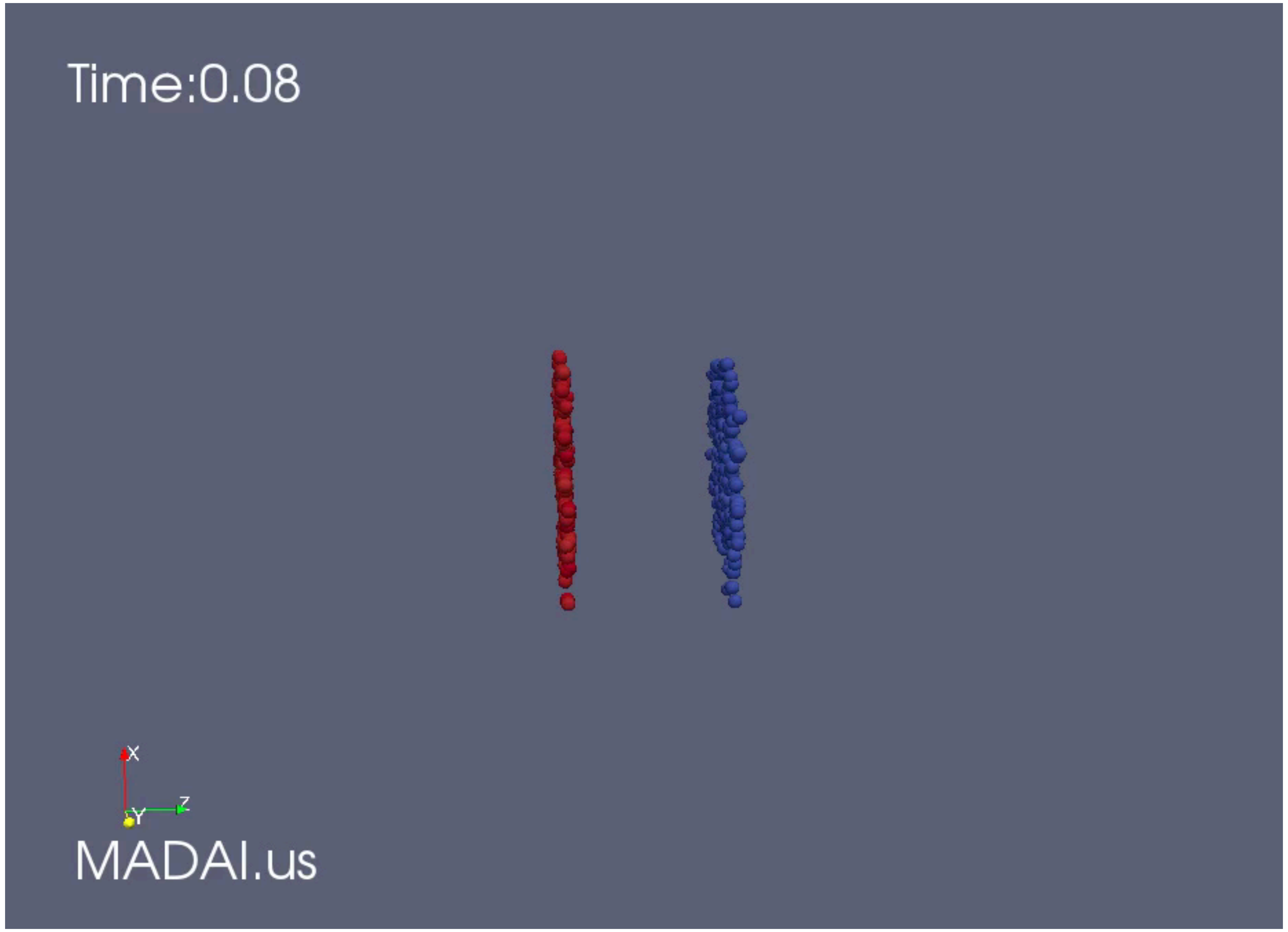

MADAI

Stages of the collision: initial stages — QGP/fluid stage — hadron formation (freeze out)

'Little Bang': recreate primordial matter in the laboratory

Azimuthal anisotropy: initial and final states

Simulated event: location of nucleons

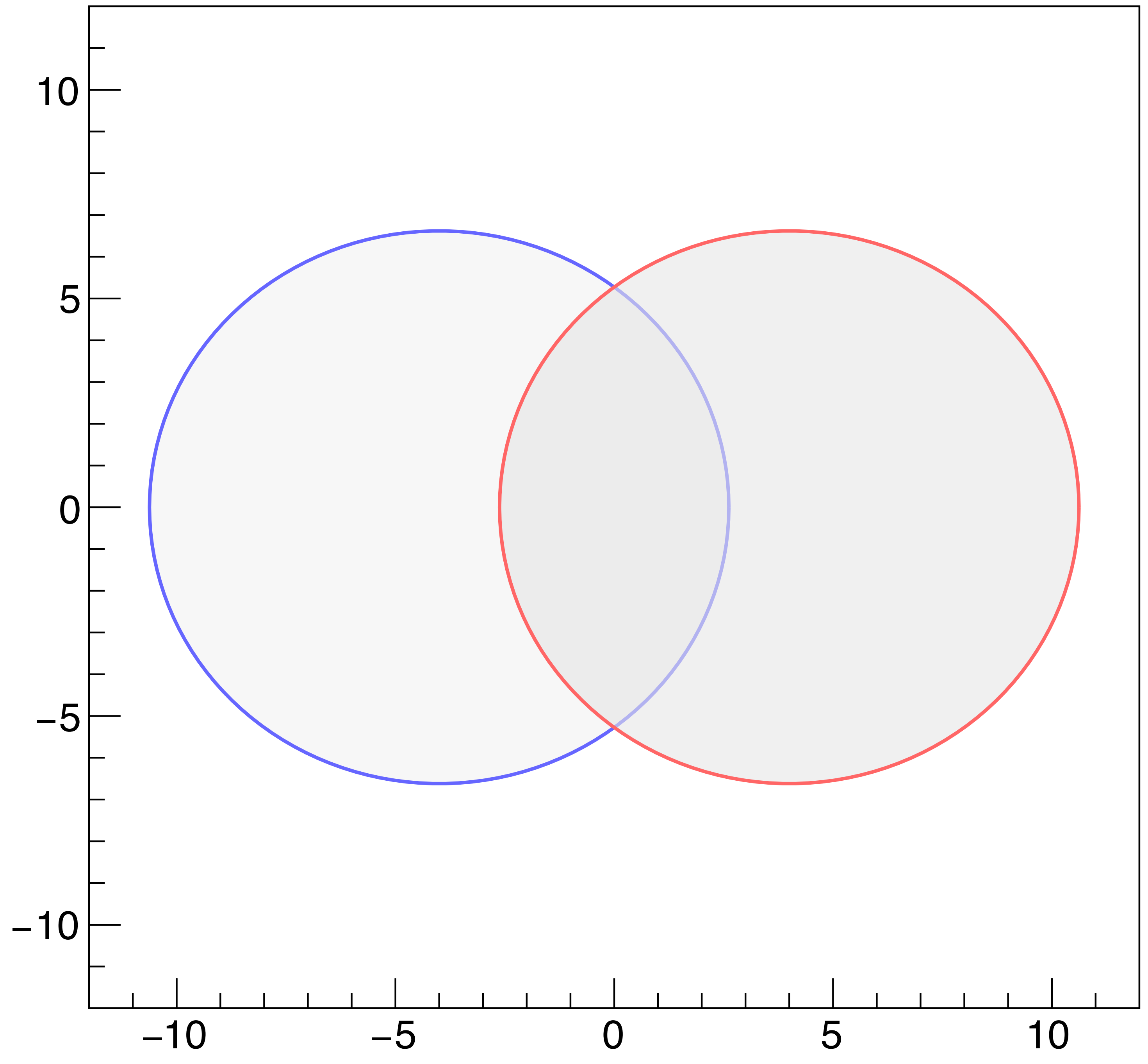

Characterise shape by harmonics:

$$\varepsilon_n = \frac{\sum r^2 (\cos^2 n\varphi + \sin^2 n\varphi)}{\sum r^2}$$

Azimuthal anisotropy: initial and final states

Simulated event: location of nucleons

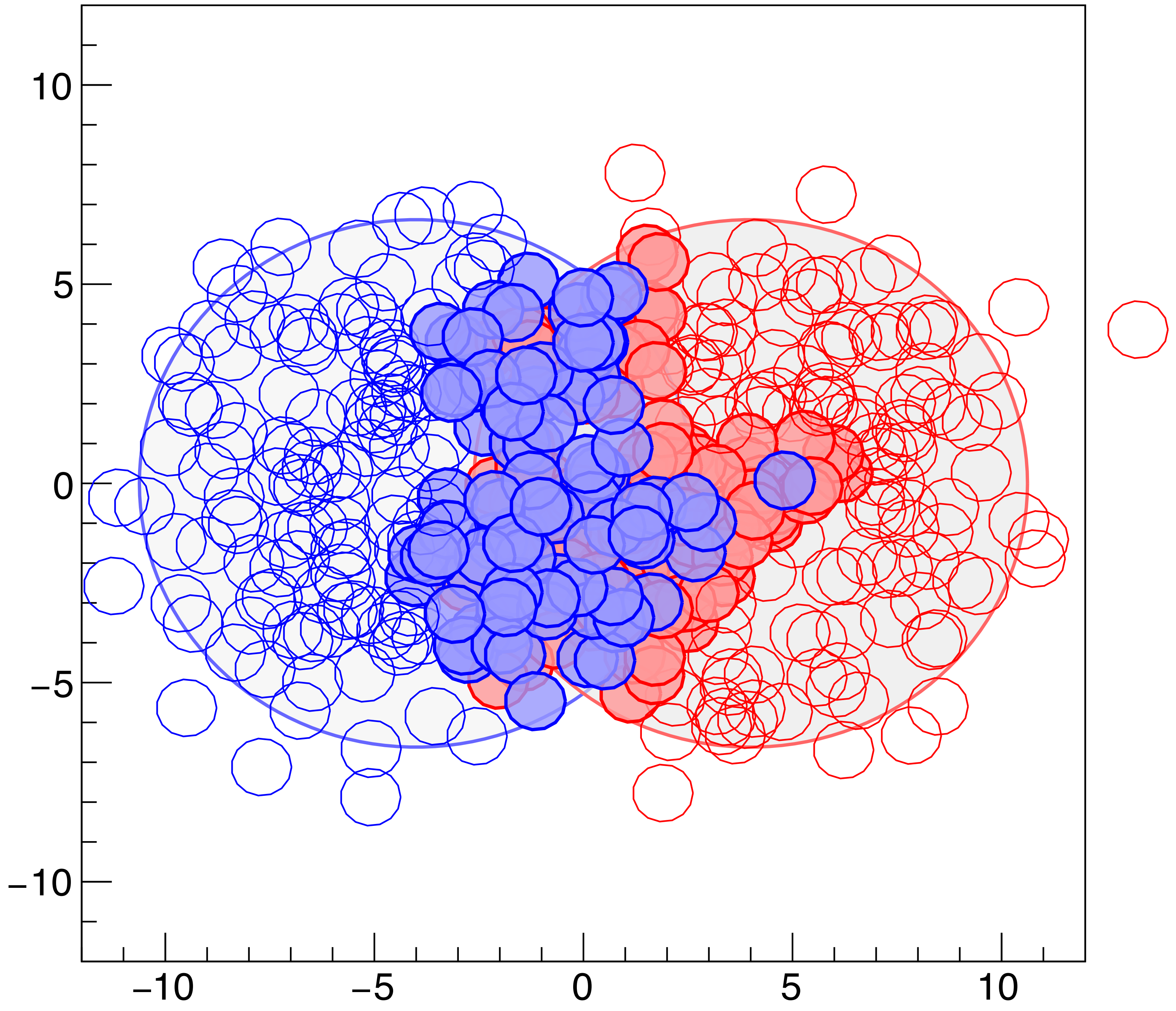

Characterise shape by harmonics:

$$\varepsilon_n = \frac{\sum r^2(\cos^2 n\varphi + \sin^2 n\varphi)}{\sum r^2}$$

Azimuthal anisotropy: initial and final states

Simulated event: location of nucleons

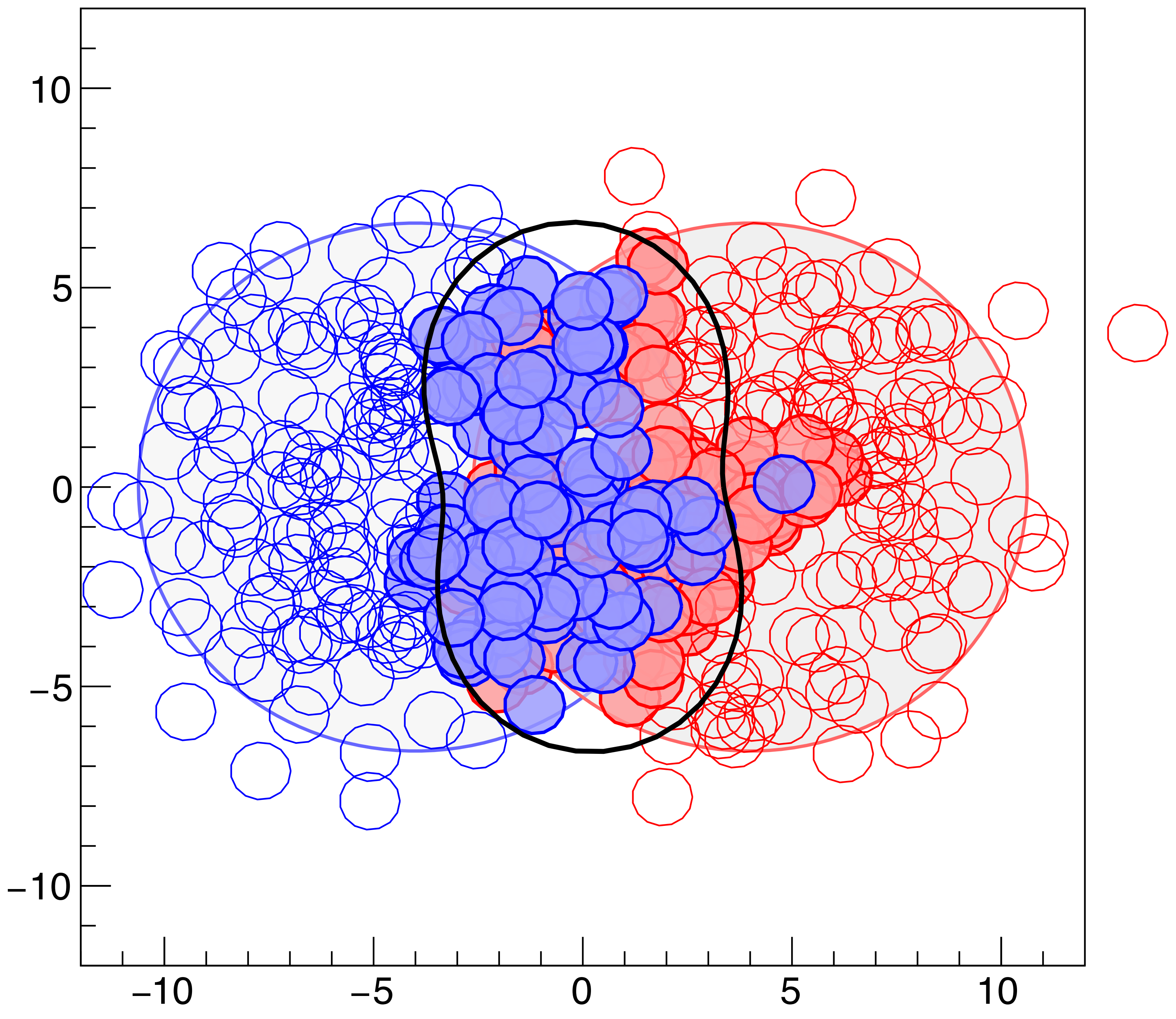

Characterise shape by harmonics:

$$\varepsilon_n = \frac{\sum r^2(\cos^2 n\varphi + \sin^2 n\varphi)}{\sum r^2}$$

Azimuthal anisotropy: initial and final states

Simulated event: location of nucleons

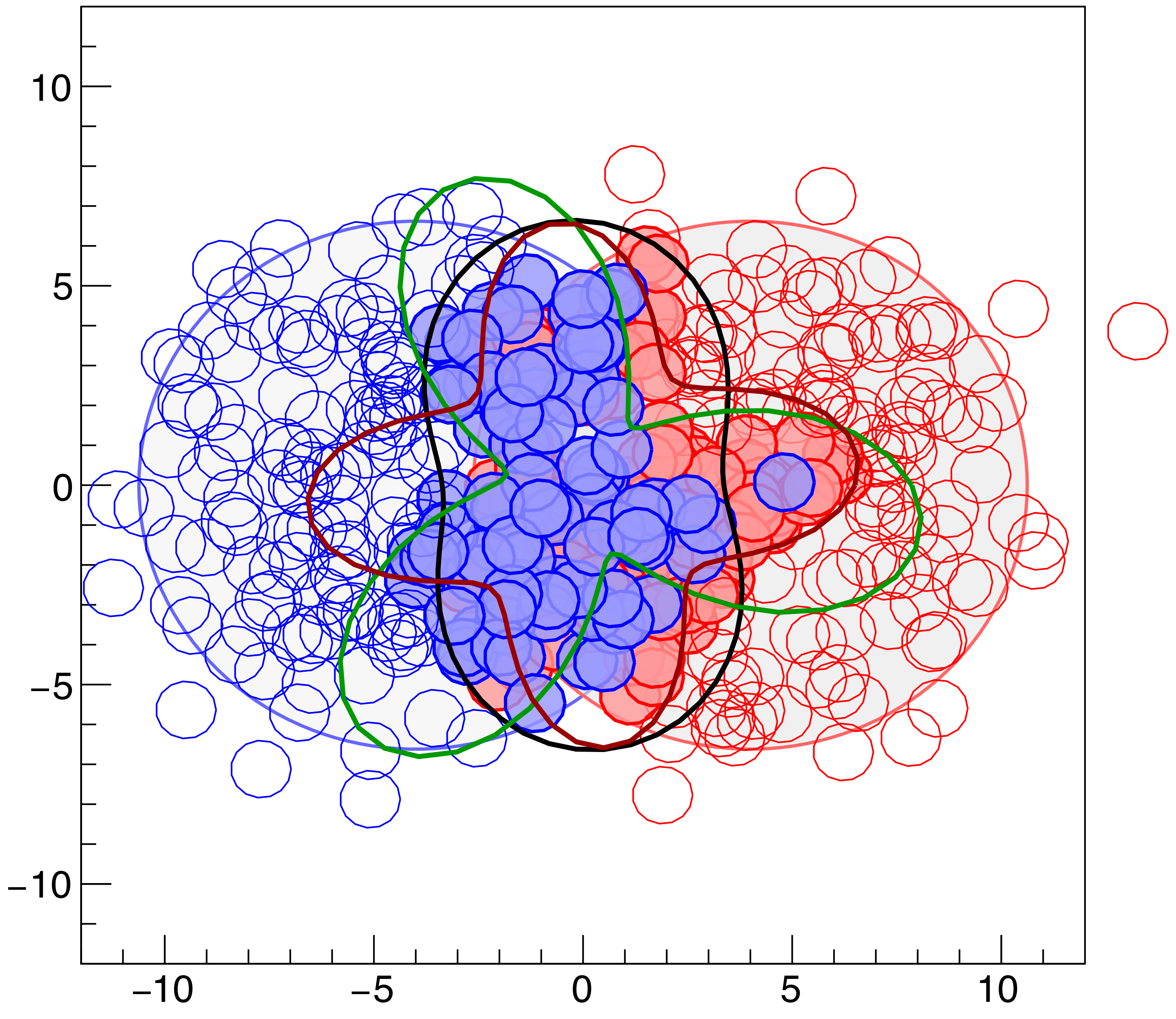

Initial state spatial anisotropies ε_n are transferred into
final state momentum anisotropies v_n
by pressure gradients, flow of the Quark Gluon Plasma

Azimuthal anisotropy: initial and final states

Simulated event: location of nucleons

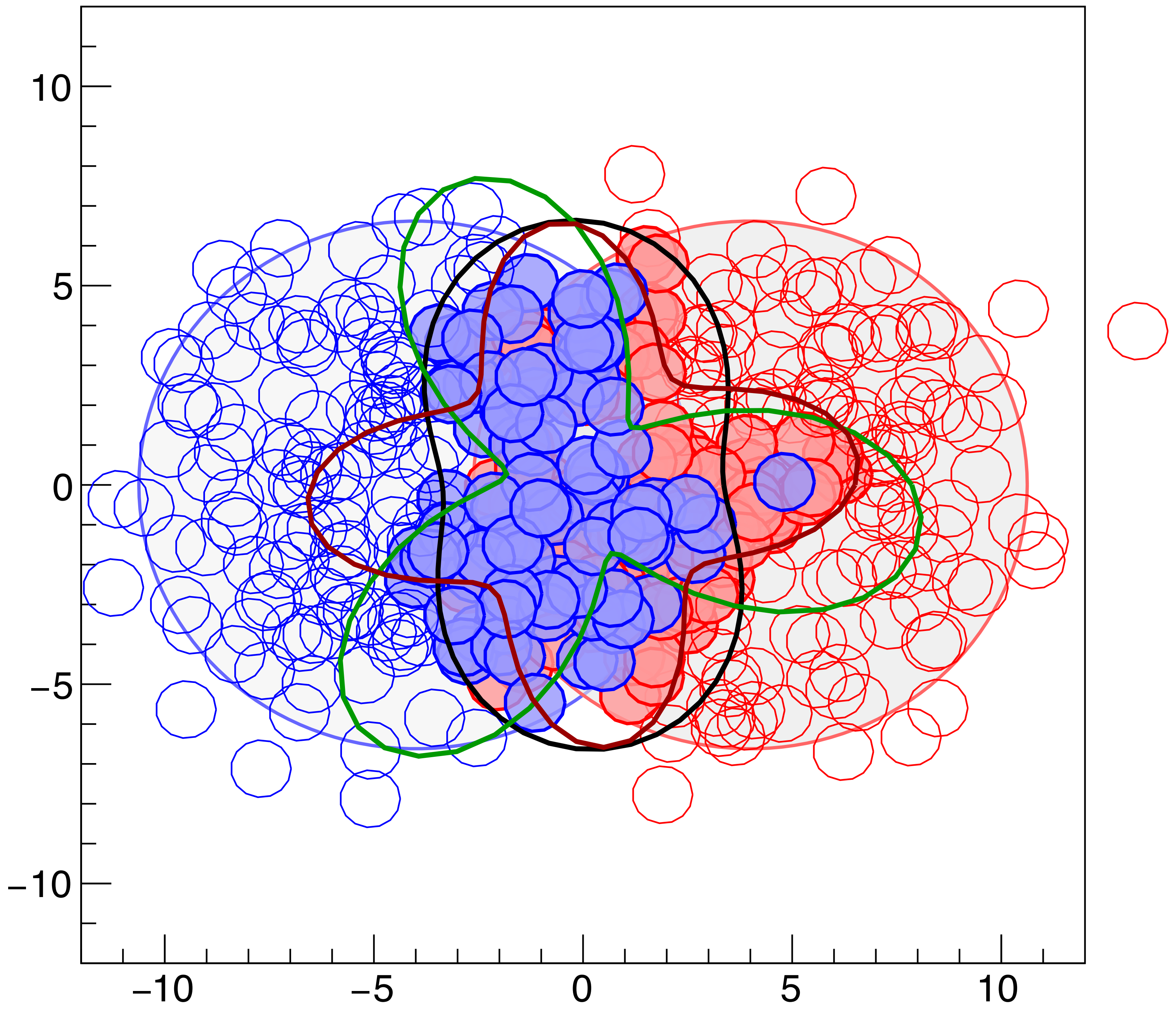

Azimuthal distribution single event

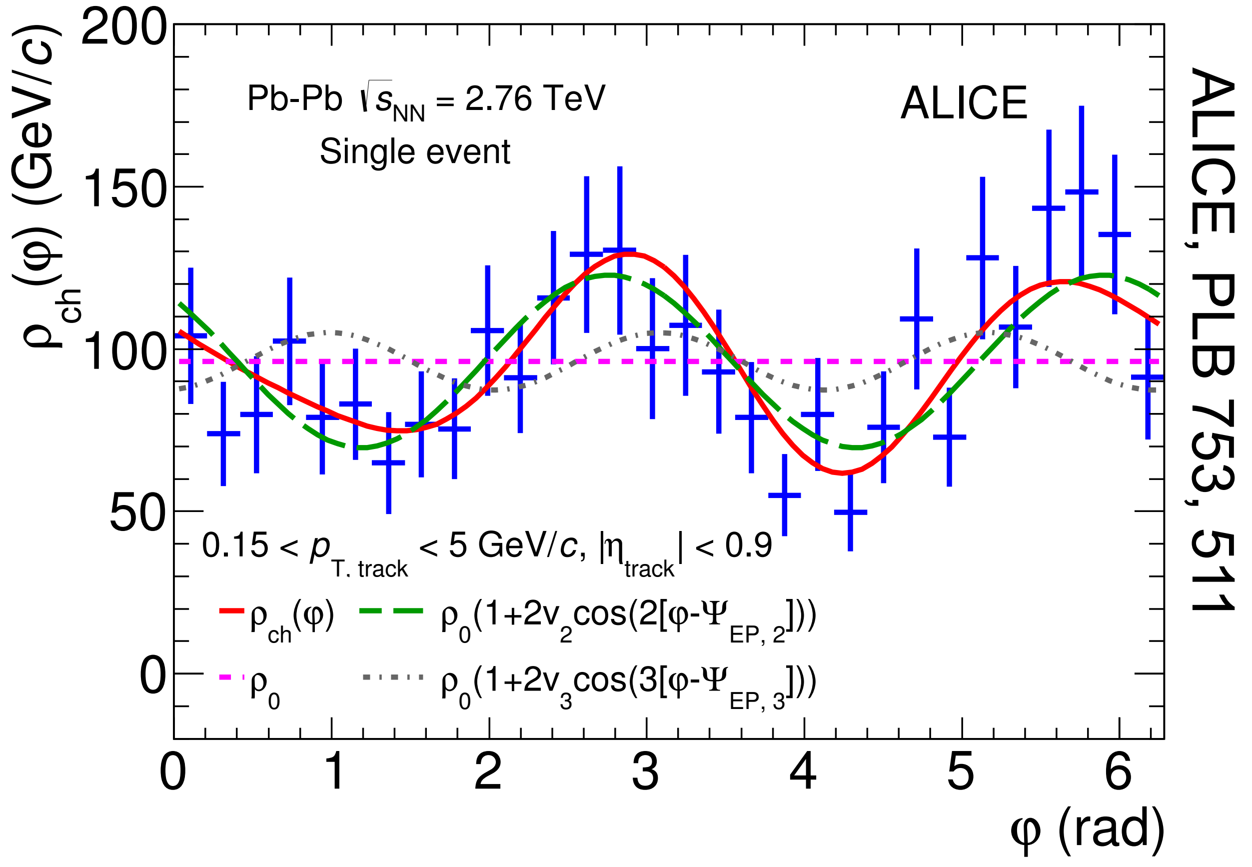

ALICE, PLB 753, 511

Initial state spatial anisotropies ε_n are transferred into
final state momentum anisotropies v_n
by pressure gradients, flow of the Quark Gluon Plasma

Azimuthal anisotropy: initial and final states

Simulated event: location of nucleons

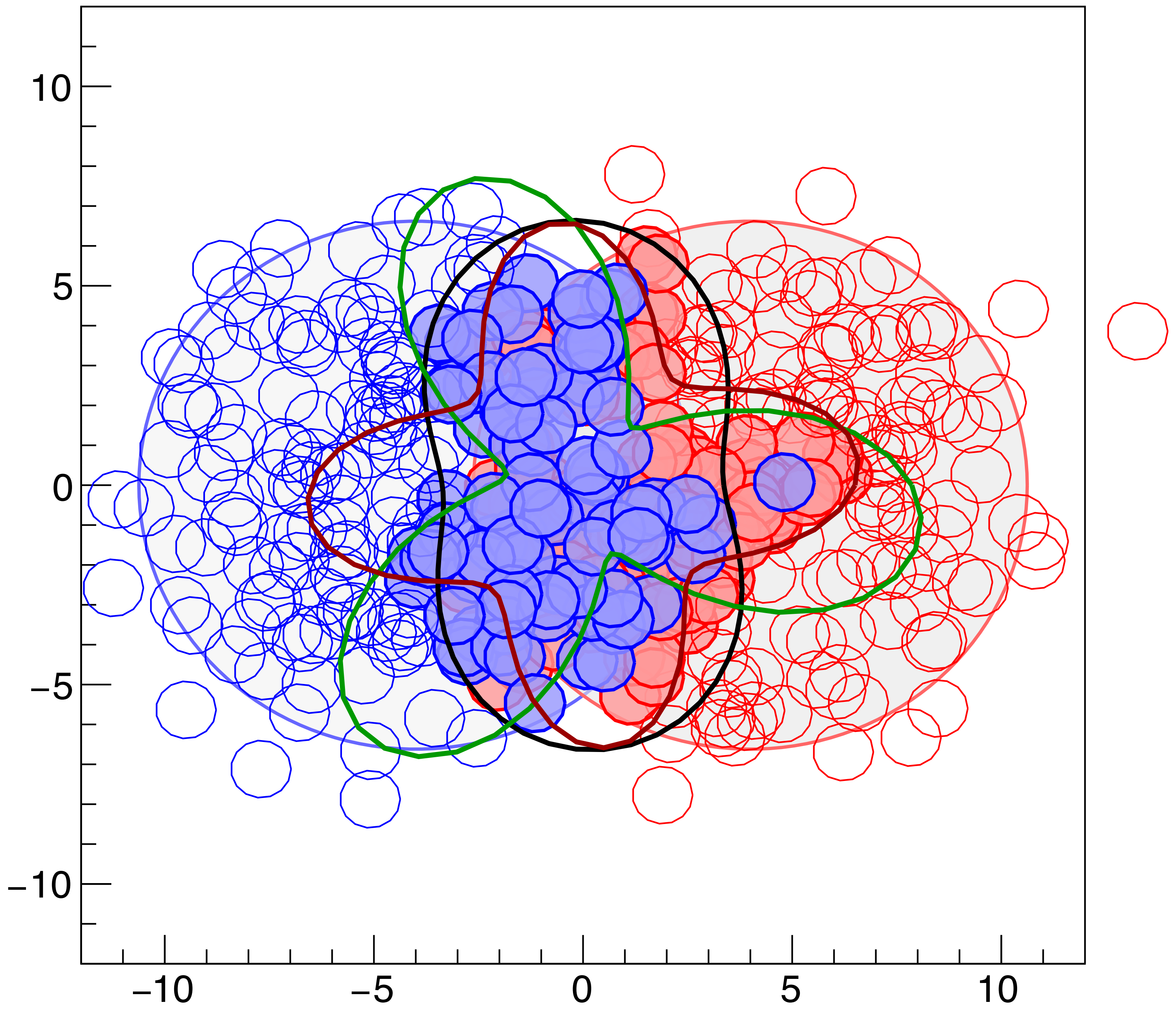

Azimuthal distribution single event

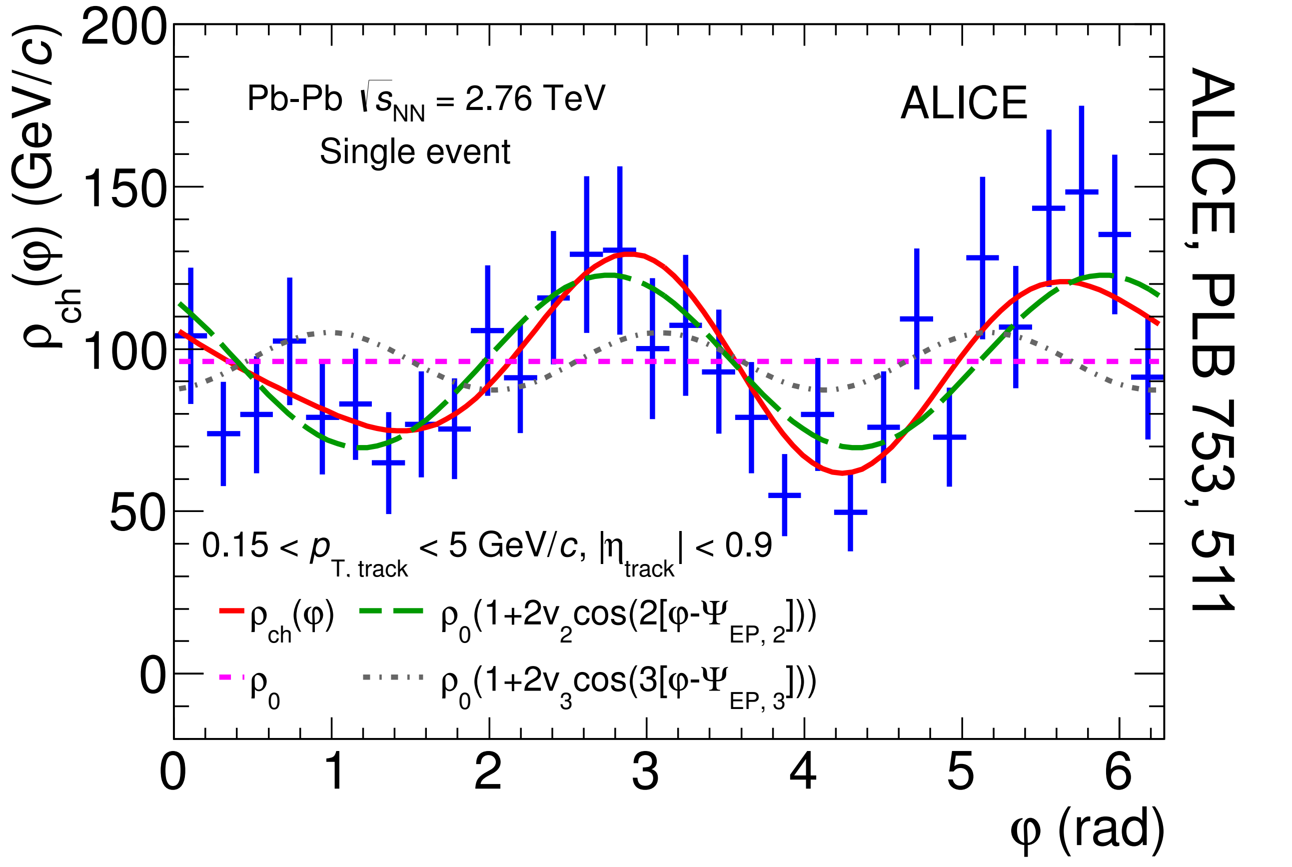

Sum over many events

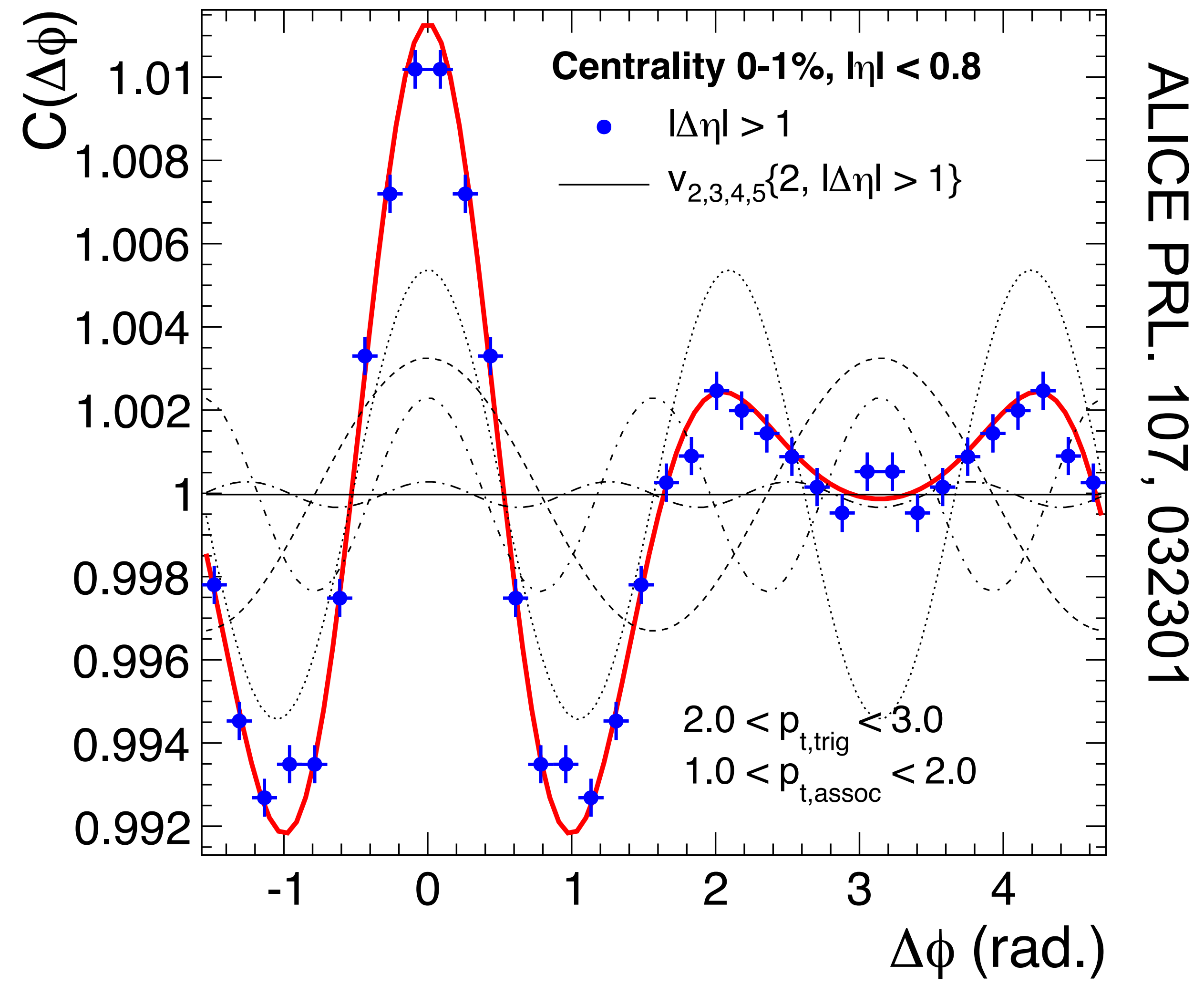

Initial state spatial anisotropies ε_n are transferred into
final state momentum anisotropies v_n
by pressure gradients, flow of the Quark Gluon Plasma

Anisotropic flow: initial state and QGP expansion

Elliptic flow v_2

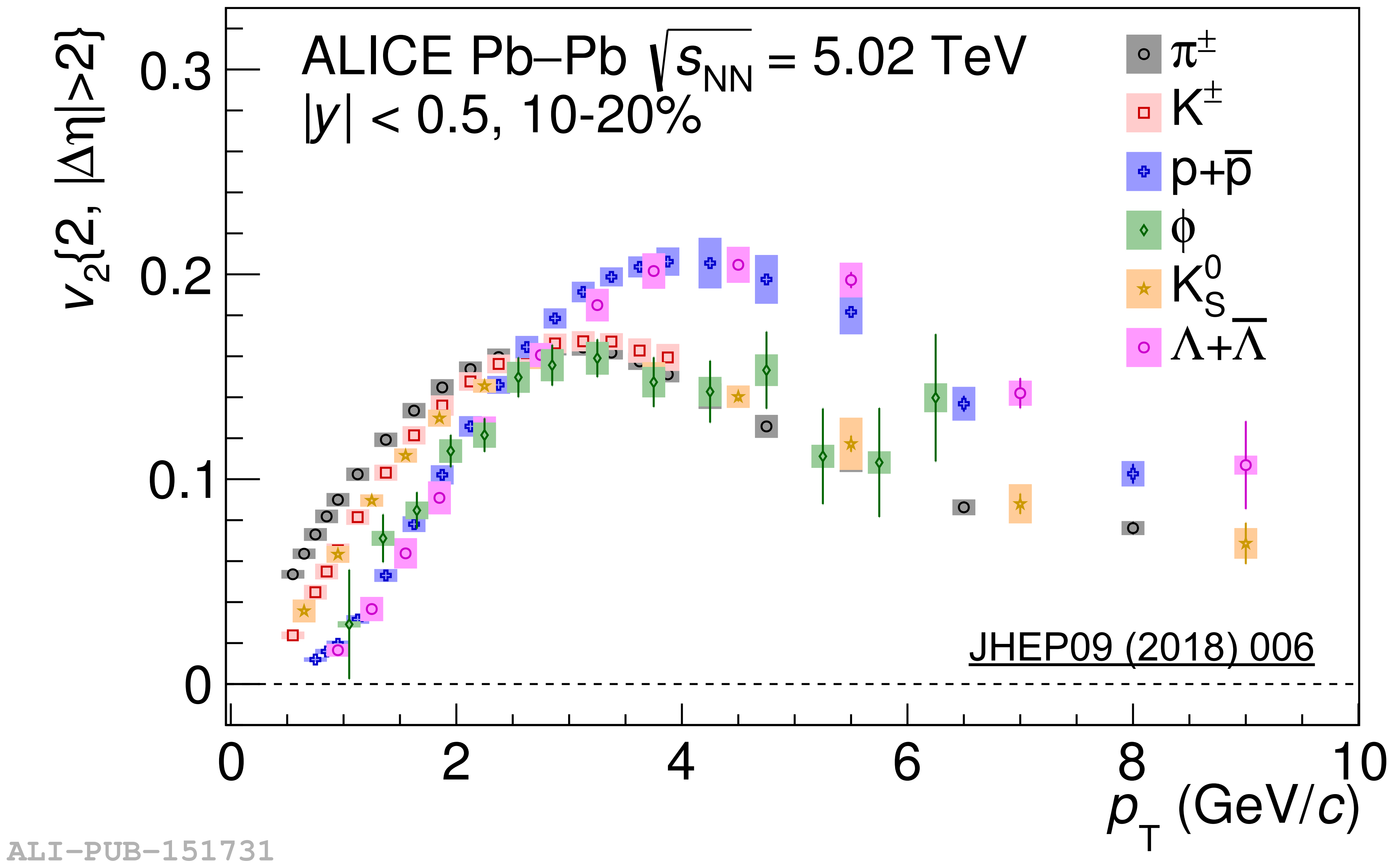

Mass-dependence of v_2 measures flow velocity

Anisotropic flow: initial state and QGP expansion

Elliptic flow v2

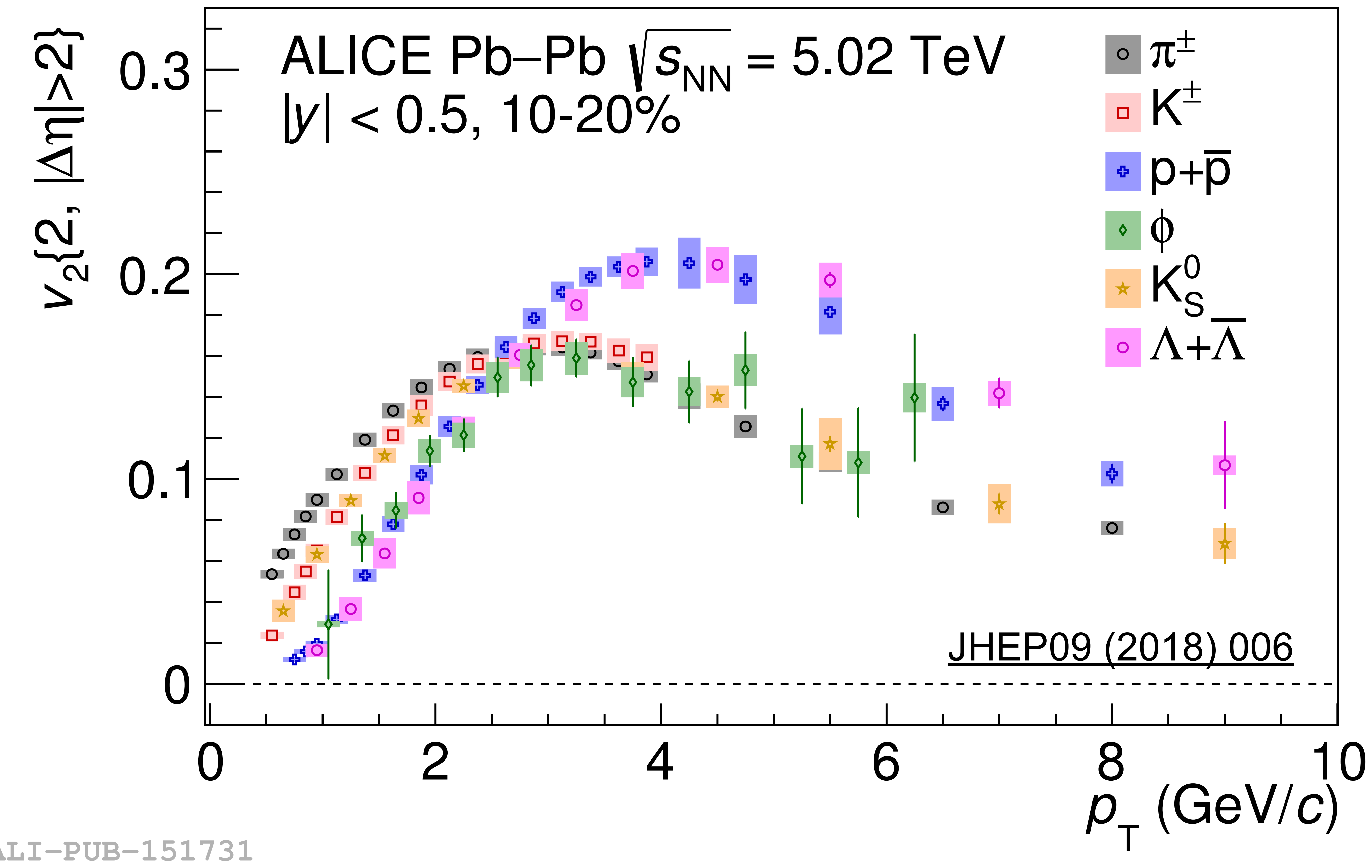

v2 of open charm

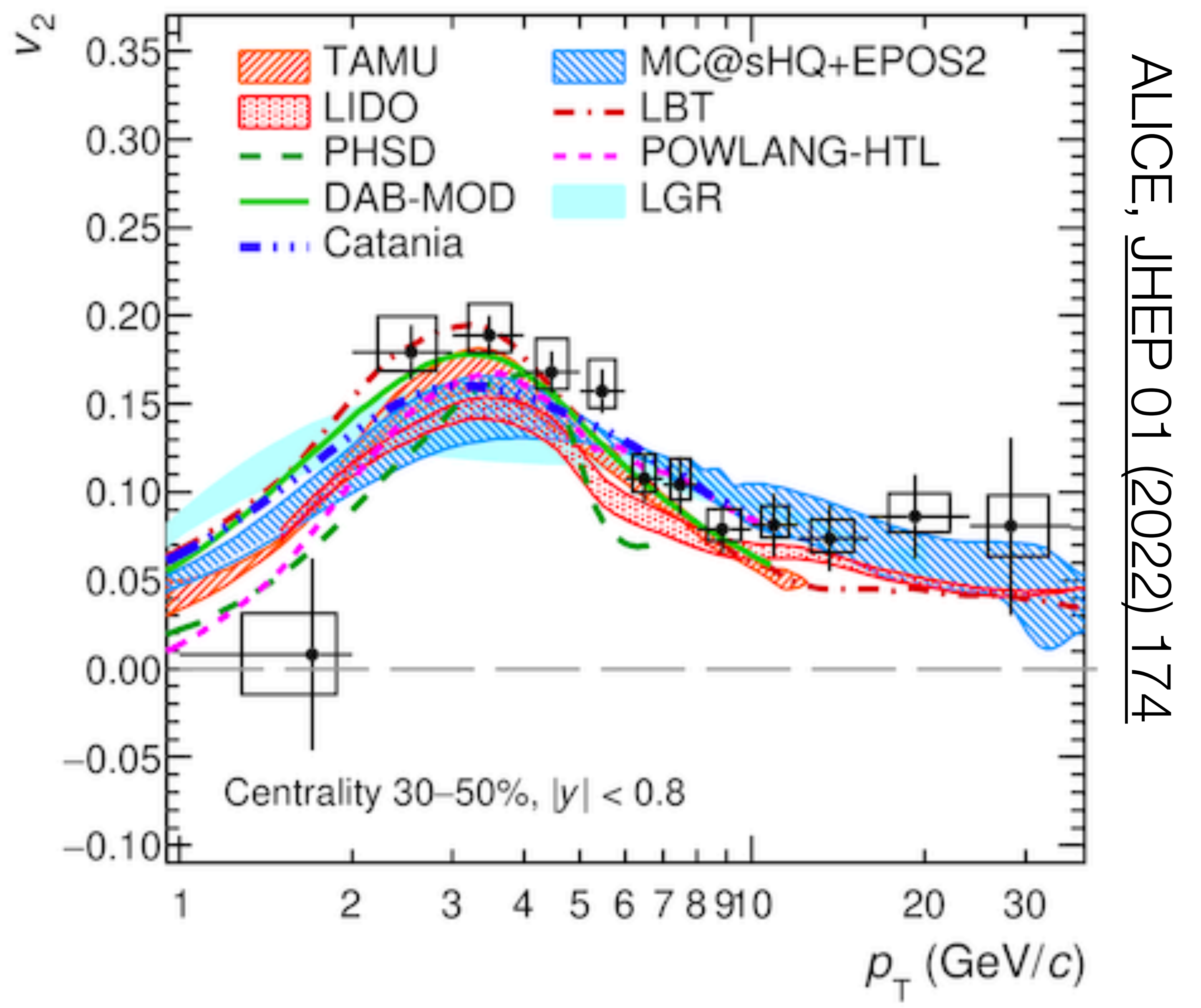

Even heavy flavour hadrons flow !

Mass-dependence of v_2 measures flow velocity

Anisotropic flow: initial state and QGP expansion

Elliptic flow v_2

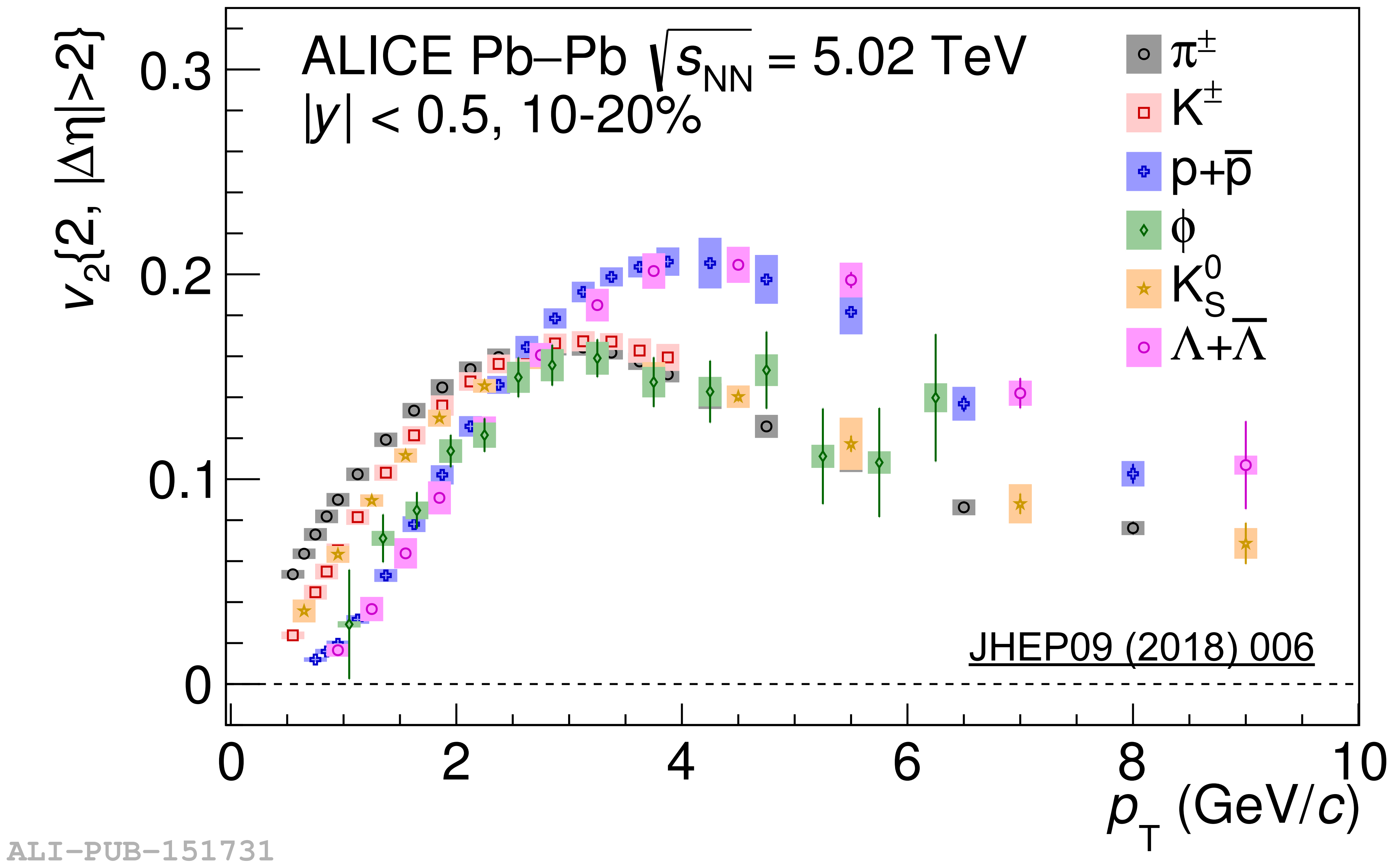

v_2 of open charm

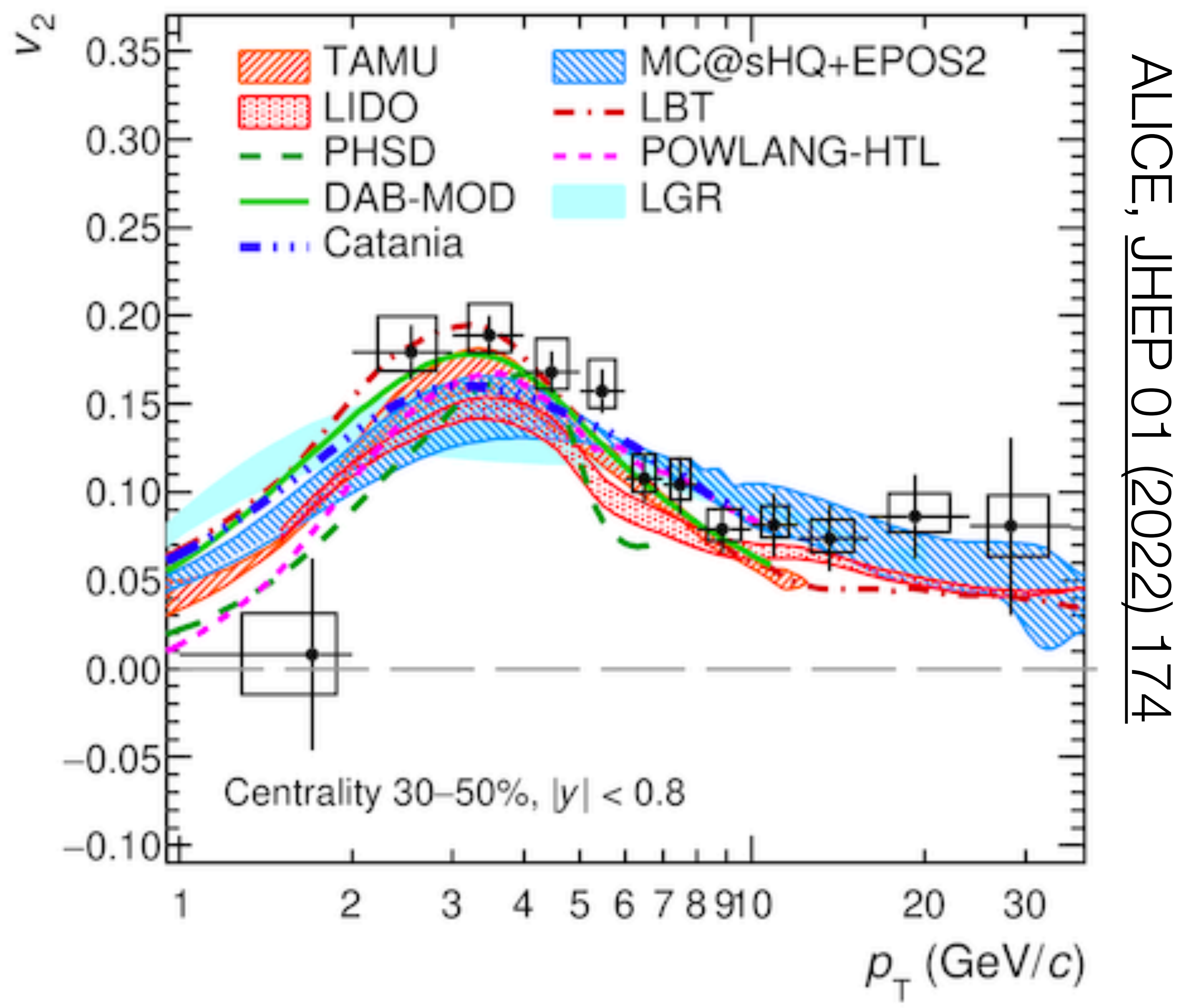

Even heavy flavour hadrons flow !

v_3

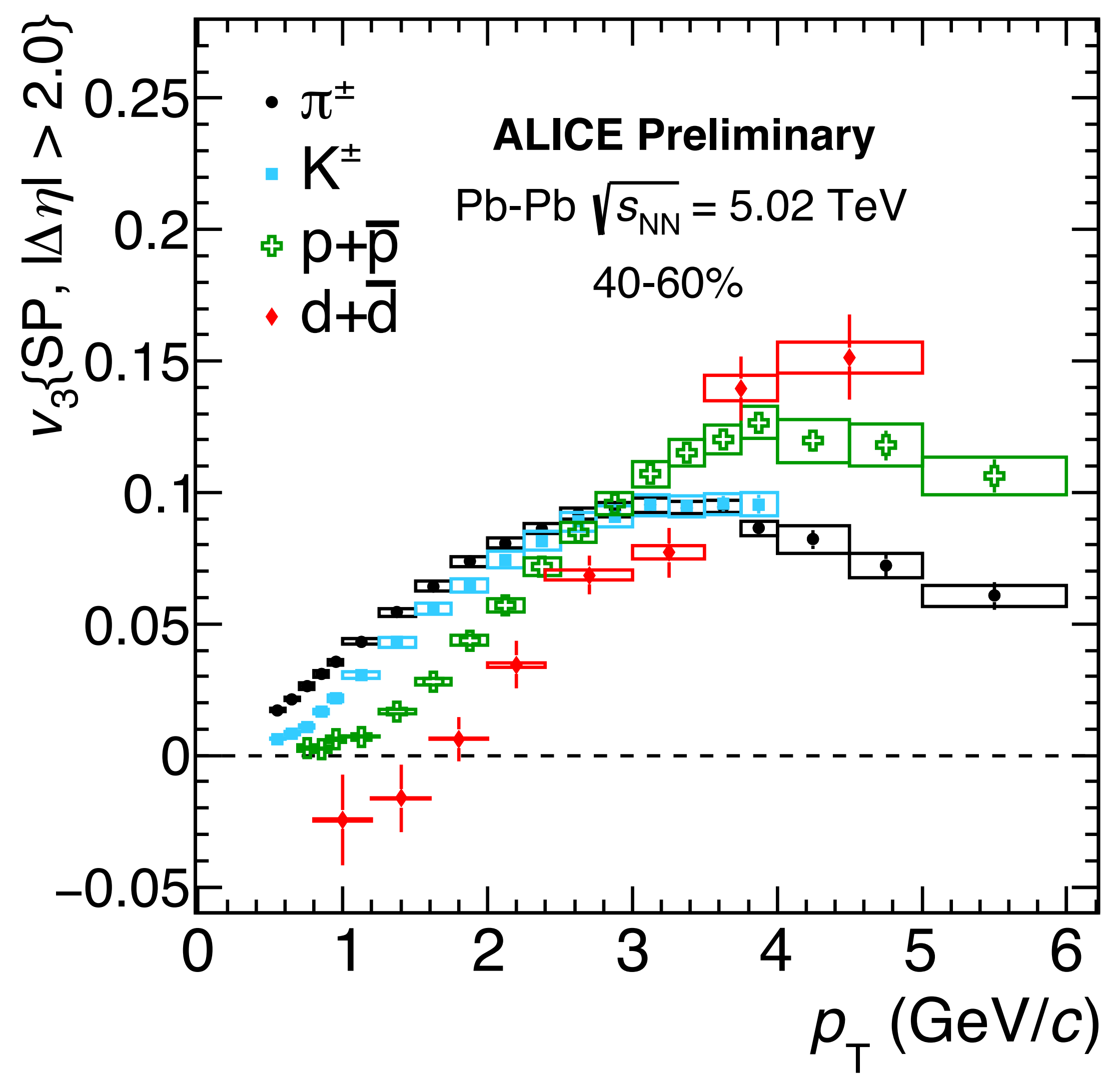

v_4

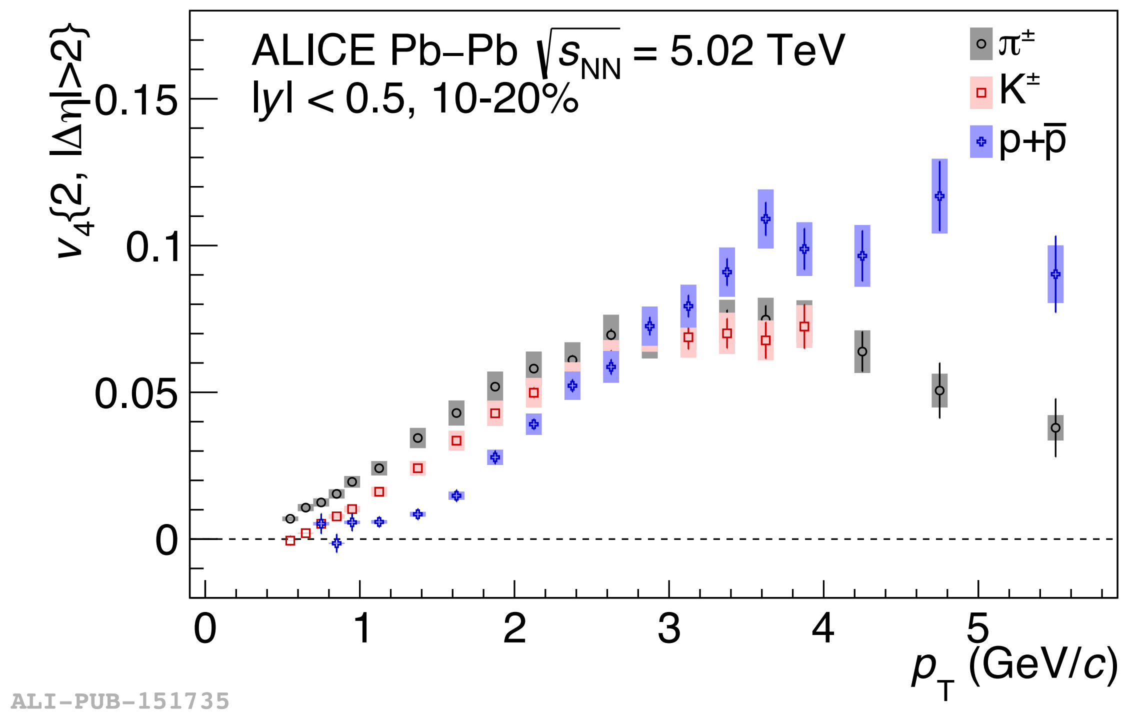

Mass-dependence of v_2 measures flow velocity

Azimuthal anisotropy: initial and final states

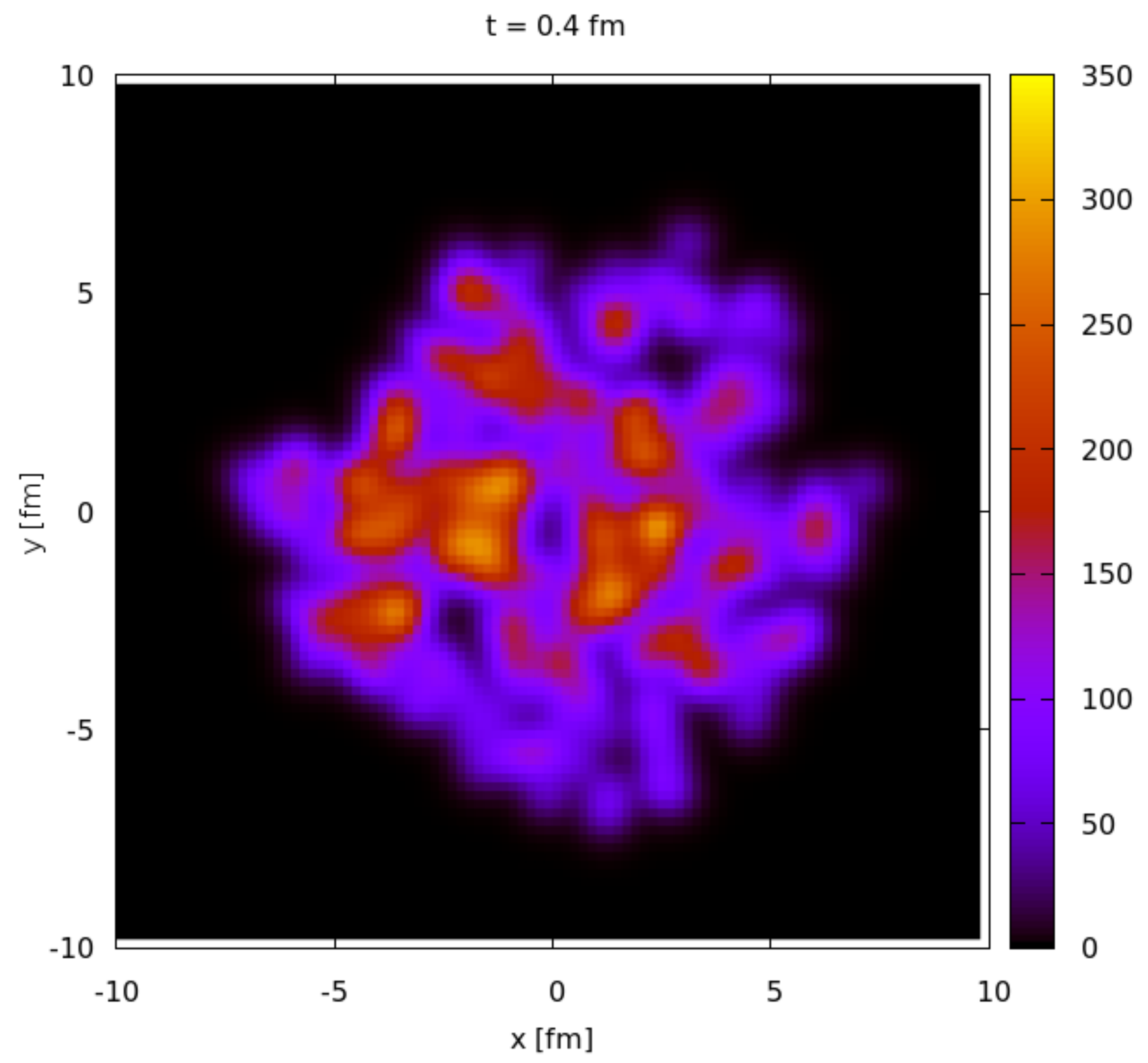

No viscosity
$\eta/s = 0$

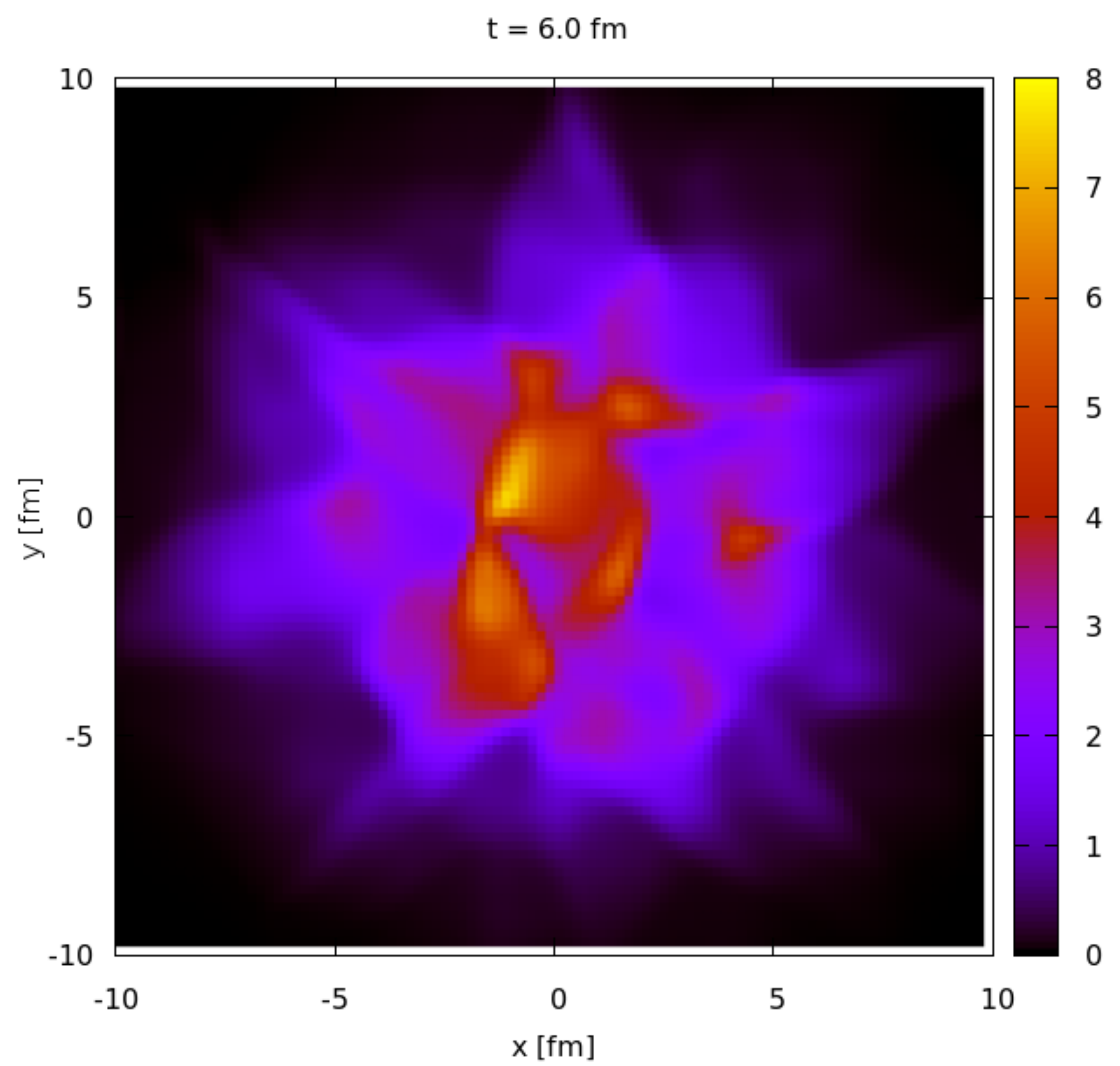

Schenke and Jeon,
Phys.Rev.Lett.106:042301

Azimuthal anisotropy: initial and final states

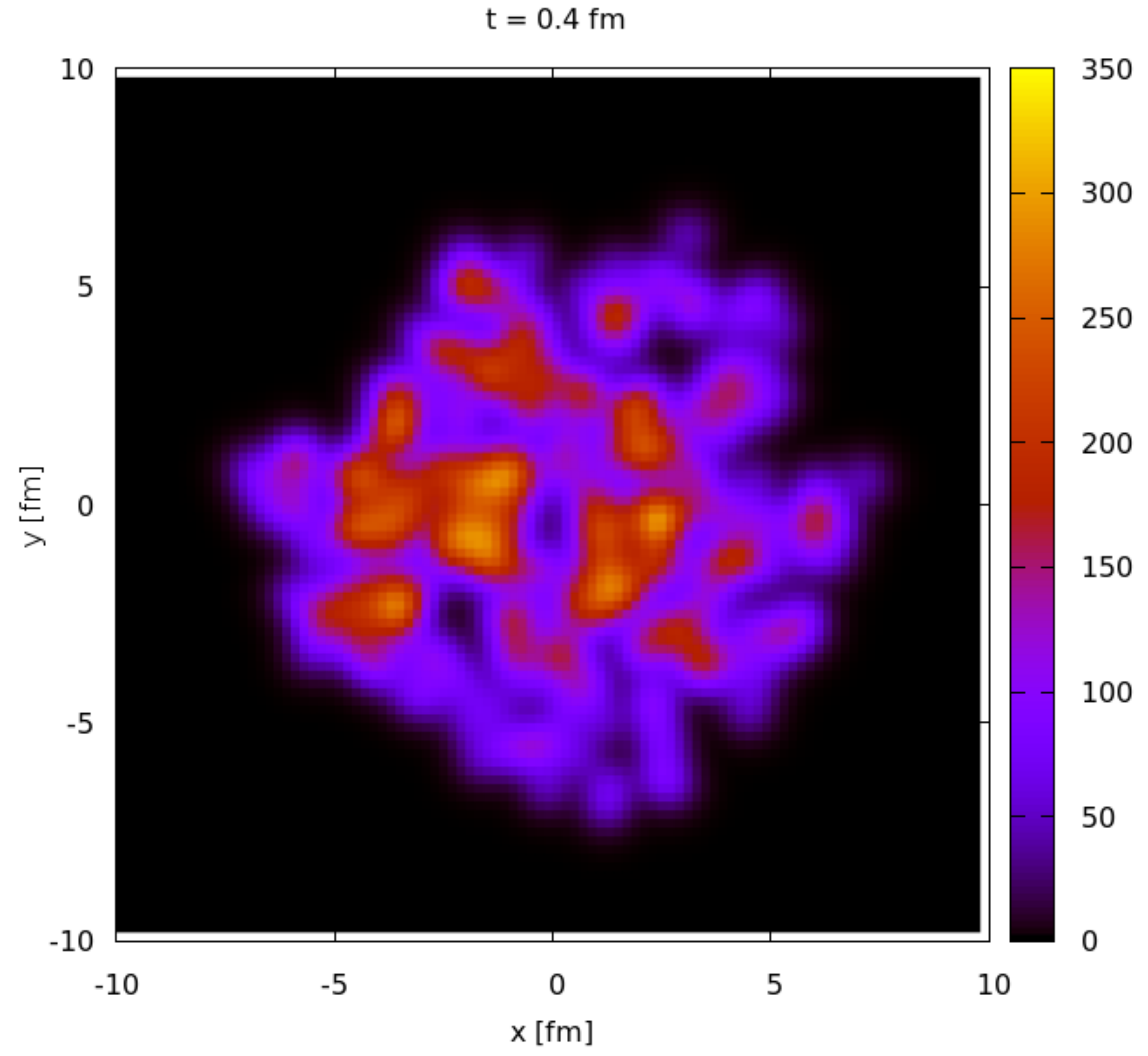

No viscosity
$\eta/s = 0$

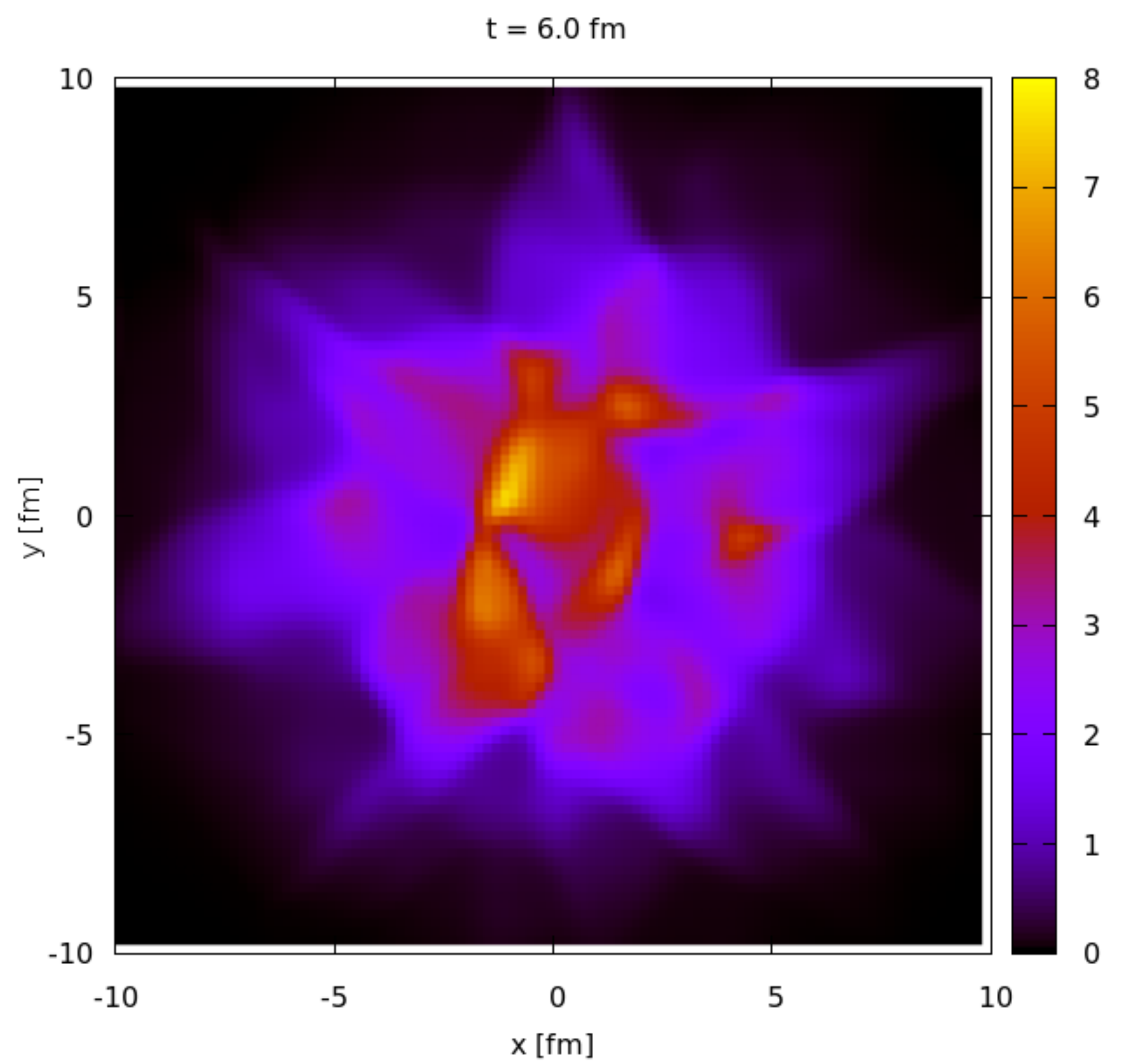

$\eta/s = 0.16$
Low viscosity

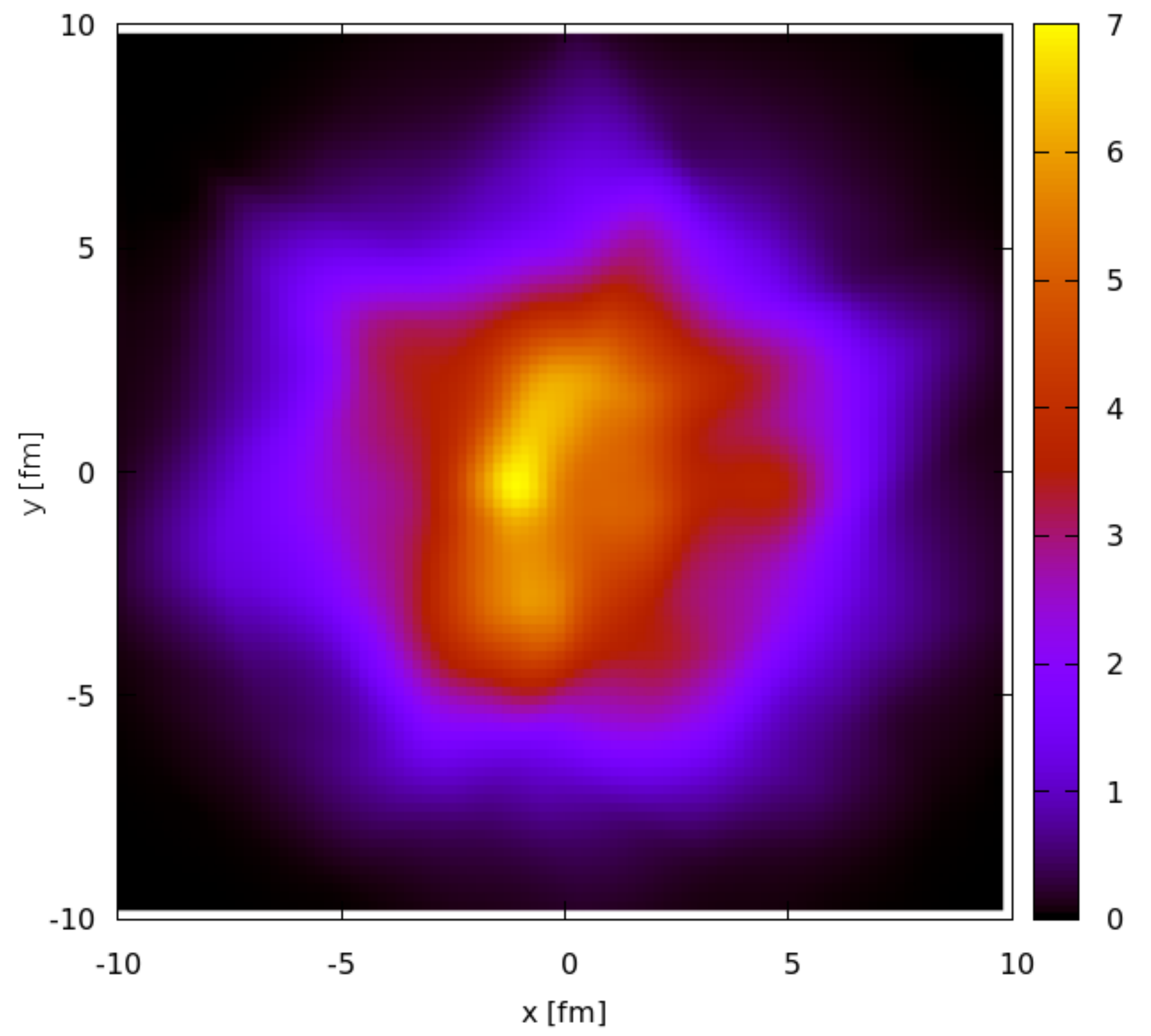

Schenke and Jeon,
Phys.Rev.Lett.106:042301

Constraining initial state and plasma properties simultaneously: Bayesian inference

J. E. Bernhard et al, arXiv: 1605.03954

Experimental input: yields, mean p_T and harmonic flow vs p_T

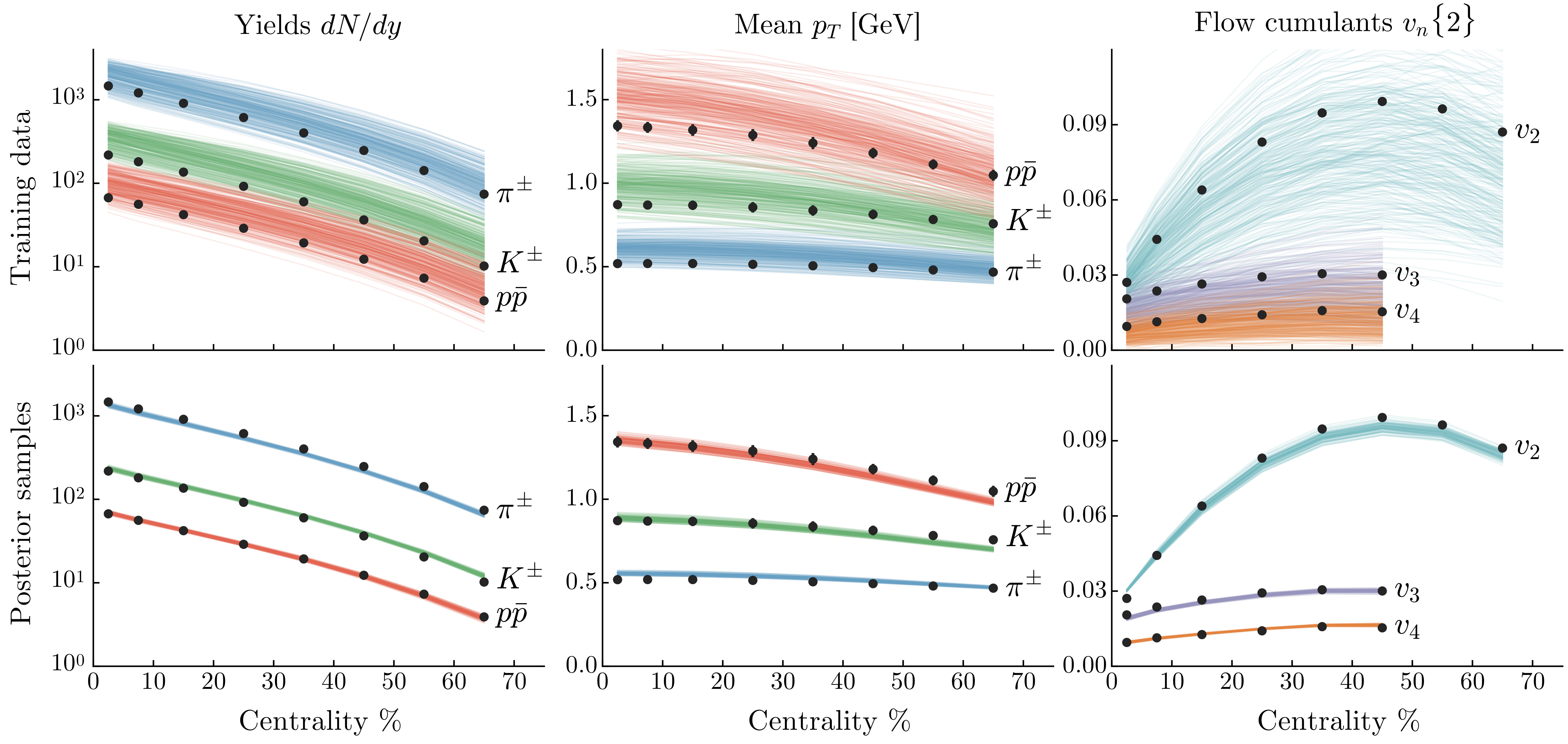

Model: initial anisotropies + medium response

Explores a large parameter space to investigate reliability/robustness of the modeling

Bayesian analysis of flow: results

Initial state geometry

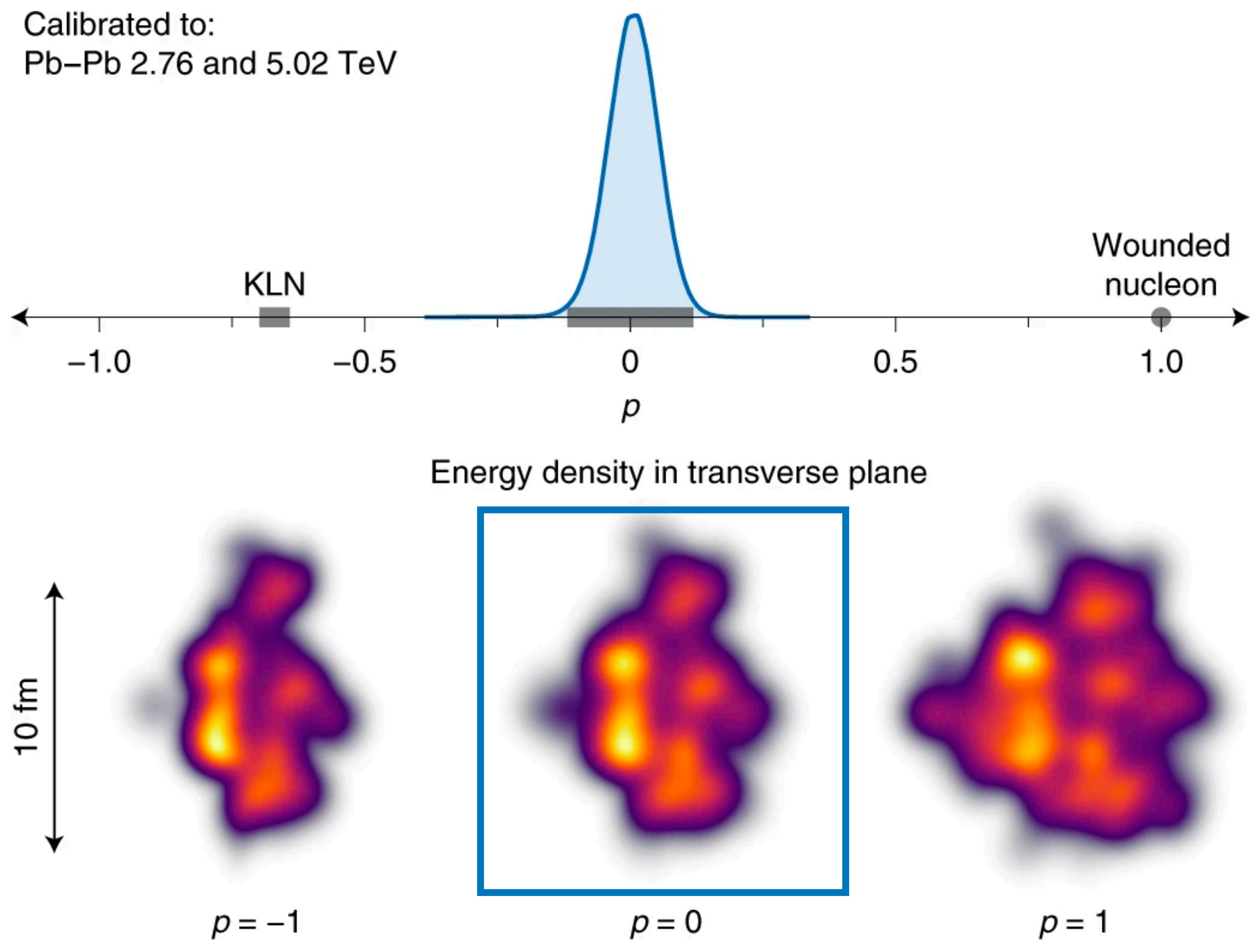

Flow data provide information on initial geometry and viscosity of the QGP at the same time

Viscosity vs *T*

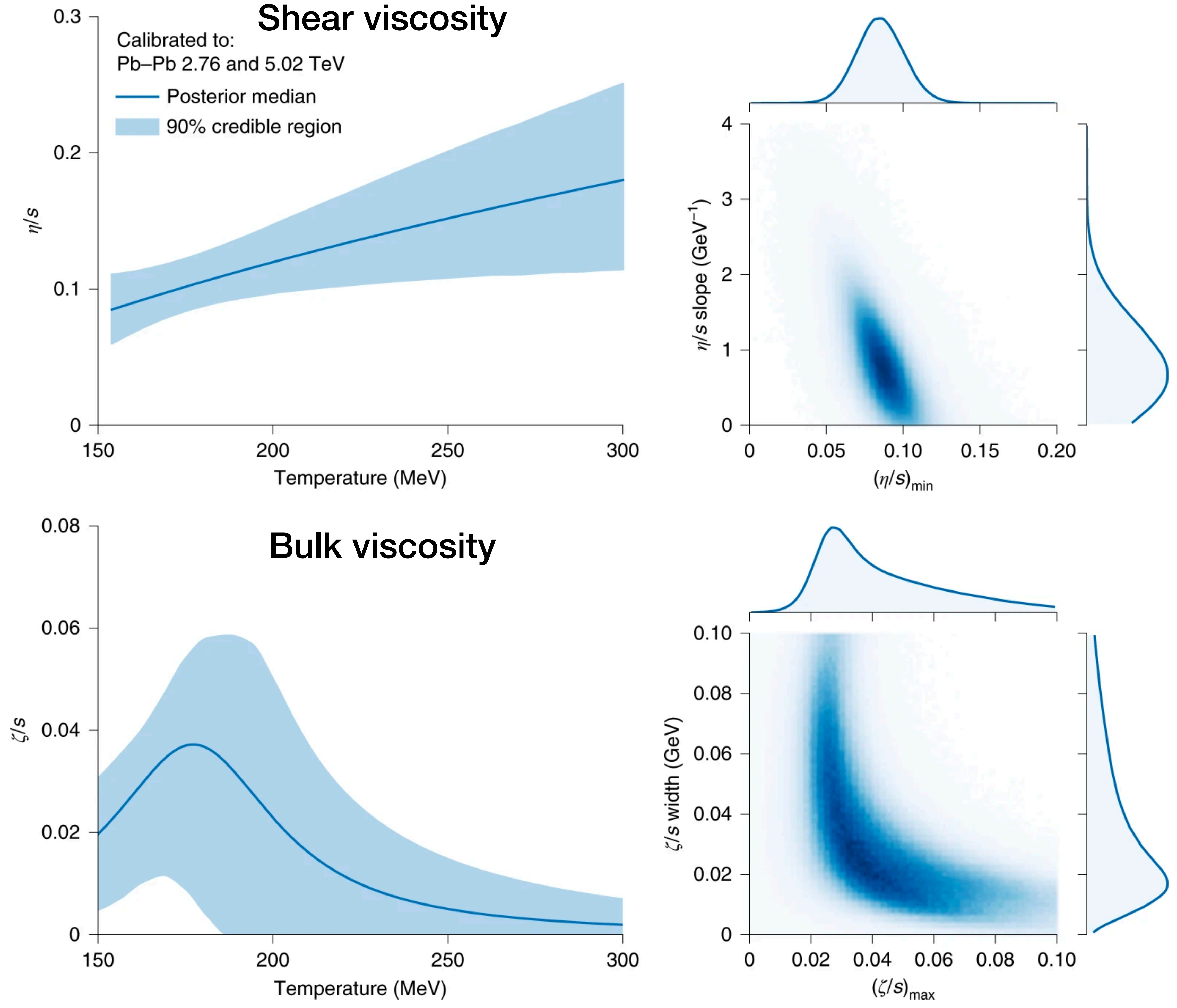

J. E. Bernhard et al, arXiv: 1605.03954

A global fit to anisotropic flow: main result

J. E. Bernhard et al, Nature Physics 15, 1113–1117, arXiv: 1605.03954

QGP has a very small ‘specific viscosity’
small mean free path

Viscosity close to fundamental lower bound

Comparison to well-known liquids

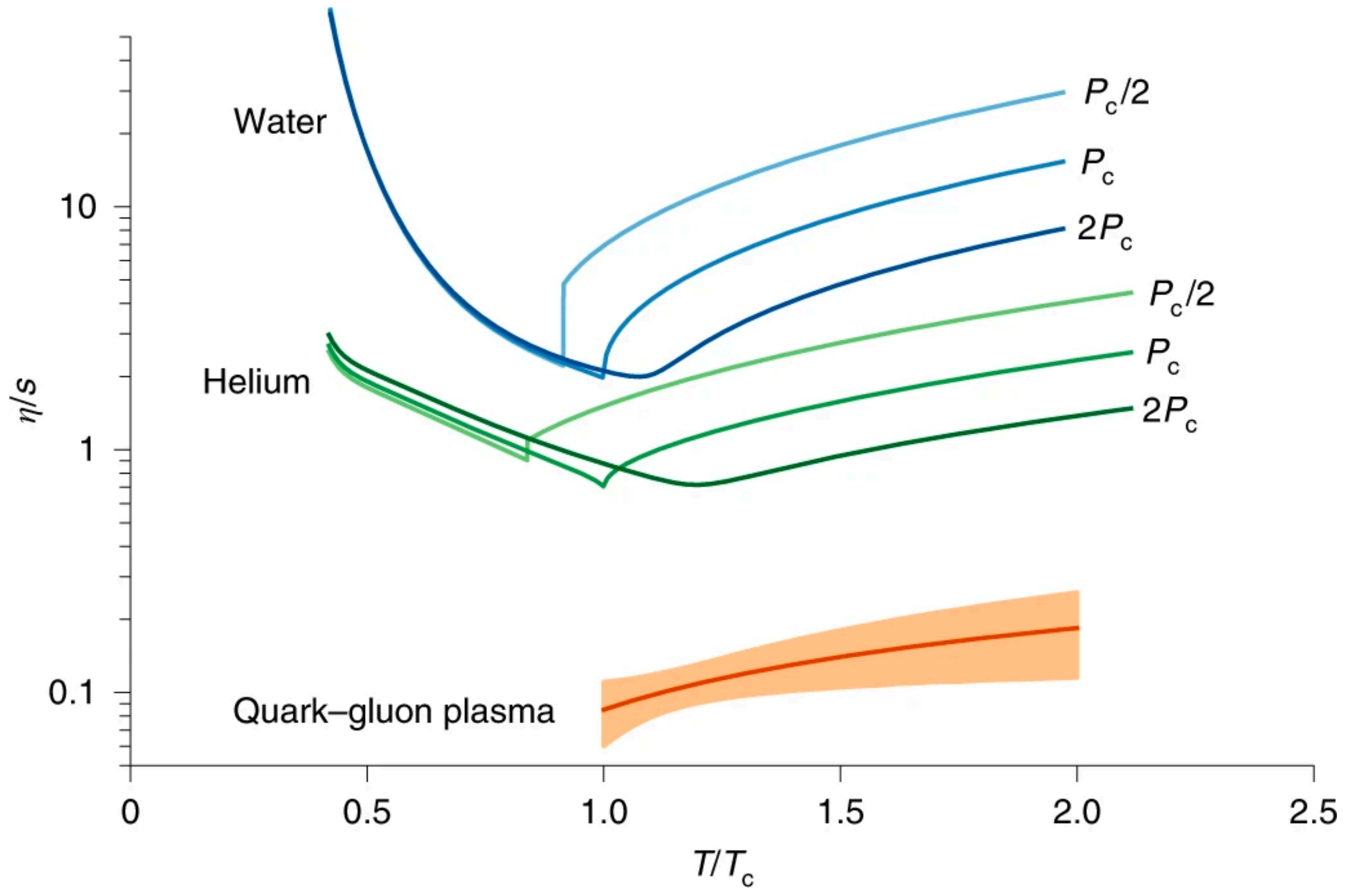

$$\eta = \frac{1}{3} n \bar{p} \lambda$$

Initial state geometry: event plane correlations

ALICE, arXiv:2302.01234

Elliptic deformation

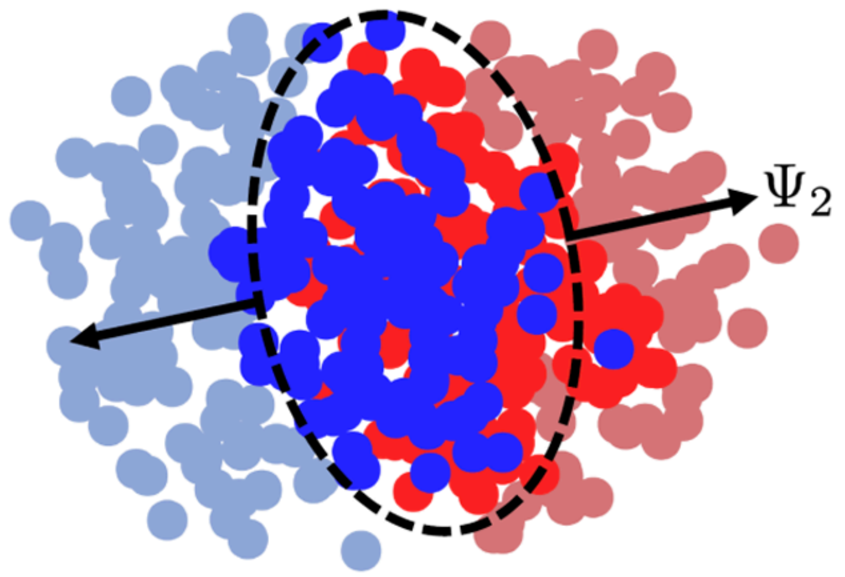

Triangular deformation

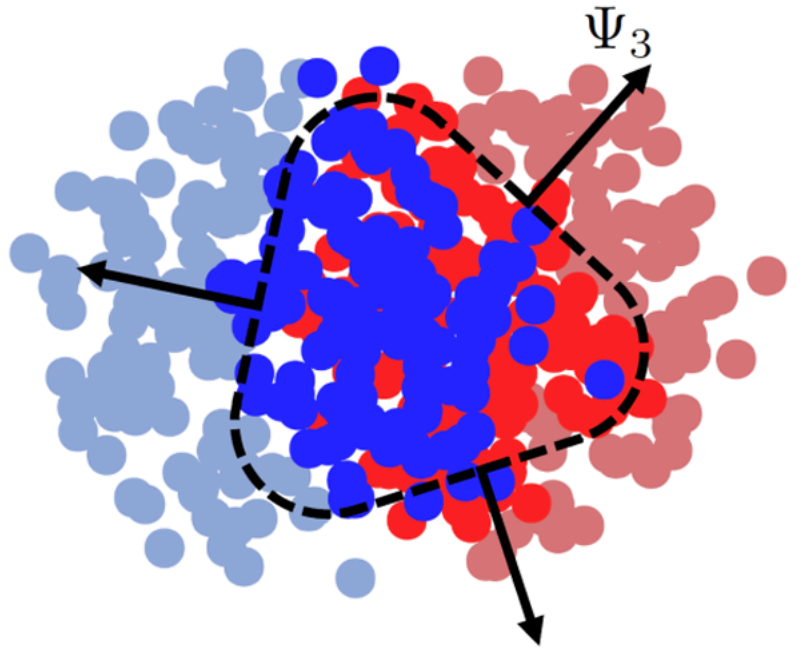

Comparison to previous results

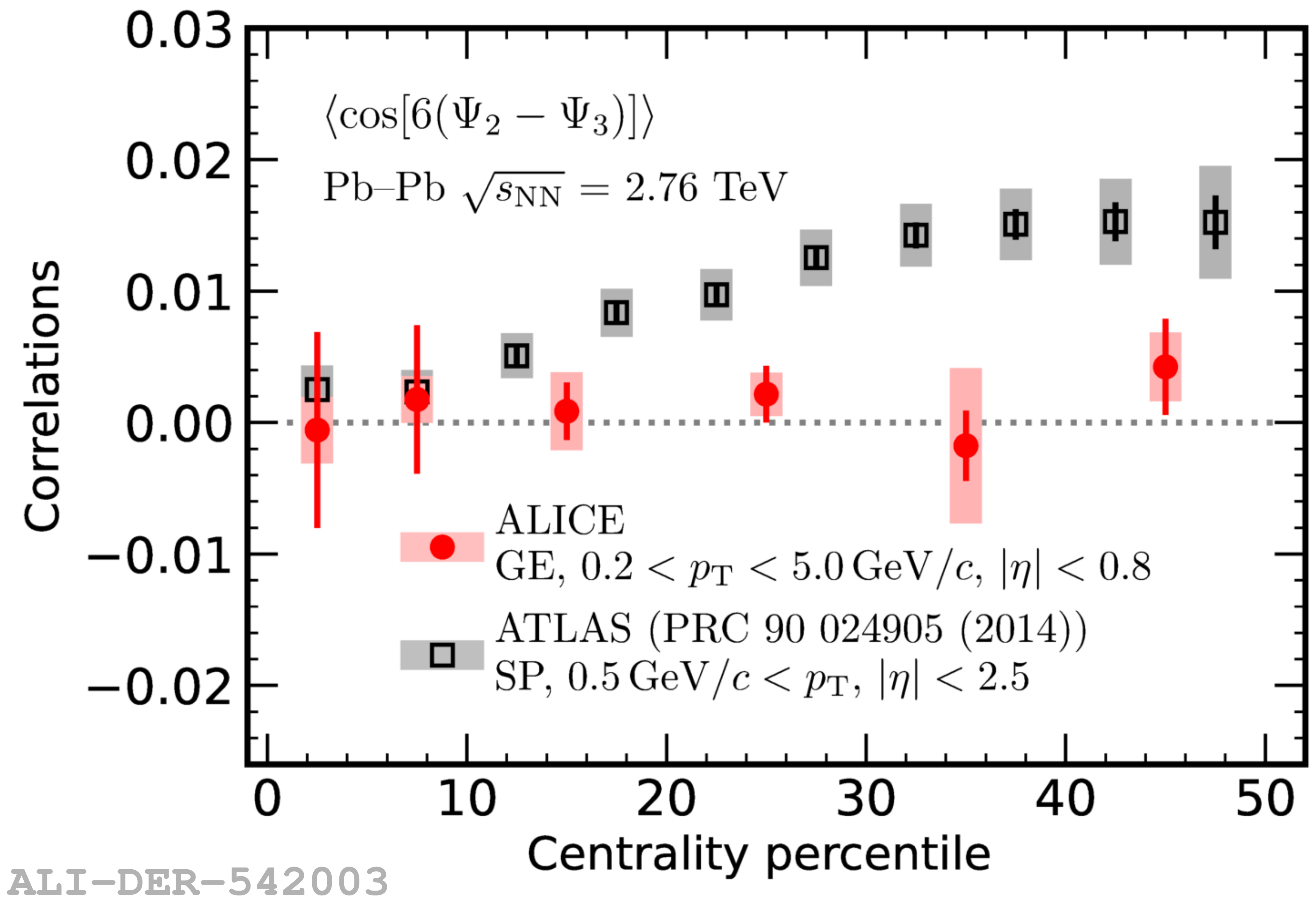

Comparison to theory

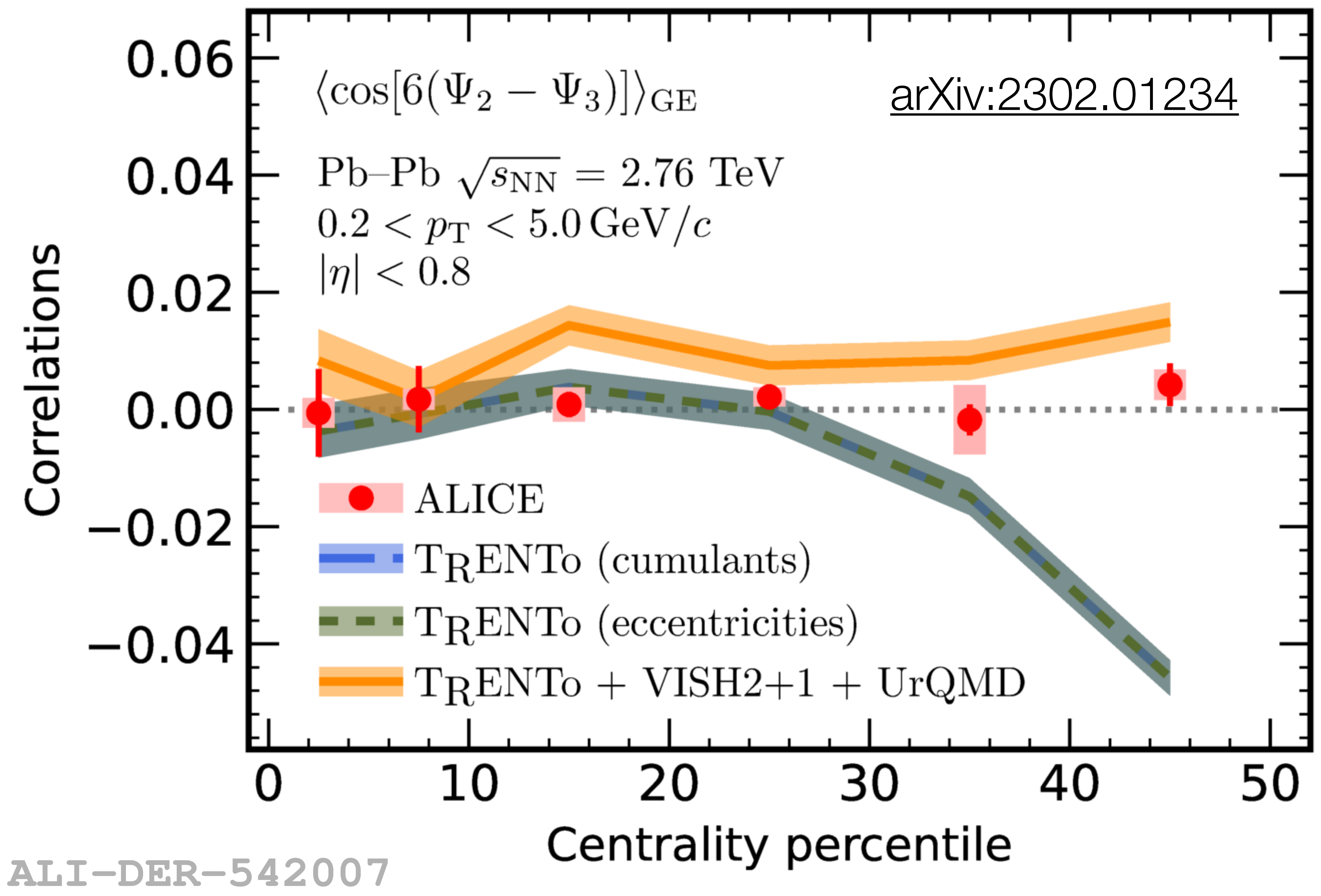

Correlations between symmetry plane orientations

- New method: reduced sensitivity to numerical fluctuations
- No significant correlation between Ψ_2 and Ψ_3

- New results more in line with expectations

Chemical freeze-out

Chemical freeze-out determines hadron yields
— end of inelastic collisions

- Hadron yields follow thermal distribution with $T = T_c$ = 155 MeV

$$N = (2J + 1)\, e^{-m/T}$$

- Chemical freeze-out at phase transition temperature:
  no inelastic collisions after phase transition

Hadron yields compared to thermal model calculation

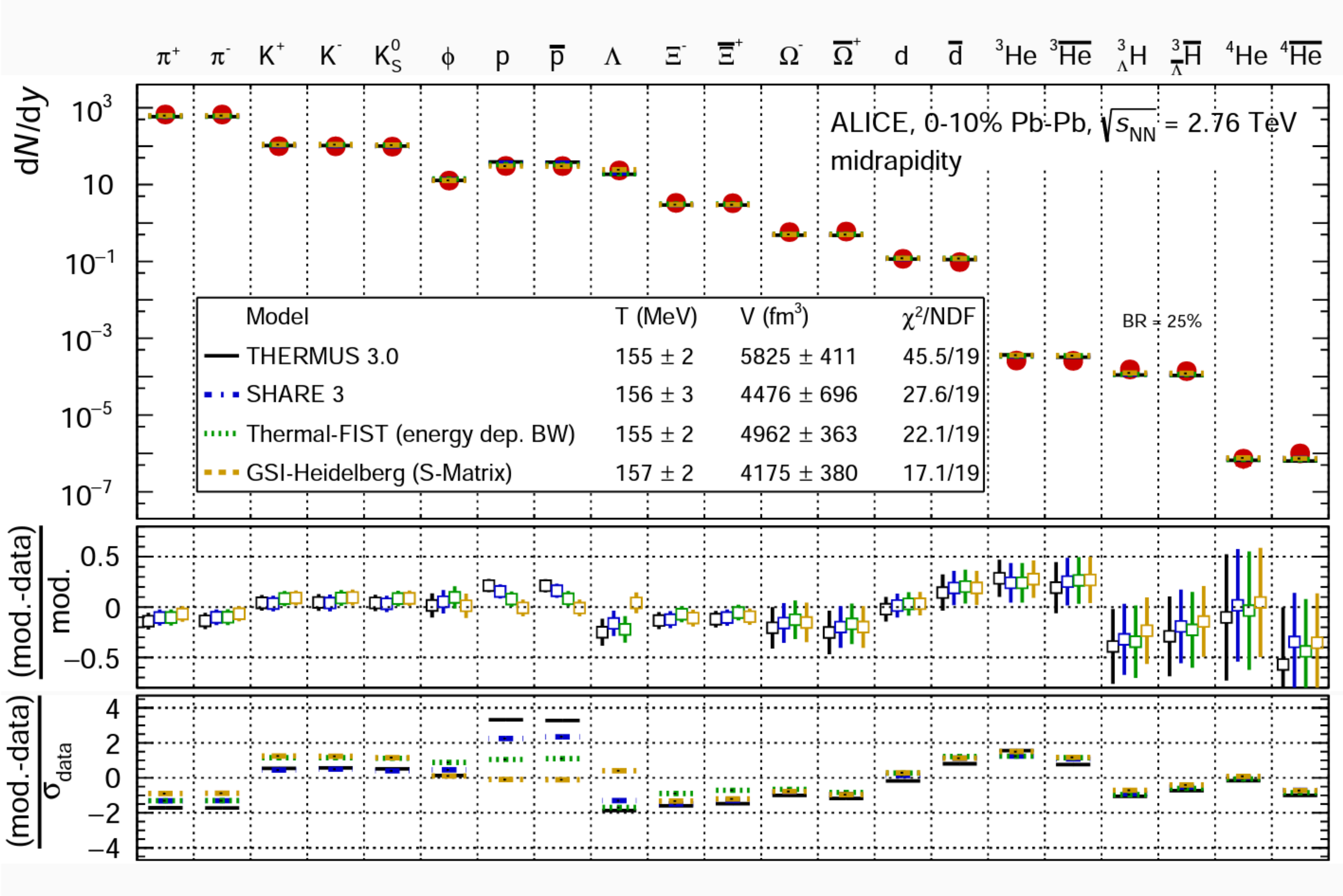

A journey through QCD, ALICE, arXiv:2211.04384

Elastic collisions in the hadronic phase: resonance yields

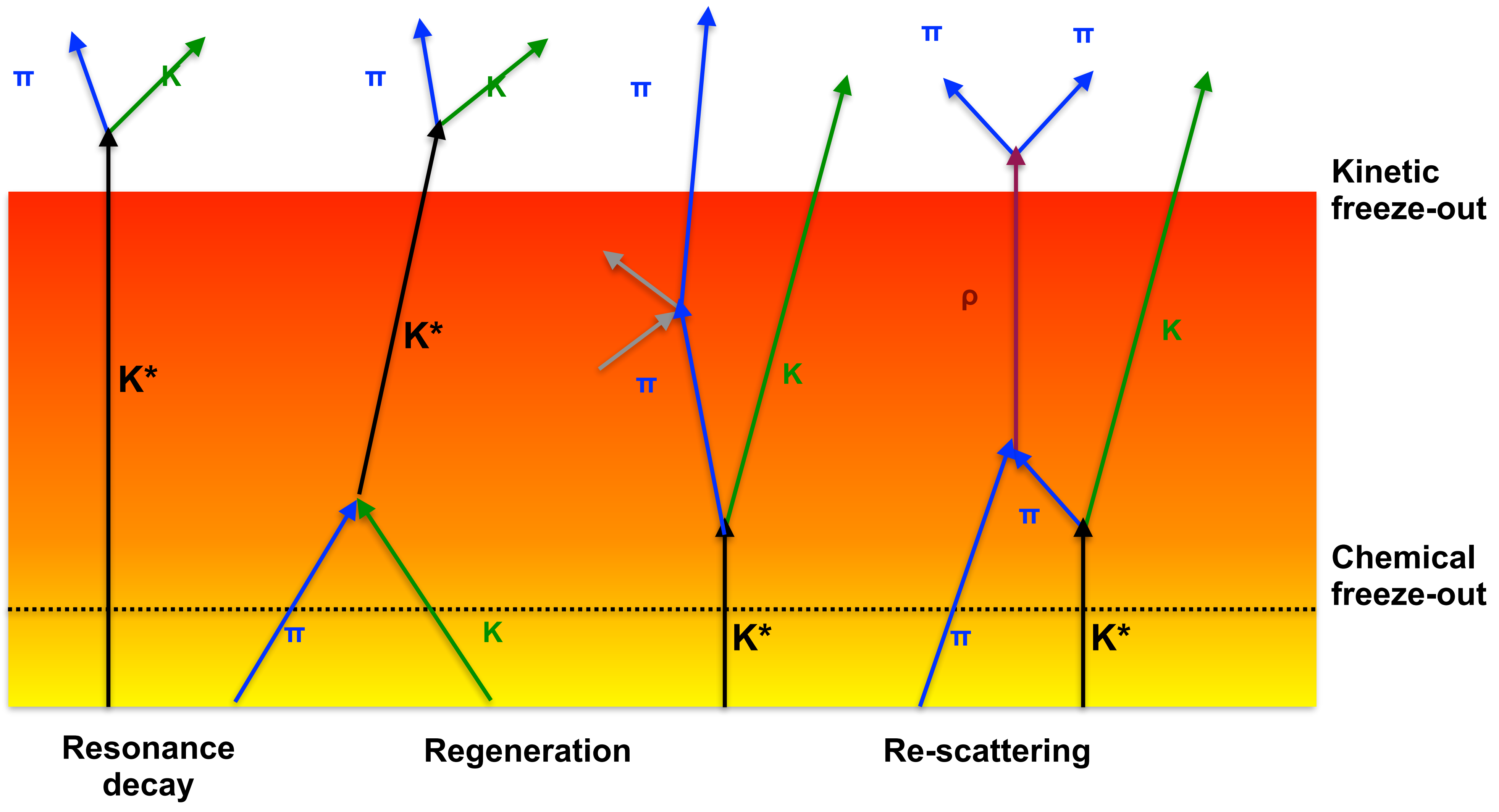

Re-scattering of decay daughters: signal loss

Regeneration: resonances formed in hadron scattering

Resonance yields vs system size

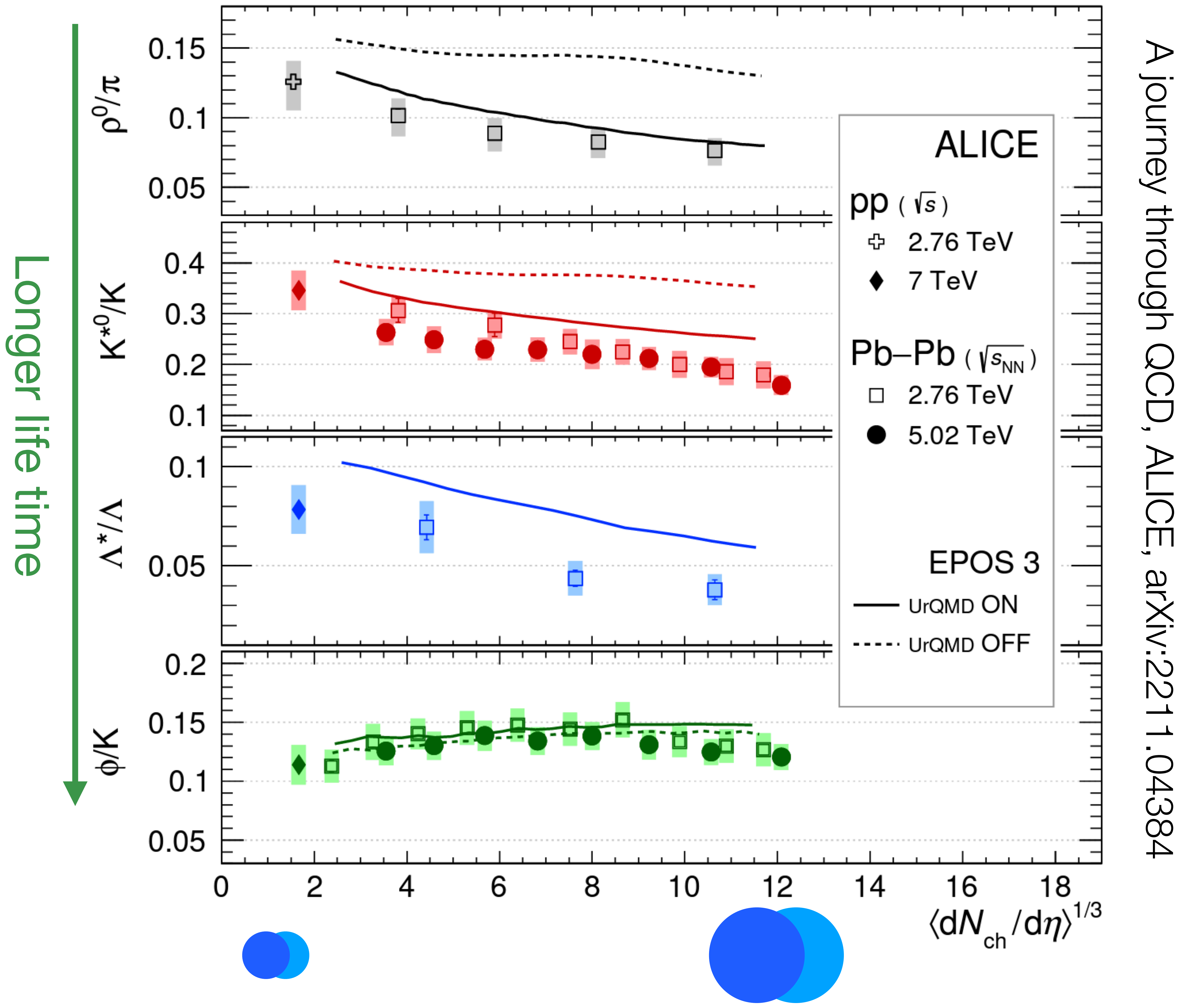

ρ, K*, Λ* reduced yield: final state scattering of decay particles

ϕ: longer life time, yield not affected

Light nuclei: a sensitive probe of the hadronic phase

Hadronic collisions at LHC produce light nuclei
d, t, ^{3}He, ^{4}He etc

- Small binding energy O(MeV) << *T* of hadronic phase
- Expect large break-up probability

Formation by coalescence of protons and neutrons?

- Expect yield $\propto \rho_p \, \rho_n$
- Model calculations use Wigner function formalism

JUNE 1, 1932 PHYSICAL REVIEW VOLUME 40

On the Quantum Correction For Thermodynamic Equilibrium

By E. WIGNER
Department of Physics, Princeton University
(Received March 14, 1932)

The probability of a configuration is given in classical theory by the Boltzmann formula exp $[-V/hT]$ where V is the potential energy of this configuration. For high temperatures this of course also holds in quantum theory. For lower temperatures, however, a correction term has to be introduced, which can be developed into a power series of h. The formula is developed for this correction by means of a probability function and the result discussed.

deuteron coalescence parameter in pp

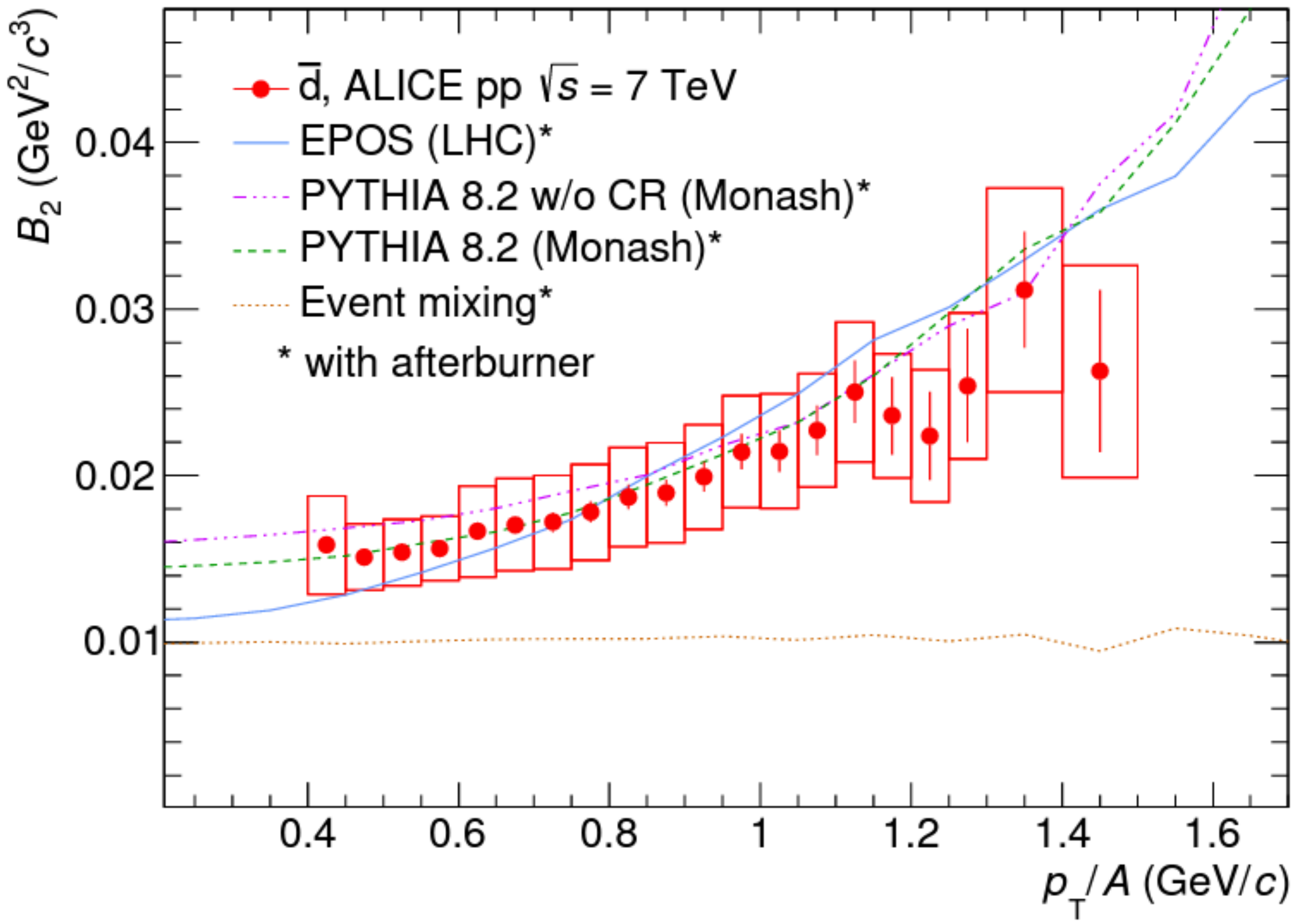

ALICE, arXiv:1709.08522

$$B_2 = E_A \frac{d^3N}{dp_A^3}(p_A) \Big/ E_p \frac{d^3N}{dp_p^3}(p_p)\, E_n \frac{d^3N}{dp_n^3}(p_n)$$

$$p_n = p_p \quad p_A = 2\,p_p$$

ALICE

The Wigner function (quantum density matrix formalism)

On the Quantum Correction For Thermodynamic Equilibrium

By E. Wigner
Department of Physics, Princeton University
(Received March 14, 1932)

It does not seem to be easy to make explicit calculations with the form (4) of the mean value. One may resort therefore to the following method.

If a wave function $\psi(x_1 \cdots x_n)$ is given one may build the following expression[2]

$$P(x_1, \cdots, x_n; p_1, \cdots, p_n) = \left(\frac{1}{h\pi}\right)^n \int_{-\infty}^{\infty} \cdots \int dy_1 \cdots dy_n \psi(x_1 + y_1 \cdots x_n + y_n)^* \psi(x_1 - y_1 \cdots x_n - y_n) e^{2i(p_1y_1 + \cdots + p_ny_n)/h} \quad (5)$$

and call it the probability-function of the simultaneous values of $x_1 \cdots x_n$ for the coordinates and $p_1 \cdots p_n$ for the momenta. In (5), as throughout

Of course $P(x_1, \cdots, x_n; p_1, \cdots, p_n)$ cannot be really interpreted as the simultaneous probability for coordinates and momenta, as is clear from the fact, that it may take negative values. But of course this must not hinder the use of it in calculations as an auxiliary function which obeys many relations we would expect from such a probability. It should be noted, furthermore,

Coalescence models for nuclear collisions/QGP combine **proximity conditions in coordinate and momentum space**

- Explored for nuclei by e.g. R Scheibl, U Heinz
- Extended to parton coalescence by J Zimányi, P Lévai, T Csörgö, T S Biró, V Greco, C M Ko, R Fries, R Hwa, and others

Production of light nuclei: thermal model vs coalescence

deuteron/proton ratio

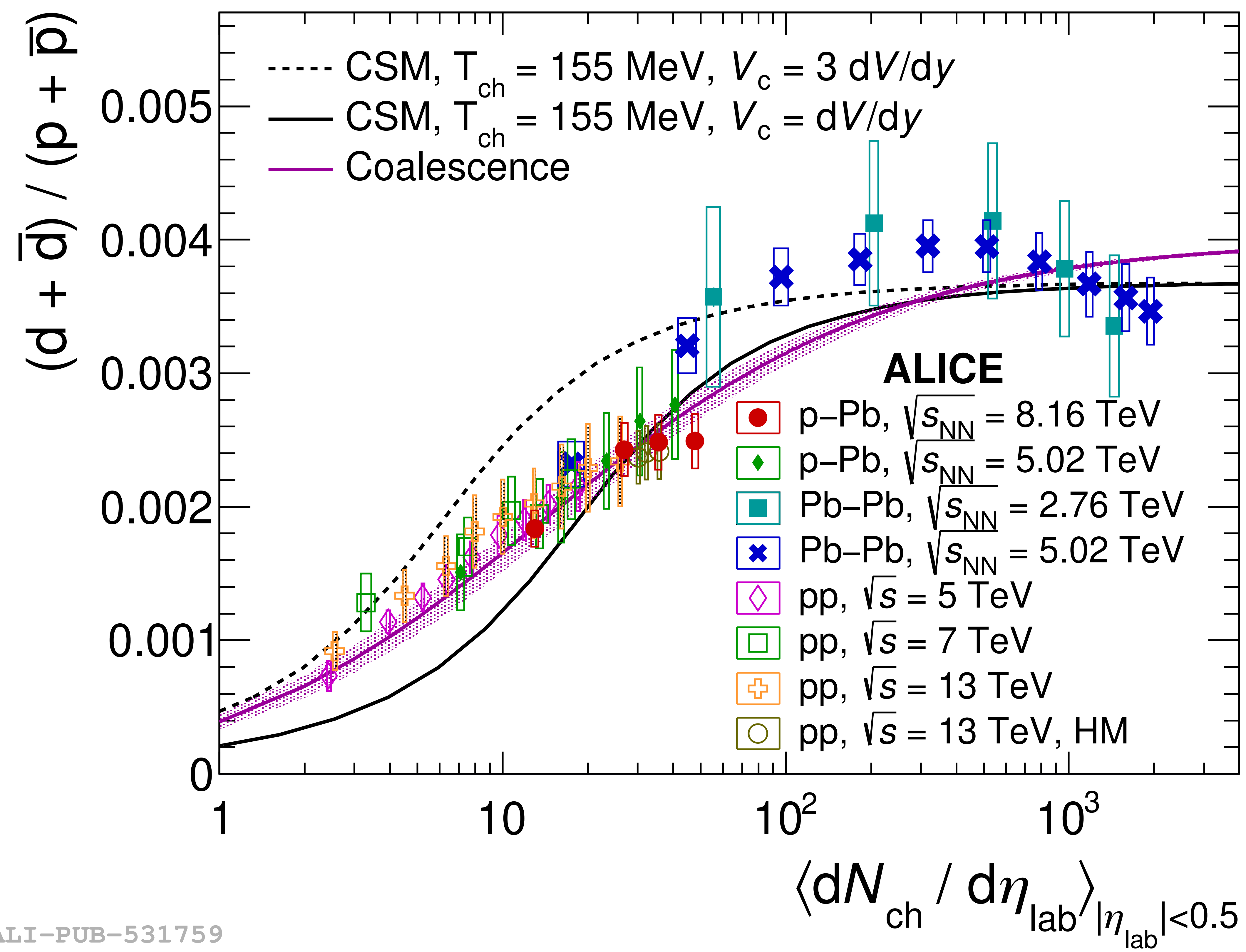

³He/proton ratio

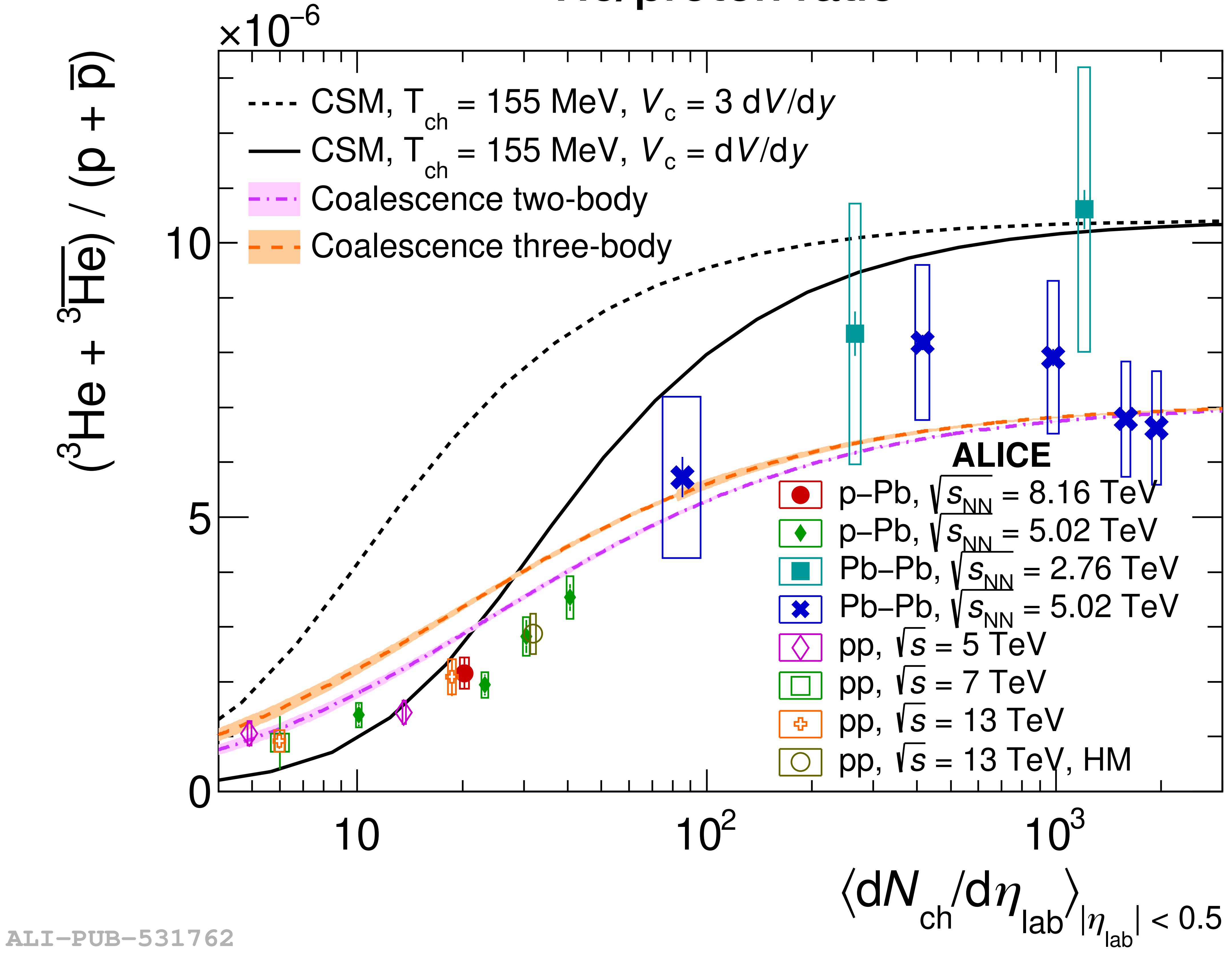

arXiv:2212.04777

Thermal and coalescence calculations give similar result for compact states; clear differences for larger states

J/ψ: melting and regeneration at the parton level

$$R_{AA} = \frac{dN/dp_T|_{AA}}{\langle N_{coll}\rangle \, dN/dp_T|_{pp}}$$

Nuclear modification factor

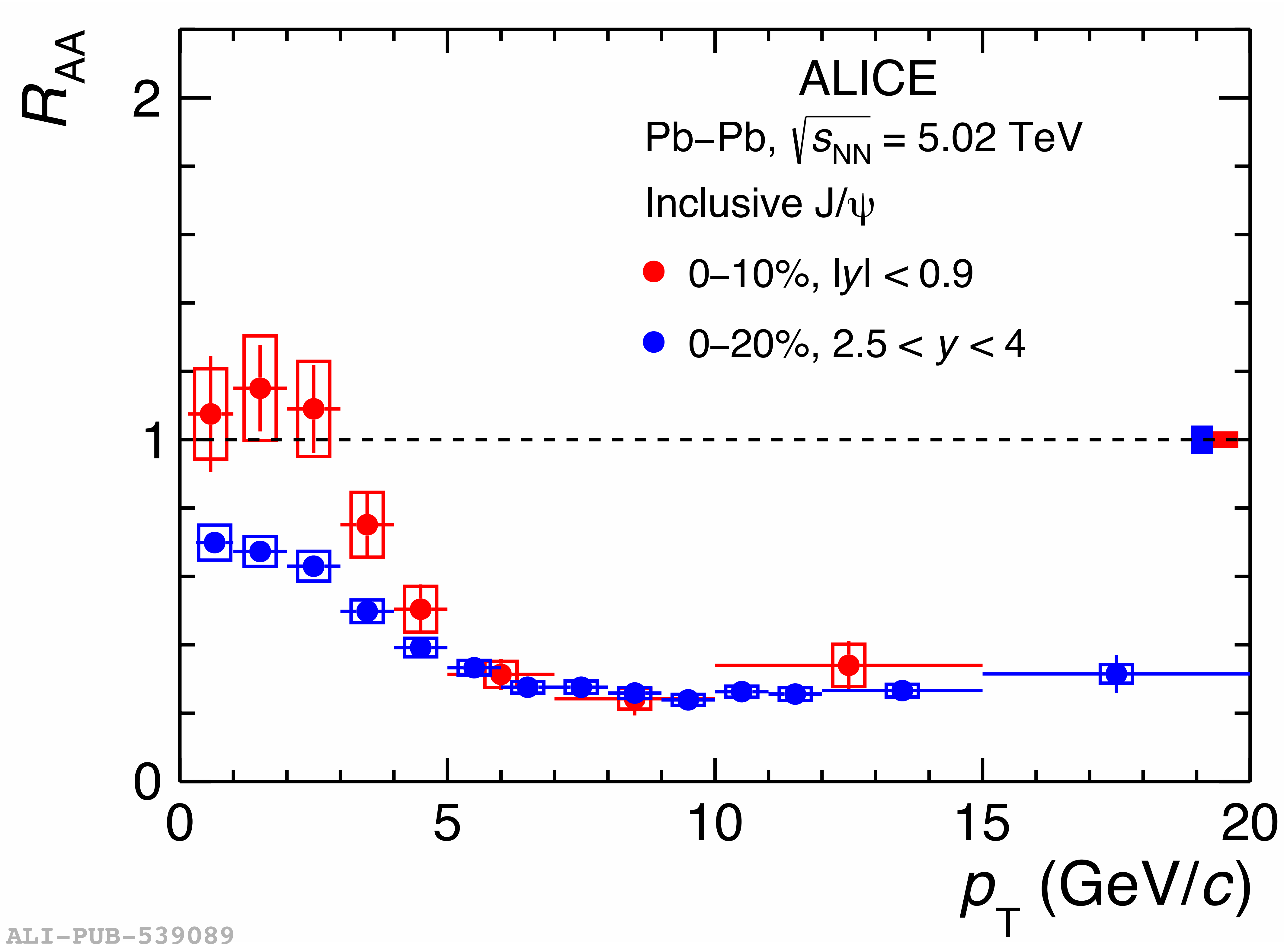

J/ψ: bound state
charm and anti-charm quark

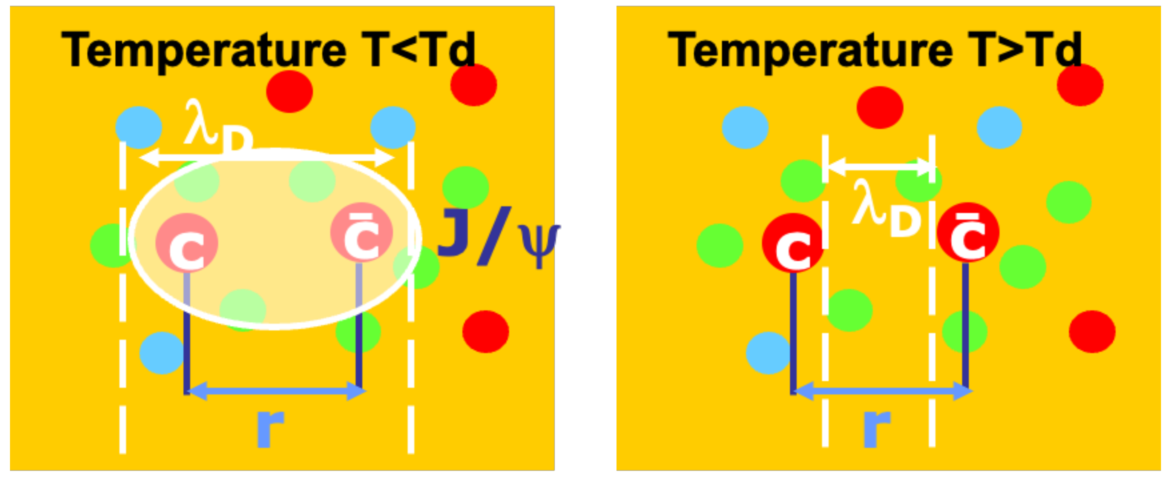

Binding force screened when
$r > \lambda_d$

J/ψ: melting and regeneration at the parton level

$$R_{AA} = \frac{dN/dp_T|_{AA}}{\langle N_{coll}\rangle \, dN/dp_T|_{pp}}$$

Nuclear modification factor

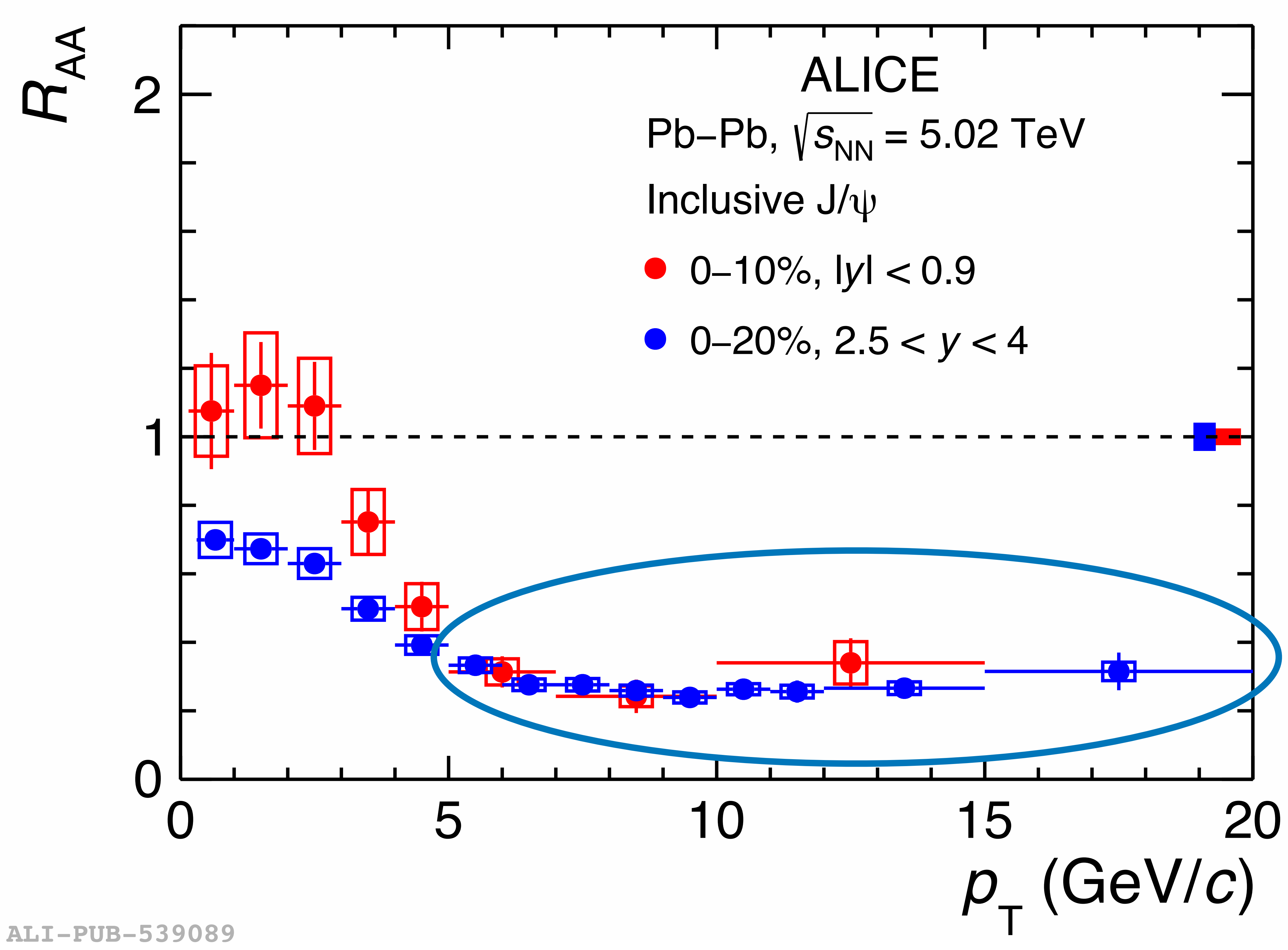

J/ψ: bound state
charm and anti-charm quark

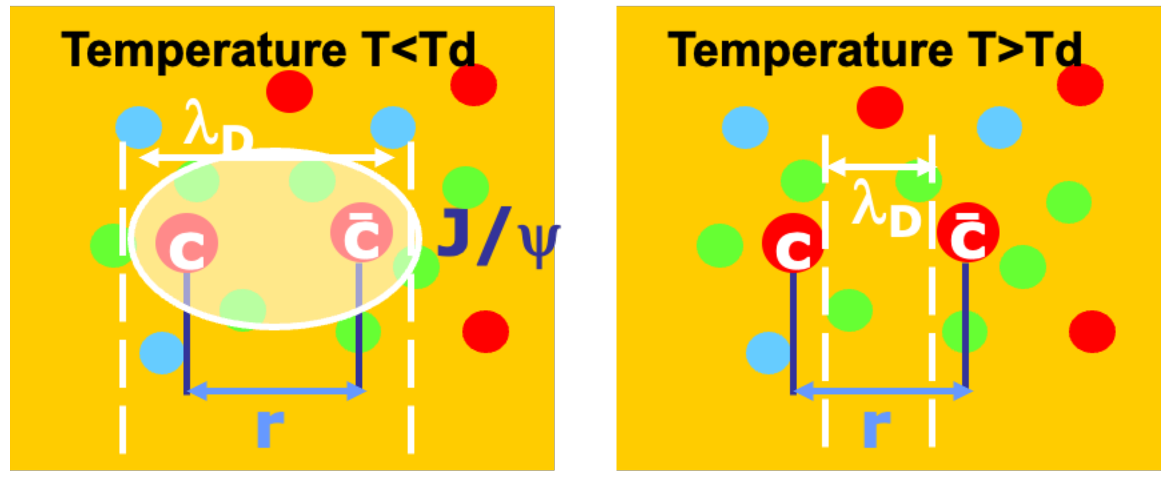

Binding force screened when
$r > \lambda_d$

High p_T - low density:
quarkonia dissociate in the QGP

J/ψ: melting and regeneration at the parton level

$$R_{AA} = \frac{dN/dp_T|_{AA}}{\langle N_{coll}\rangle \, dN/dp_T|_{pp}}$$

Nuclear modification factor

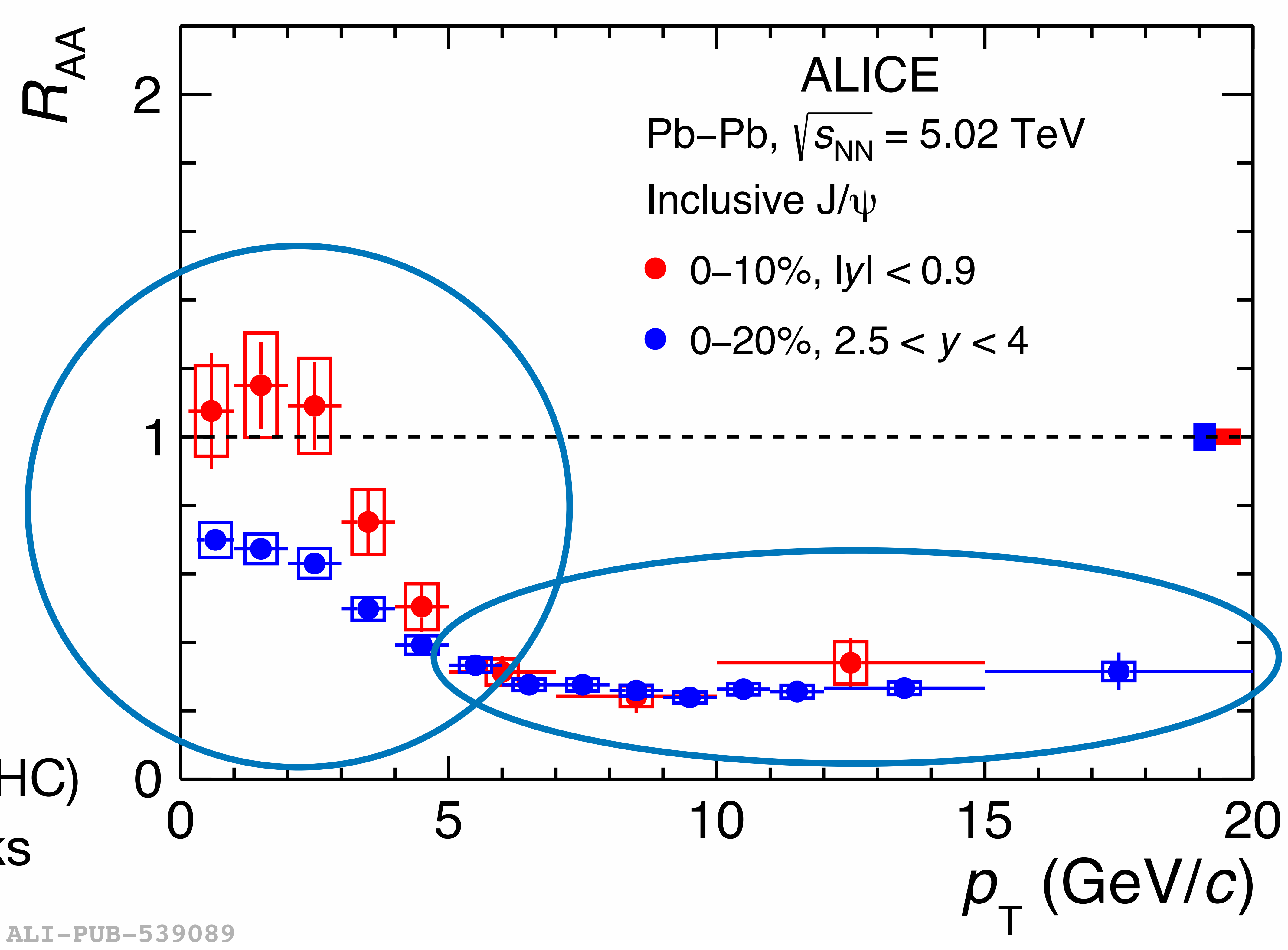

Low p_T:
large density of charm quarks (at LHC)
regeneration: coalescence of quarks

J/ψ: bound state
charm and anti-charm quark

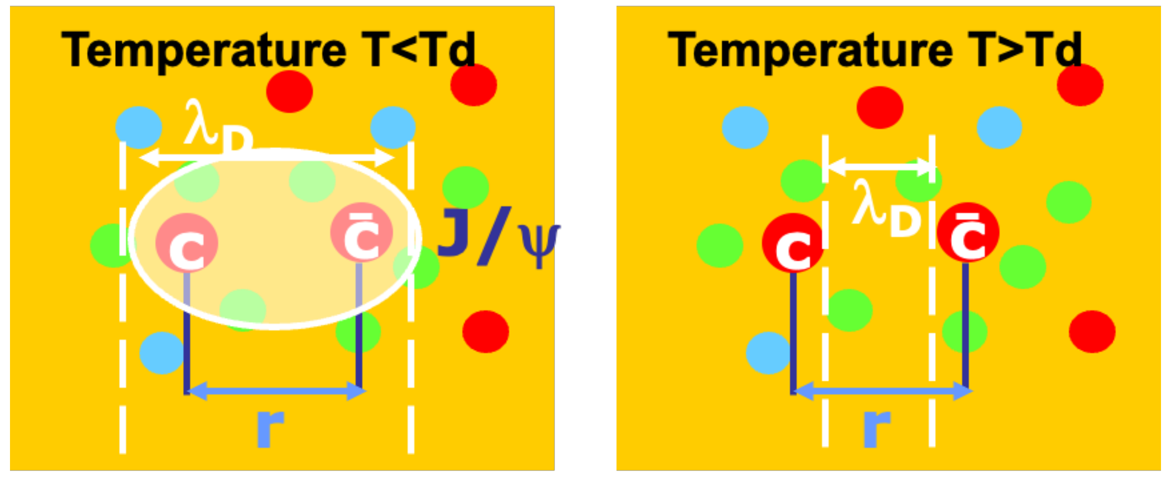

Binding force screened when
$r > \lambda_d$

High p_T - low density:
quarkonia dissociate in the QGP

J/ψ production in Pb-Pb collisions: melting and recombination

arXiv:2303.13361

Mid-rapidity

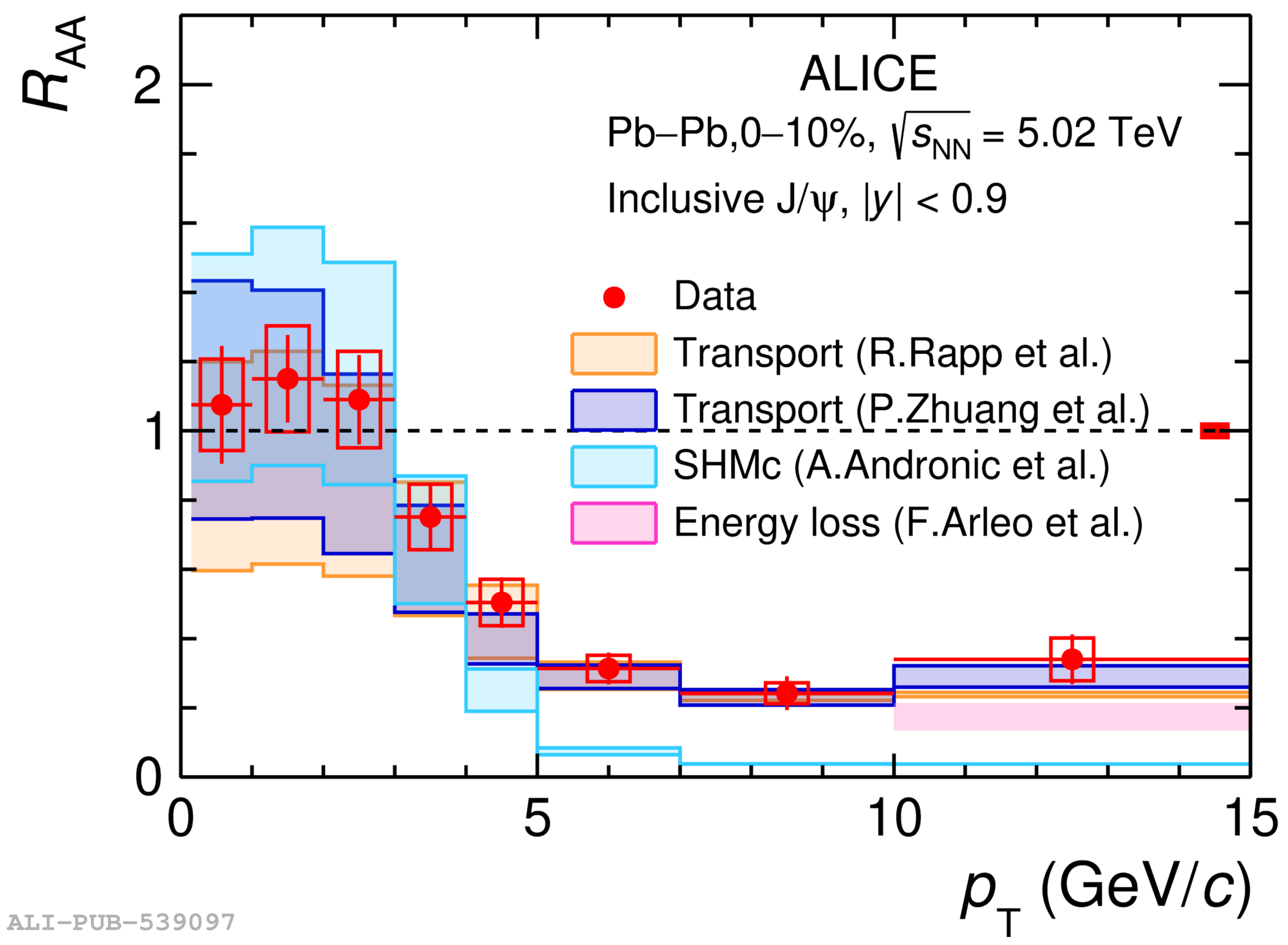

Forward rapidity

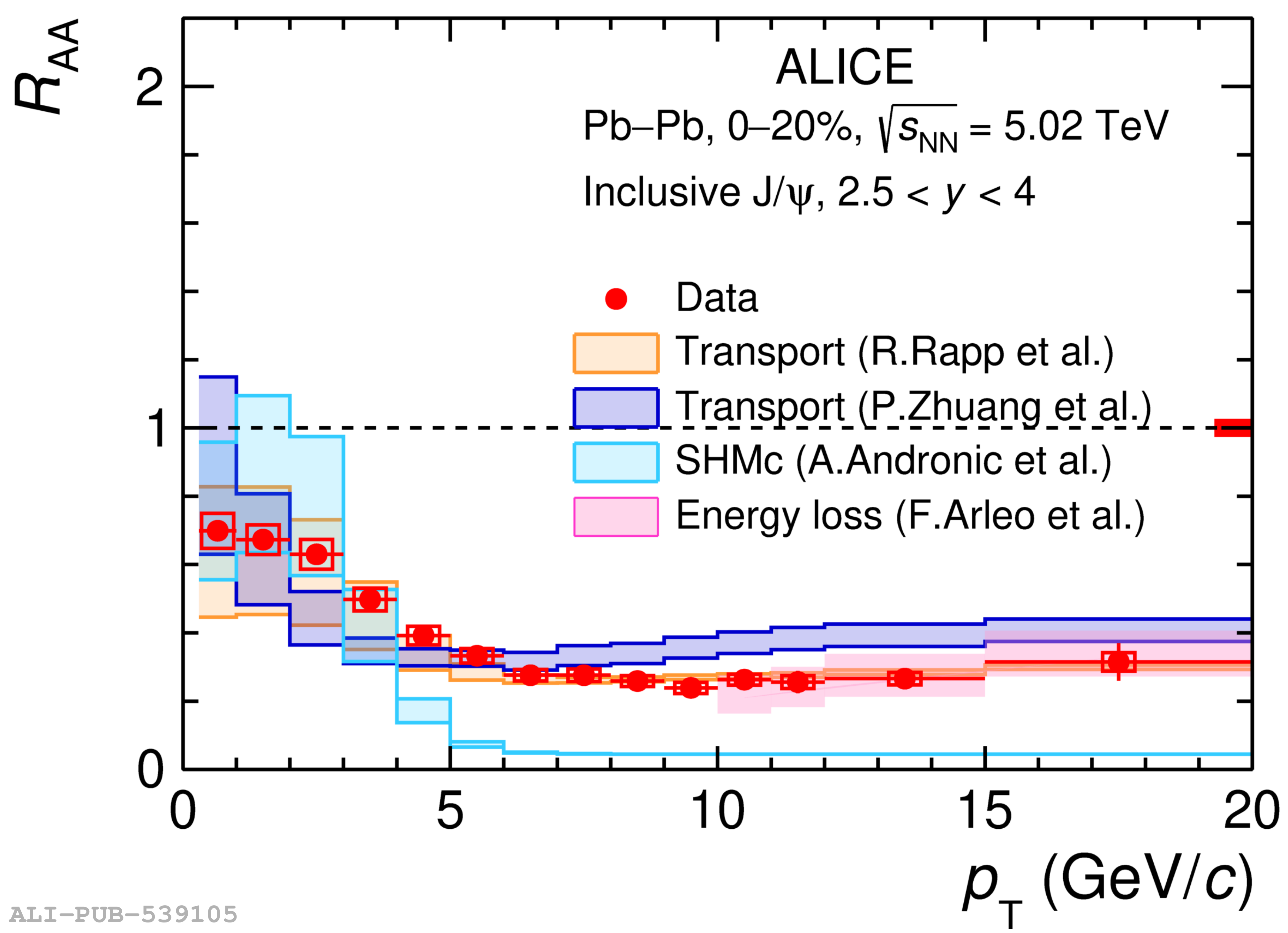

$$R_{AA} = \frac{dN/dp_T|_{AA}}{\langle N_{coll}\rangle \, dN/dp_T|_{pp}}$$

- Balance between melting and recombination at low p_T
- Rapidity dependence exposes density dependence

Back to the earliest stages: direct photon production

Large background: decay photons from π^0, η, …

⇒ Challenging measurement

Main sources:

- High p_T: hard scattering; quark-gluon Compton process
- Low p_T: thermal radiation

Excess at low p_T: thermal photons

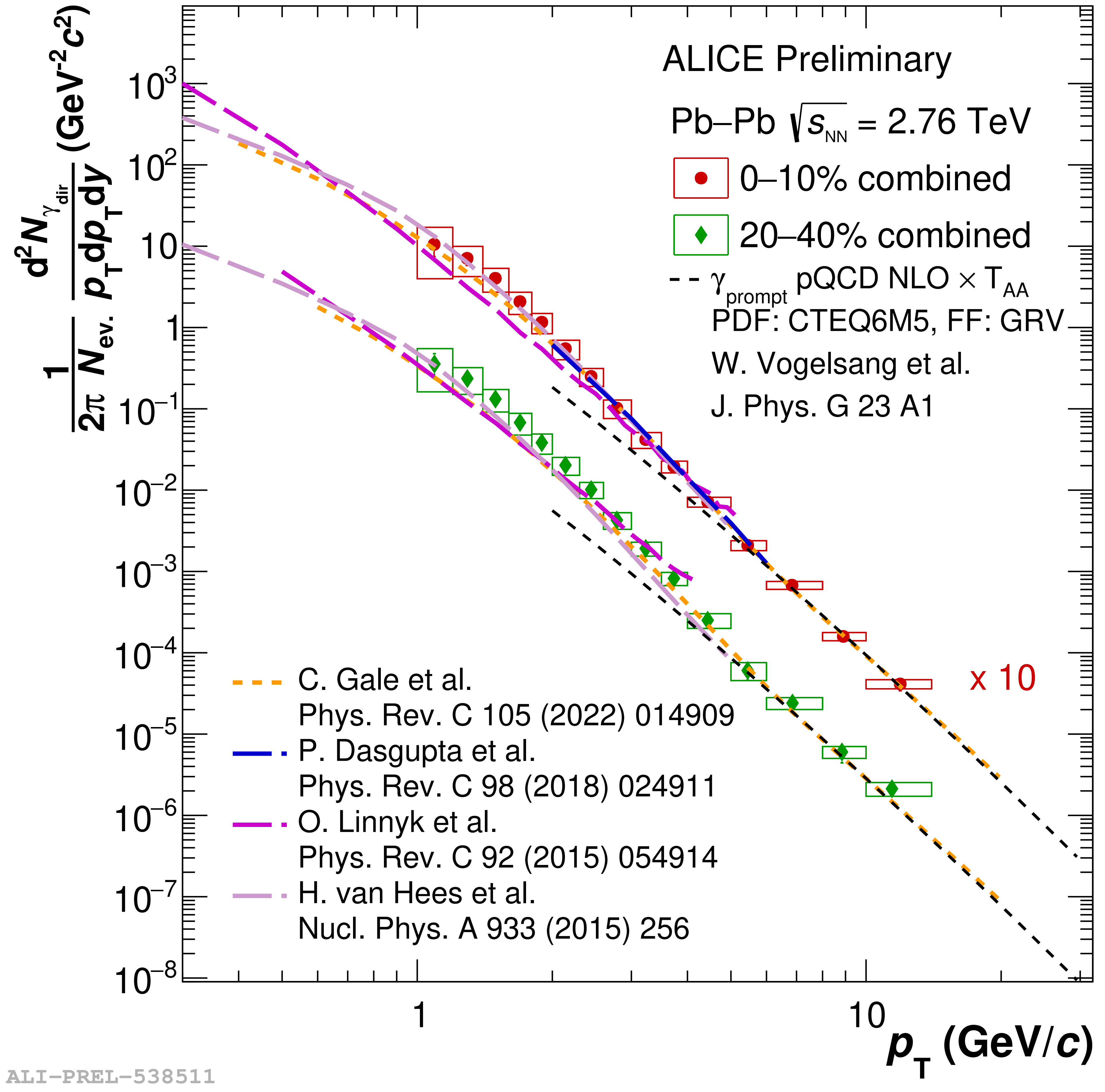

ALICE, PLB 754, 235

Direct photon excess: thermal production

Direct photon excess spectrum

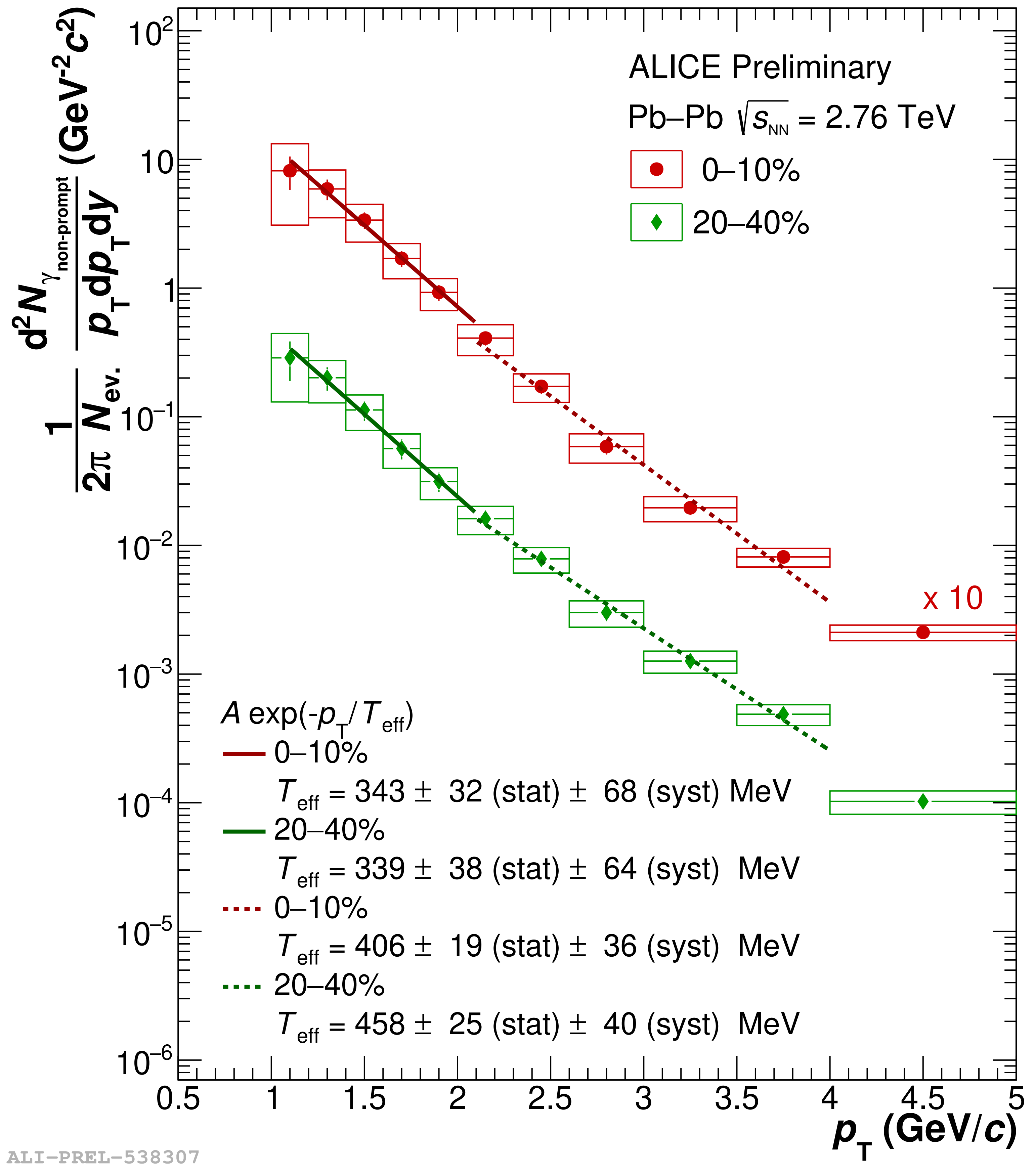

Thermal emission visible for mid-central and central events

Spectral slope: apparent temperature

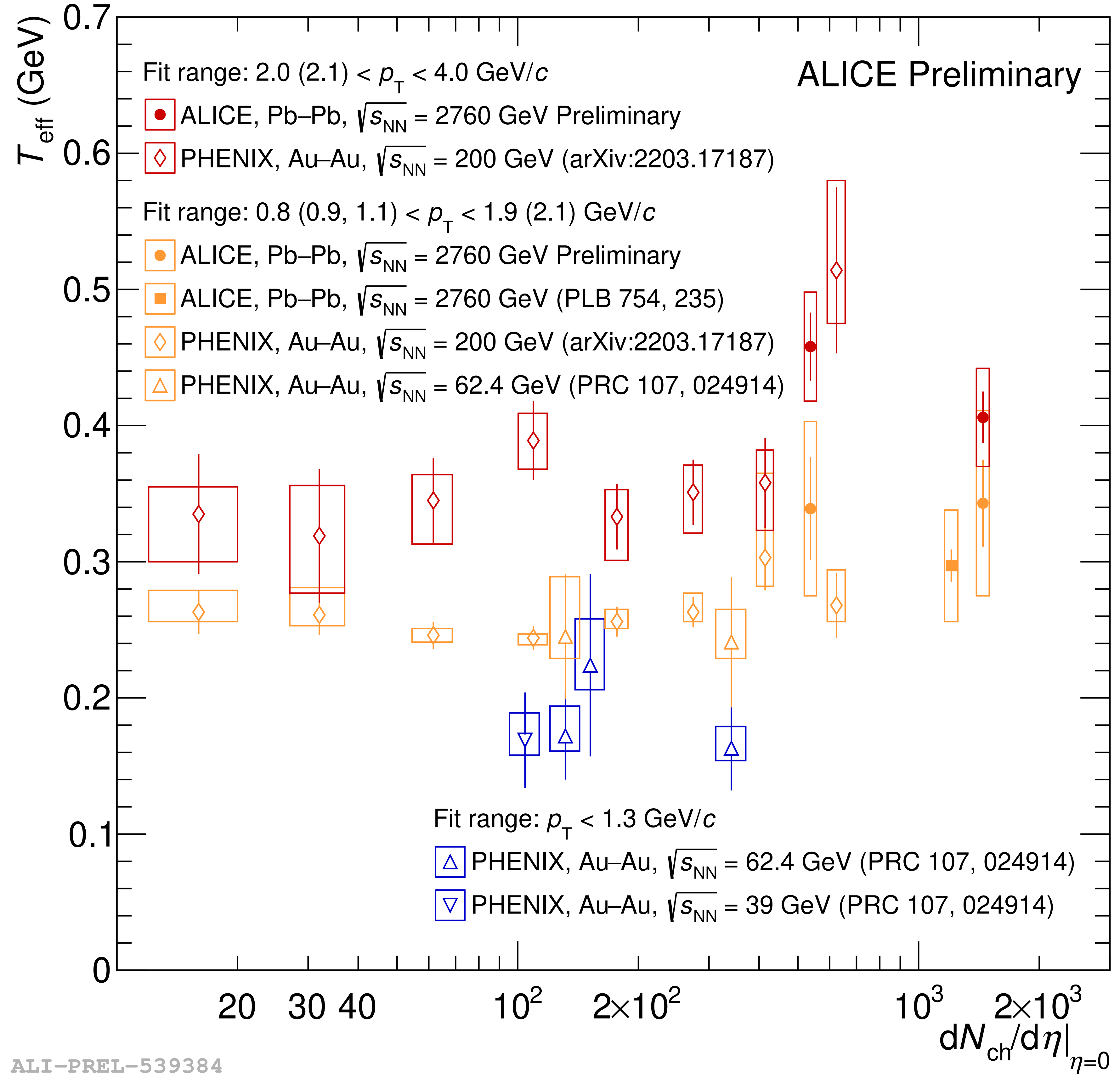

Apparent temperature larger at LHC than RHIC
Absolute temperature depends on blue shift

The ALICE detector

A general purpose detector for heavy-ion physics

- **Low material budget**
- **High-resolution tracking**
  - Silicon tracker
  - Time projection chamber
- **Particle identification**
  - TPC *dE/dx*
  - Time of Flight
  - Ring-imaging Cherenkov (high p_T)
  - Muon ID (forward)
  - Transition radiation detector
- **EM calorimeters**

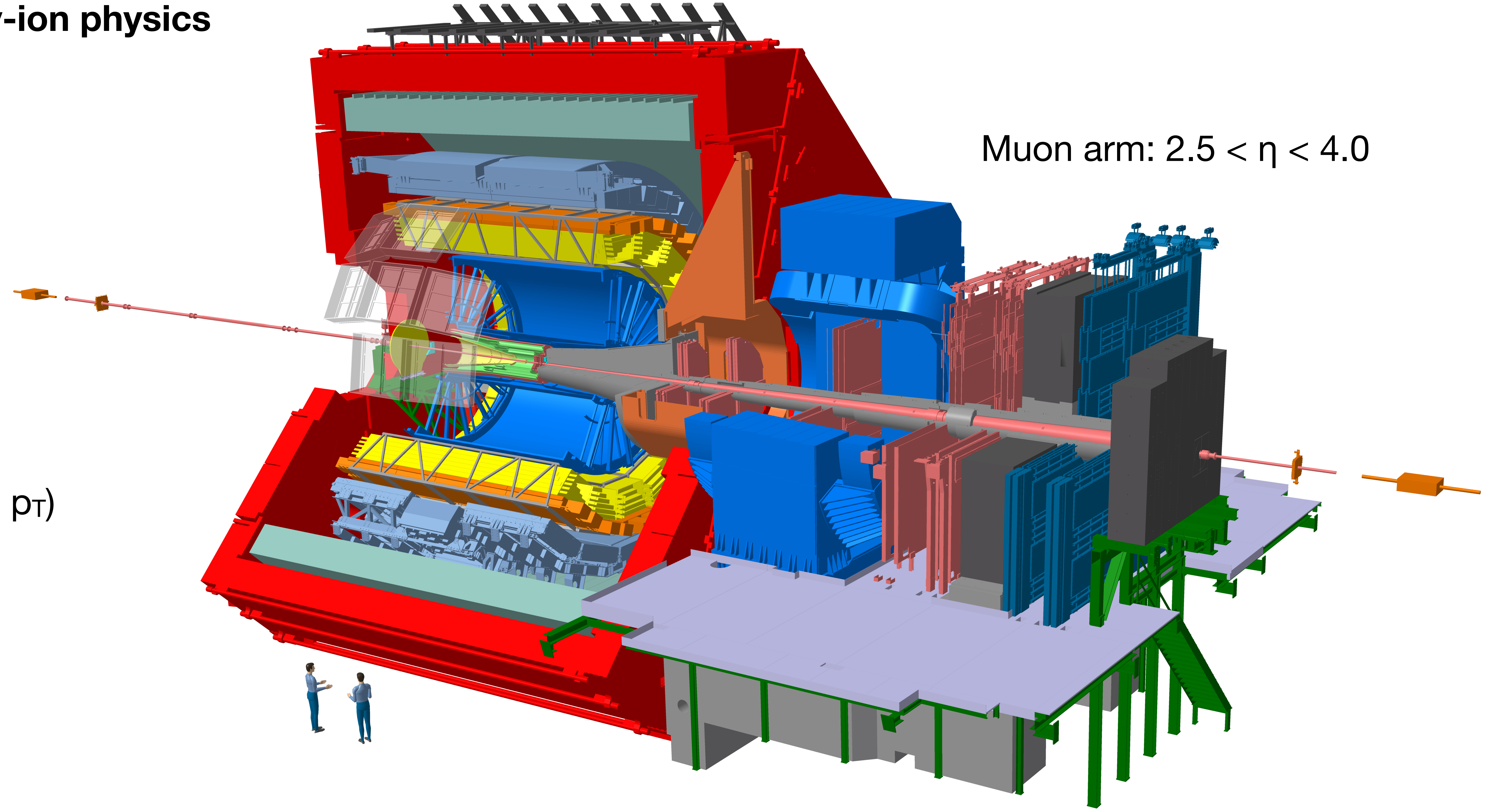

ALICE upgrades in Long Shutdown 2 (2019-2021)

New ITS and MFT

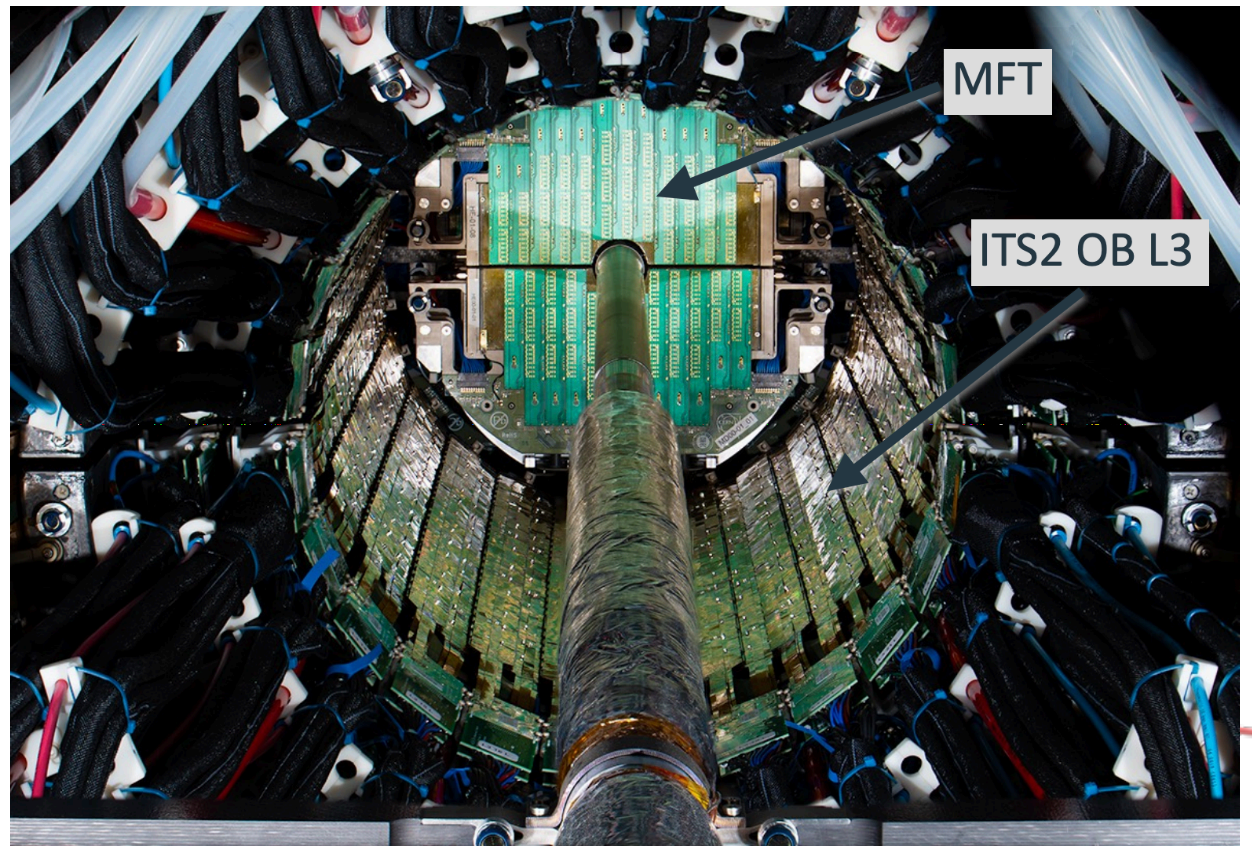

Full pixel detector

Improved spatial resolution

Fast Interaction Trigger

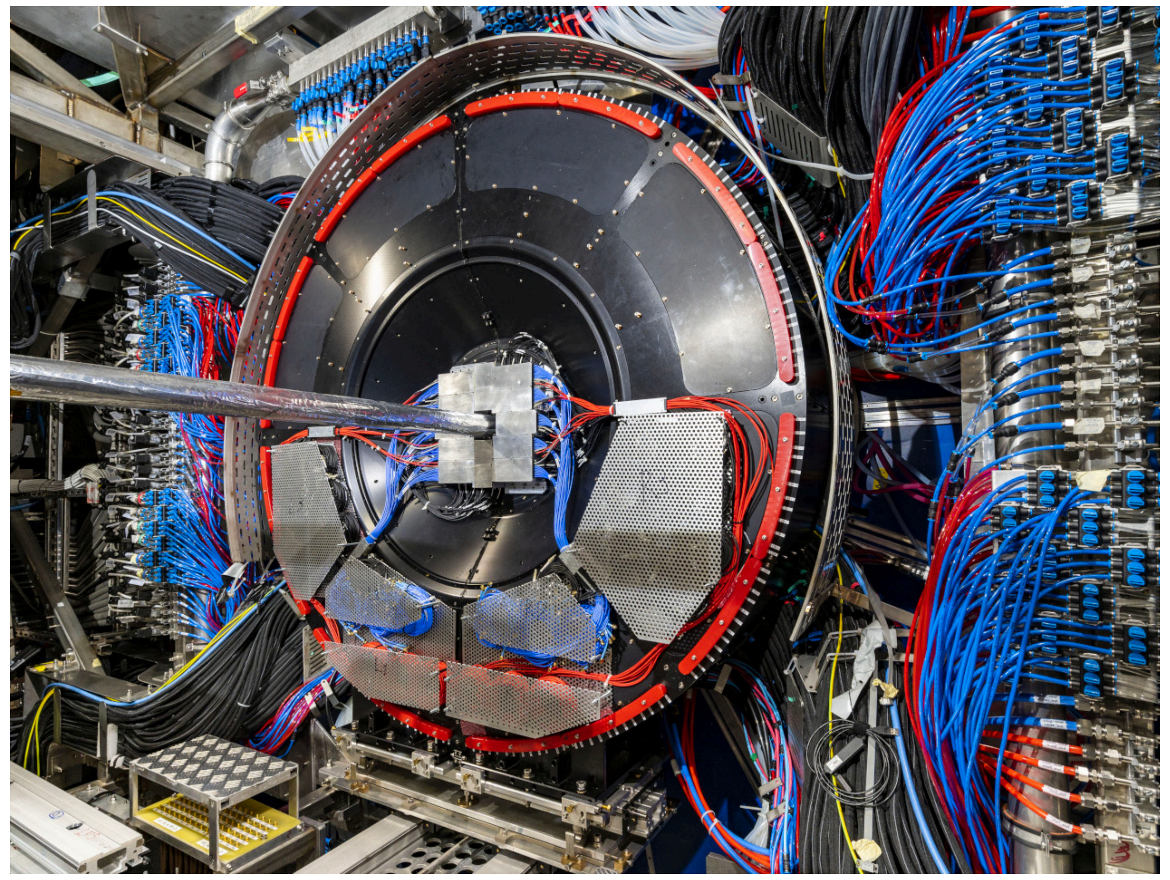

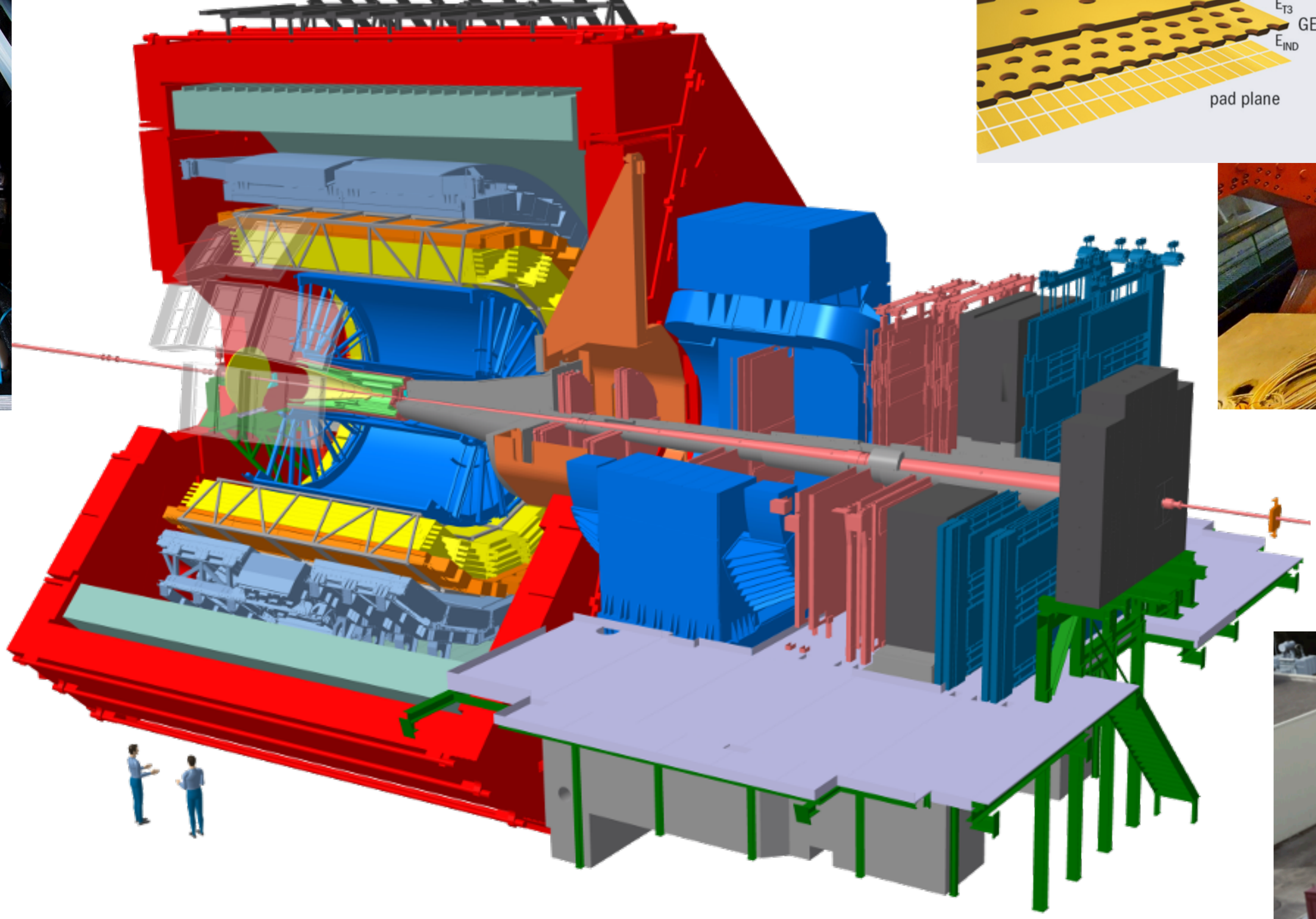

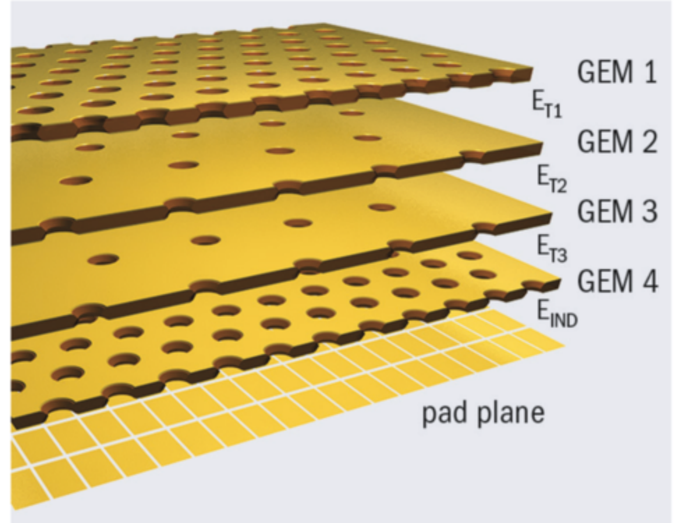

TPC: GEM readout

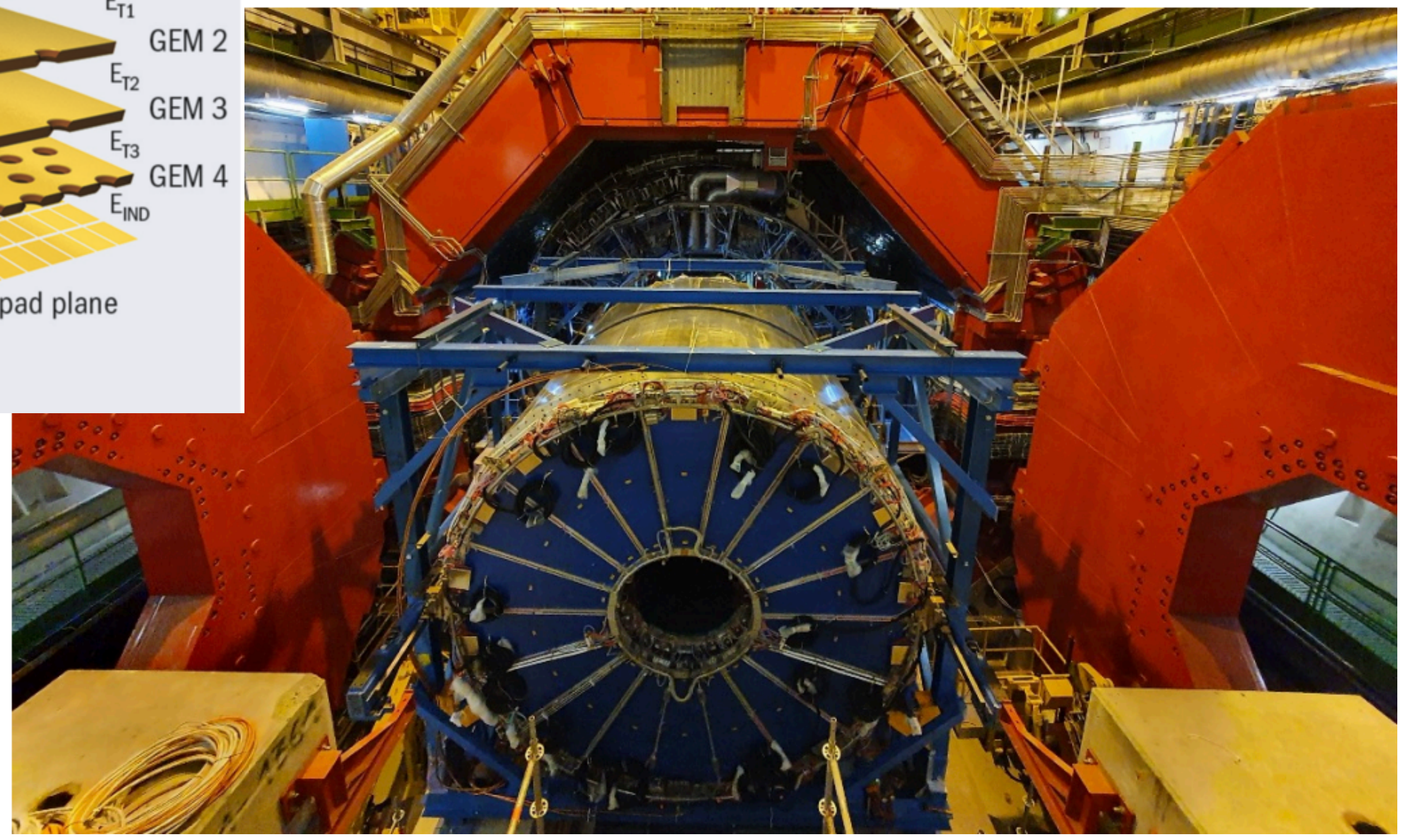

Continuous readout

Online event processing

ALICE LS2 upgrade paper: arXiv:2302.01238

Run 3, 4: collect 13 nb^{-1} Pb-Pb: 50x more minimum bias data; 10x more triggered data

Future upgrades: ITS 3 and FoCal

ITS 3: ultra-light, fully cylindrical tracking layers

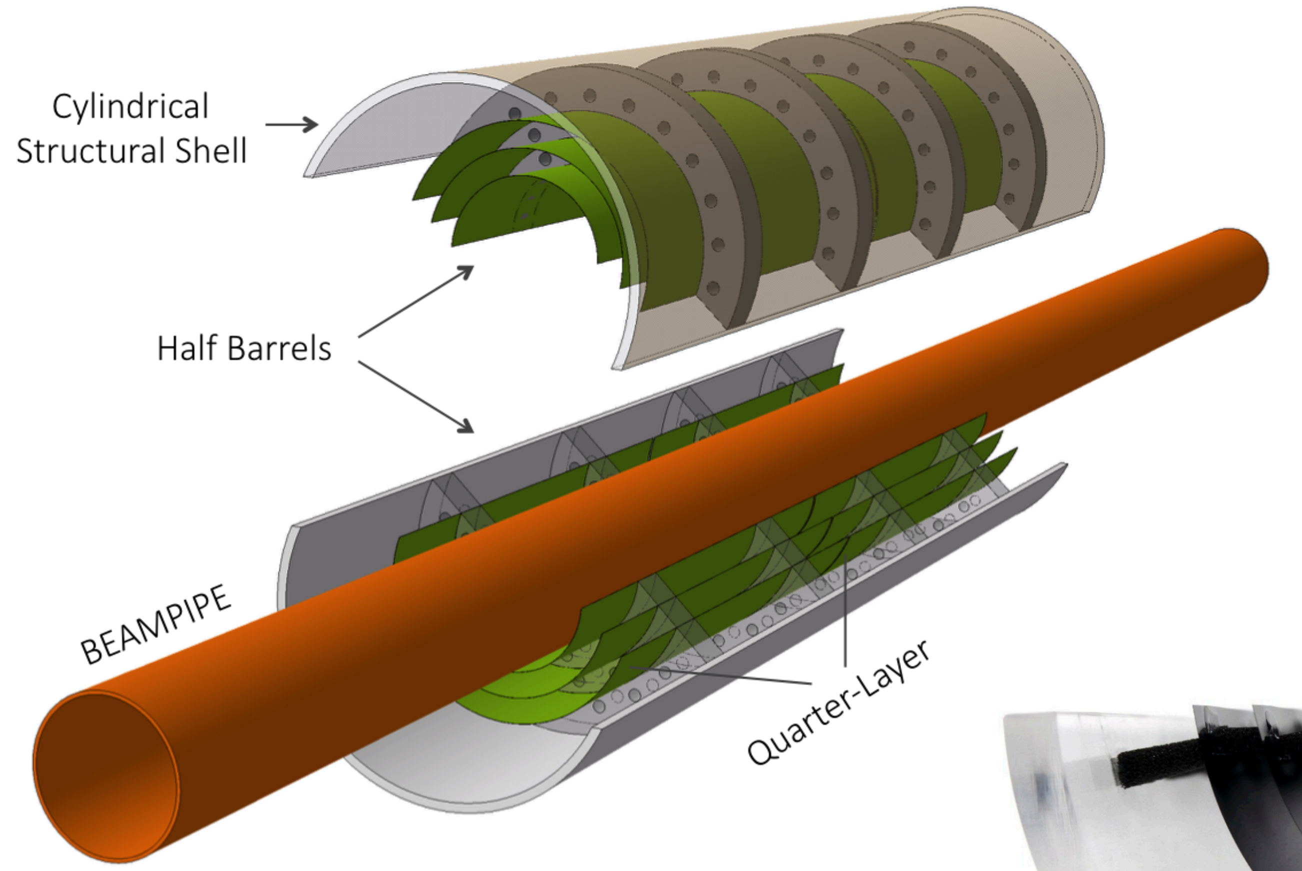

DPTS test sensor

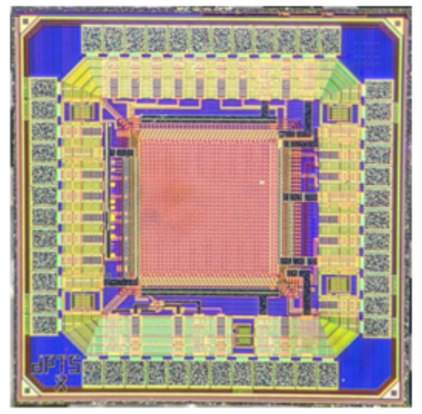

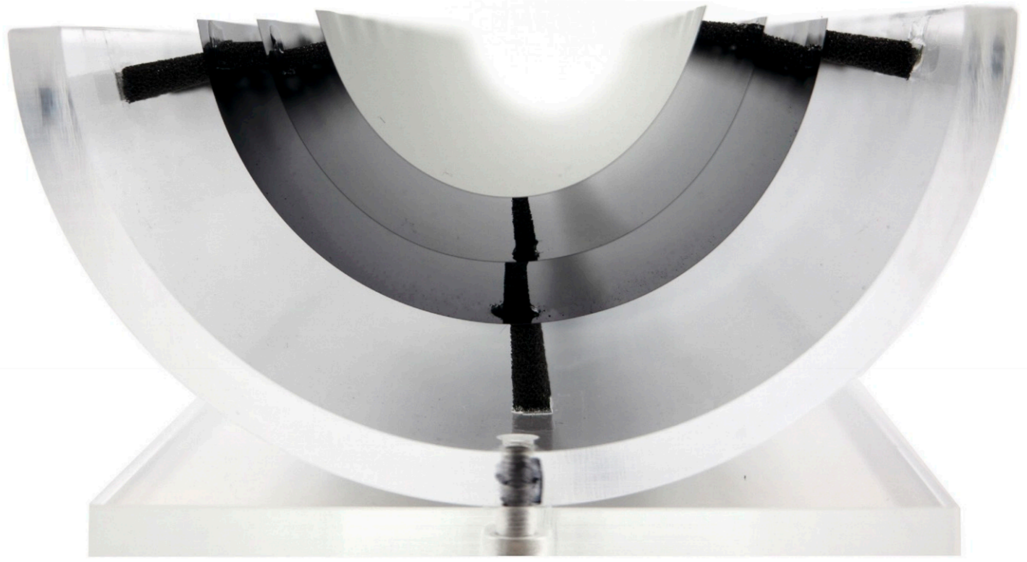

LoI: CERN-LHCC-2019-018

DPTS test paper arXiv:2212.08621

Improved performance for

- Heavy flavour reconstruction
- **Di-lepton measurements**

FoCal: high-granularity forward calorimeter

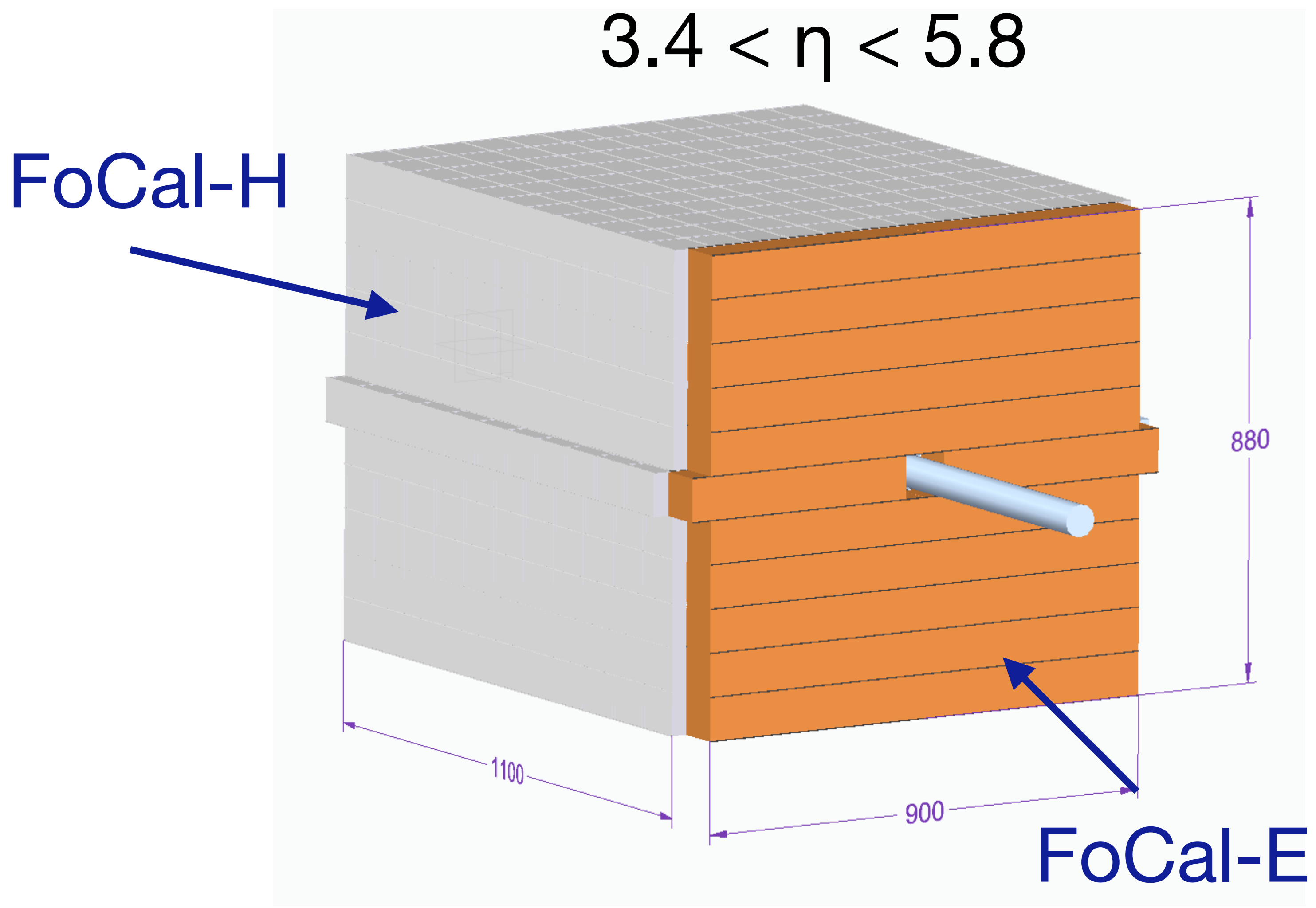

Longitudinal profile (2γ showers)

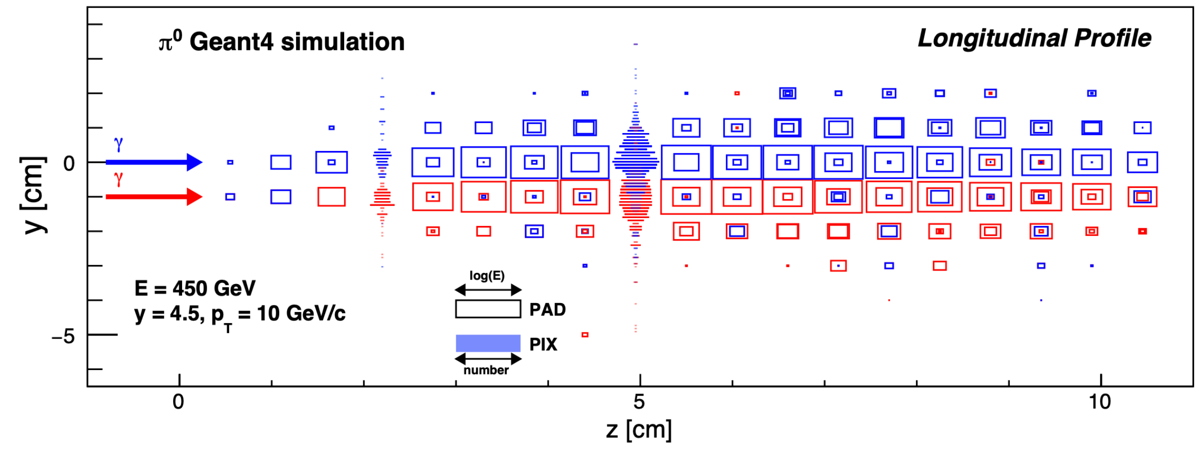

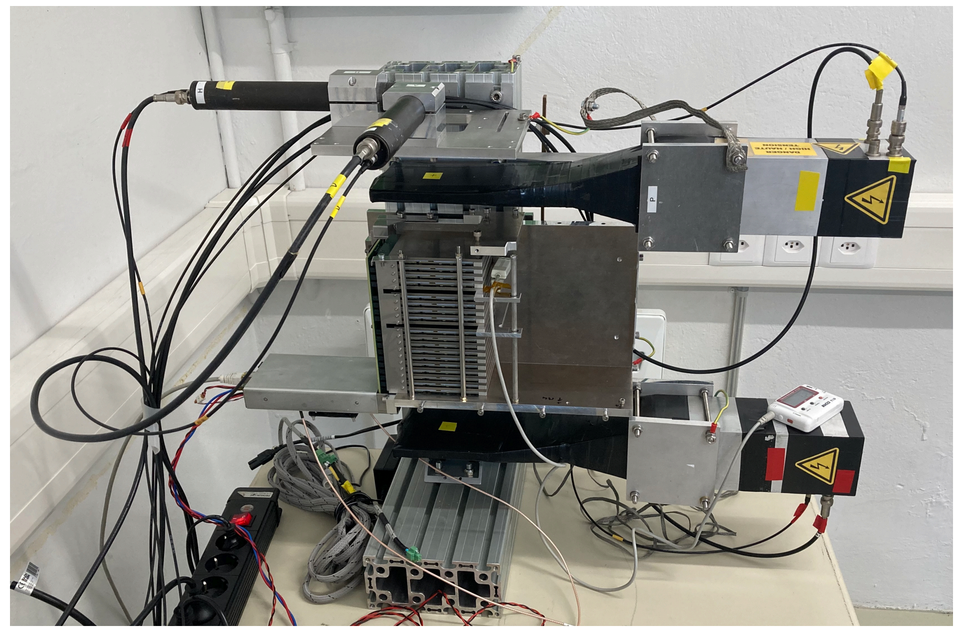

LoI: CERN-LHCC-2020-009

High-granularity Si-W EM calorimeter for **photons and π^0**

- **Small-x physics** in pp and p-Pb
- Forward π^0 in Pb-Pb

LHC Run 5 and 6: ALICE 3

- Compact all-silicon tracker
  with high-resolution vertex detector
- Particle Identification over large acceptance:
  muons, electrons, hadrons, photons
- Fast read-out and online processing

Improvement of detector performance for the upgrades

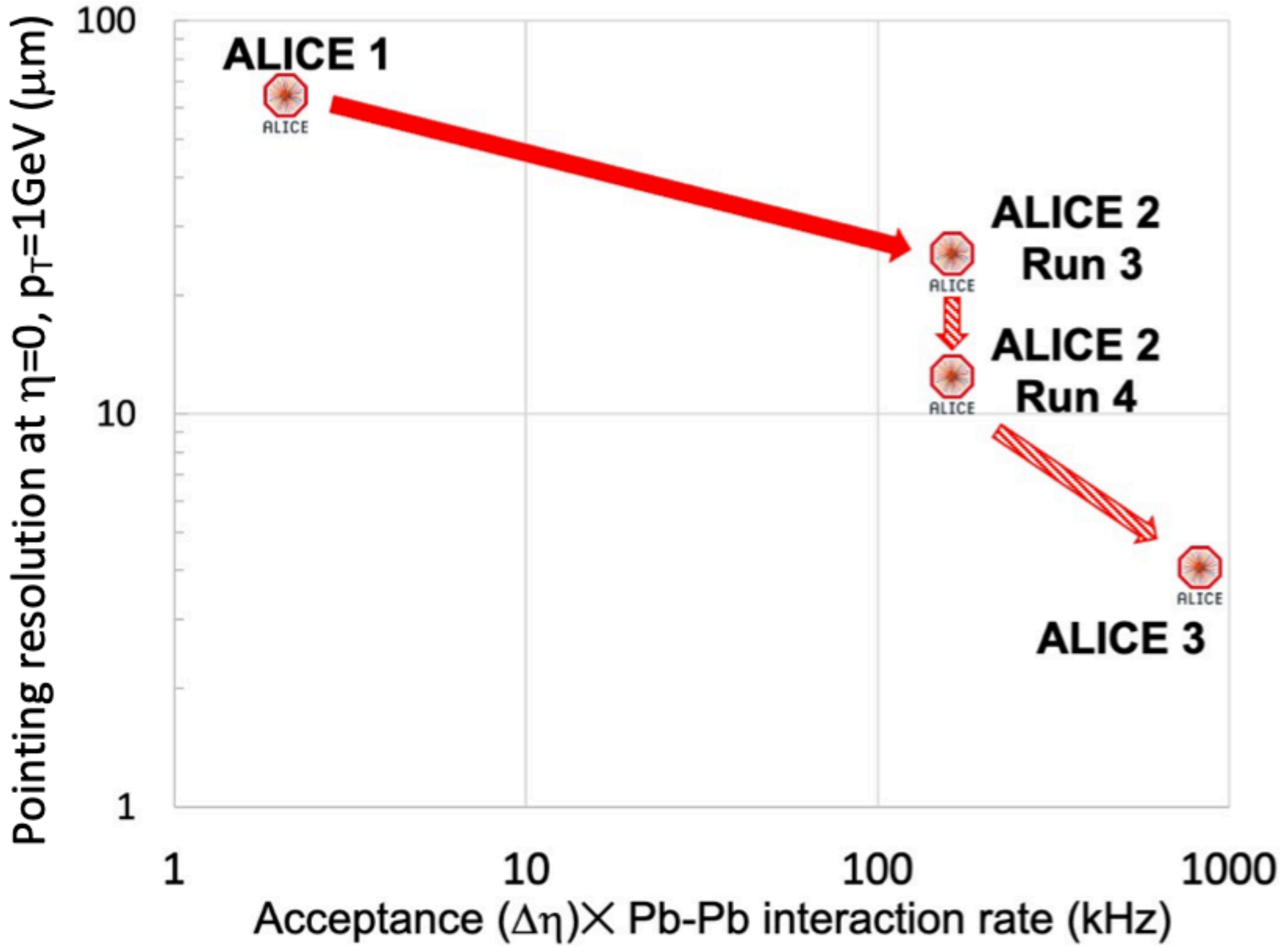

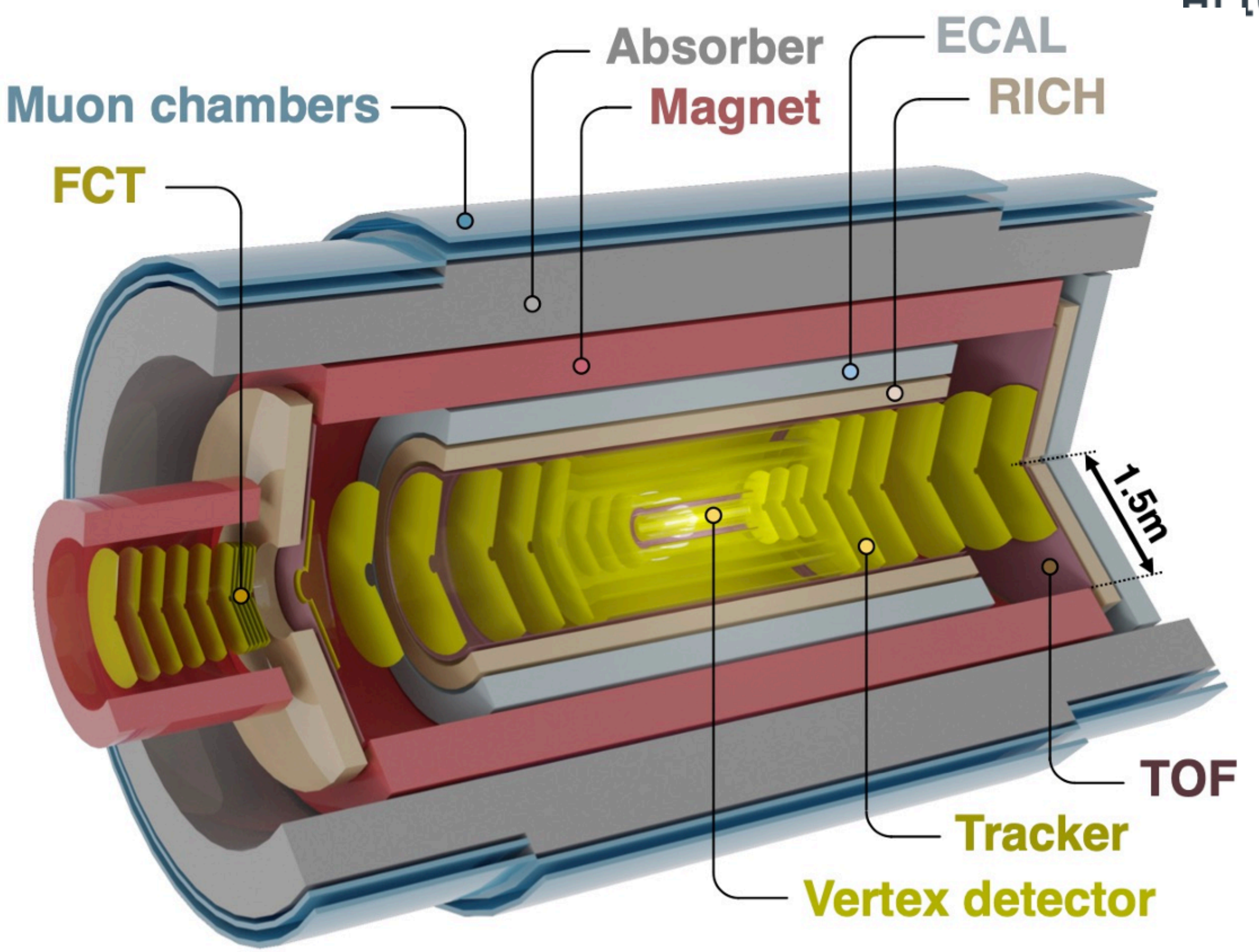

Letter of Intent: LHCC-2022-009

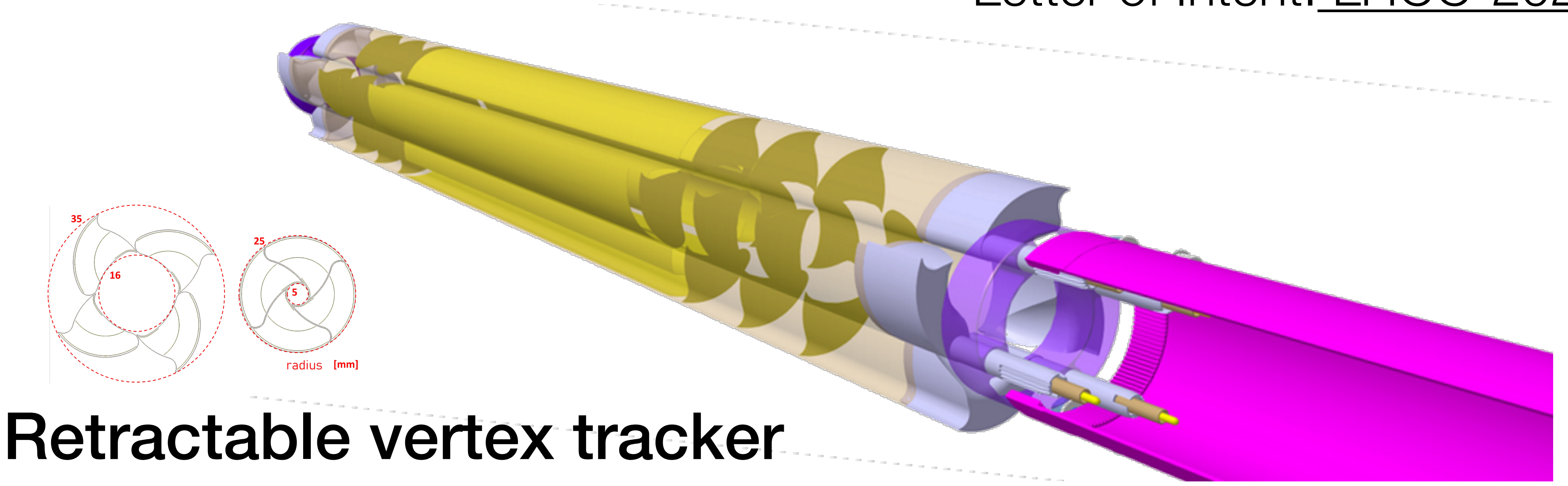

Retractable vertex tracker

Di-lepton emission: virtual photons

- Virtual photons: e+e- pairs
- Cleaner signal:
  - $m_{ee} > 1\ \mathrm{GeV}/c^2$ removes light flavour decay background
  - Remaining background: heavy flavour pairs
- Slope of mass spectrum not blue-shifted
- Vector meson spectral functions sensitive to chiral symmetry restoration

Di-lepton mass distribution

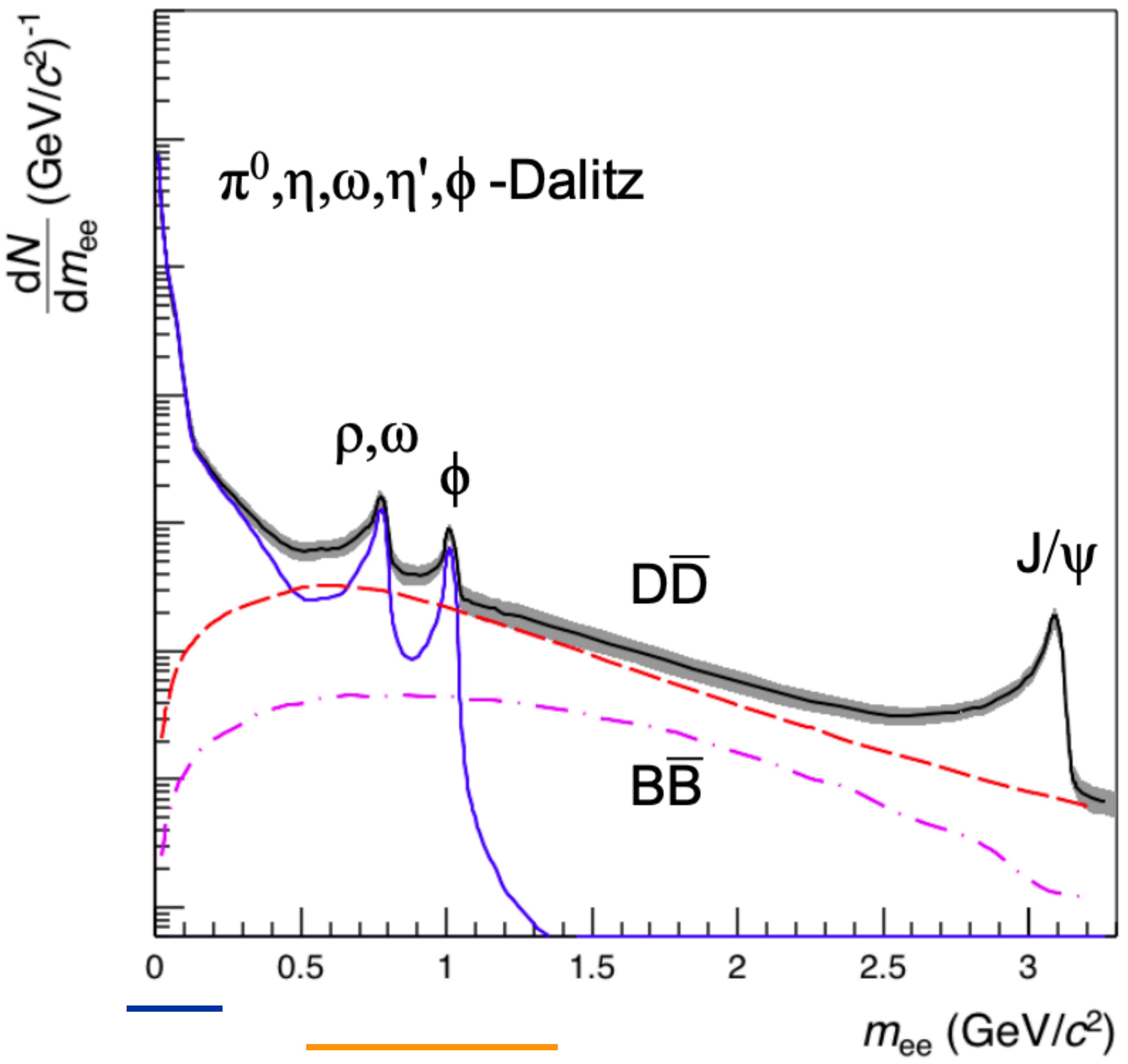

Very low mass:
π_0 decay background
conductivity

ω/φ region:
chiral symmetry and
ρ-a_1 mixing

Large mass:
thermal emission,
early times

Dielectrons: chiral symmetry and thermal emission

Dileptons in run 3 and 4

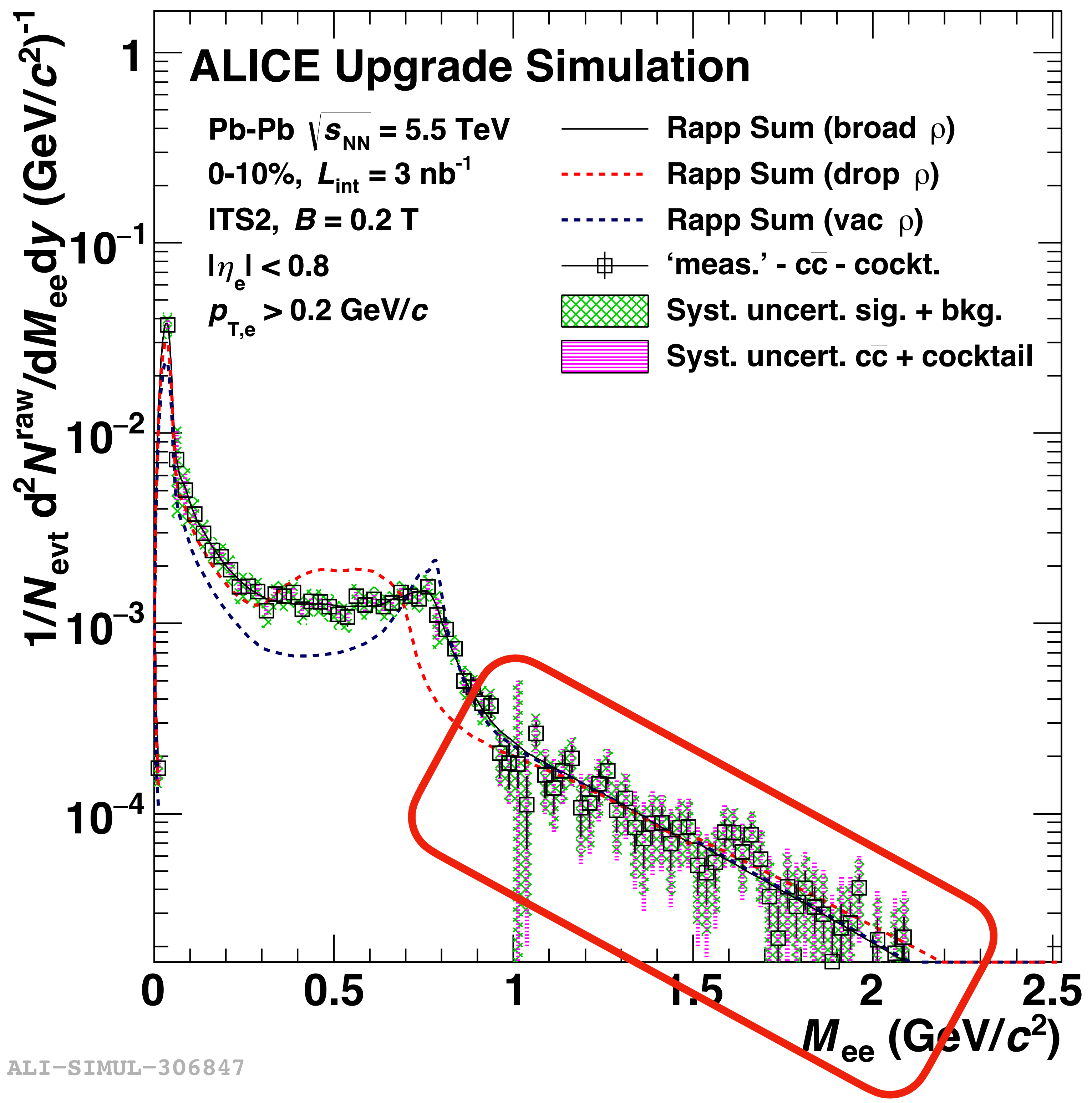

Run 3 and 4: first measurements
of thermal dilepton emission at LHC

Dielectrons: chiral symmetry and thermal emission

Dileptons in run 3 and 4

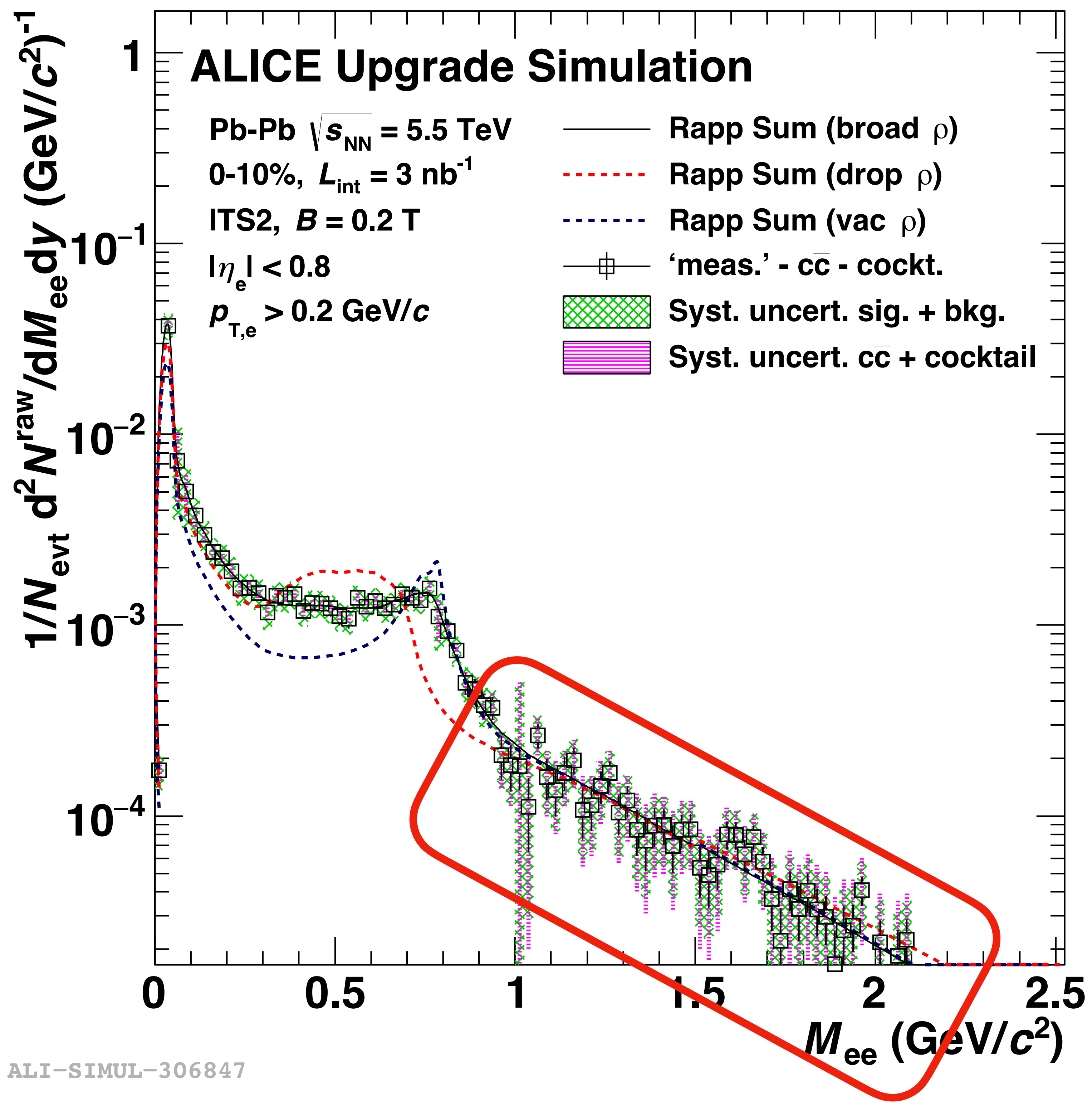

Run 3 and 4: first measurements of thermal dilepton emission at LHC

ALICE 3 mass spectrum

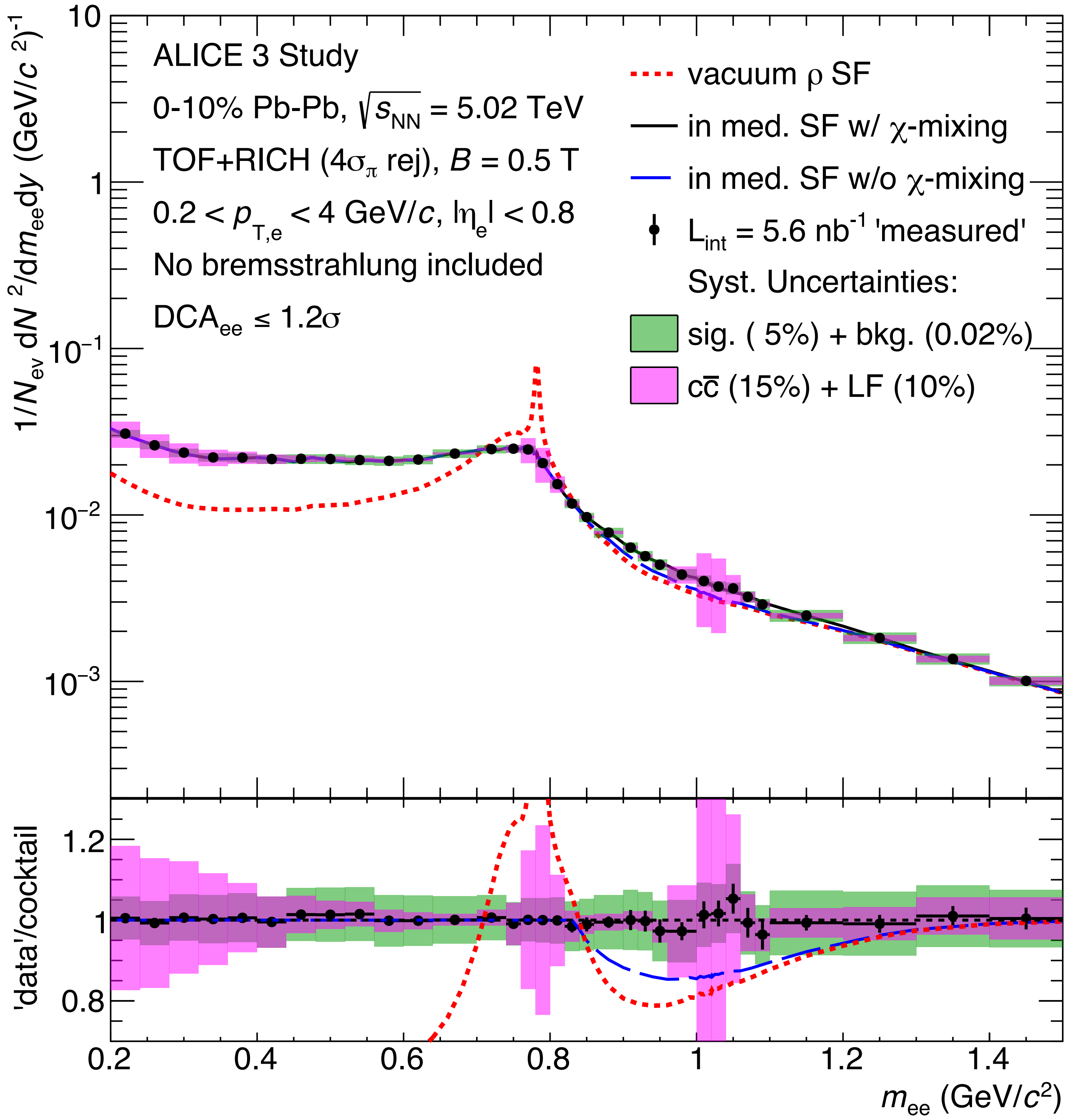

High precision:

access $\rho - a_1$ mixing

Dielectrons: chiral symmetry and thermal emission

Dileptons in run 3 and 4

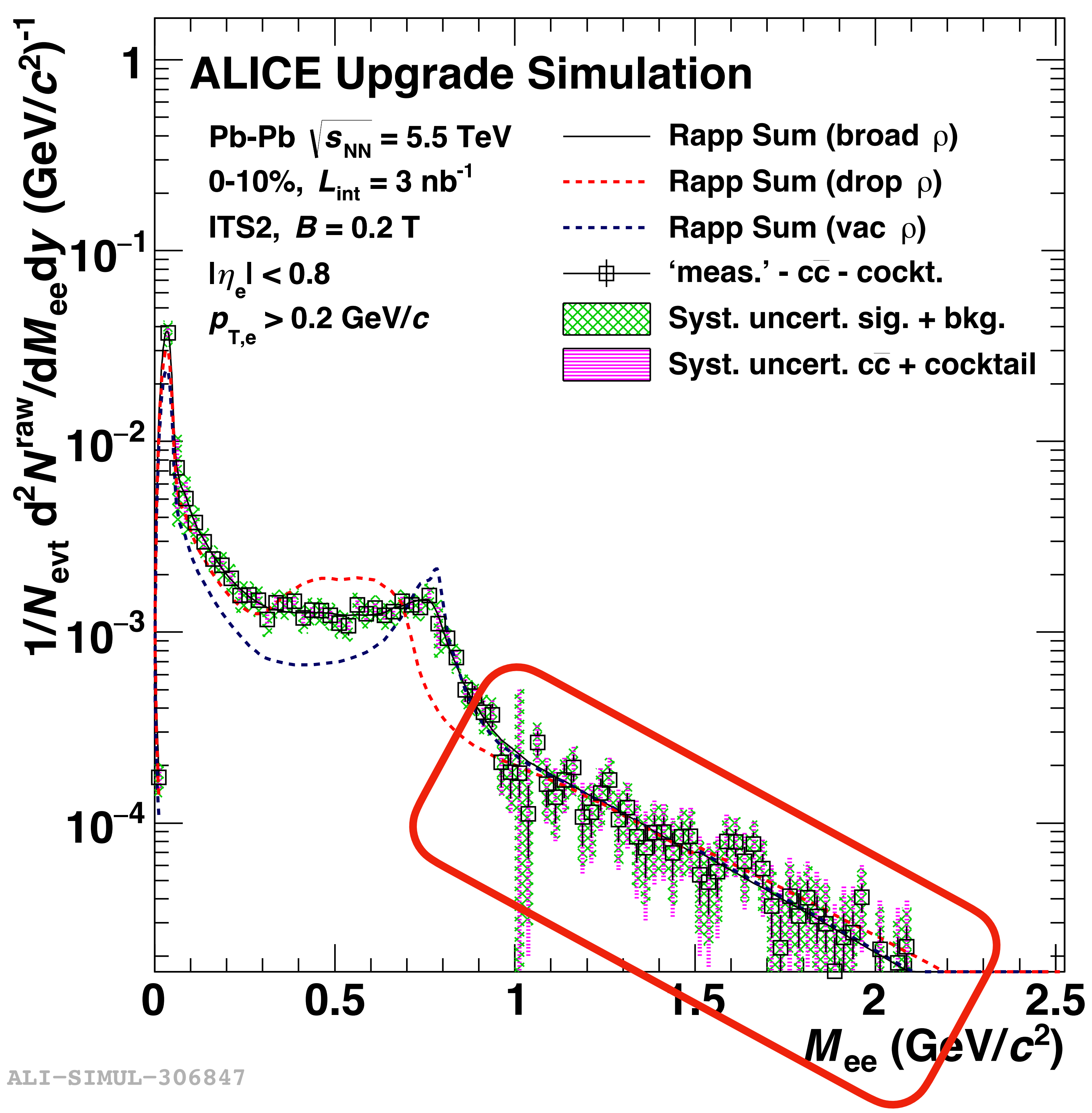

Run 3 and 4: first measurements of thermal dilepton emission at LHC

ALICE 3 mass spectrum

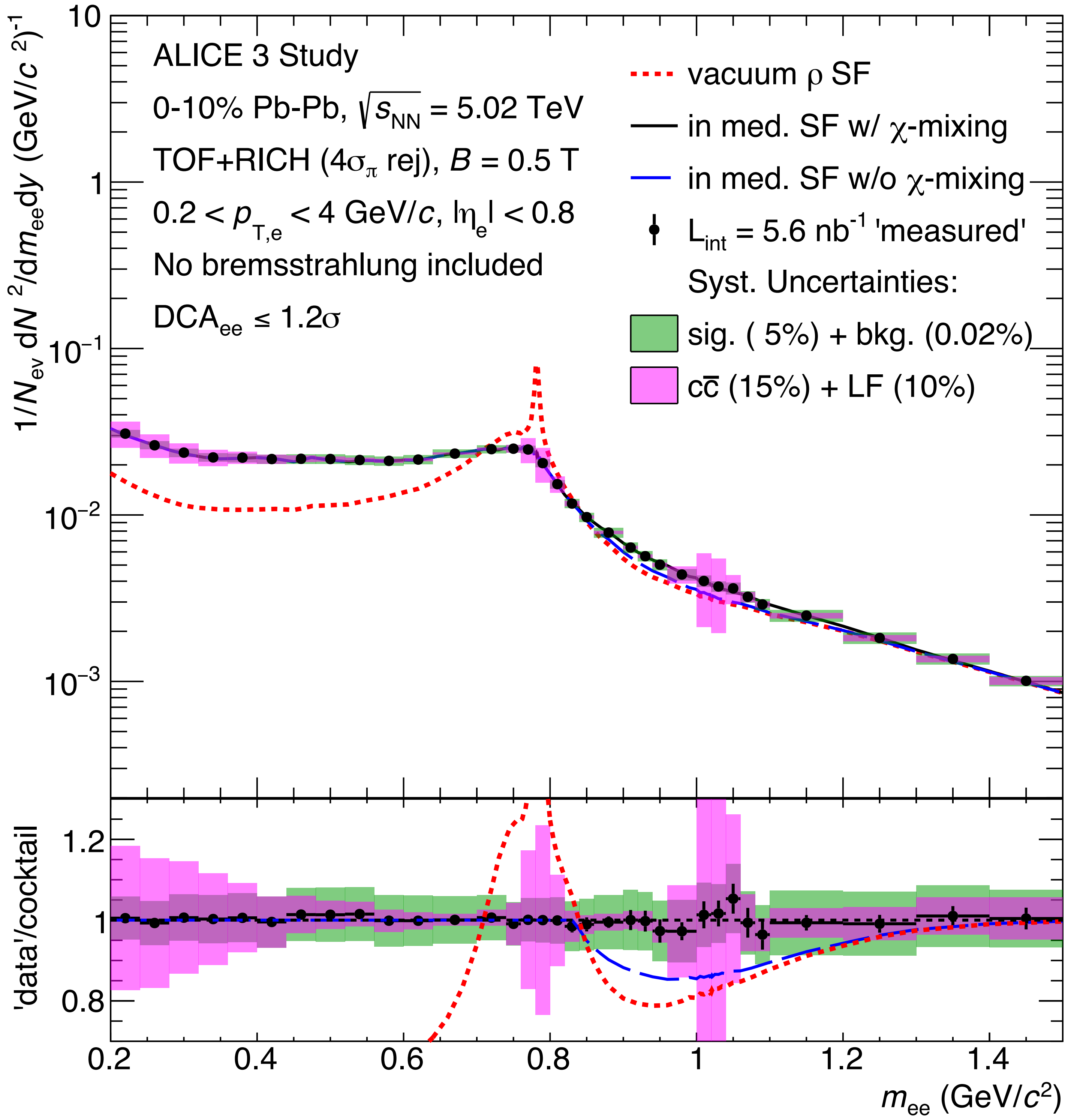

High precision:
access $\rho - a_1$ mixing

Dielectron v_2

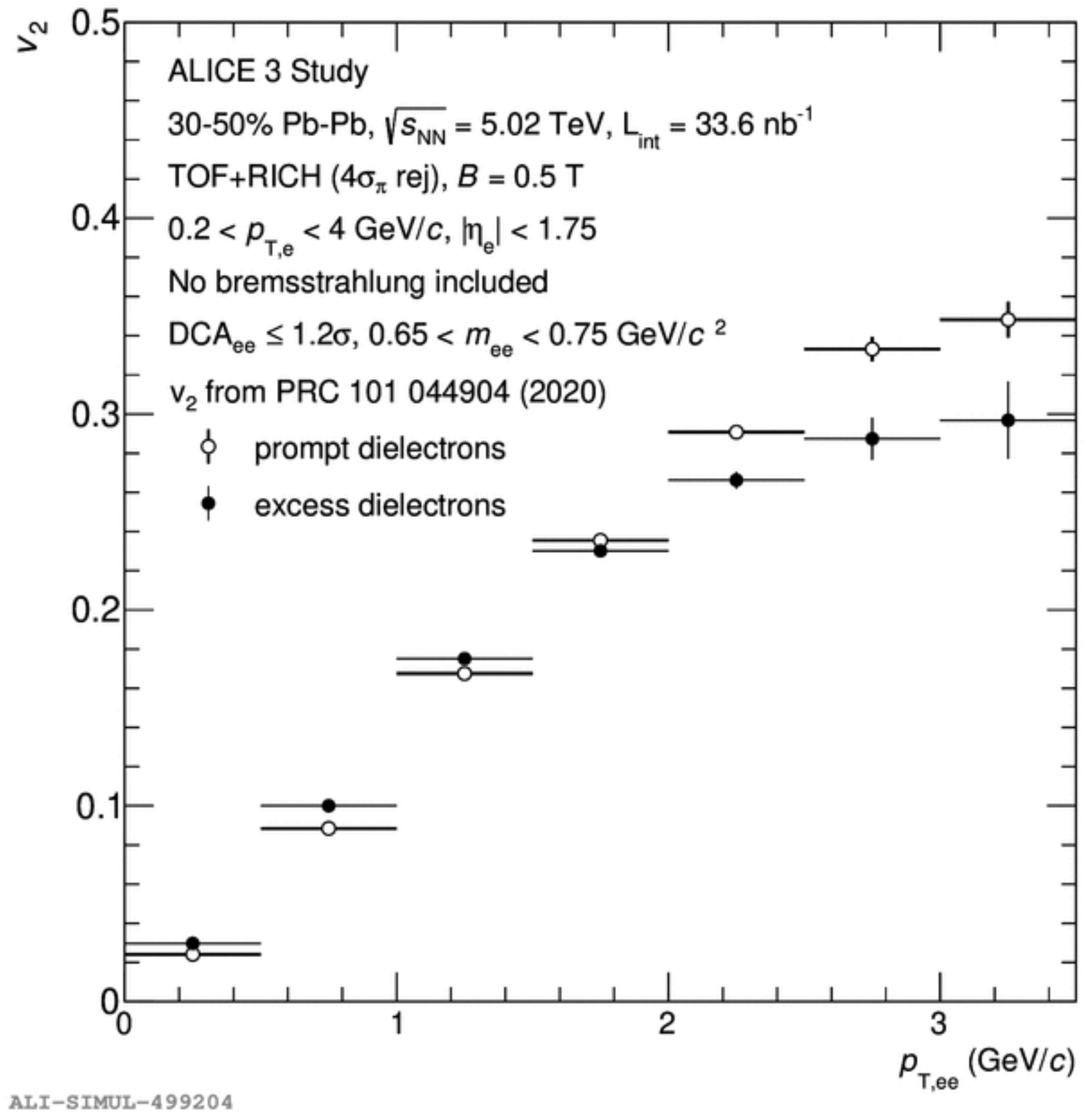

Excellent precision for dilepton v_2 vs p_T in different mass ranges
→ time evolution of emission

DD̄ azimuthal correlations

Charm azimuthal correlations

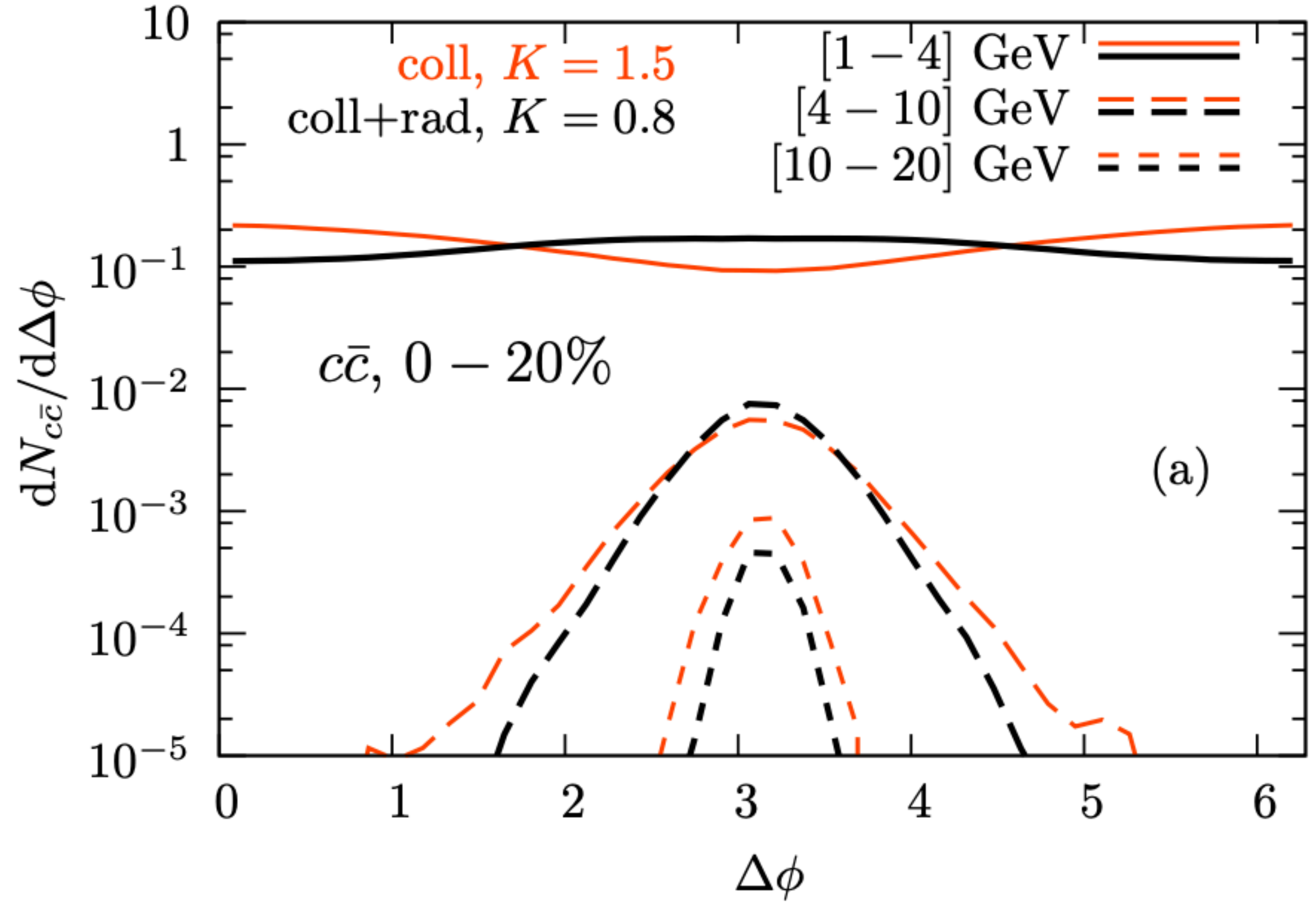

M Nahrgang et al, PRC 90, 024907

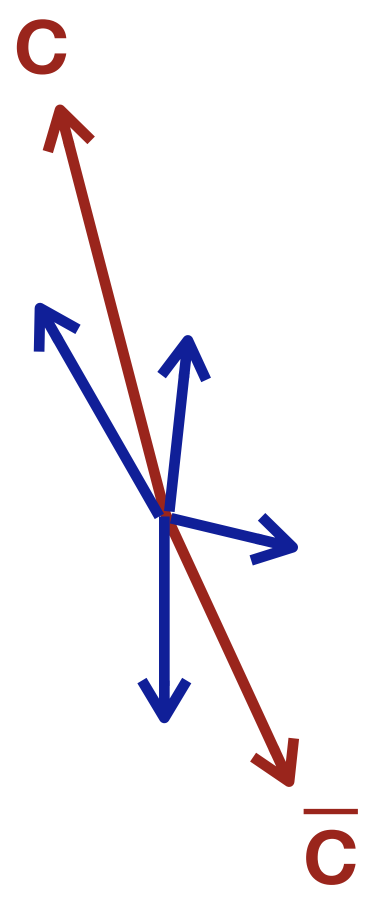

- Angular decorrelation directly probes QGP scattering
  - Signal strongest at low p_T
- Very challenging measurement:
  need good purity, efficiency and η coverage
  → heavy-ion measurement only possible with ALICE 3

$D\bar{D}$ azimuthal correlations

Charm azimuthal correlations

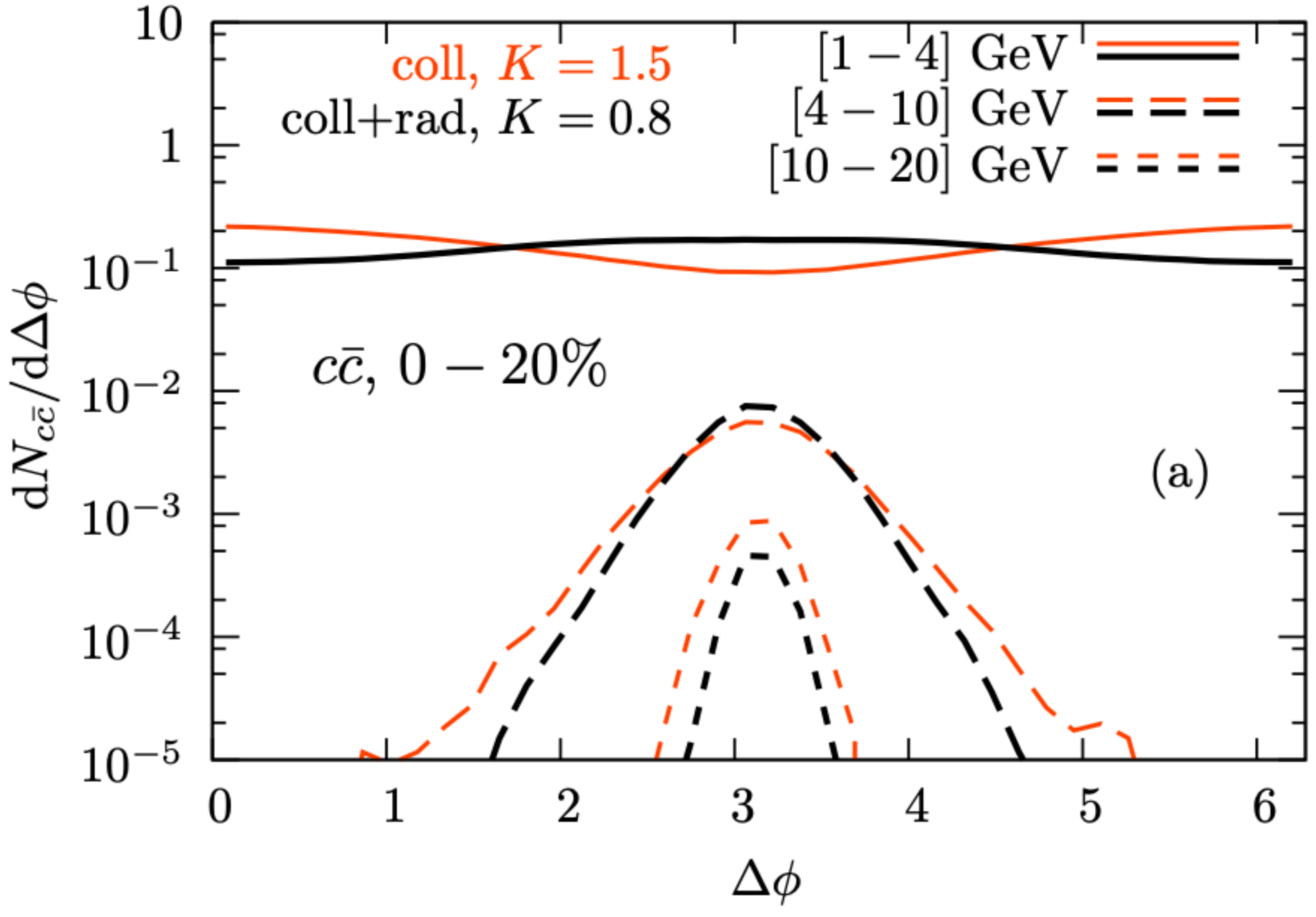

M Nahrgang et al, PRC 90, 024907

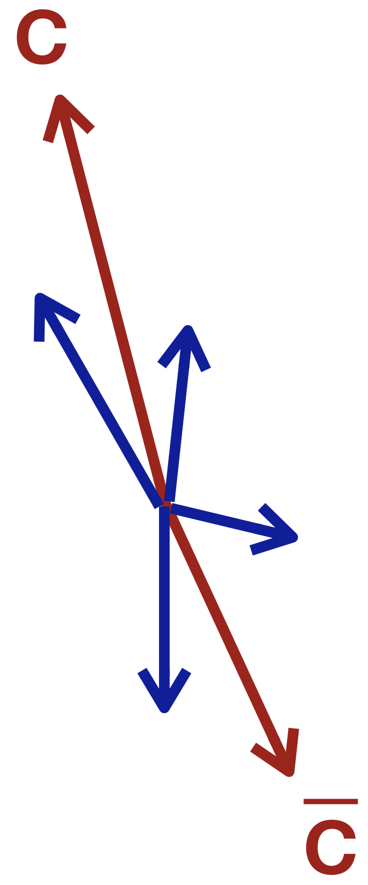

ALICE 3 projection: $D\bar{D}$ correlations

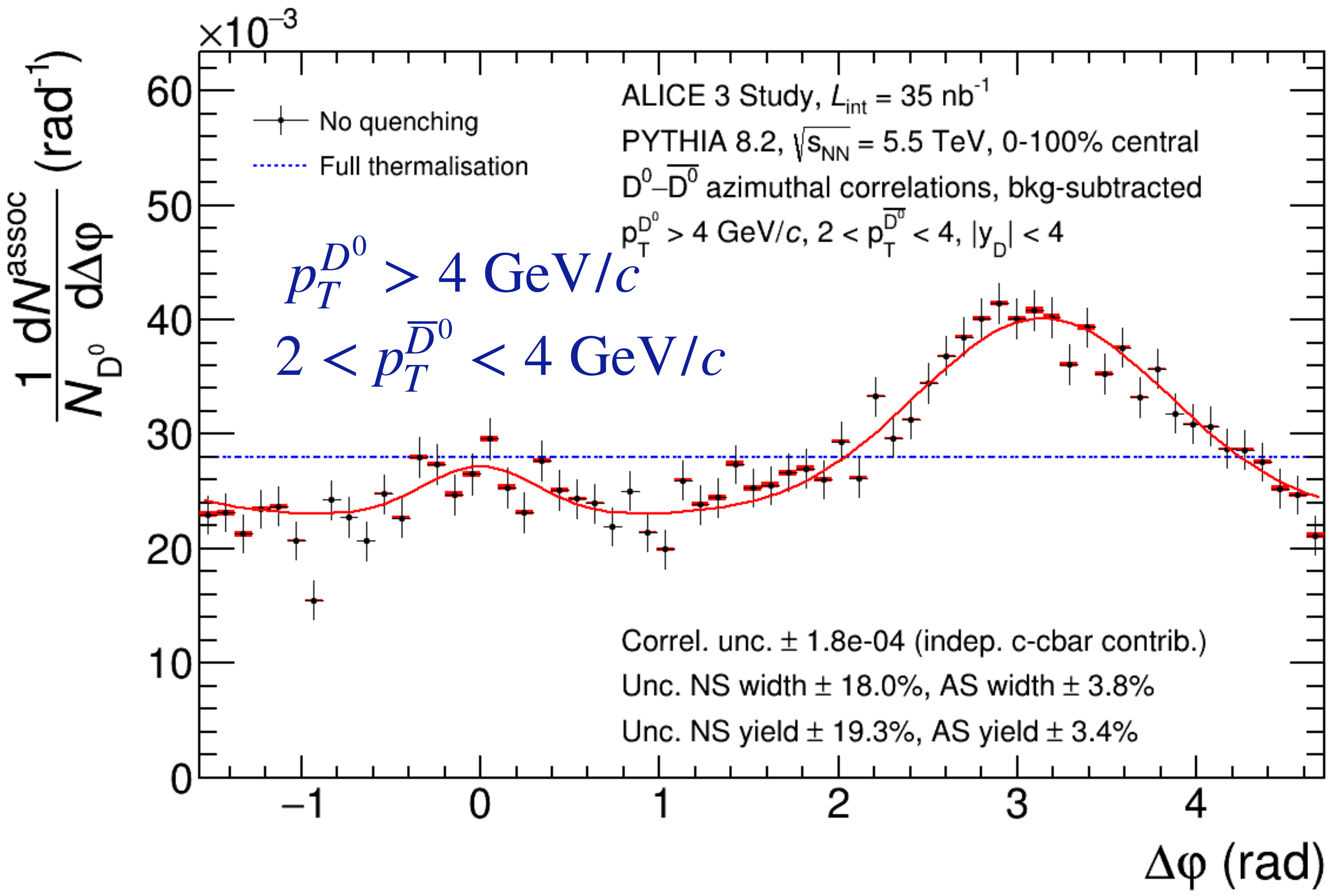

- Angular decorrelation directly probes QGP scattering
  - Signal strongest at low p_T
- Very challenging measurement:
  need good purity, efficiency and η coverage
  → heavy-ion measurement only possible with ALICE 3

$D\bar{D}$ azimuthal correlations

Charm azimuthal correlations

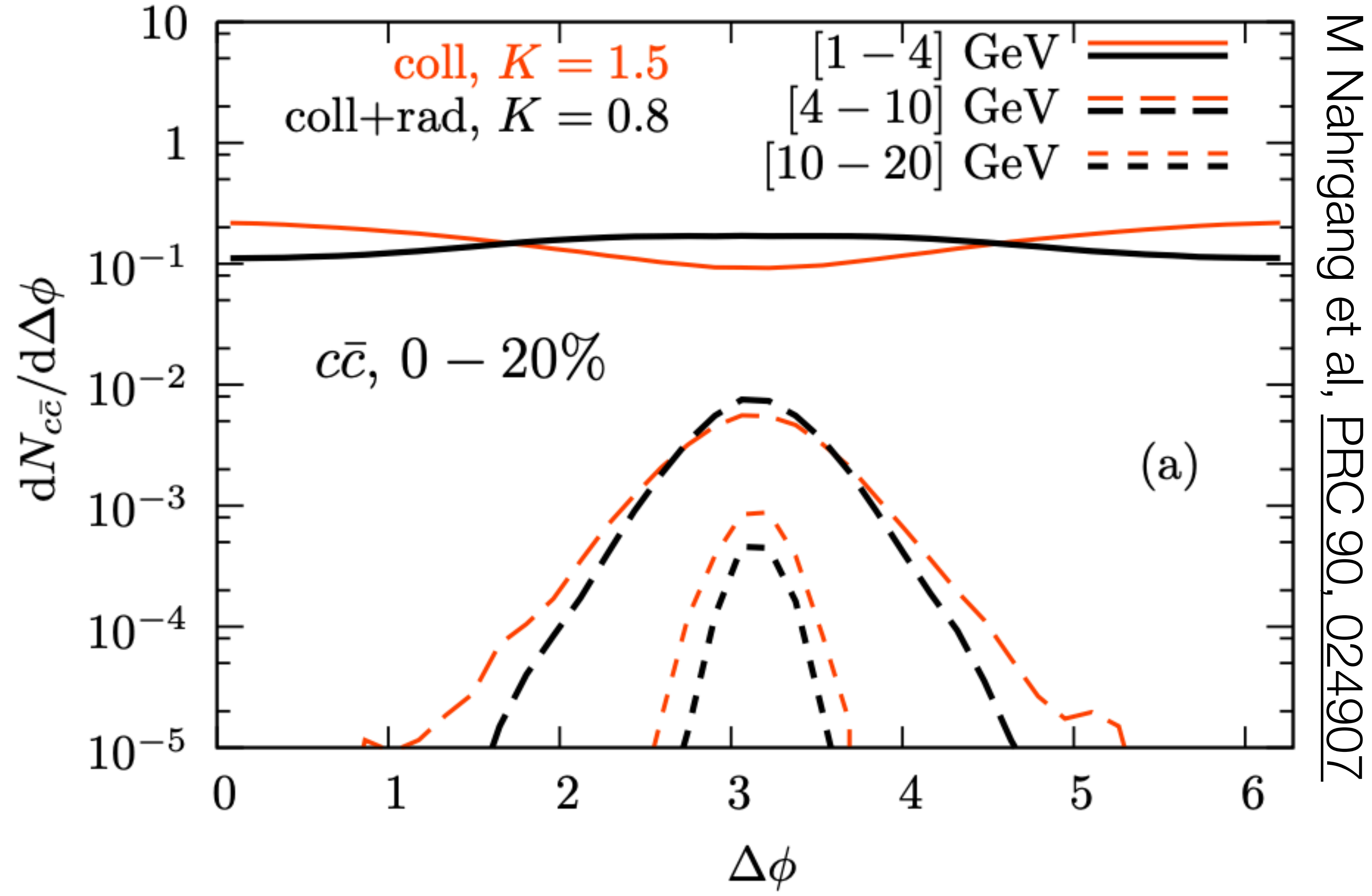

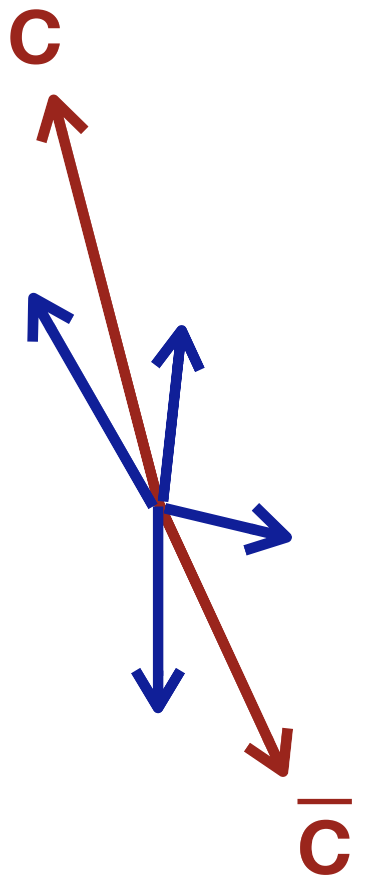

ALICE 3 projection: $D\bar{D}$ correlations

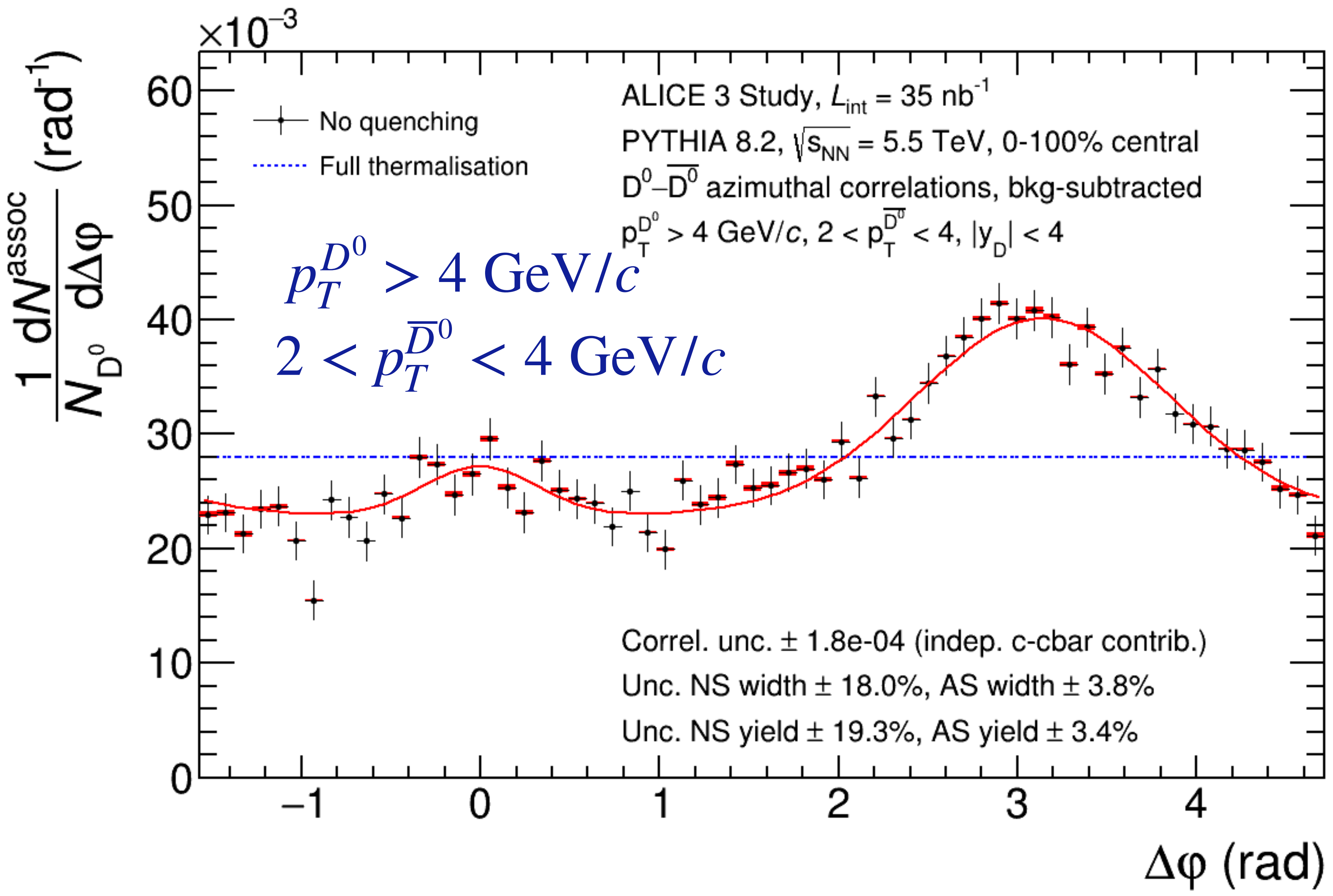

ALICE Run 3 + 4 projection

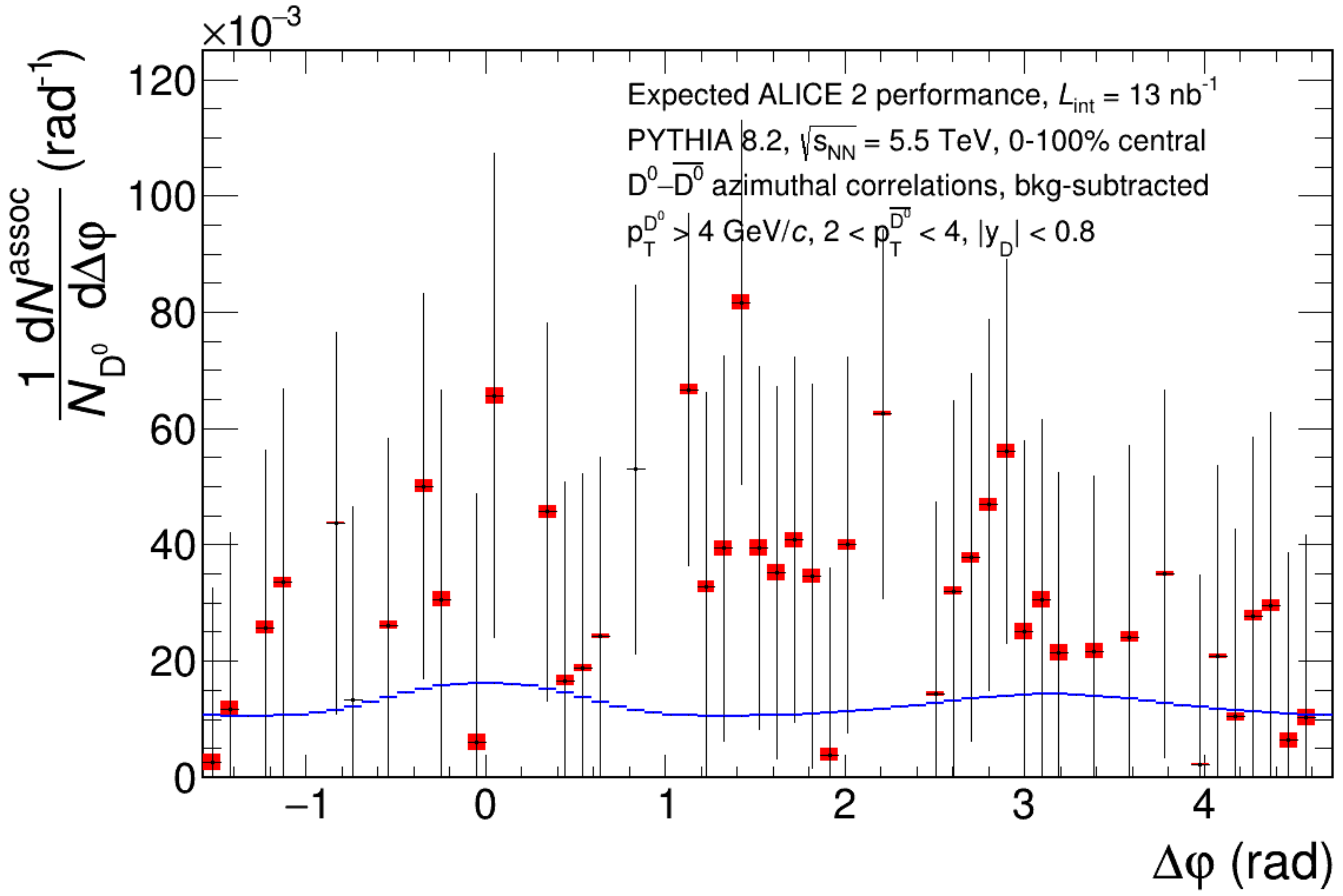

- Angular decorrelation directly probes QGP scattering
  - Signal strongest at low p_T
- Very challenging measurement:
  need good purity, efficiency and η coverage
  → heavy-ion measurement only possible with ALICE 3

Strategic detector R&D for ALICE 3

- **Vertex tracker mechanics**
- **Silicon tracking sensor development**
  - Improve read-out speed, radiation hardness
  - Low-power for cooling, large scale application
  - Module integration
- **Integrated timing sensor development**
  - Goal: achieve monolithic timing sensors
  - Improve time resolution to 20 ps
  - Combine photon sensors and timing sensors?
- **Muon detector development**
  - Large area, low noise detectors

R&D for ALICE 3 is starting up
Many exciting opportunities

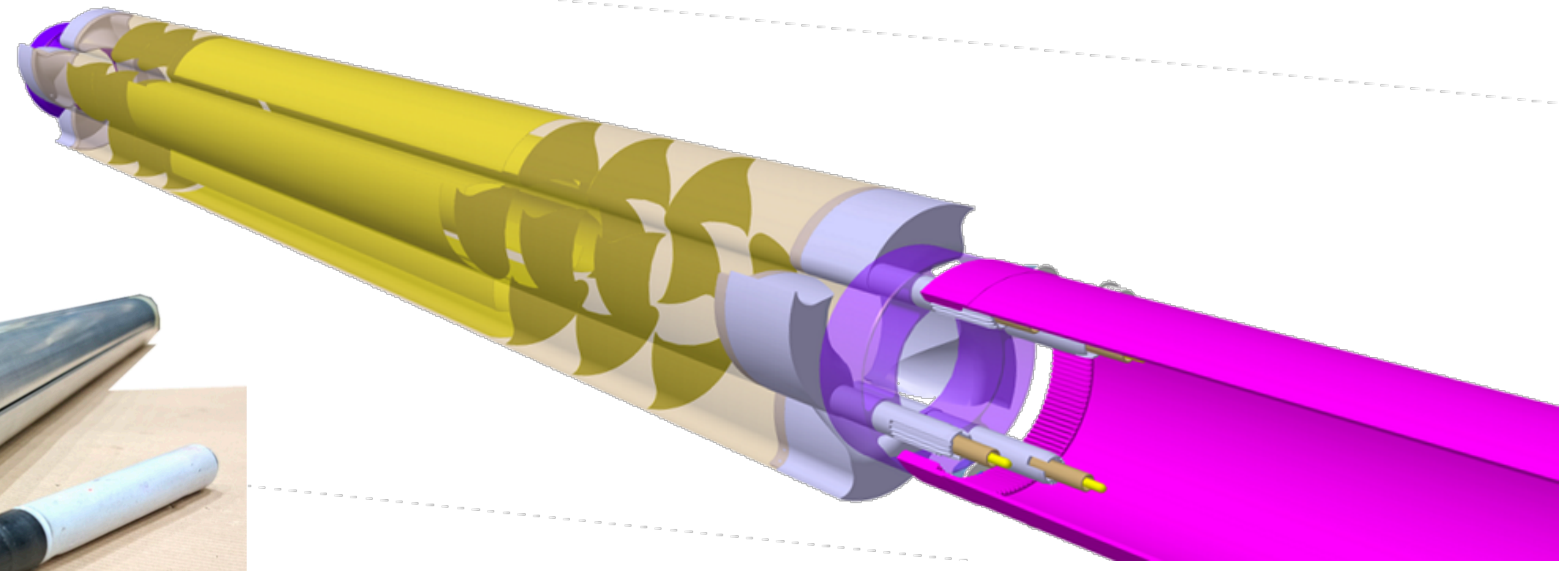

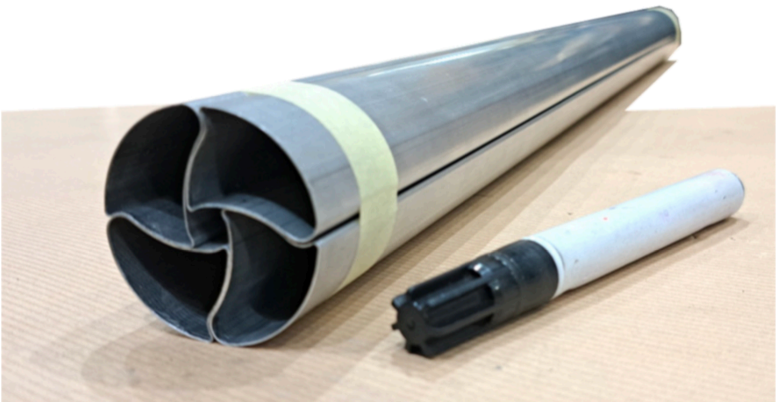

First very thin LGAD prototypes produced by FBK

25 μm and **35 μm**-thick FBK single channel
Area = **1x1 mm²**

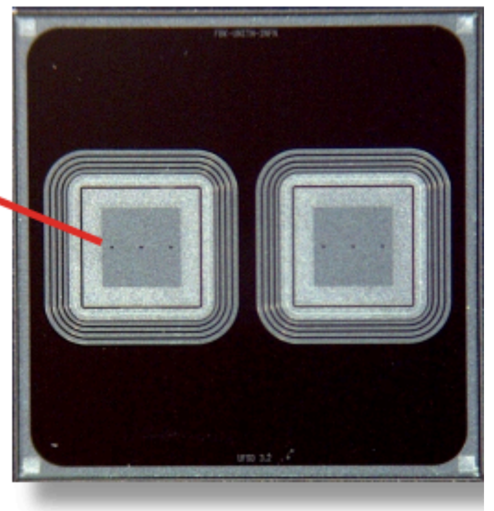

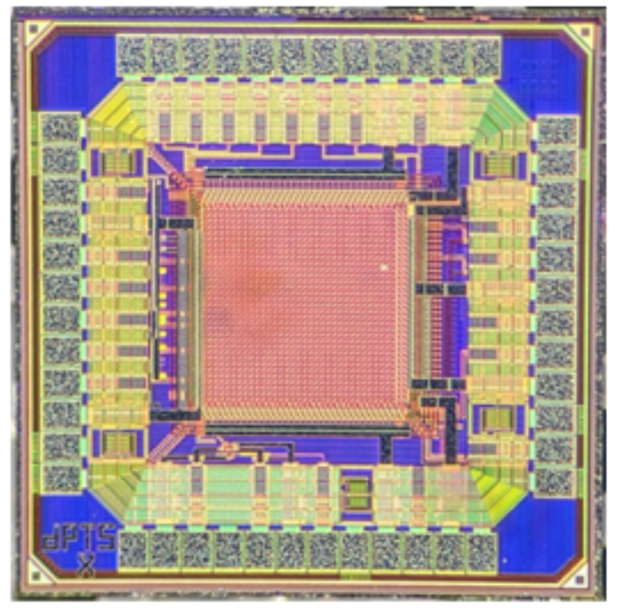

LGAD time resolution

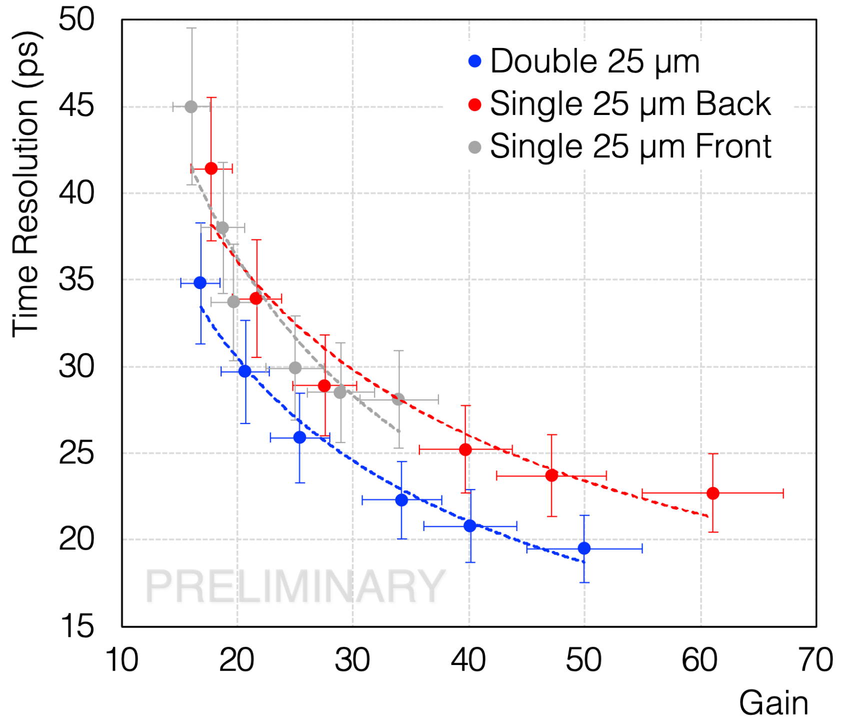

F. Carnesecchi et al, EPJ Plus 138 1, 99

SiPM hadron response tests

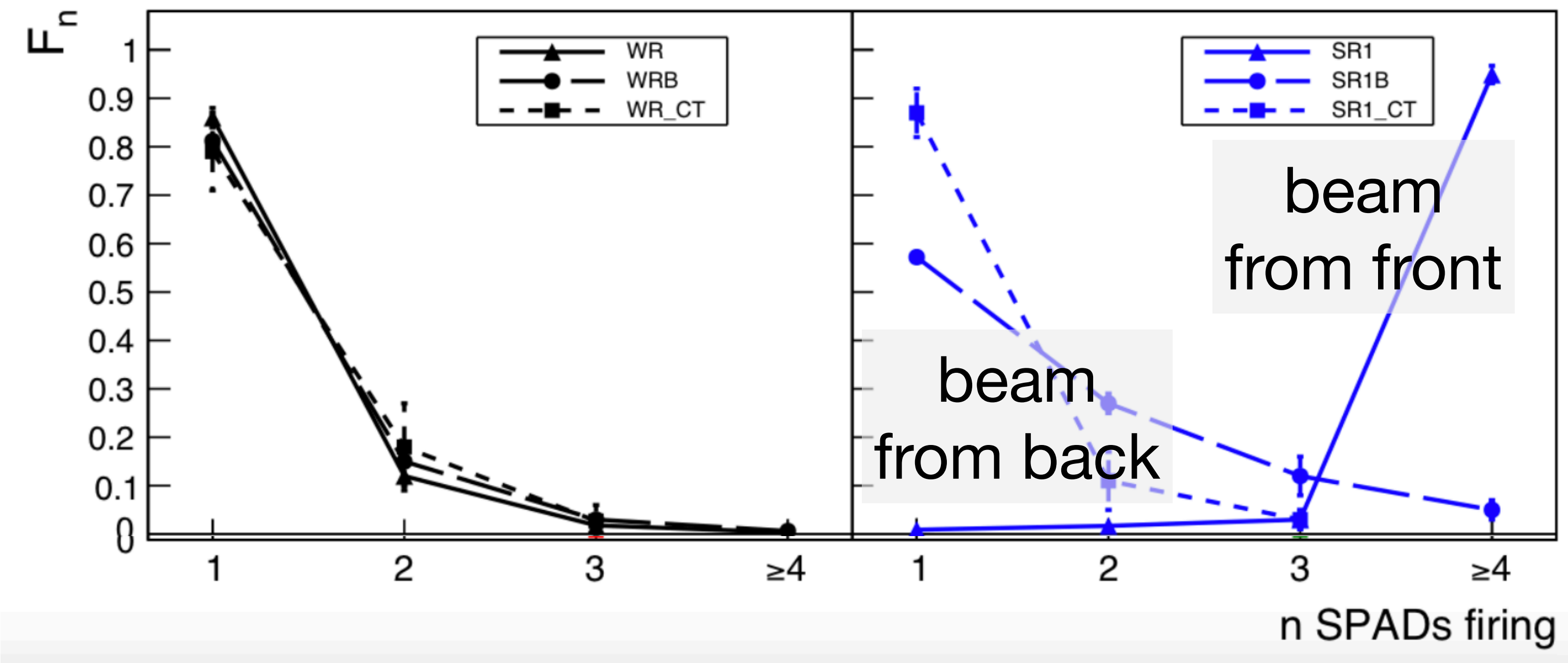

F Carnesecchi et al, arXiv:2202.04169

Summary

- ALICE studies the *condensed matter* of the strong interaction at high temperature: **the Quark Gluon Plasma**
- Key properties of the plasma are being determined from data:
  - Shear viscosity: close to lower bound
  - First constraints on bulk viscosity
- Charm quarks move with the fluid expansion: **rapid thermalisation**
  - Beauty less so? $\Longrightarrow$ Run 3 and 4 to improve precision
- **Indicate short mean free path strong (residual) interactions**
- Future directions
  - Measurement of **initial temperature in reach for upcoming runs**
  - Future upgrades to understand interactions, thermalisation

Thank you for your attention!

Probing the Quark-Gluon Plasma

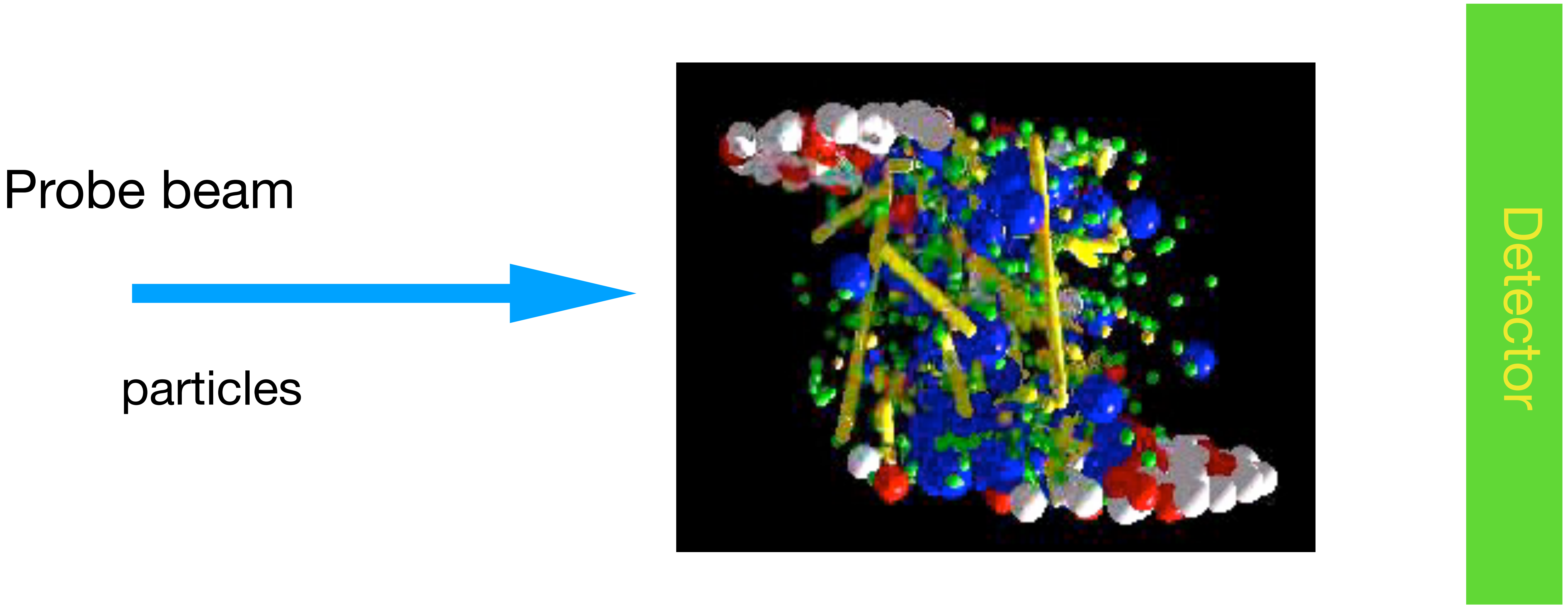

Probing the Quark-Gluon Plasma

Probe beam

particles

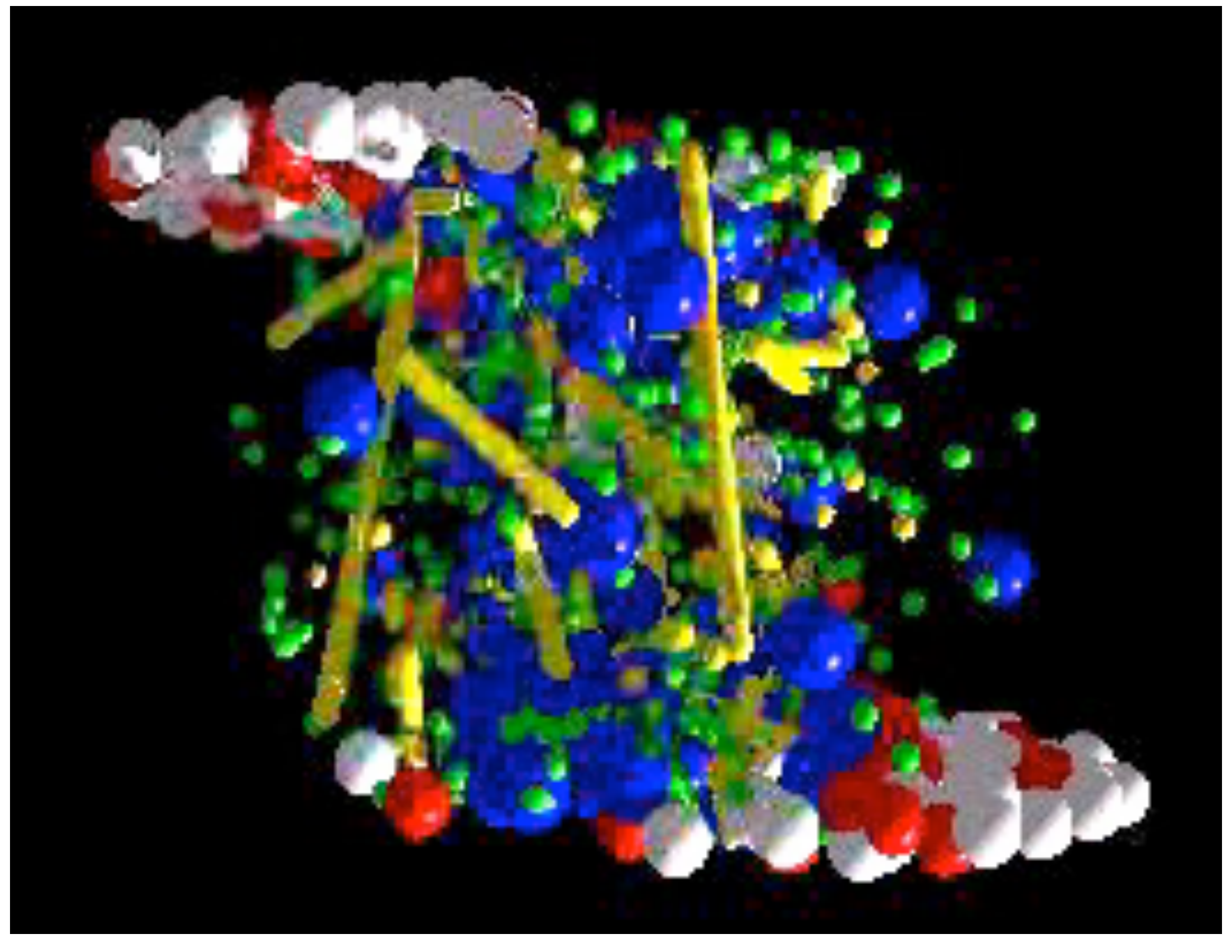

Detector

Not feasible:
Short life time
Small size (~10 fm)

Probing the Quark-Gluon Plasma

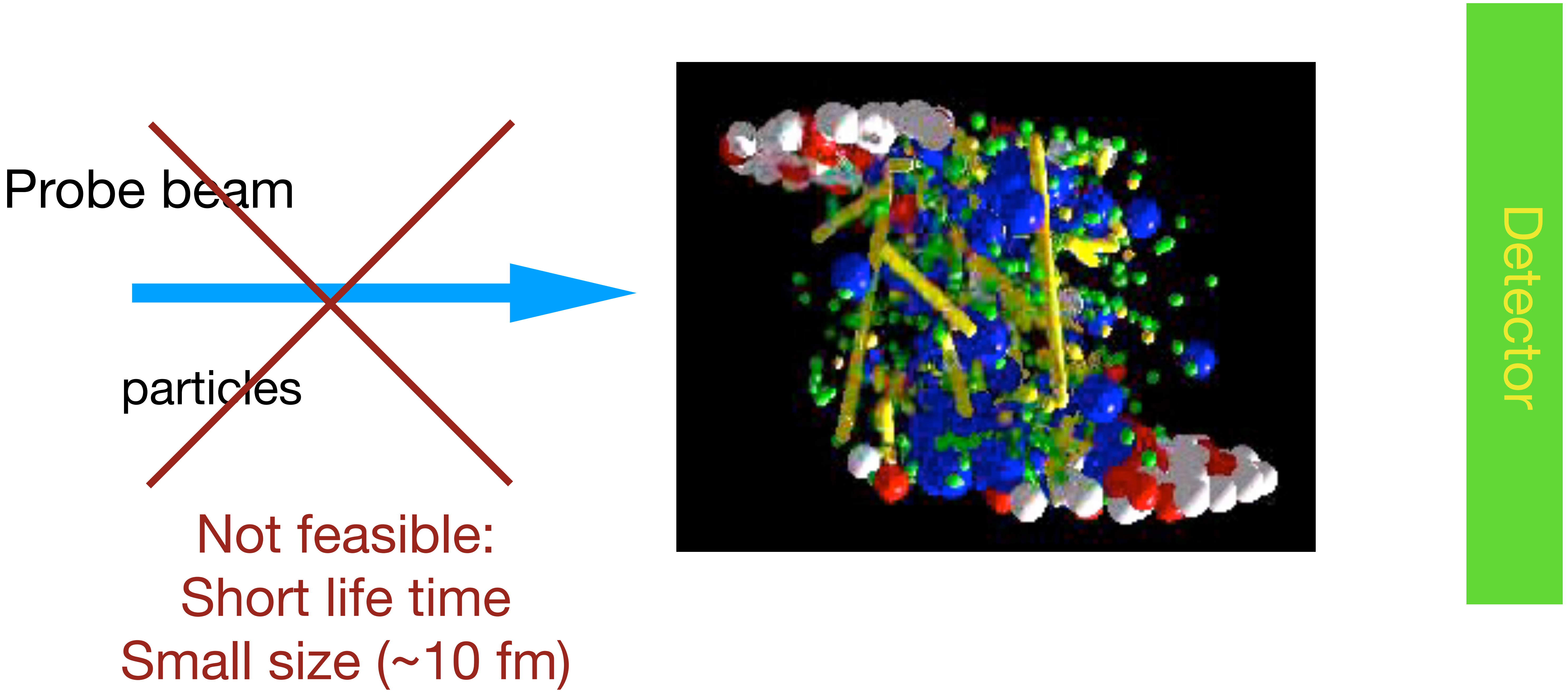

Probing the Quark-Gluon Plasma

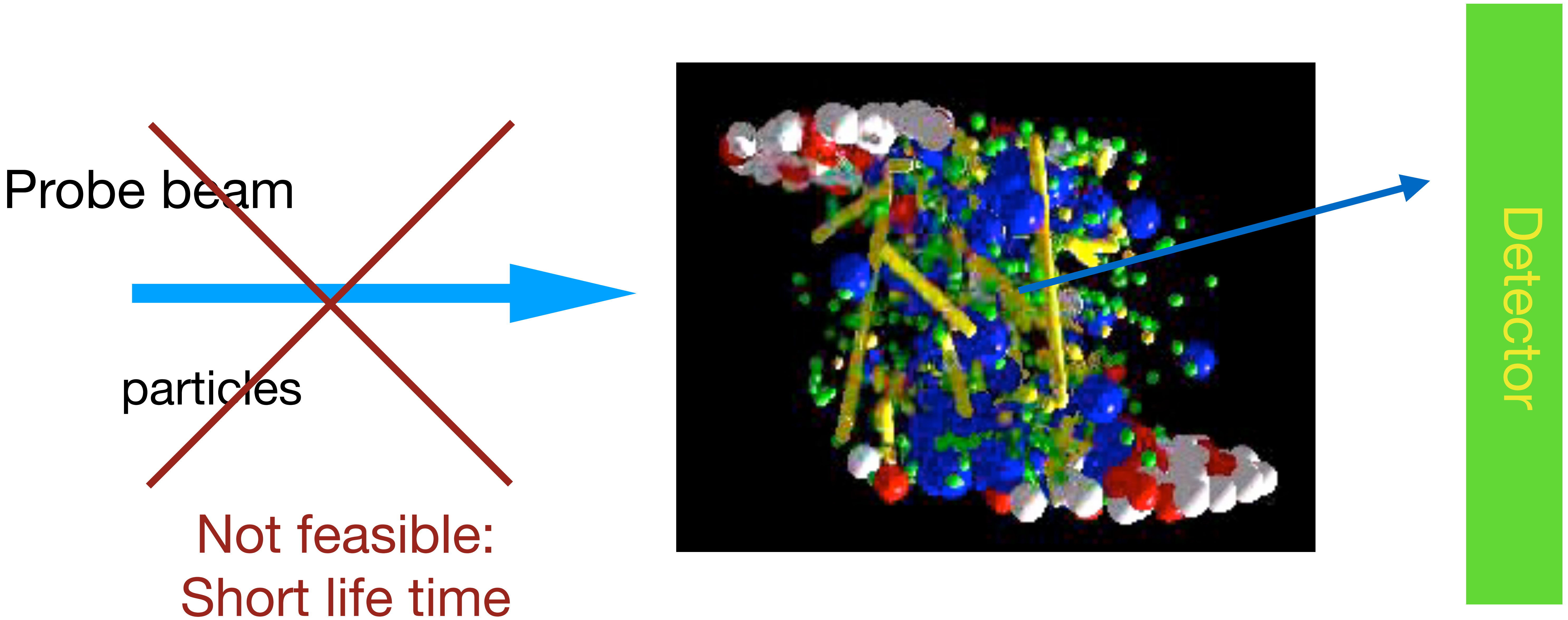

Not feasible:
Short life time
Small size (~10 fm)

Use self-generated probe:
quarks, gluons from hard scattering
large transverse momentum

Nuclear modification of p_T spectra

ALICE, PLB720, 52
CMS, EPJC, 72, 1945
ATLAS, arXiv:1504.04337

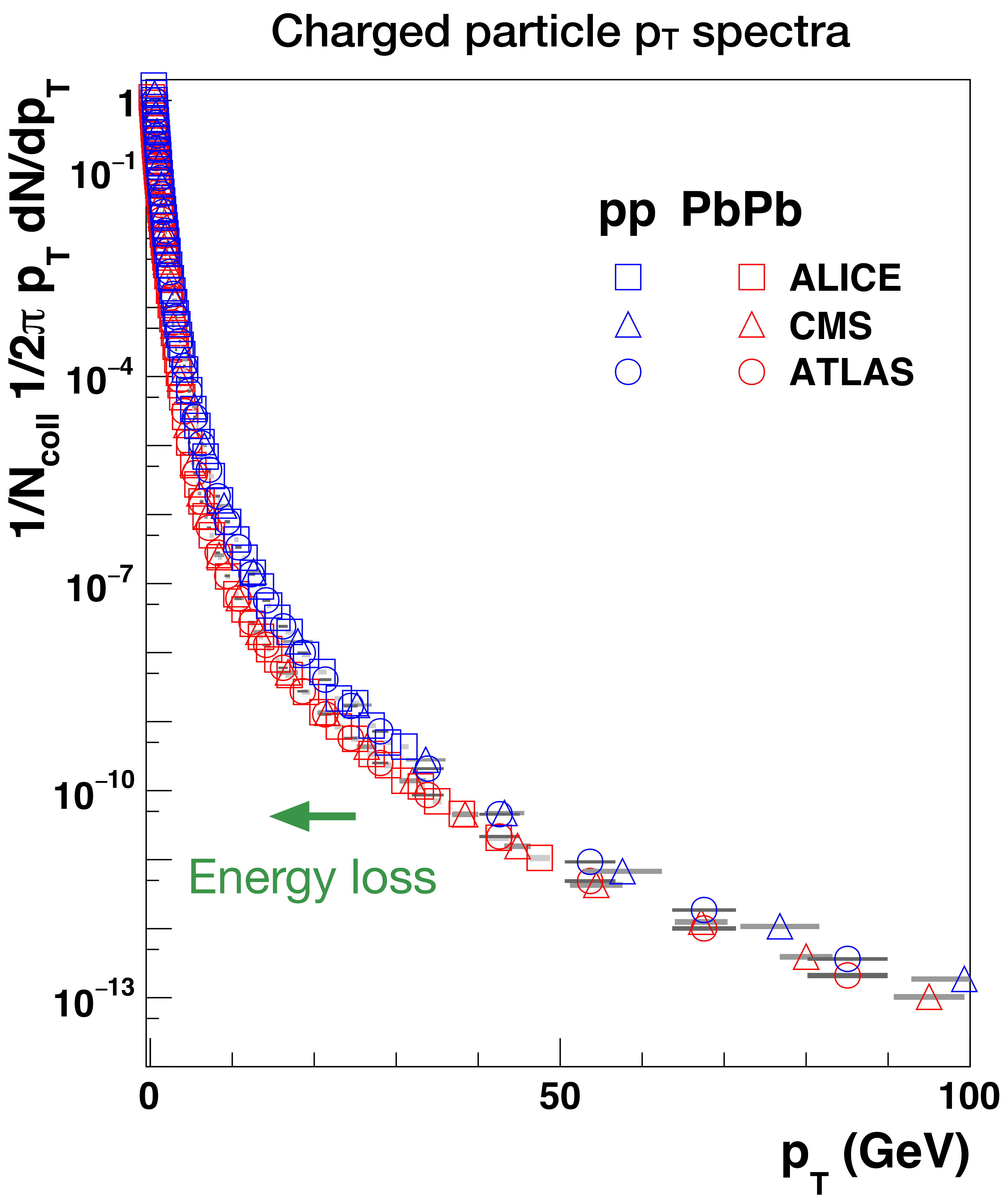

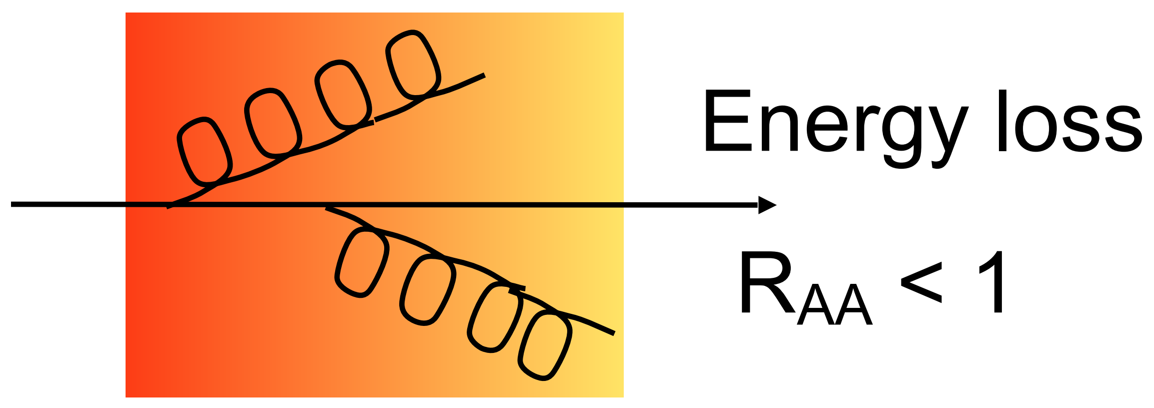

Nuclear modification of p_T spectra

ALICE, PLB720, 52
CMS, EPJC, 72, 1945
ATLAS, arXiv:1504.04337

ALICE

Charged particle p_T spectra

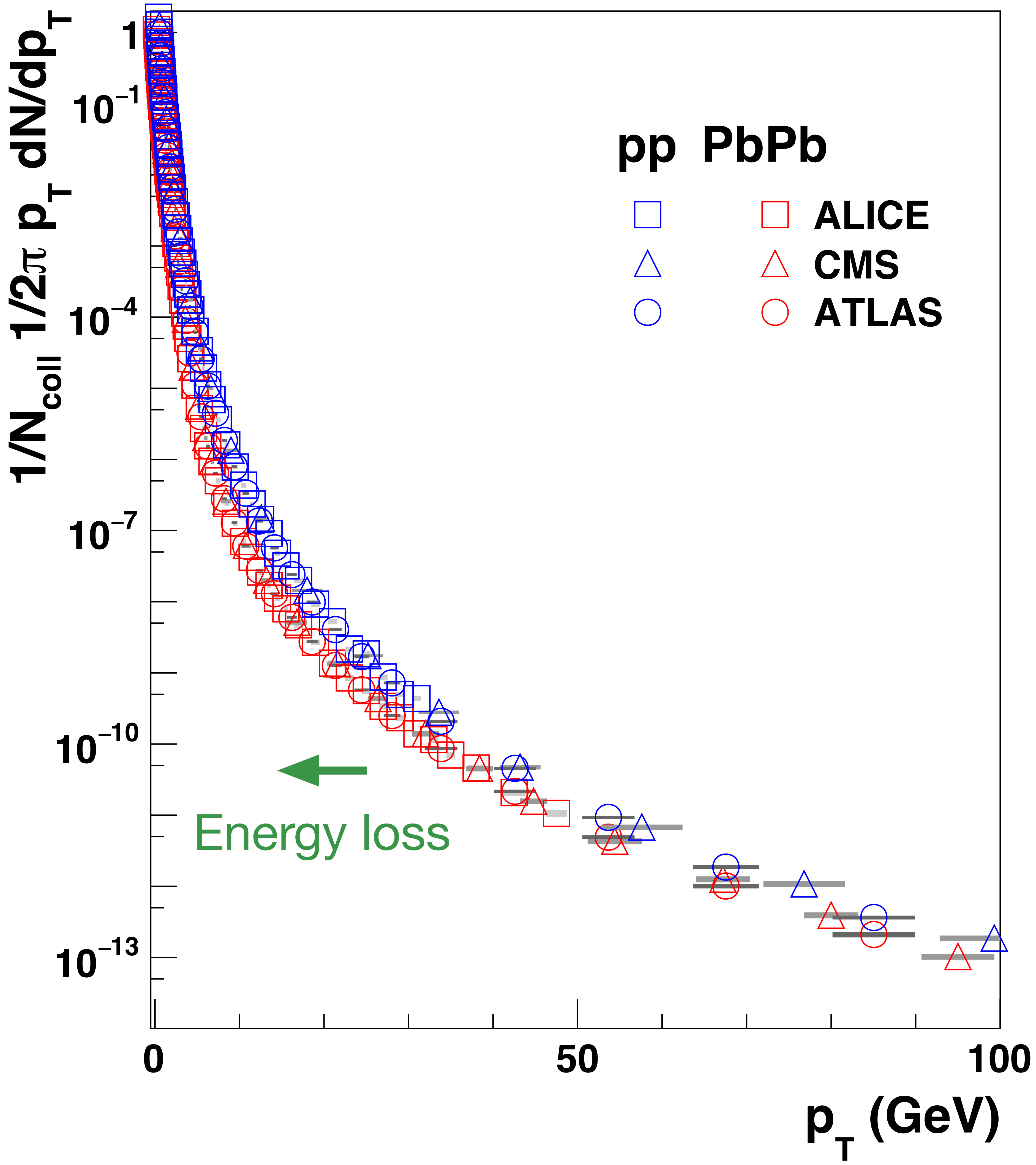

Nuclear modification factor

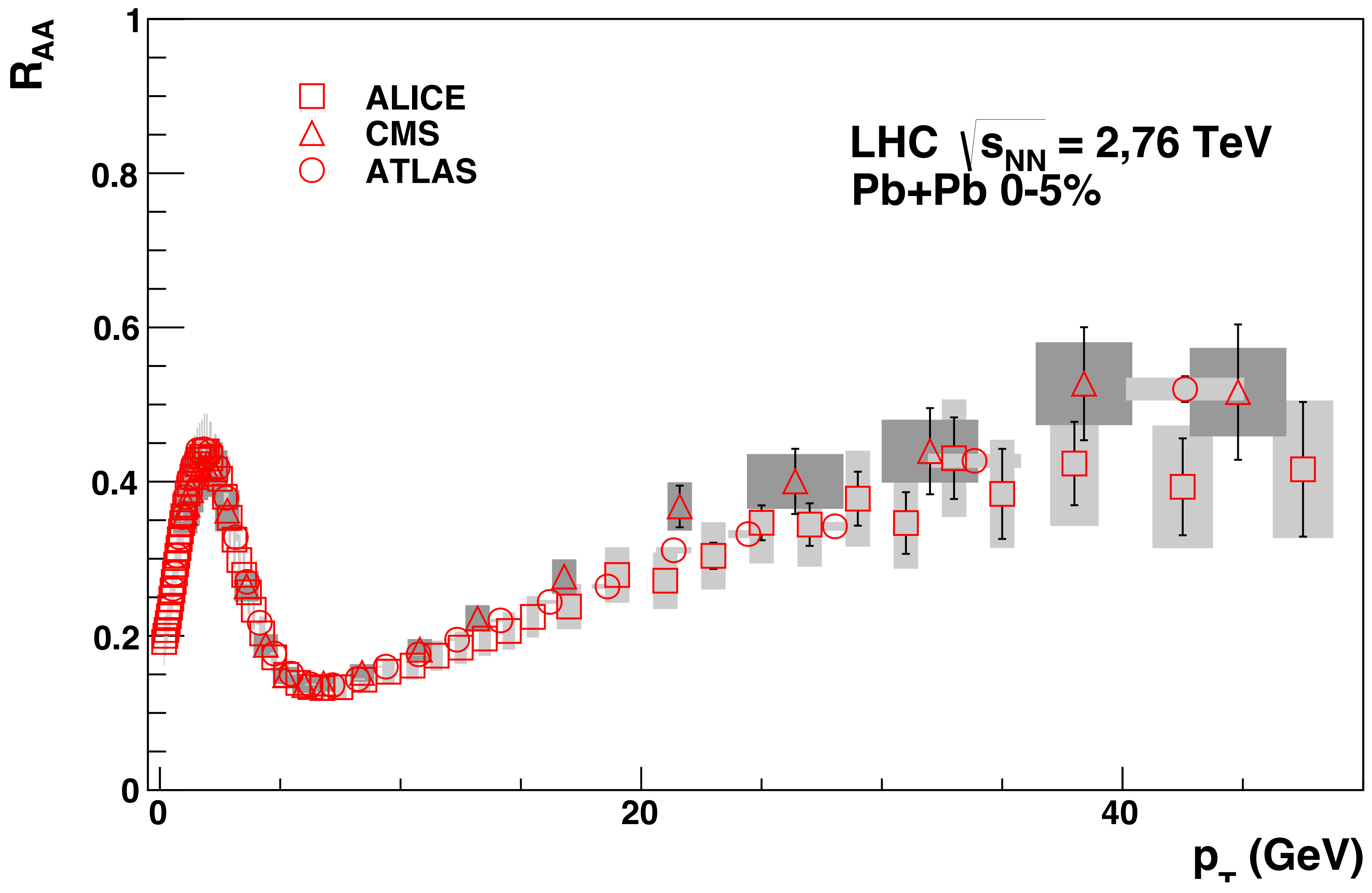

$$R_{AA} = \frac{dN/dp_T|_{A+A}}{N_{coll}\ dN/dp_T|_{p+p}}$$

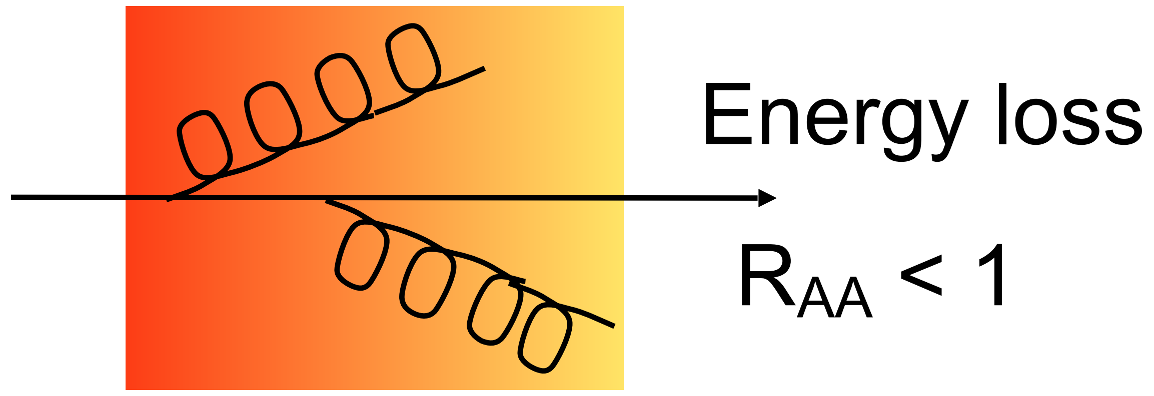

Pb+Pb: clear suppression ($R_{AA} < 1$): parton energy loss

Nuclear modification of p_T spectra

ALICE, PLB720, 52
CMS, EPJC, 72, 1945
ATLAS, arXiv:1504.04337

Charged particle p_T spectra

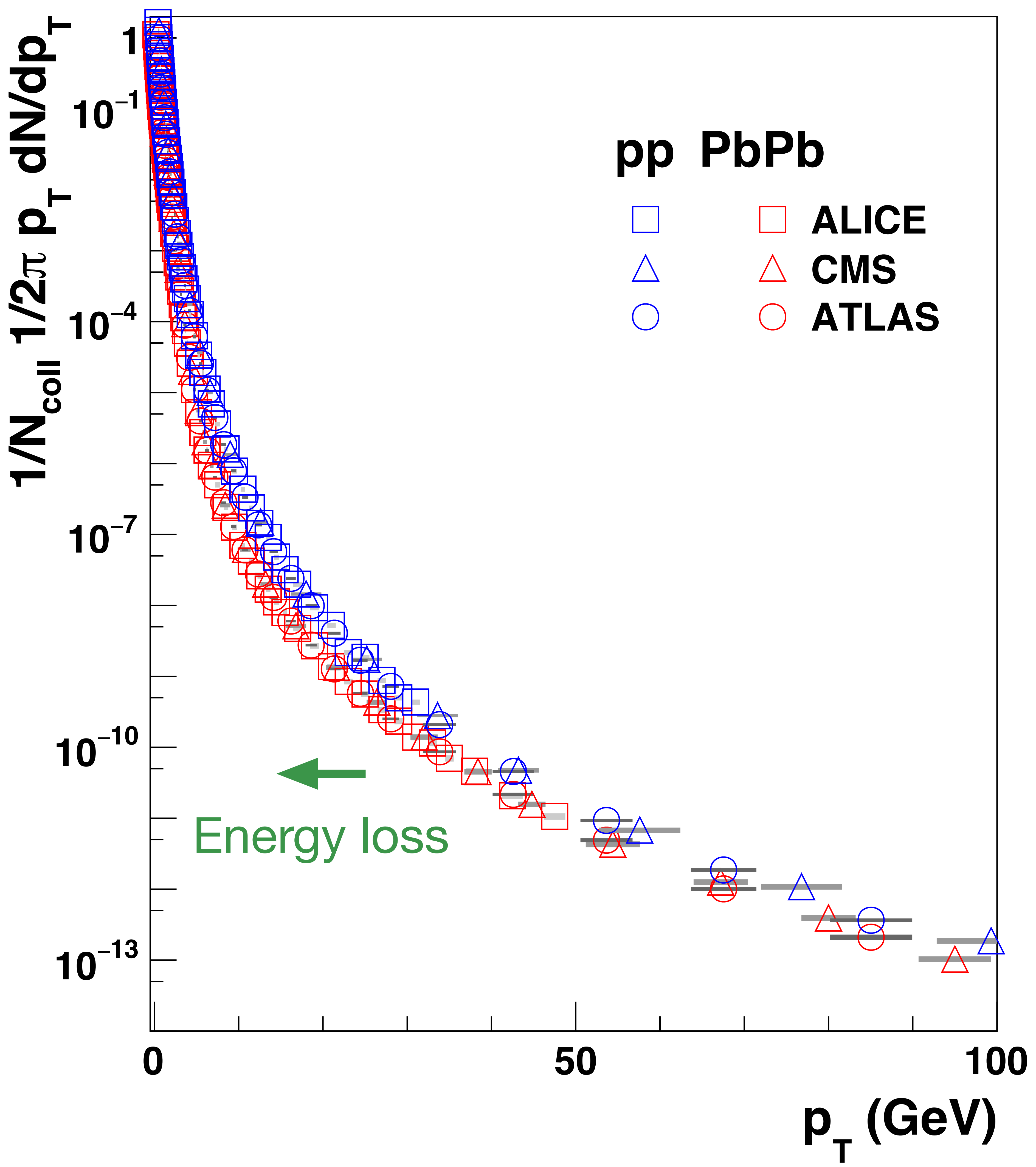

Nuclear modification factor

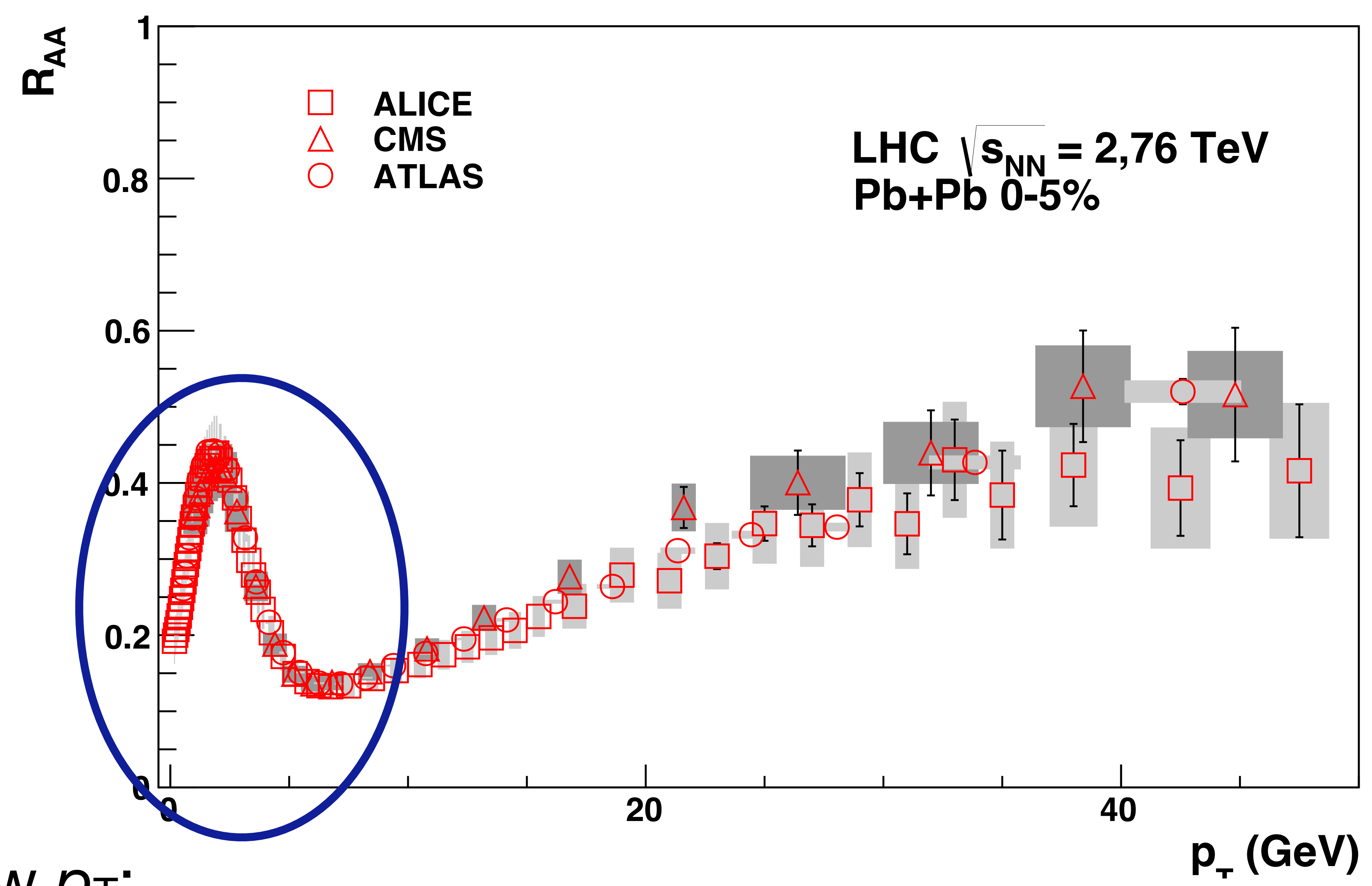

Low p_T:
soft production,
N_{part} scaling

$$R_{AA} = \frac{dN/dp_T|_{A+A}}{N_{coll}\ dN/dp_T|_{p+p}}$$

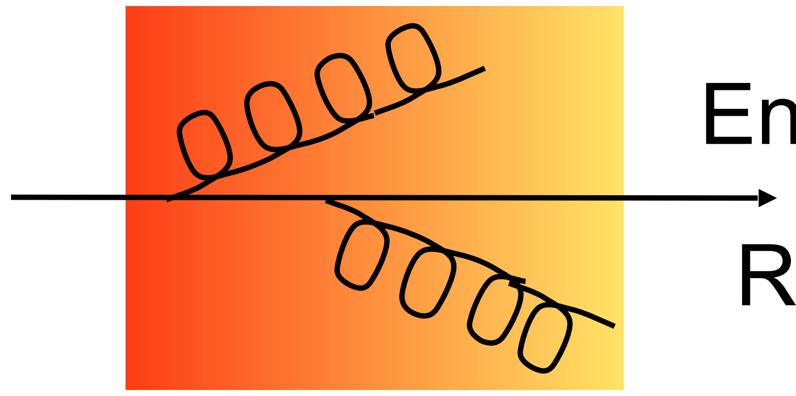

Energy loss

$R_{AA} < 1$

Pb+Pb: clear suppression ($R_{AA} < 1$): parton energy loss

Nuclear modification and elliptic flow of D mesons

D mesons contain a charm quark m >> T, that is produced in an initial hard scattering

Nuclear modification factor

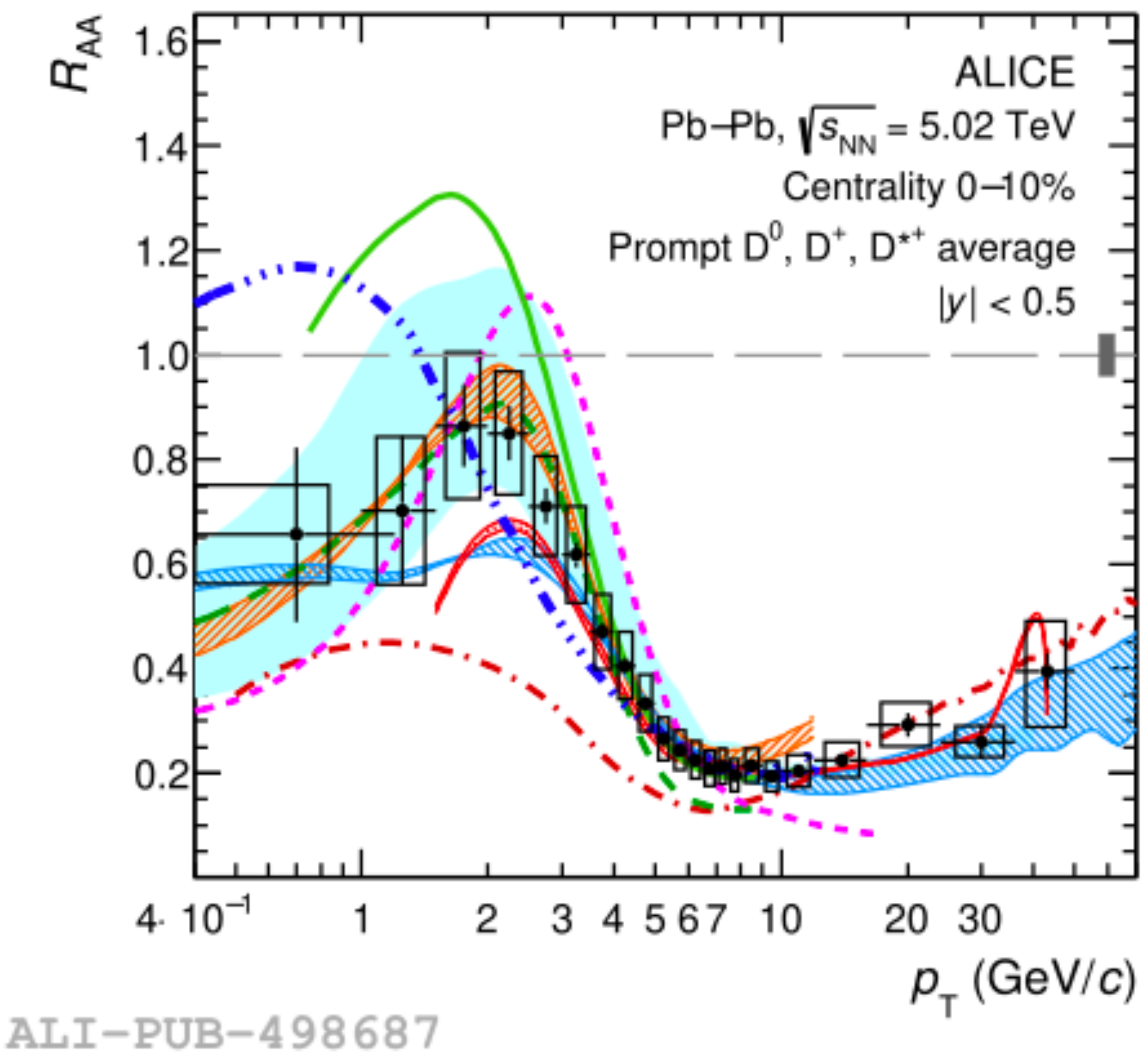

ALICE, JHEP 01 (2022) 174

Elliptic flow v_2

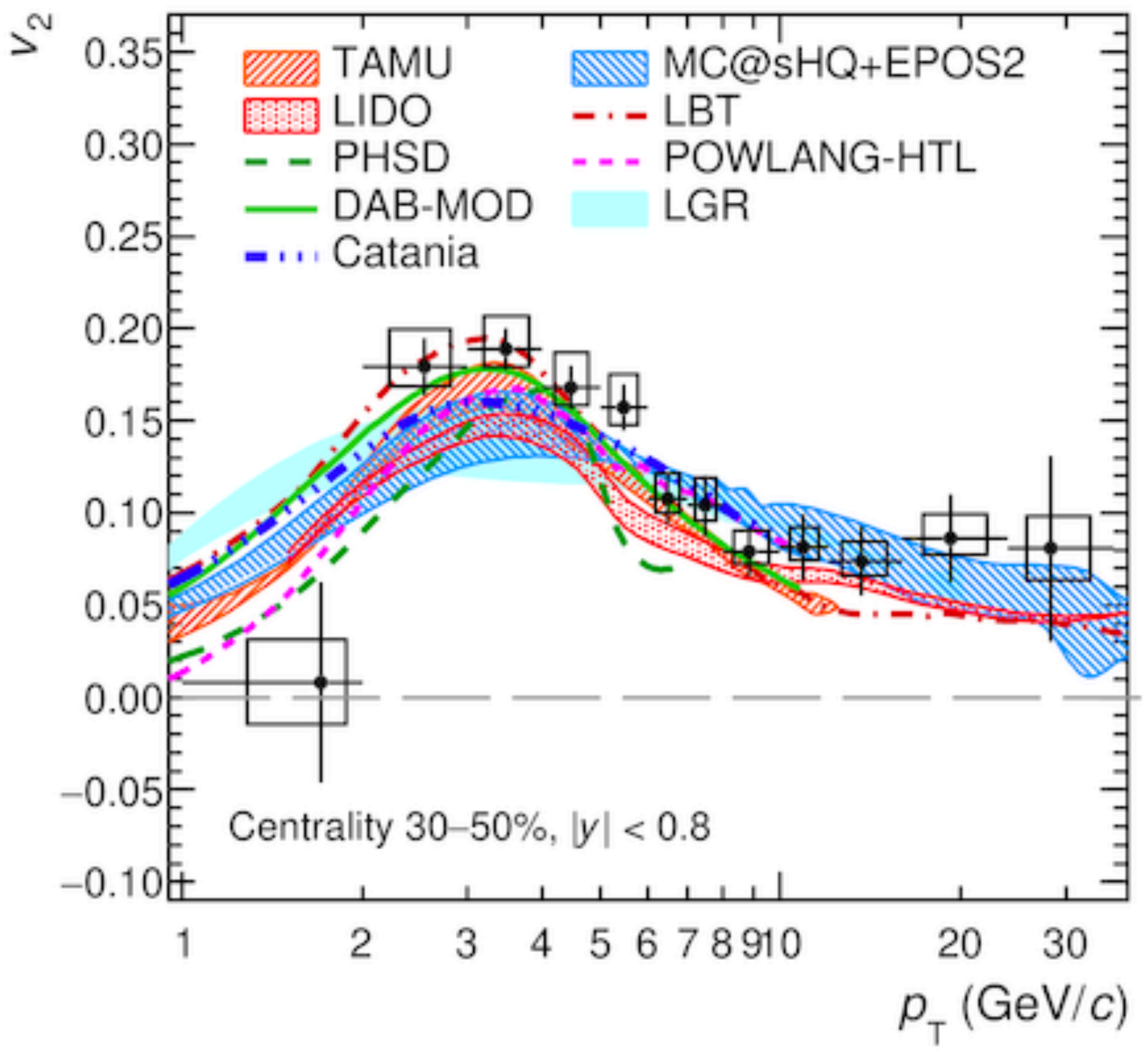

ALICE, JHEP 01 (2022) 174

Nuclear modification and elliptic flow of D mesons

D mesons contain a charm quark m >> T, that is produced in an initial hard scattering

Nuclear modification factor

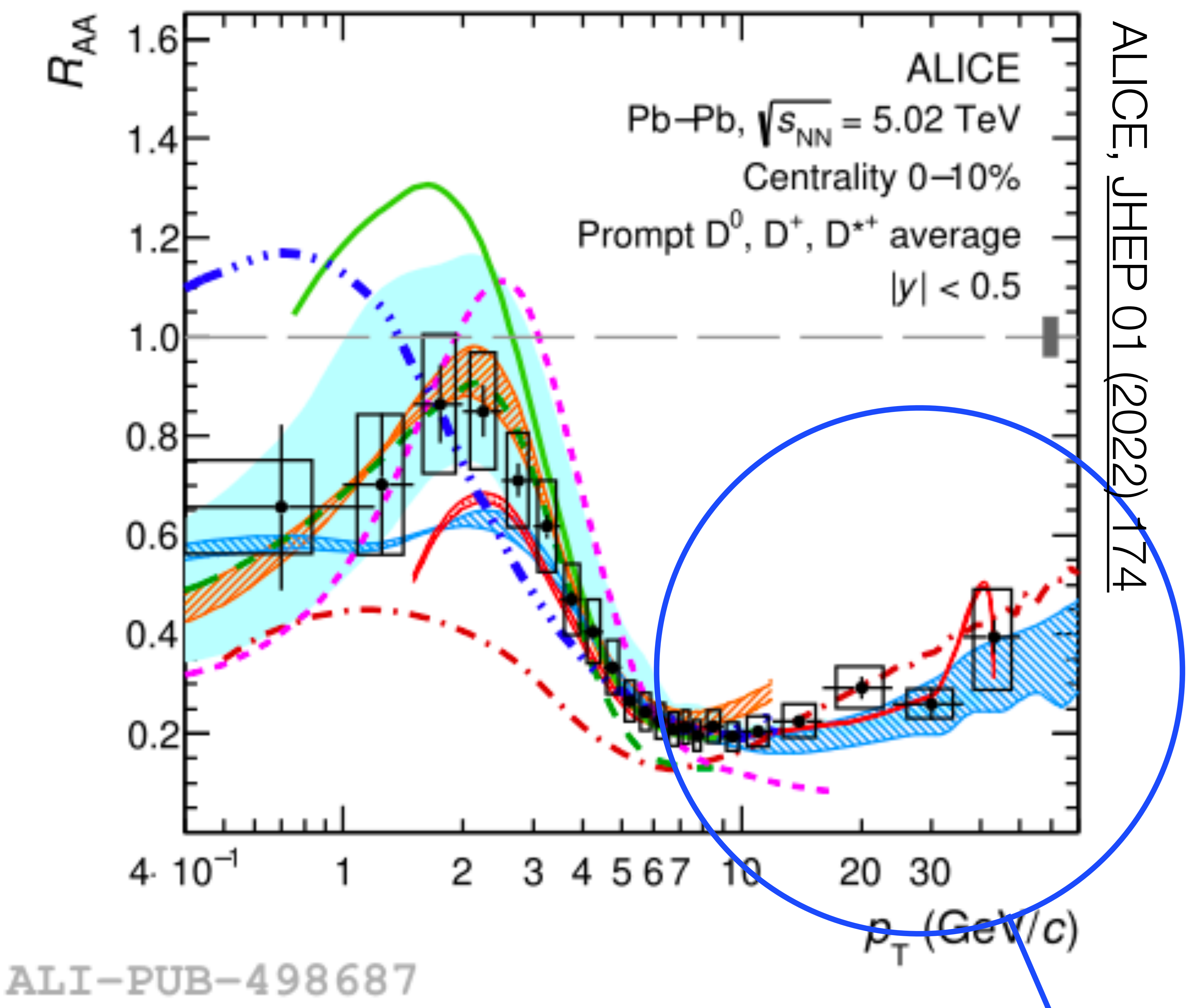

ALICE, JHEP 01 (2022) 174

Elliptic flow v2

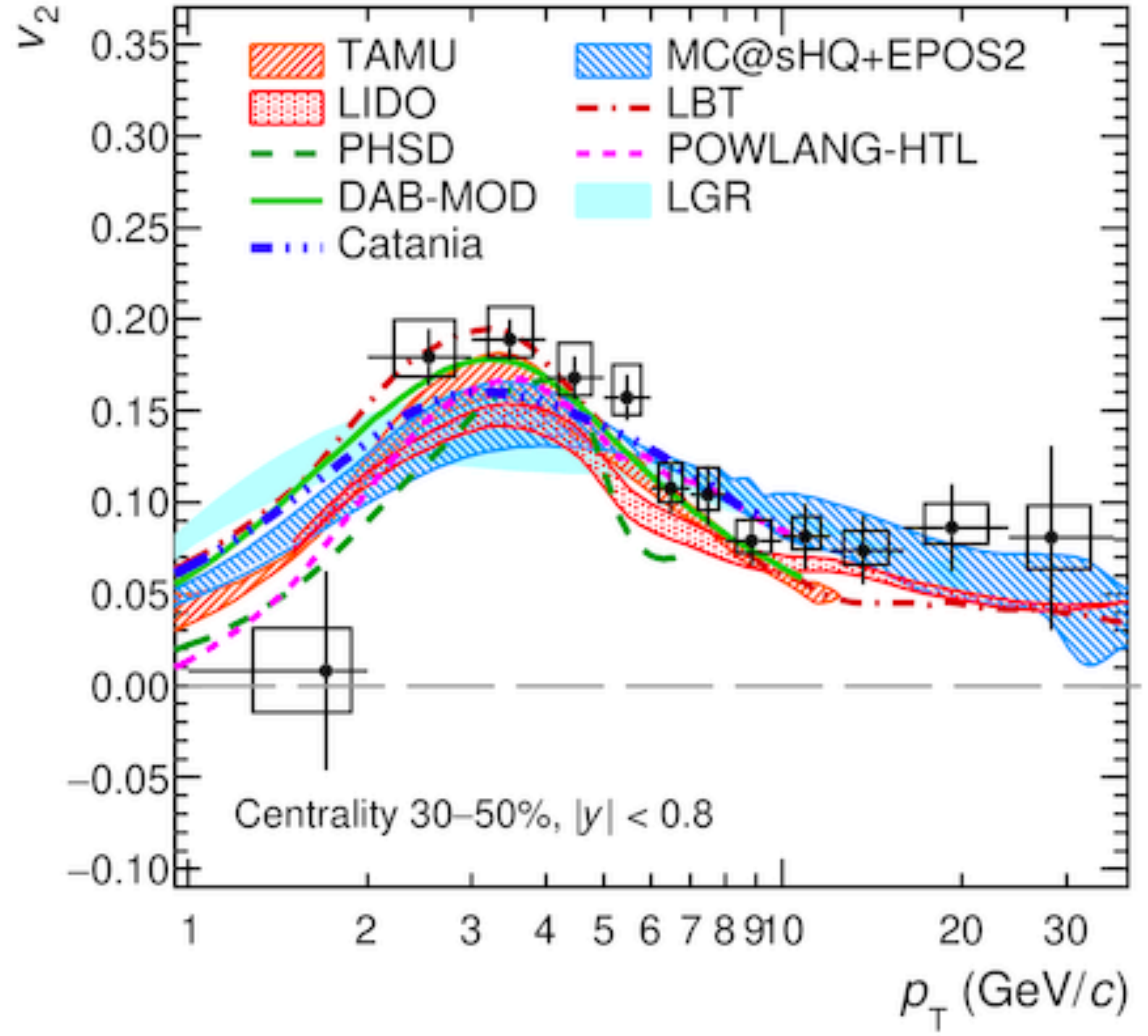

ALICE, JHEP 01 (2022) 174

High-p_T suppression:
due to energy loss

Nuclear modification and elliptic flow of D mesons

D mesons contain a charm quark m >> T, that is produced in an initial hard scattering

Nuclear modification factor

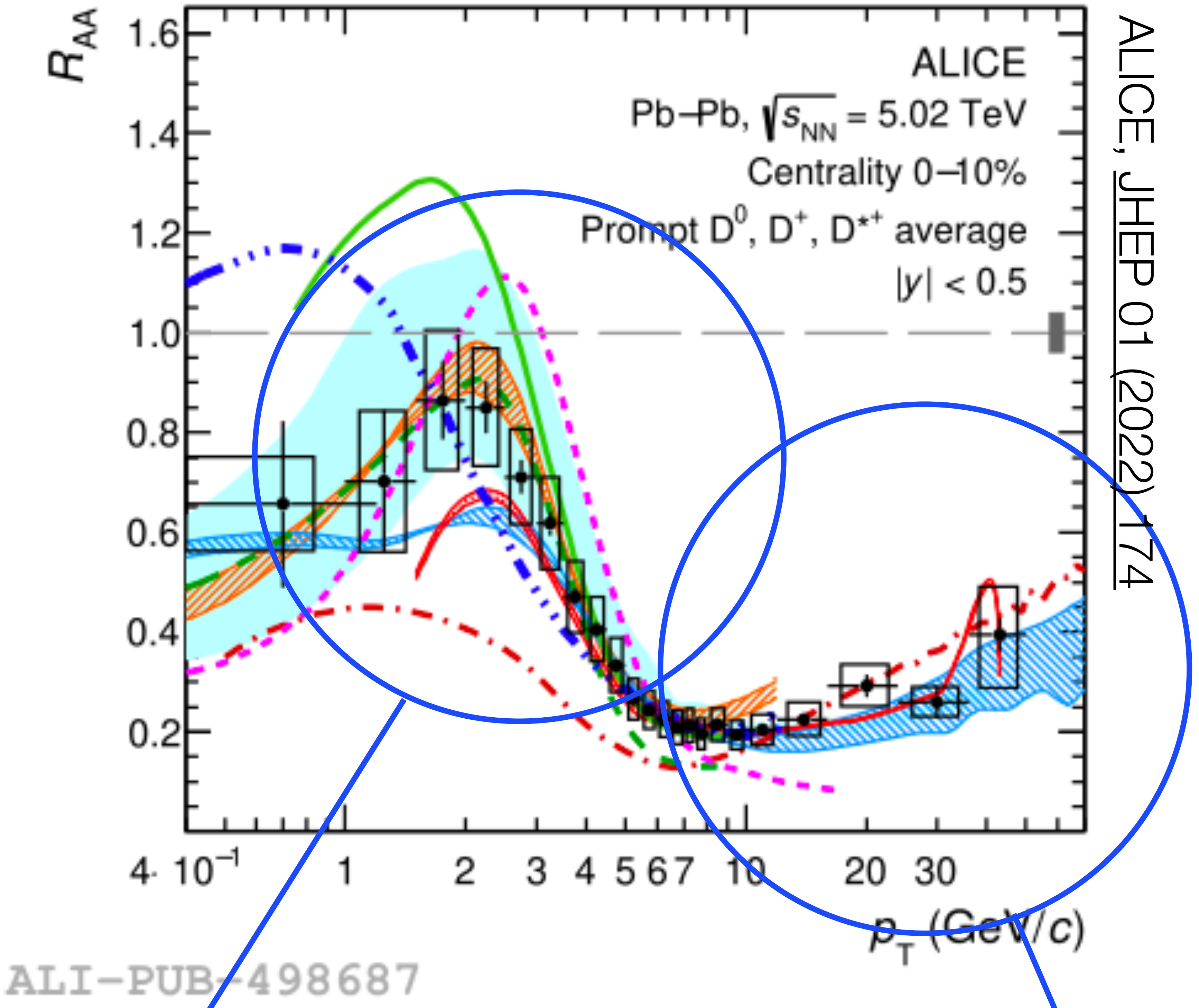

Low p_T: no change/enhancement: charm conservation + diffusion

High-p_T suppression: due to energy loss

Elliptic flow v_2

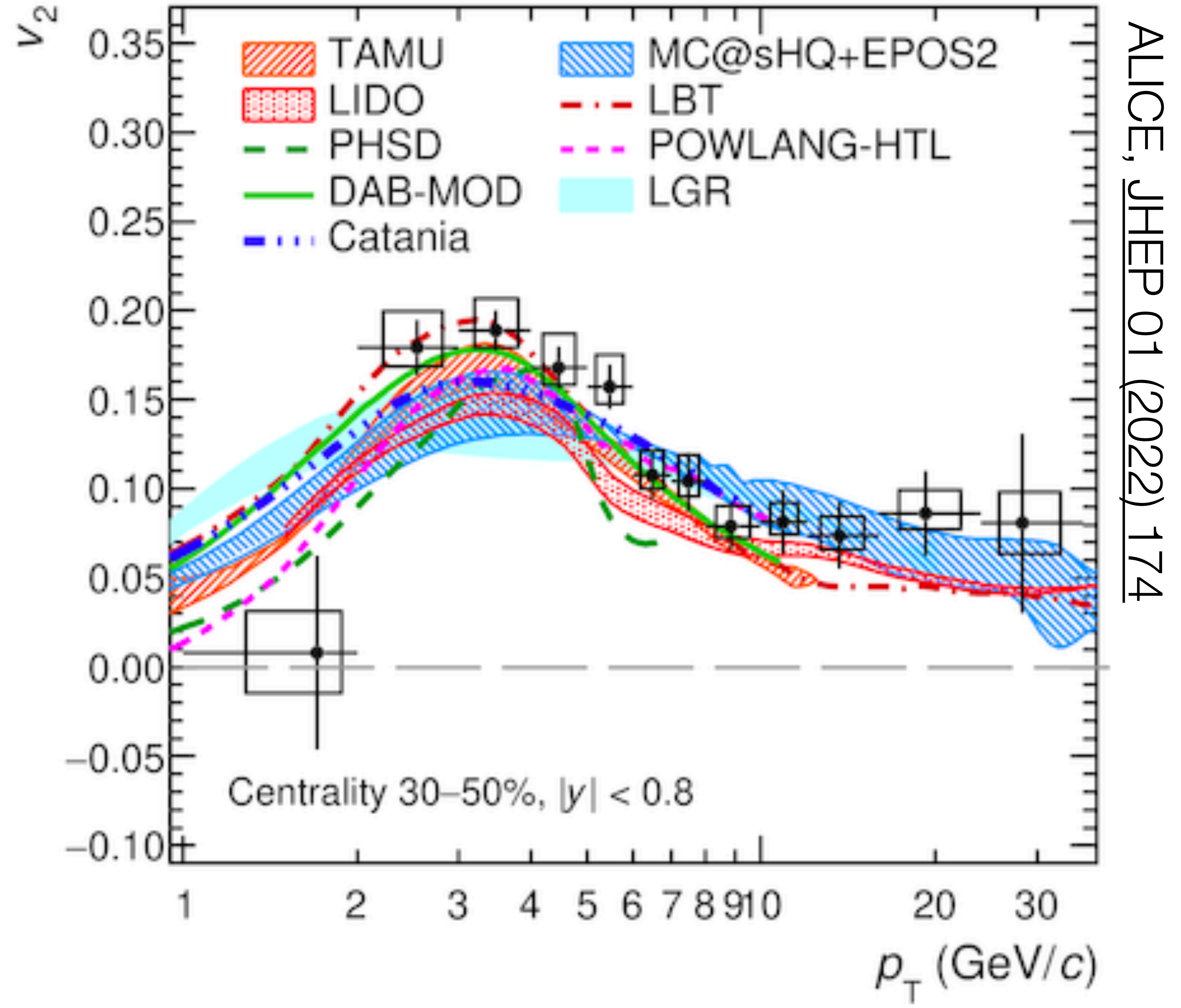

Nuclear modification and elliptic flow of D mesons

D mesons contain a charm quark m >> T, that is produced in an initial hard scattering

Nuclear modification factor

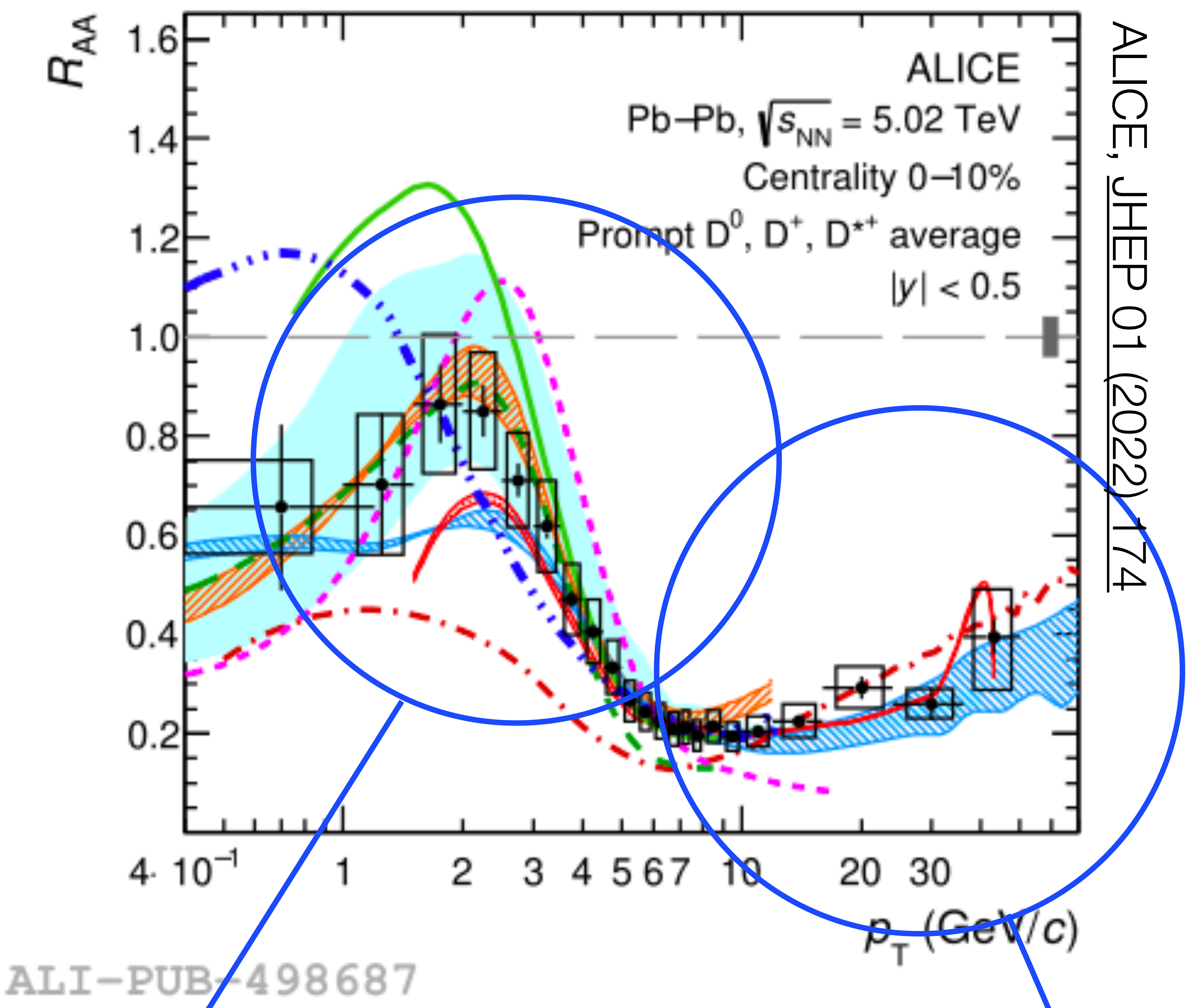

Low p_T: no change/enhancement: charm conservation + diffusion

High-p_T suppression: due to energy loss

Elliptic flow v_2

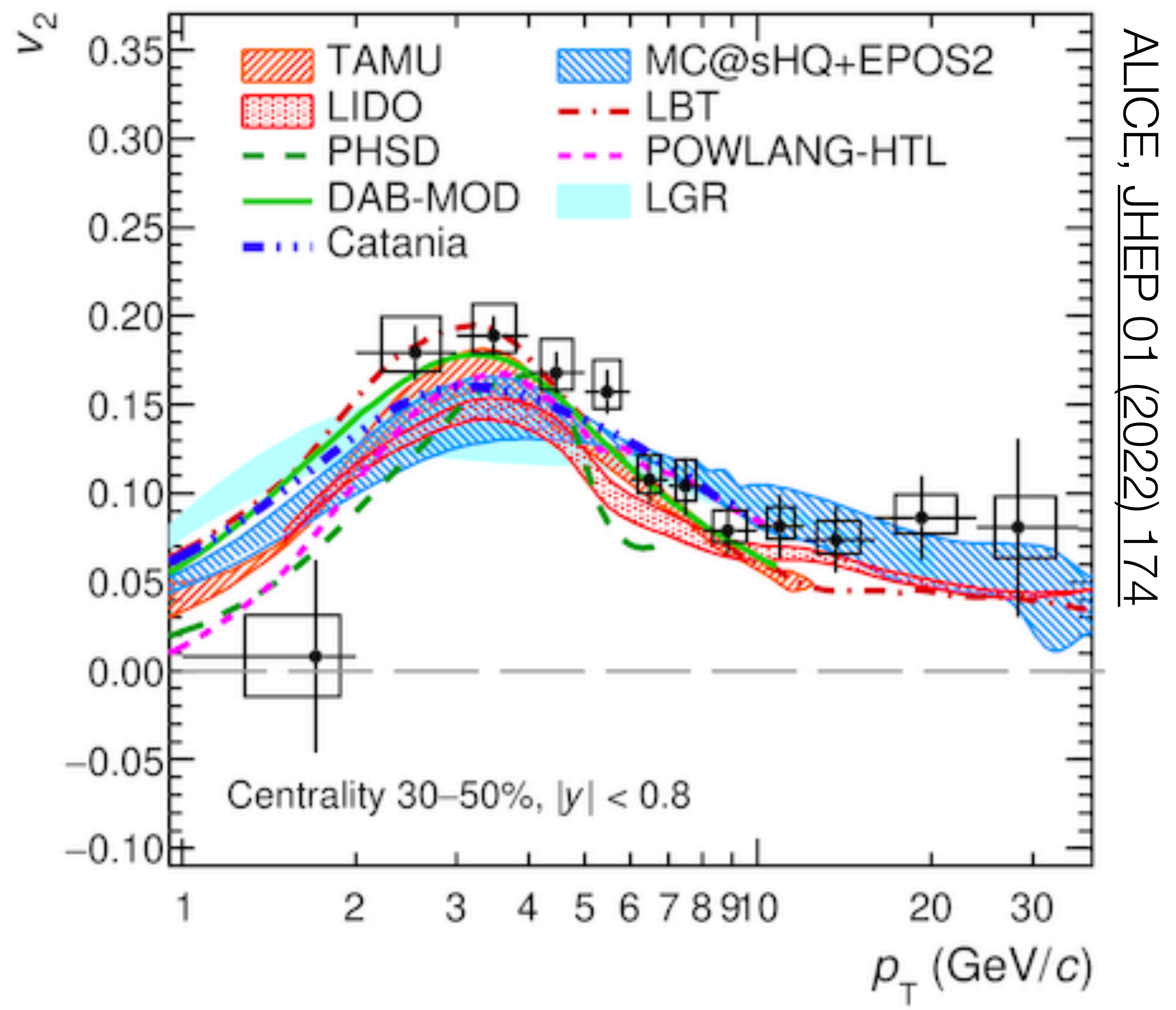

Azimuthal anisotropy: Full effect generated by interactions

Determining the transport coefficients

Run model for different parameter settings

interpolate with Gaussian process emulator

Posterior

Range of model settings that agree with data

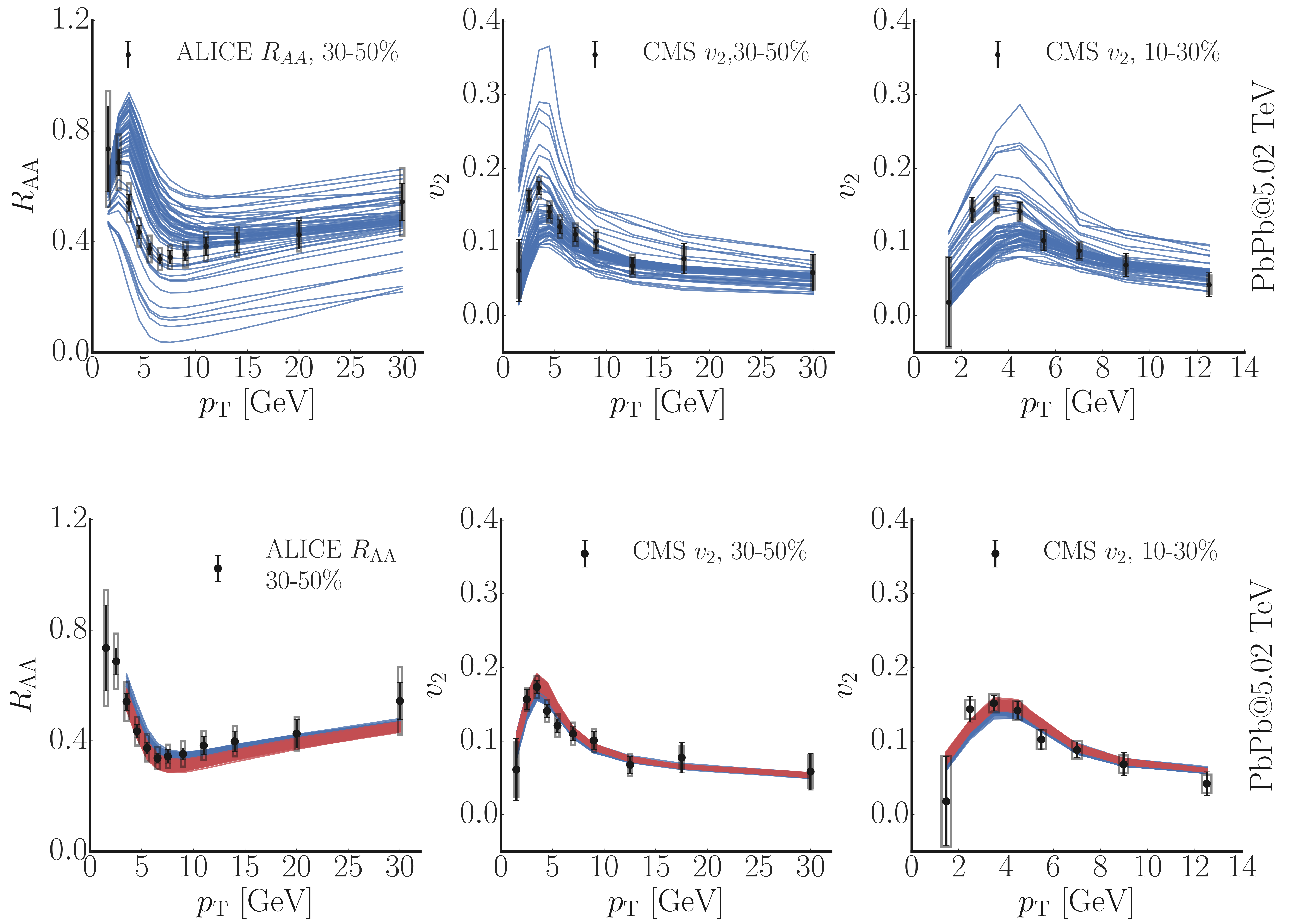

Heavy flavor transport coefficient: Bayesian fit

Diffusion coefficient D_s | **Transport coefficient $\hat{q}$**

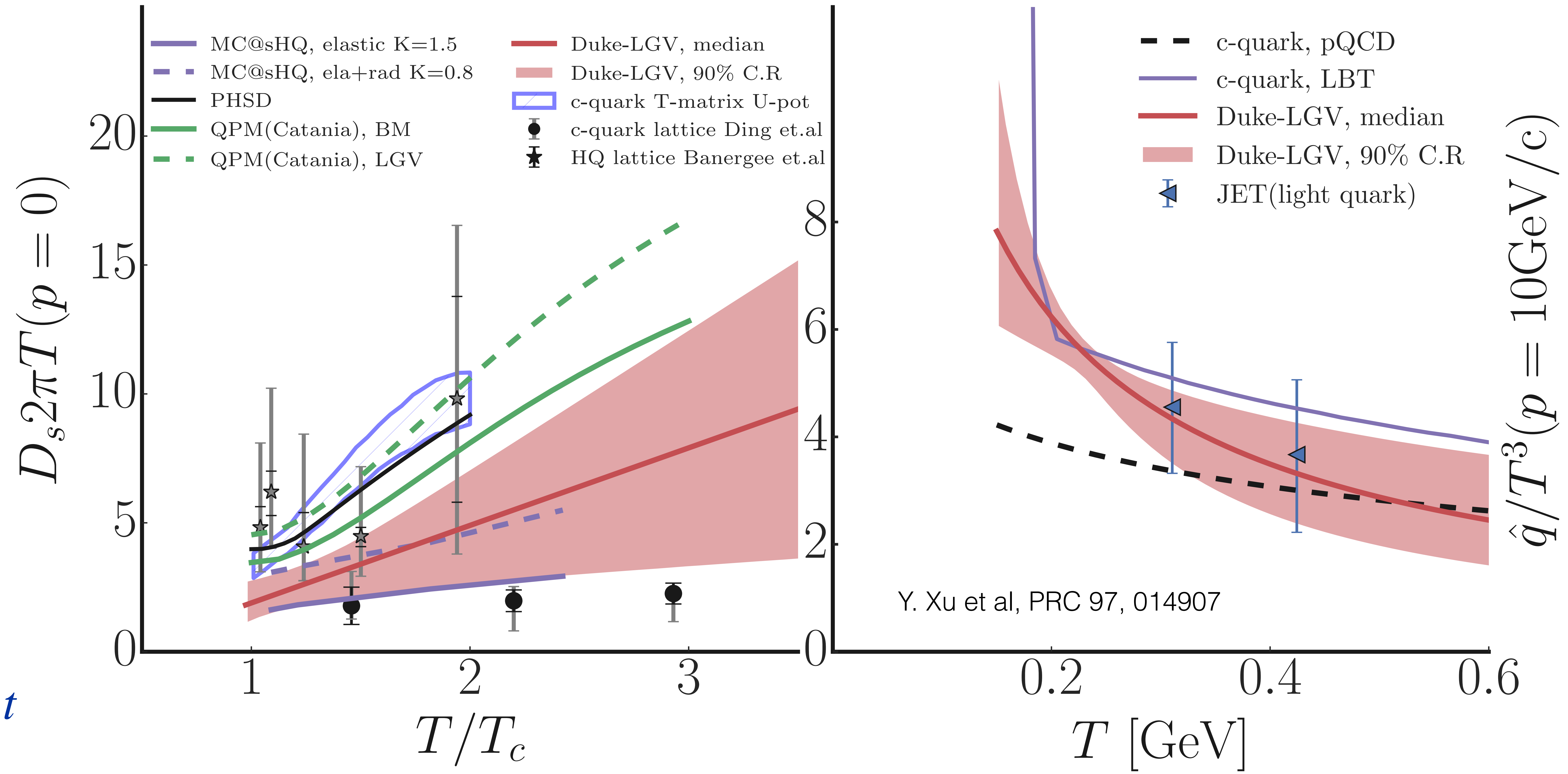

$$\langle r^2 \rangle = 6\, D_s\, t$$

$$\hat{q} = \frac{\langle q_\perp^2 \rangle}{\lambda}$$

Data constrain transport properties of the QGP

Results agree with lattice QCD/pQCD expectations
and between light and heavy flavour sector

Heavy-ion collisions as a laboratory for nuclear and hadron physics

Example: life time of strange baryons and nuclei

Proper decay length distribution

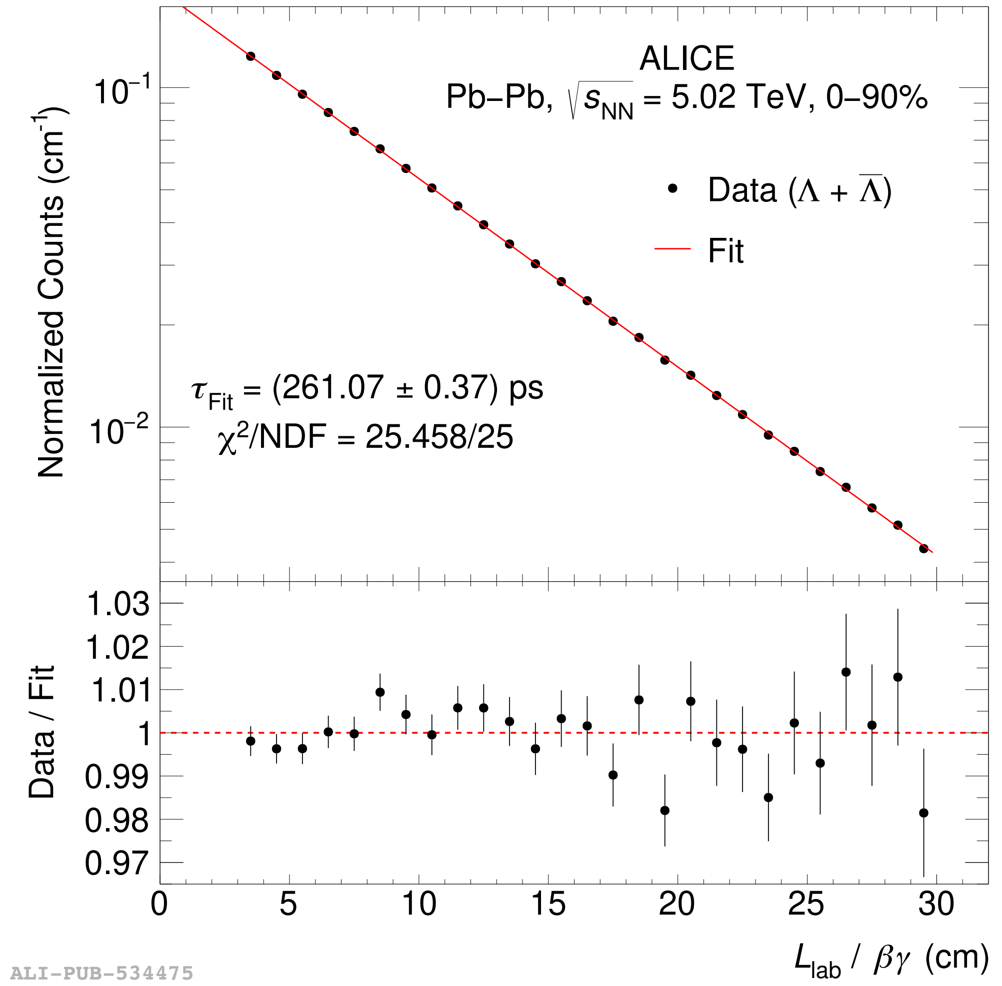

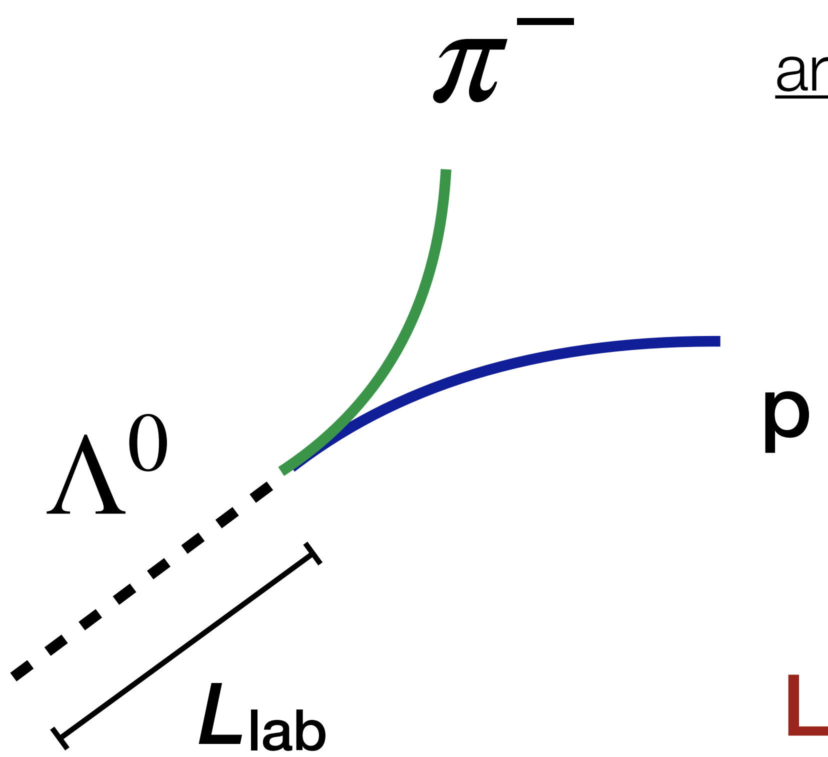

arXiv:2303.00606

Life time: comparison to existing results

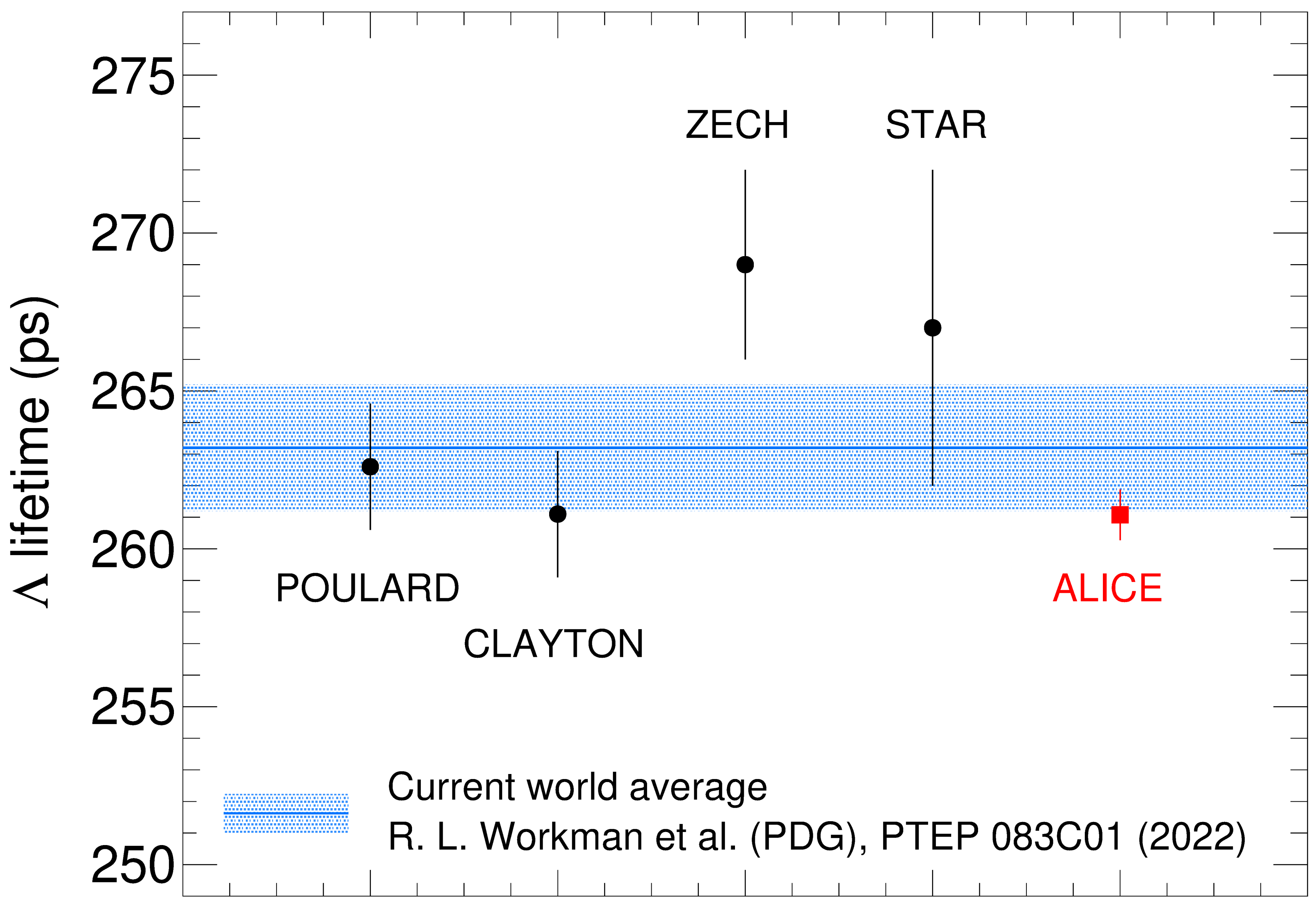

ALI-PUB-534483

$$\tau_{\Lambda+\bar{\Lambda}} = [261.07 \pm 0.37(\mathrm{stat.}) \pm 0.72(\mathrm{syst.})]\ \mathrm{ps}.$$

Hypernuclei life time

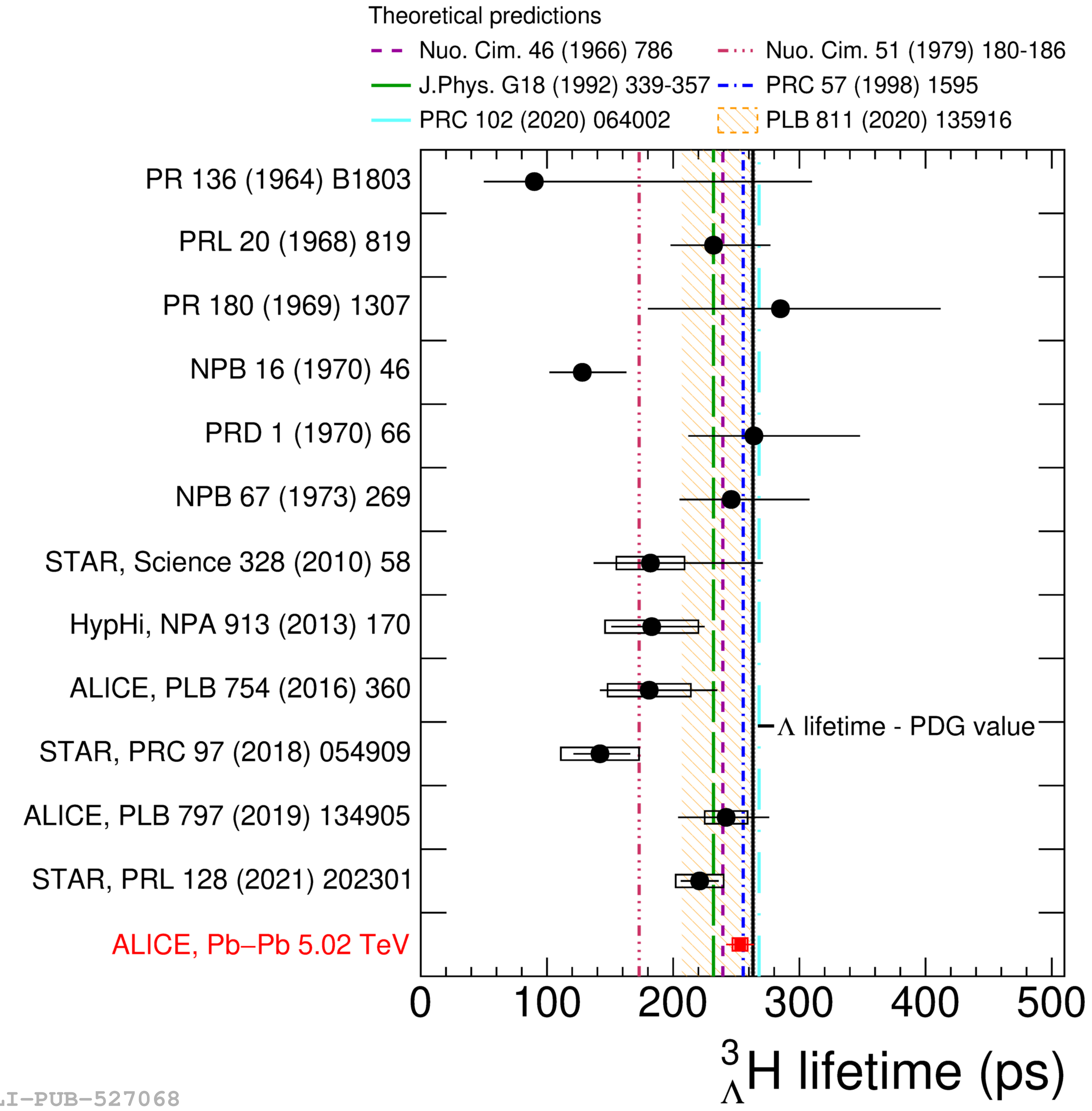

ALI-PUB-527068

arXiv:2209.07360

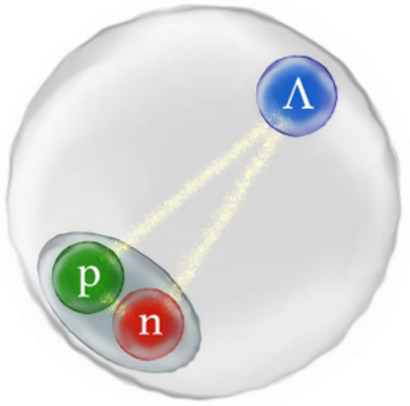

Life time measurements of hyperons and hypernuclei competitive with world data

Thermalisation of heavy quarks

Λ_b v_2 performance

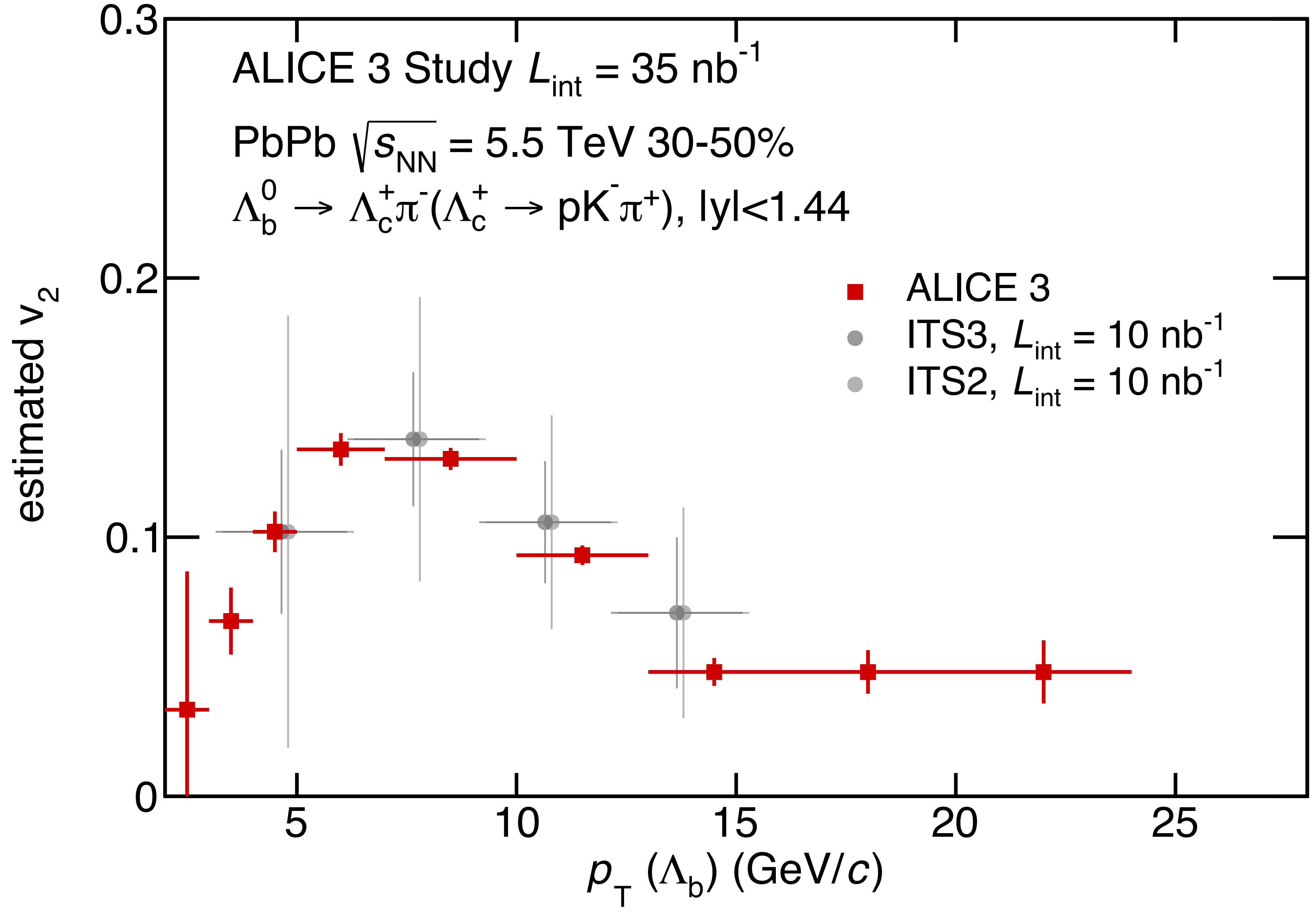

Thermalisation of heavy quarks

Λ_b v_2 performance

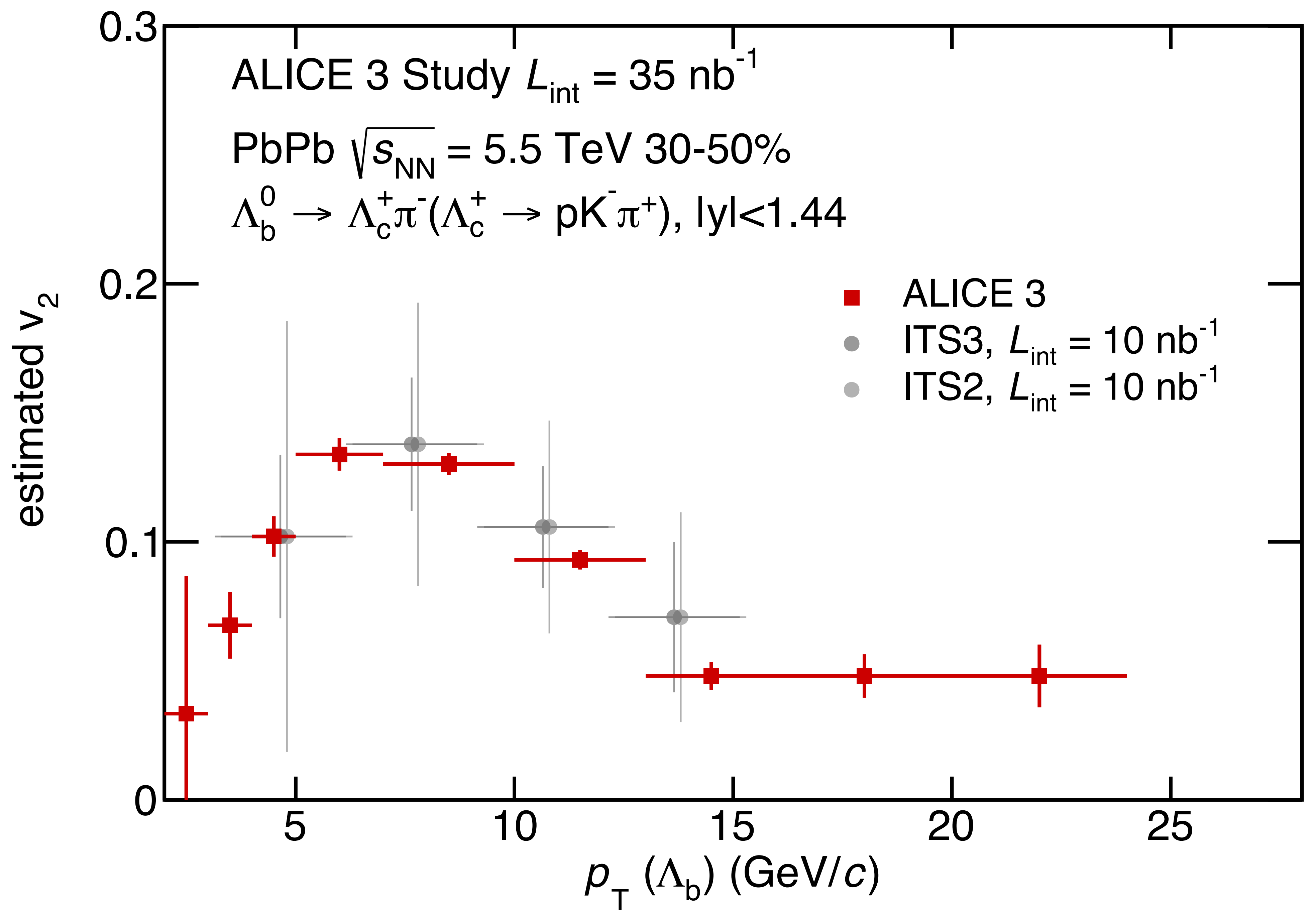

Multi-charm baryon yields

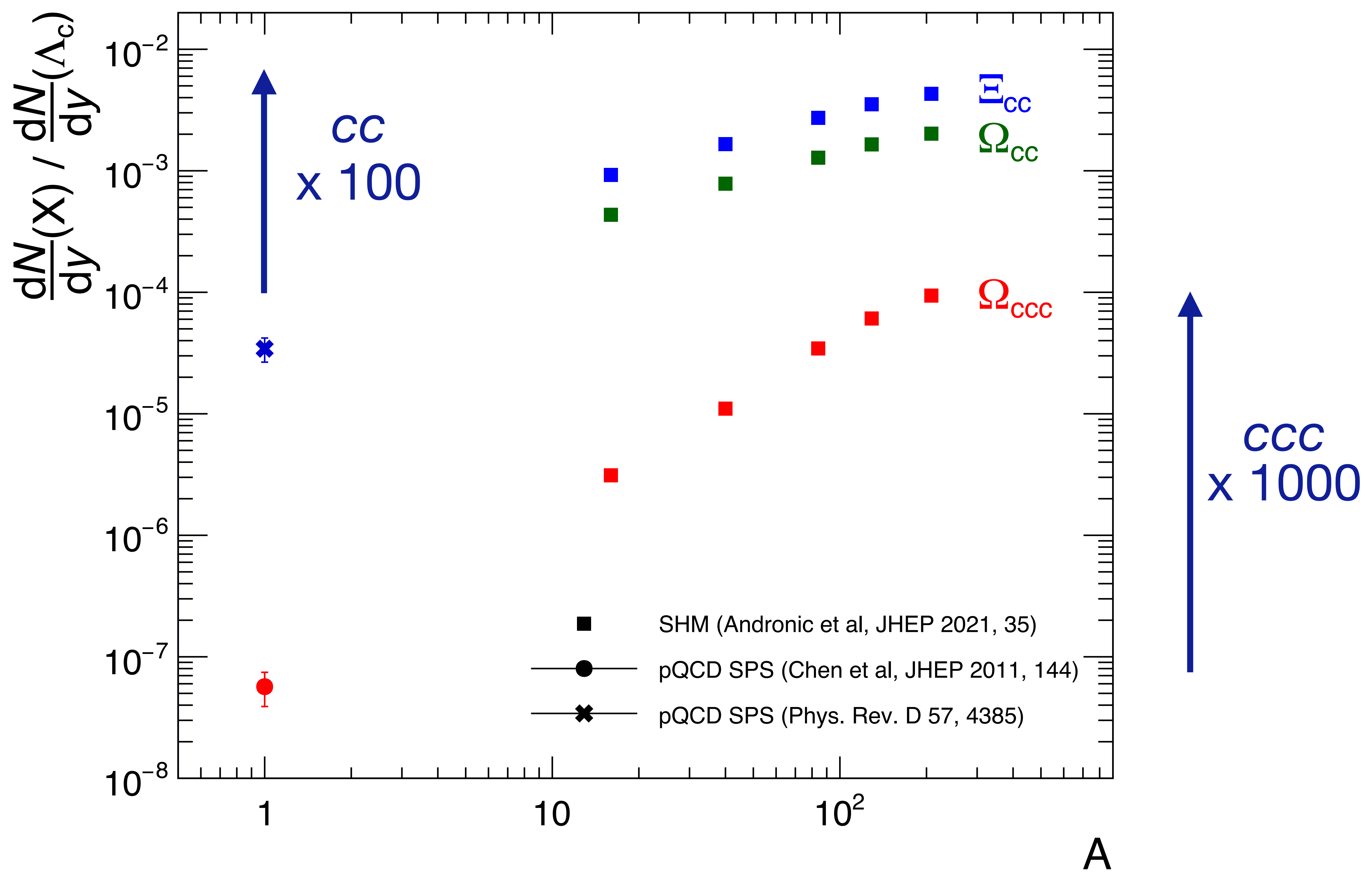

Multi-charm baryons: unique probe

- Large expected enhancement
- Theoretically clean: charm quarks conserved

Messengers of the Plasma: soft and hard processes

Soft probes: particles produced by the QGP

Azimuthal anisotropy

Light-flavour particle ratios

Thermal radiation

Messengers of the Plasma: soft and hard processes

Soft probes: particles produced by the QGP

Azimuthal anisotropy

Light-flavour particle ratios

Thermal radiation

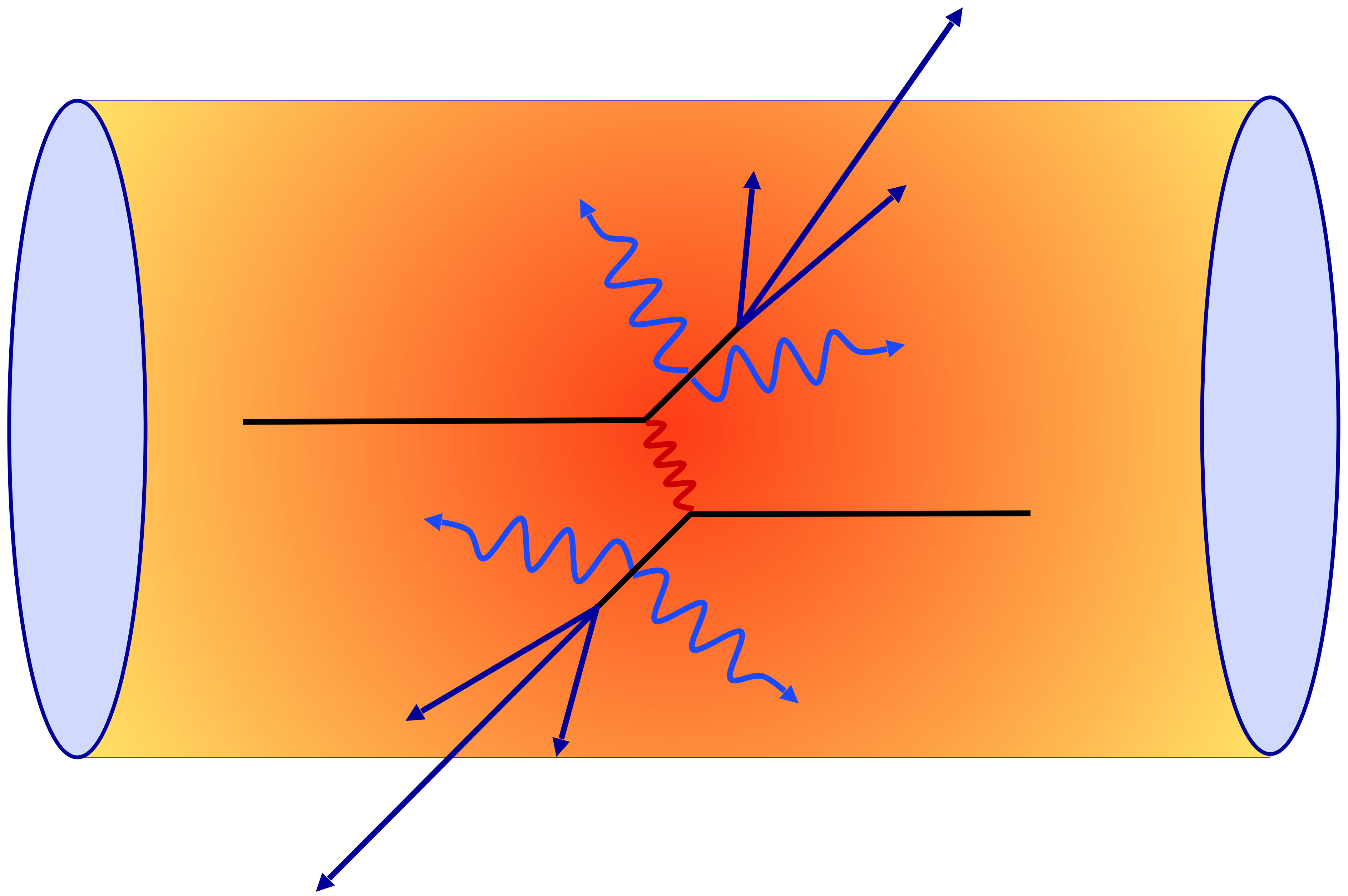

Hard scattering products probe the QGP as they propagate out

Heavy quarks charm and beauty:

- $m >> T$: Only produced in initial hard scattering
- Flavour conserved during evolution

ALICE

Azimuthal anisotropy: two mechanisms

Hydrodynamical expansion

Conversion of pressure gradients into momentum space anisotropy

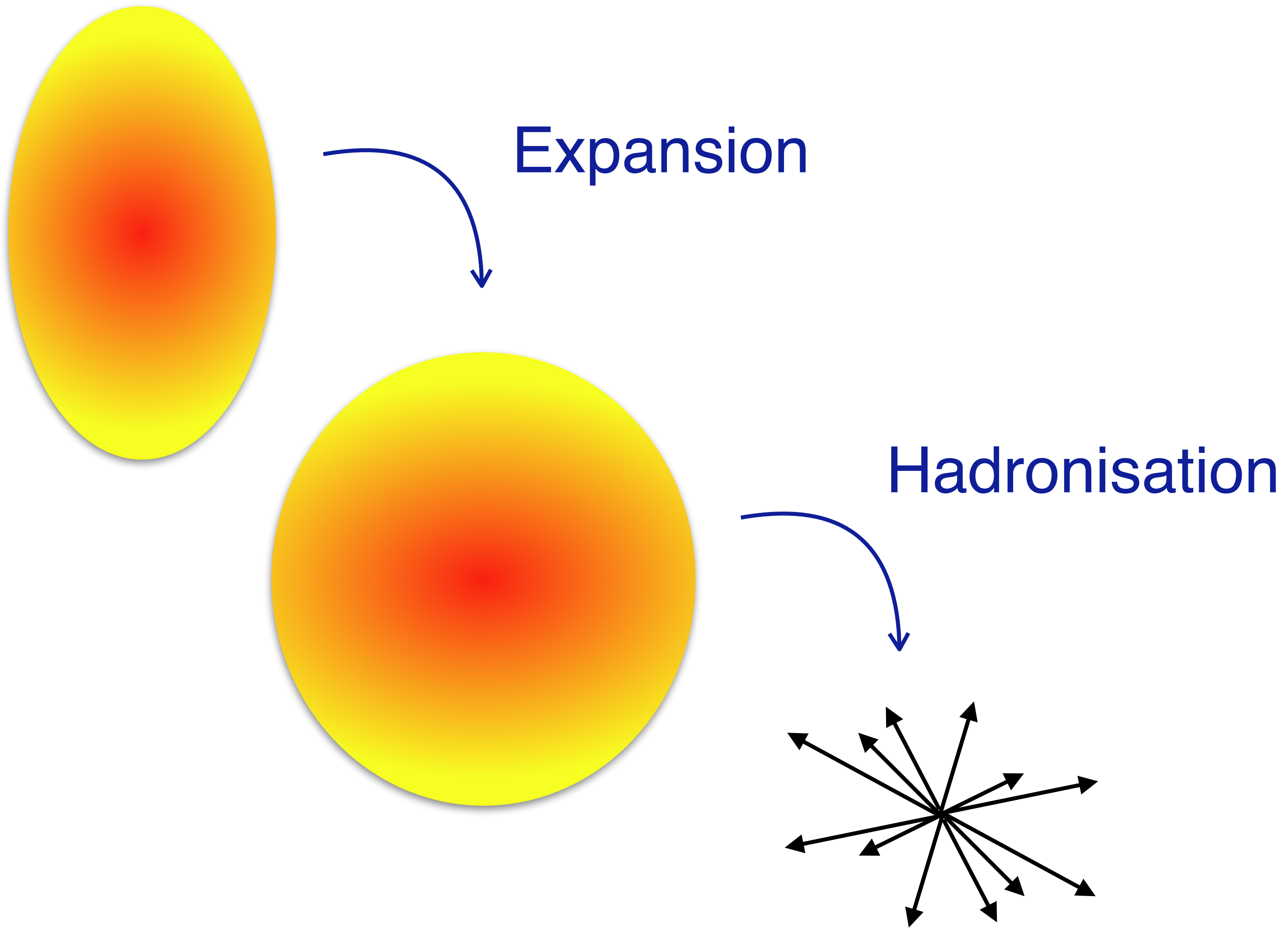

$$\nabla p = \rho \frac{d\vec{v}}{dt}$$

Dominant effect for late formation times:
light flavour at low p_T

Parton energy loss

Anisotropy due to energy loss and path length differences

Dominant effect at high p_T

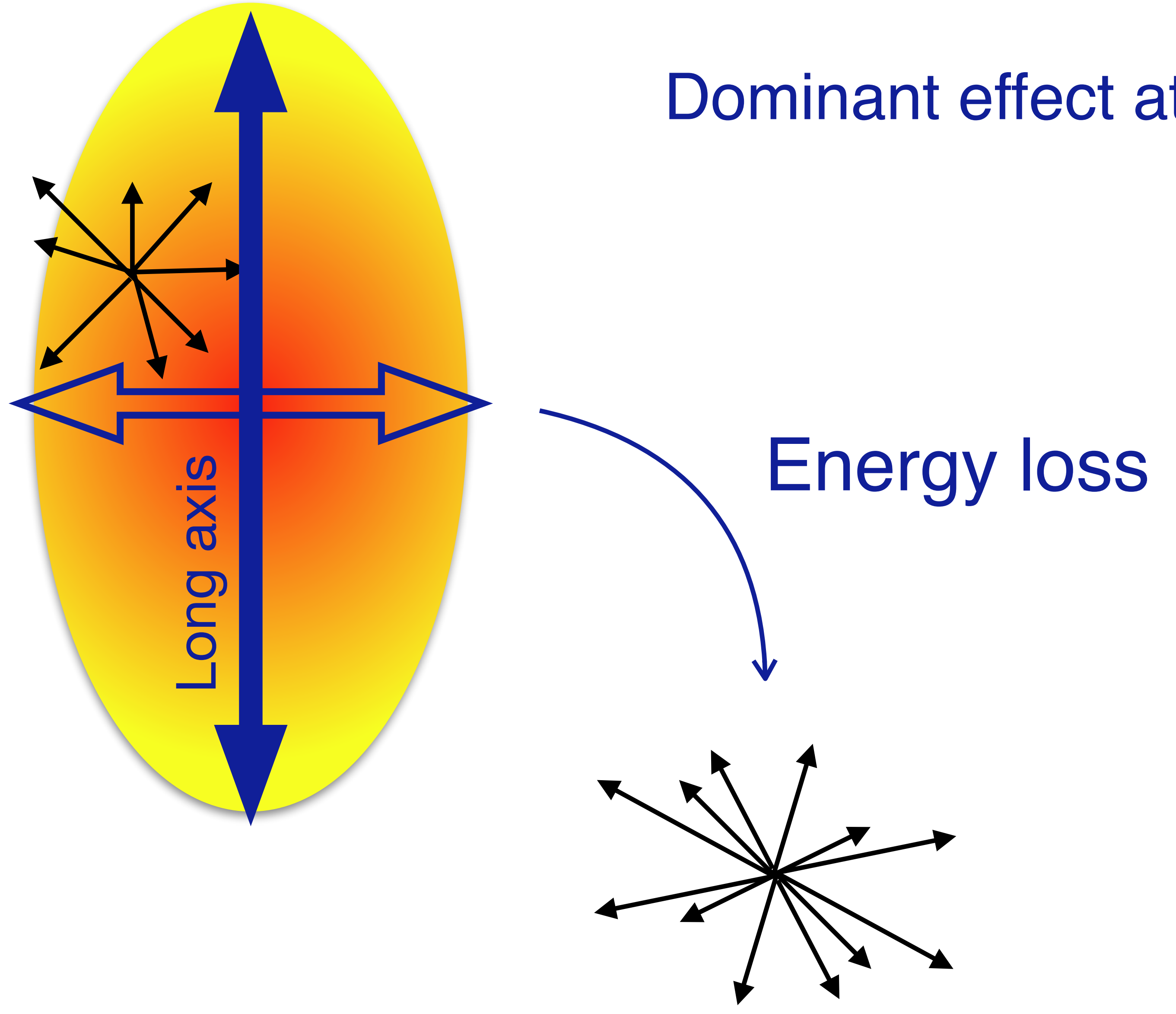

More energy loss along
long axis than short axis

$$\Delta E_{med} \sim \alpha_S \hat{q} L^2$$

Dominant effect for early formation times:
heavy flavour, high p_T probes

Jets and parton showers

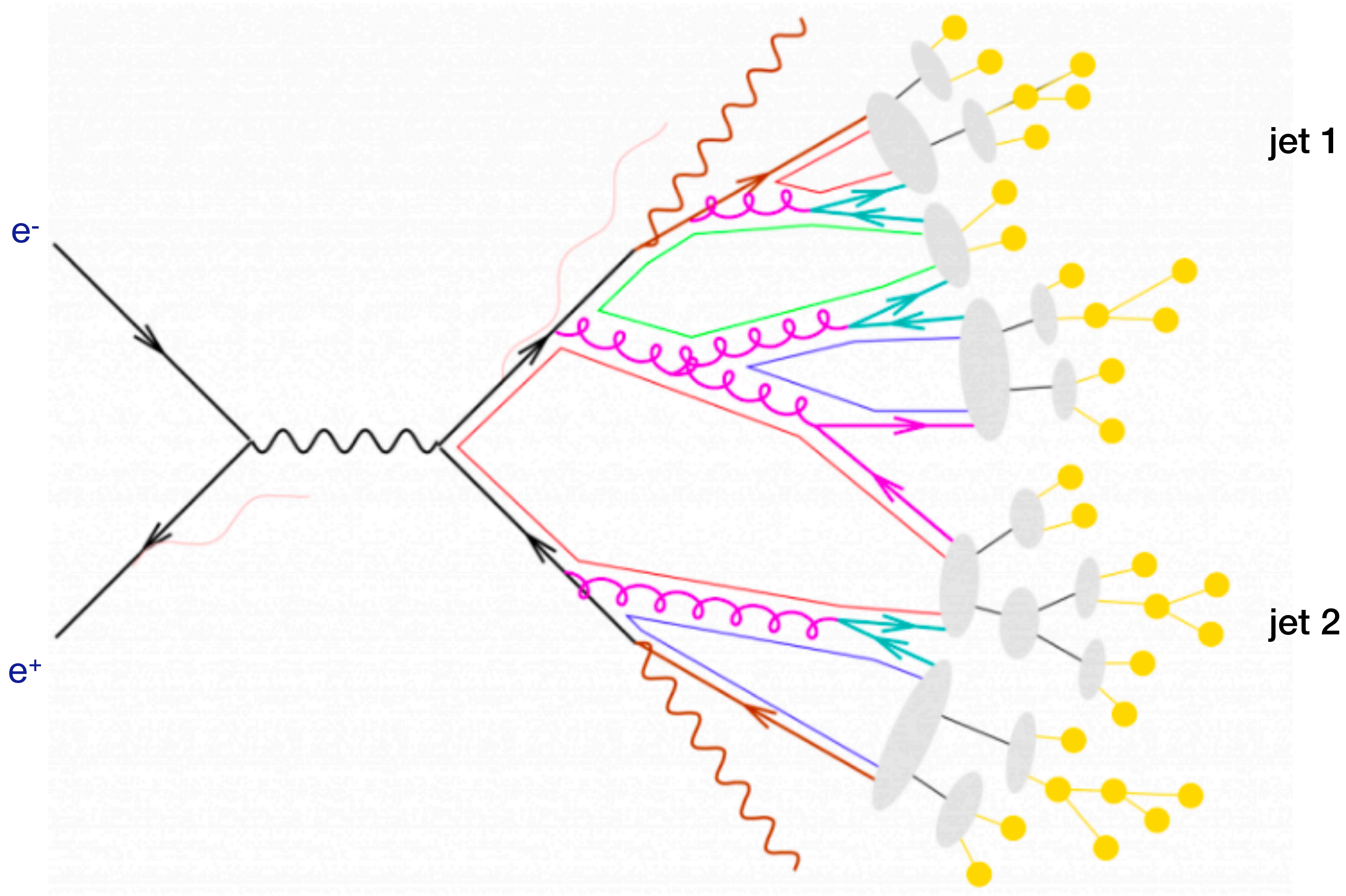

Jets and parton showers

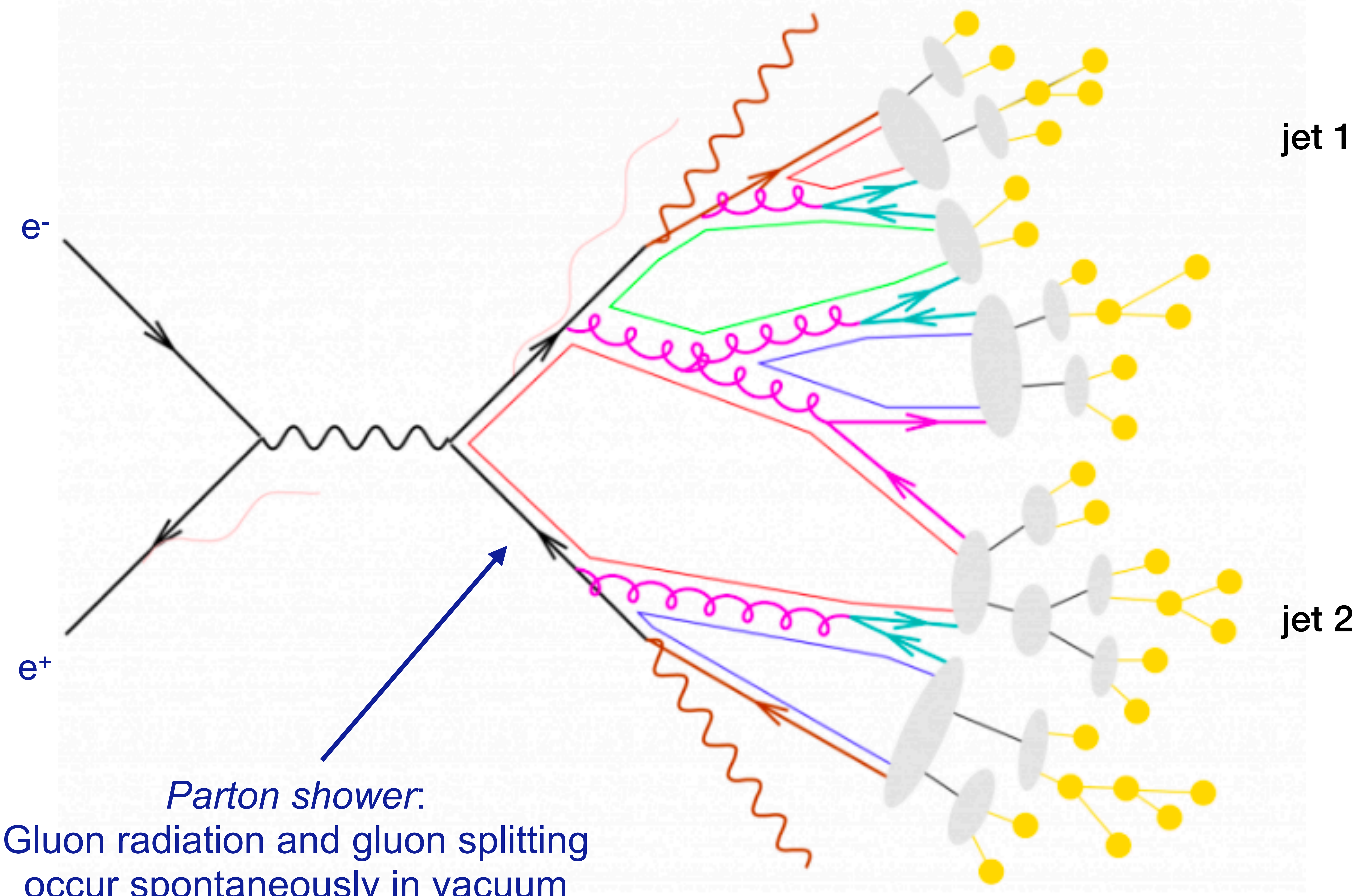

Parton shower:
Gluon radiation and gluon splitting occur spontaneously in vacuum

Jets and parton showers

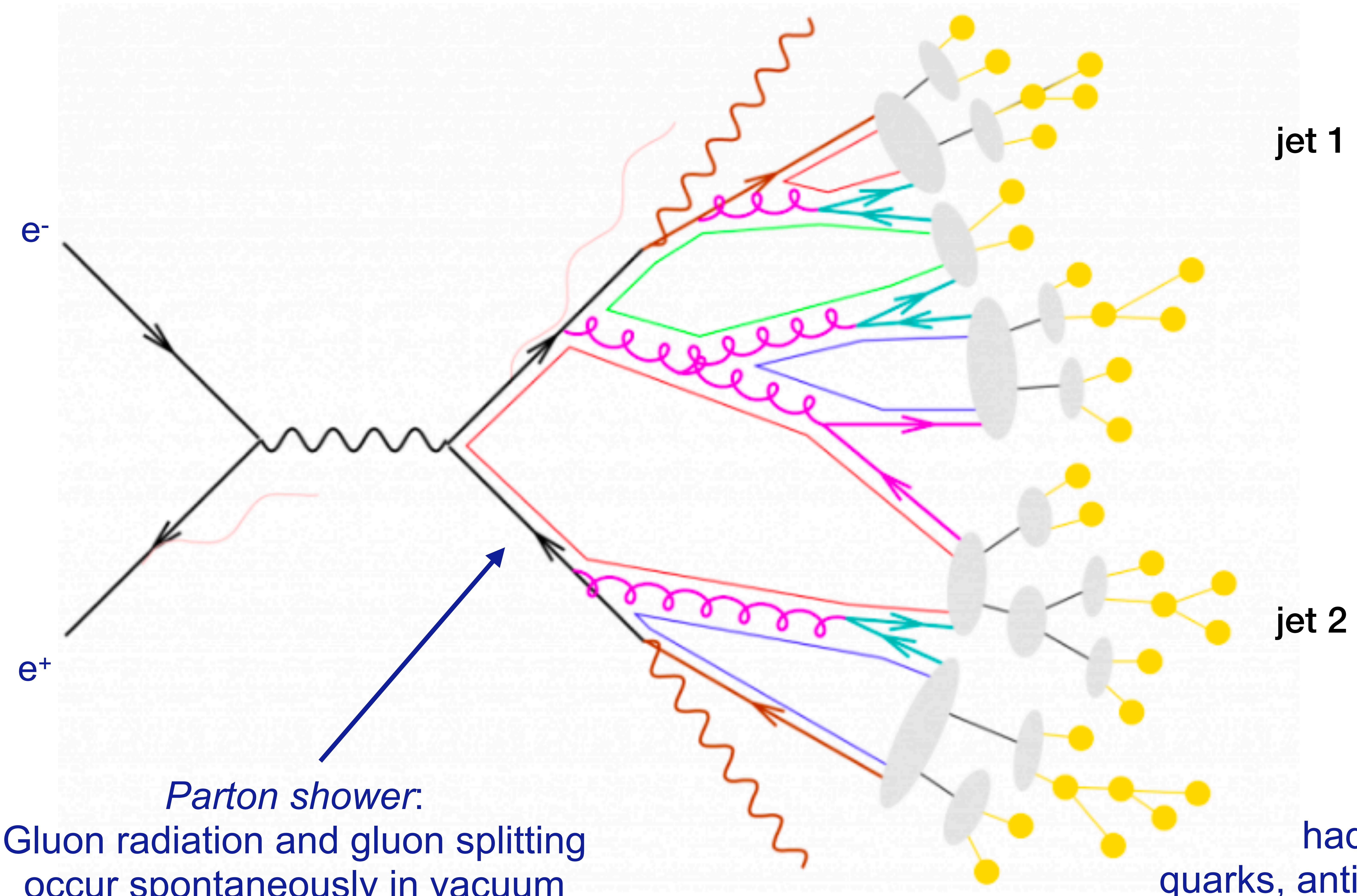

Parton shower:
Gluon radiation and gluon splitting occur spontaneously in vacuum

hadronisation:
quarks, anti-quarks and gluons form hadrons

Yields, mean p_T

Particle/pion ratios

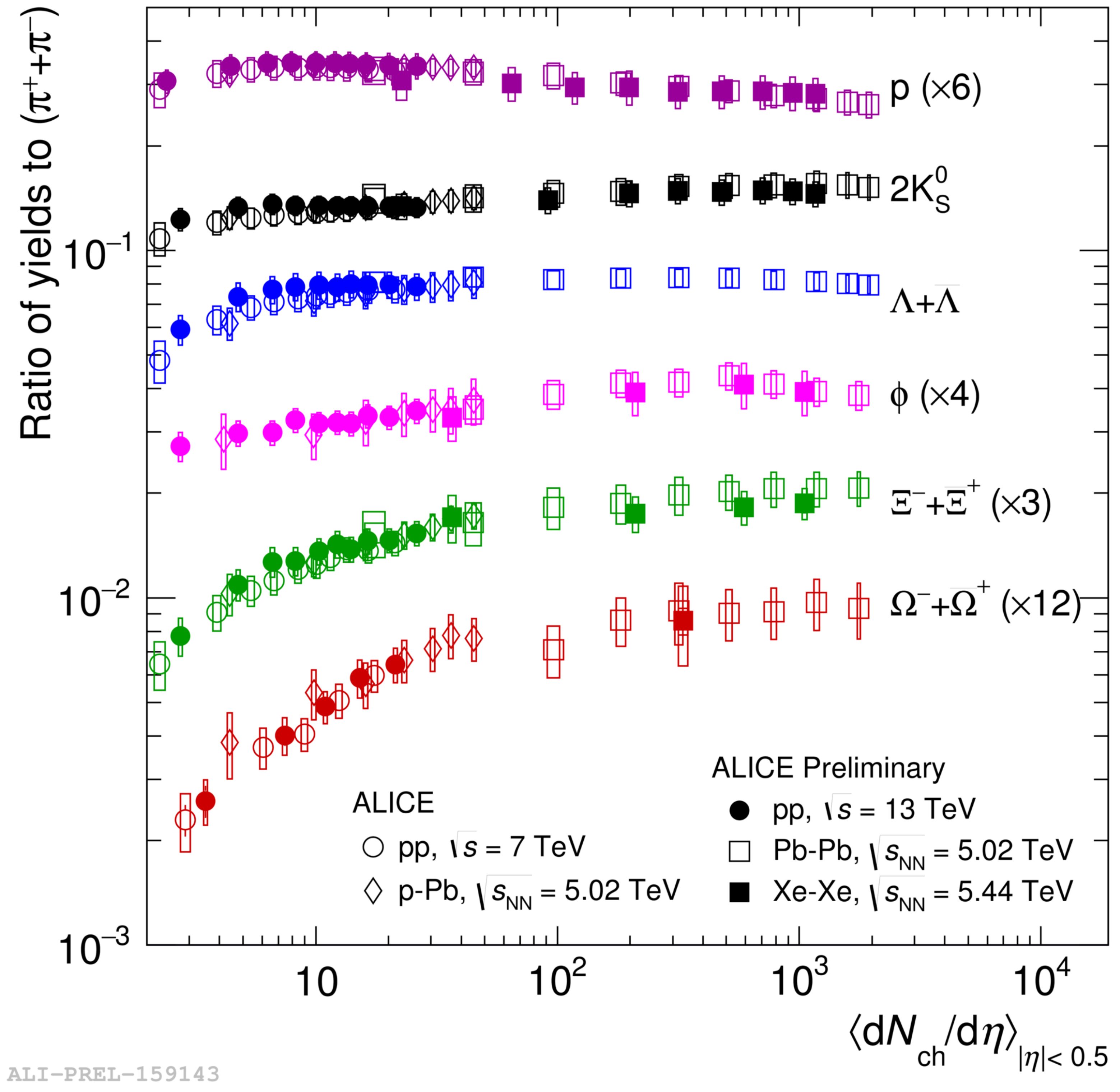

Yields ‘scale’ with multiplicity

Mean p_T

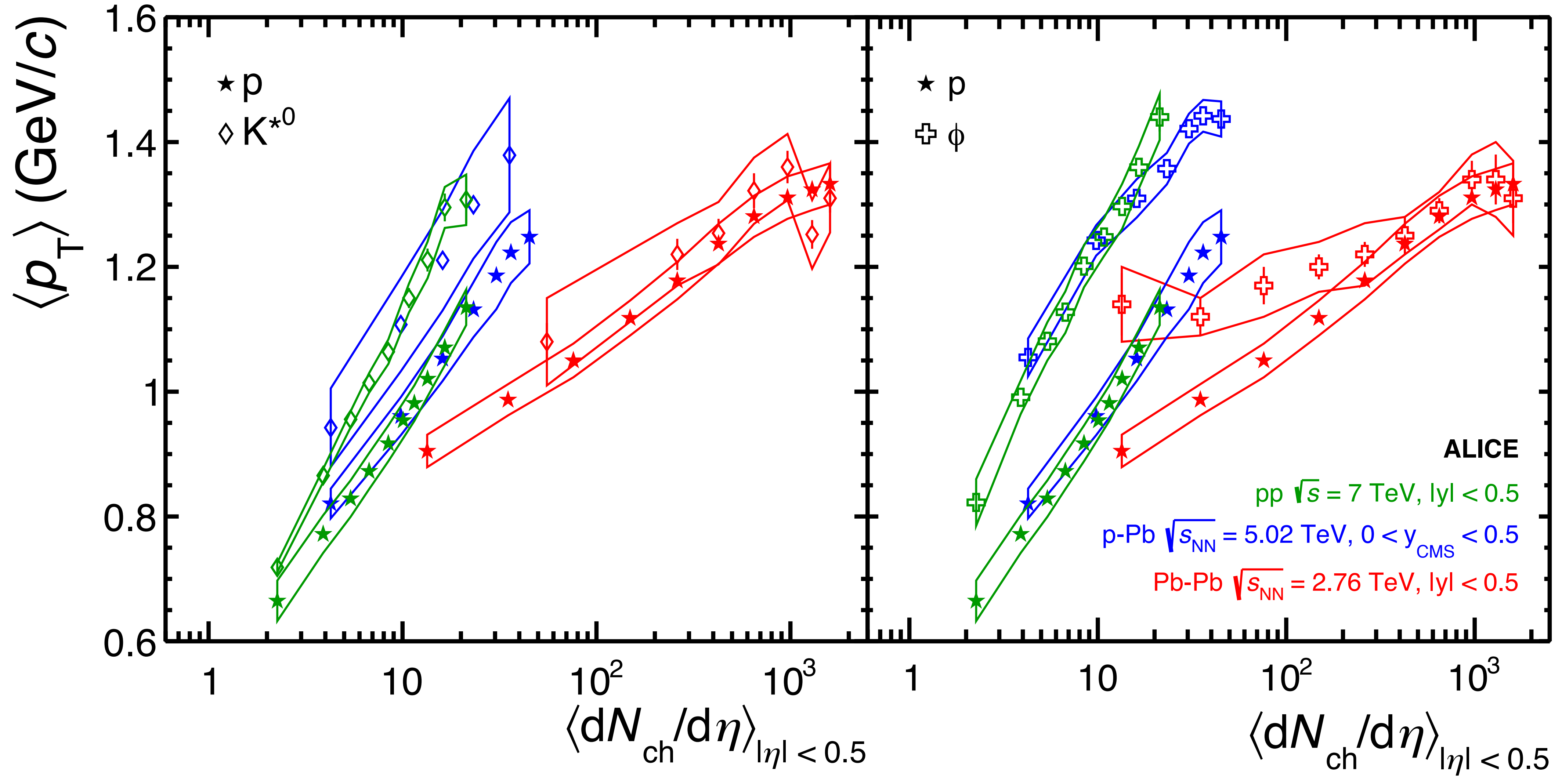

Mean p_t: disconnect between high-mult small systems and PbPb

A multiplicity selection introduces more bias in small system

Yield, mean p_T are convenient to summarise results, but a lot of physics enters

Flow of nuclei: coalescence vs thermal production

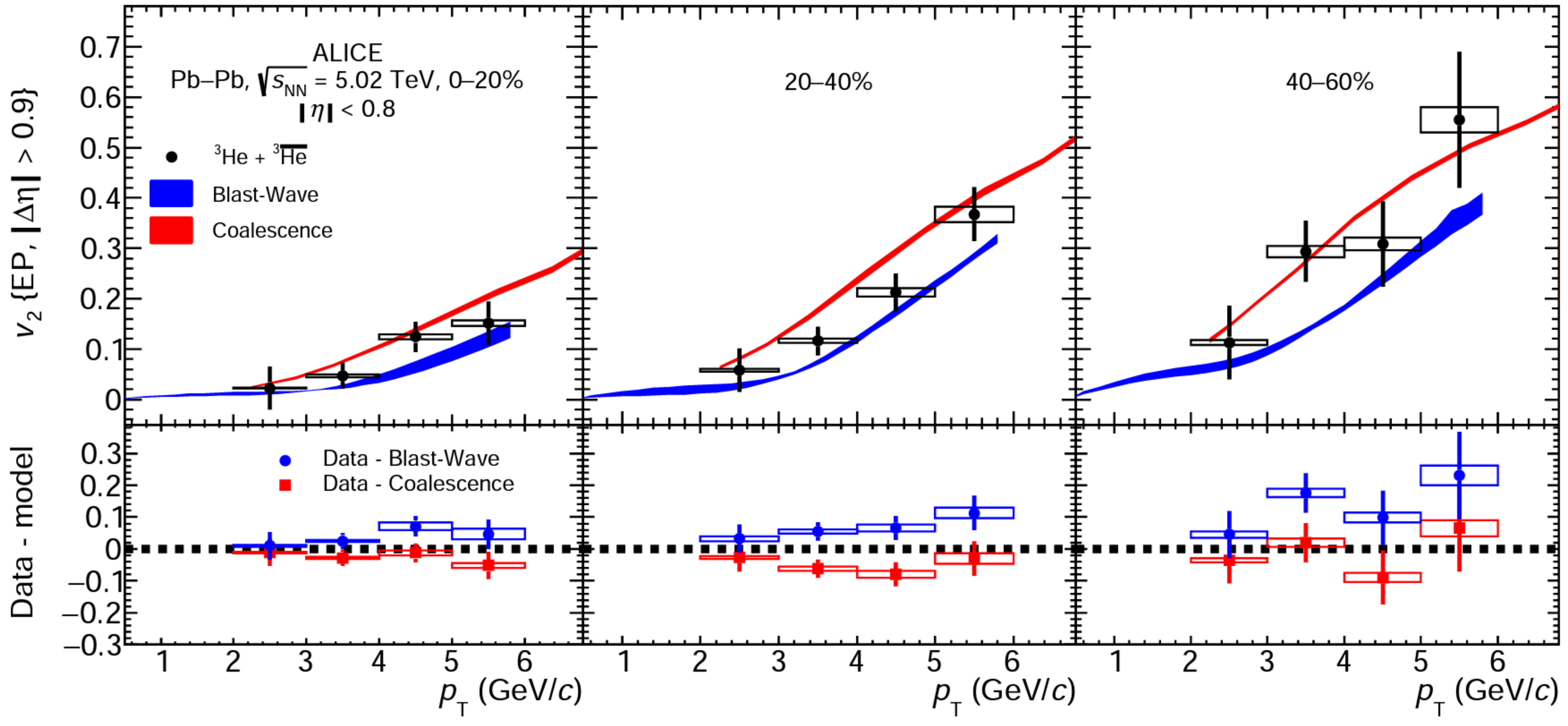

ALICE, arXiv:1910.09718

Λ_c production in pp and Pb-Pb

Λ_c/D in pp

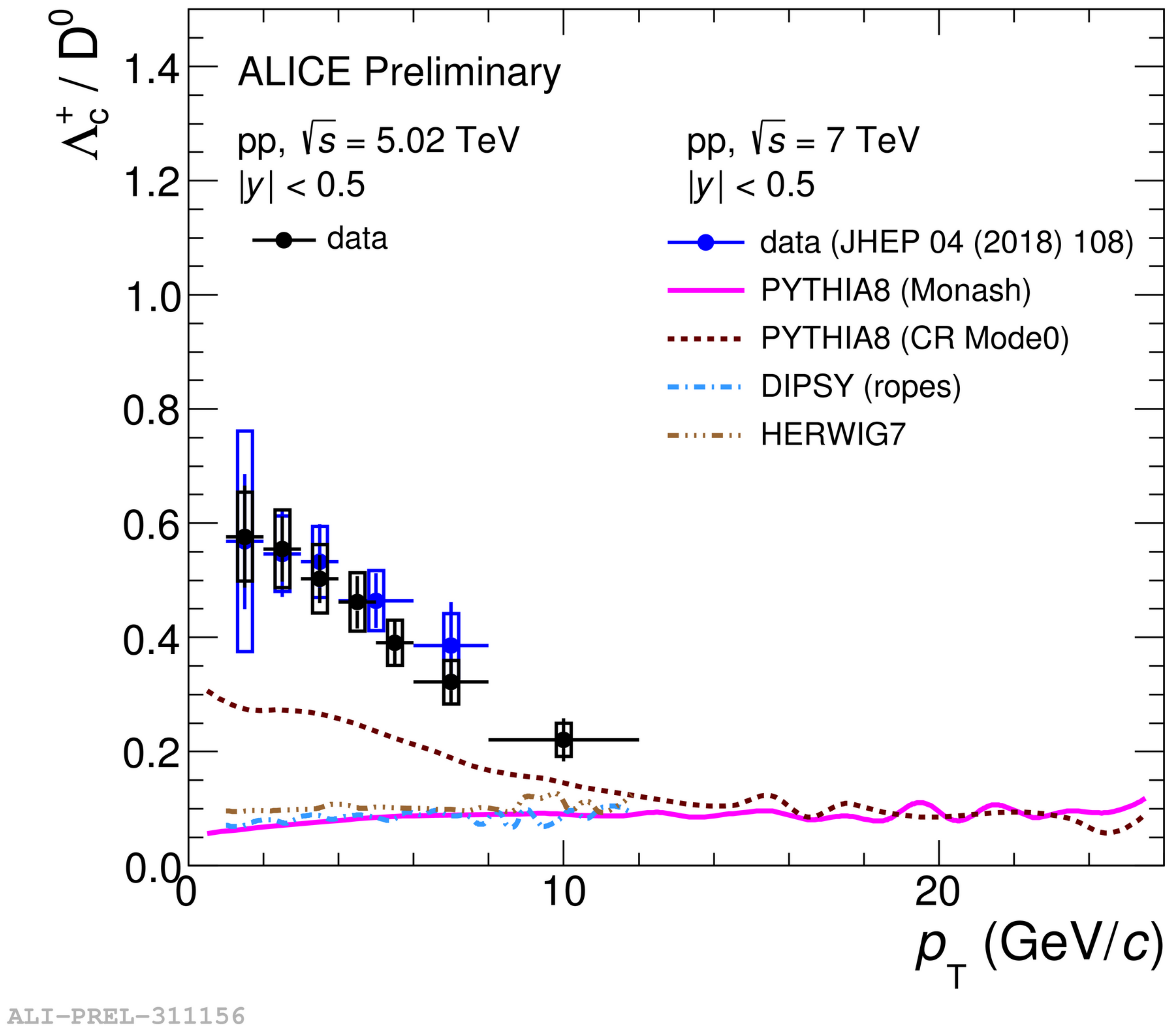

Λ_c/D^0 in pp significantly larger than expected from e^+e^-

Λ_c production in pp and Pb-Pb

Λ_c/D in pp

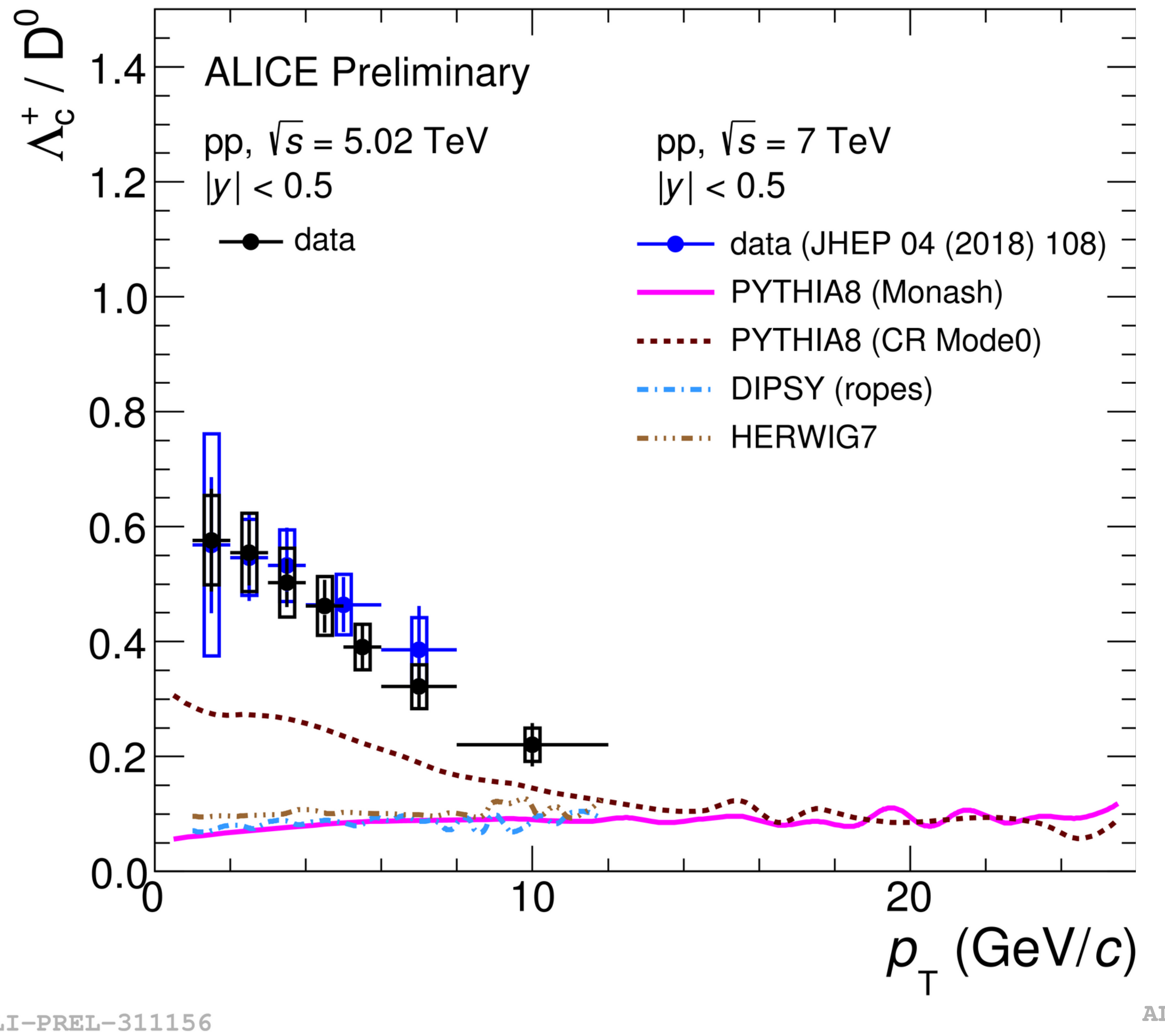

Λ_c/D in pp, Pb-Pb

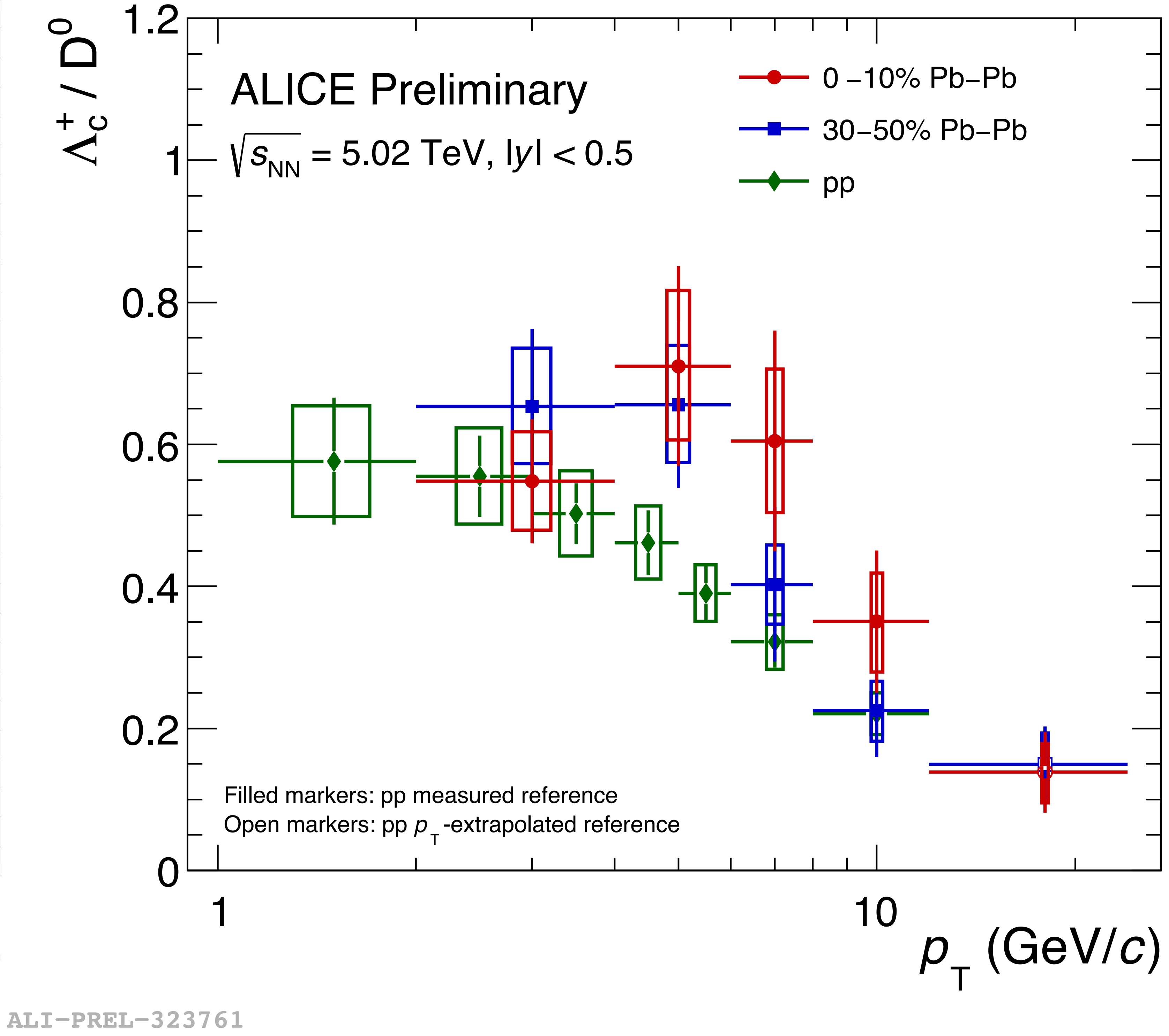

Λ_c/D^0 in pp significantly larger than expected from e^+e^-

New result: Λ_c in Pb-Pb;
Λ_c/D similar or slightly larger than in pp

Λ_c production in pp and Pb-Pb

Λ_c/D in pp

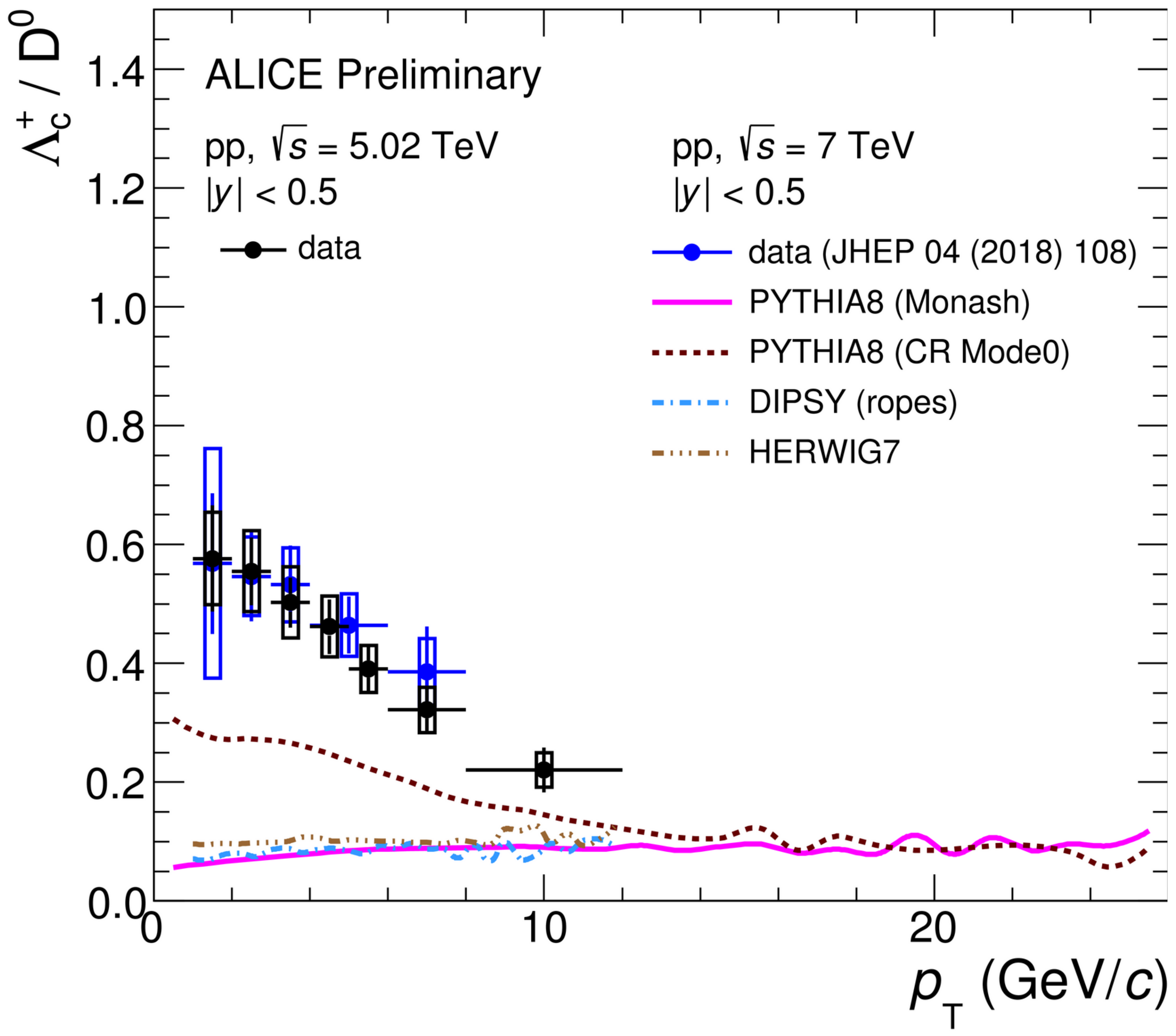

Λ_c/D in pp, Pb-Pb

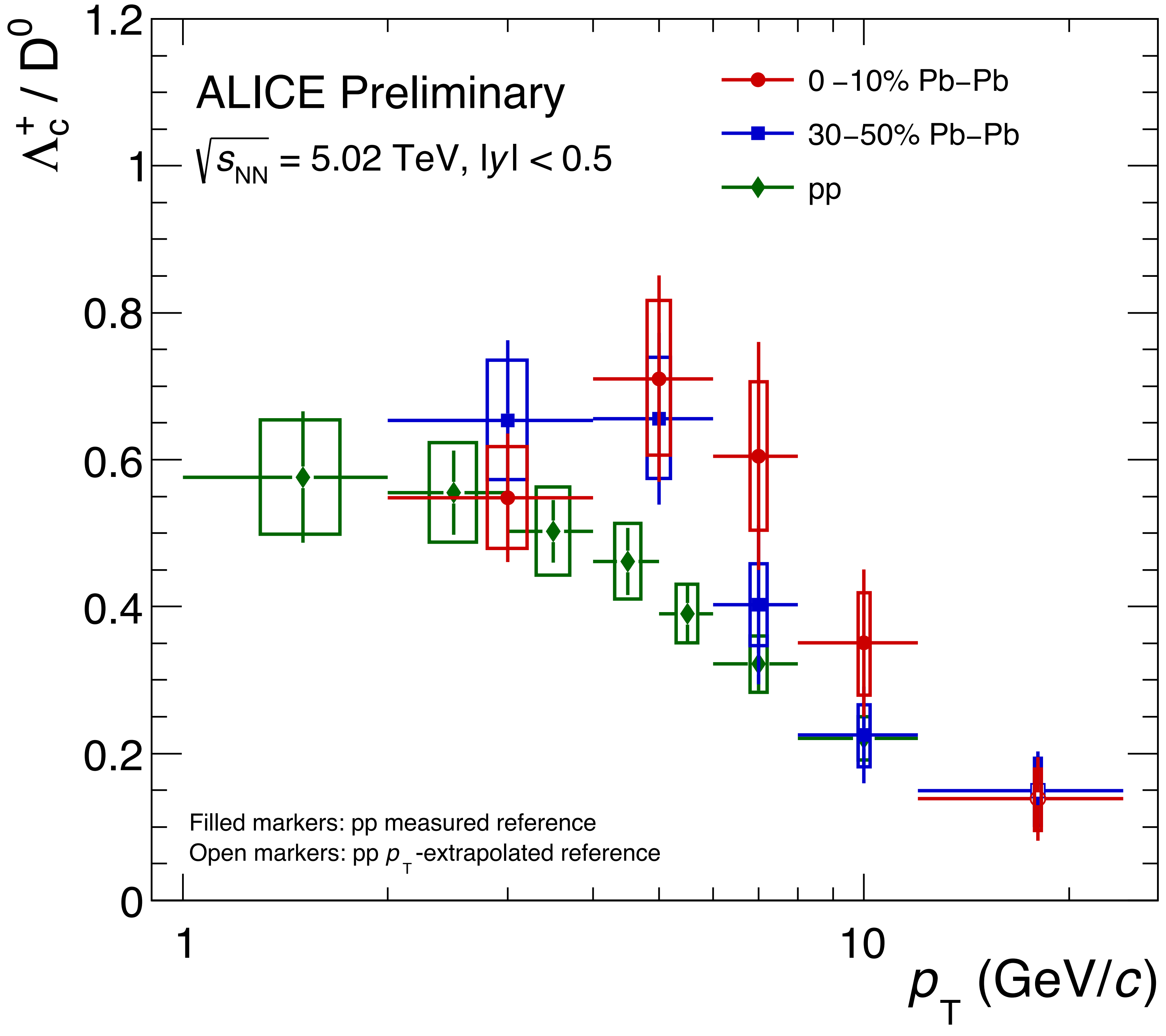

Λ_c/D in Pb-Pb

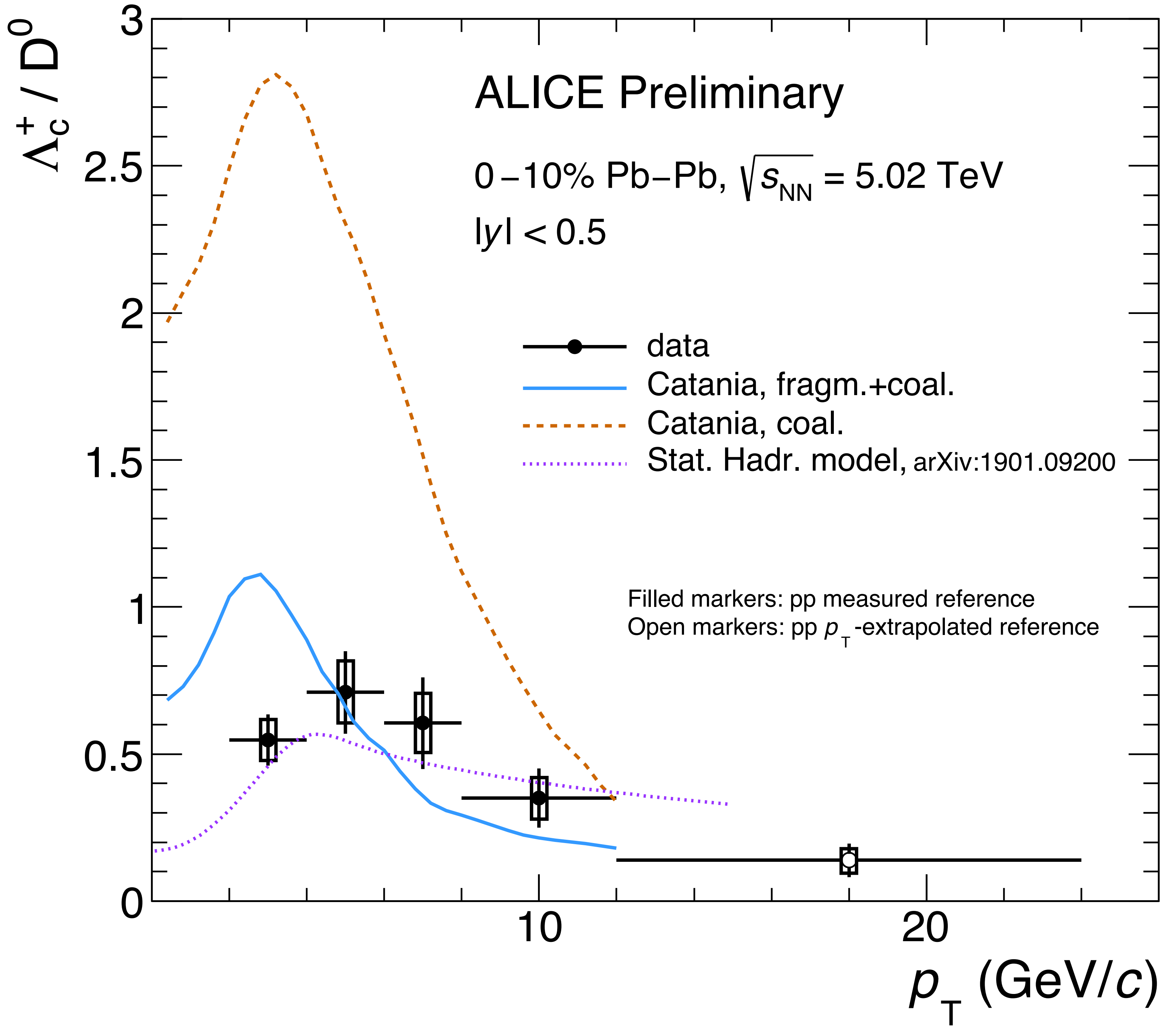

Λ_c/D^0 in pp significantly larger than expected from e^+e^-

New result: Λ_c in Pb-Pb;
Λ_c/D similar or slightly larger than in pp

Does hadronisation by recombination play a role? Or ‘just’ fragmentation?

Production of light (anti-)nuclei

- Increased production in Pb-Pb collisions
- Two possible explanations:
  - Coalescence: density impacts coalescence rate
  - Thermal-statistical (CSM): baryon number conservation suppresses multi-baryon states in pp

Deuteron production rate in pp, Pb-Pb

arxiv: 2211.14015. arxiv: 2212.04777

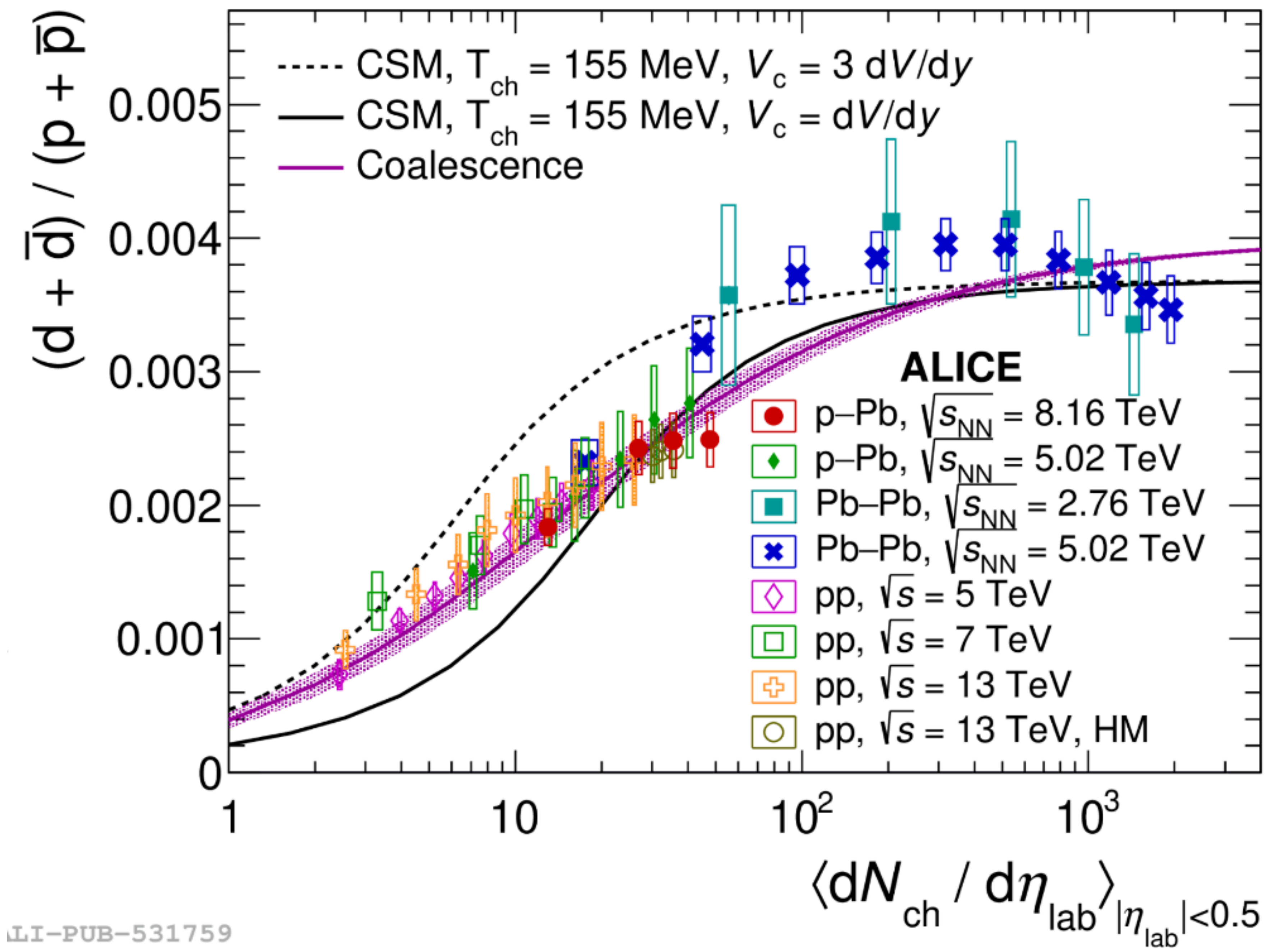

Deuteron production in jets

pp collisions

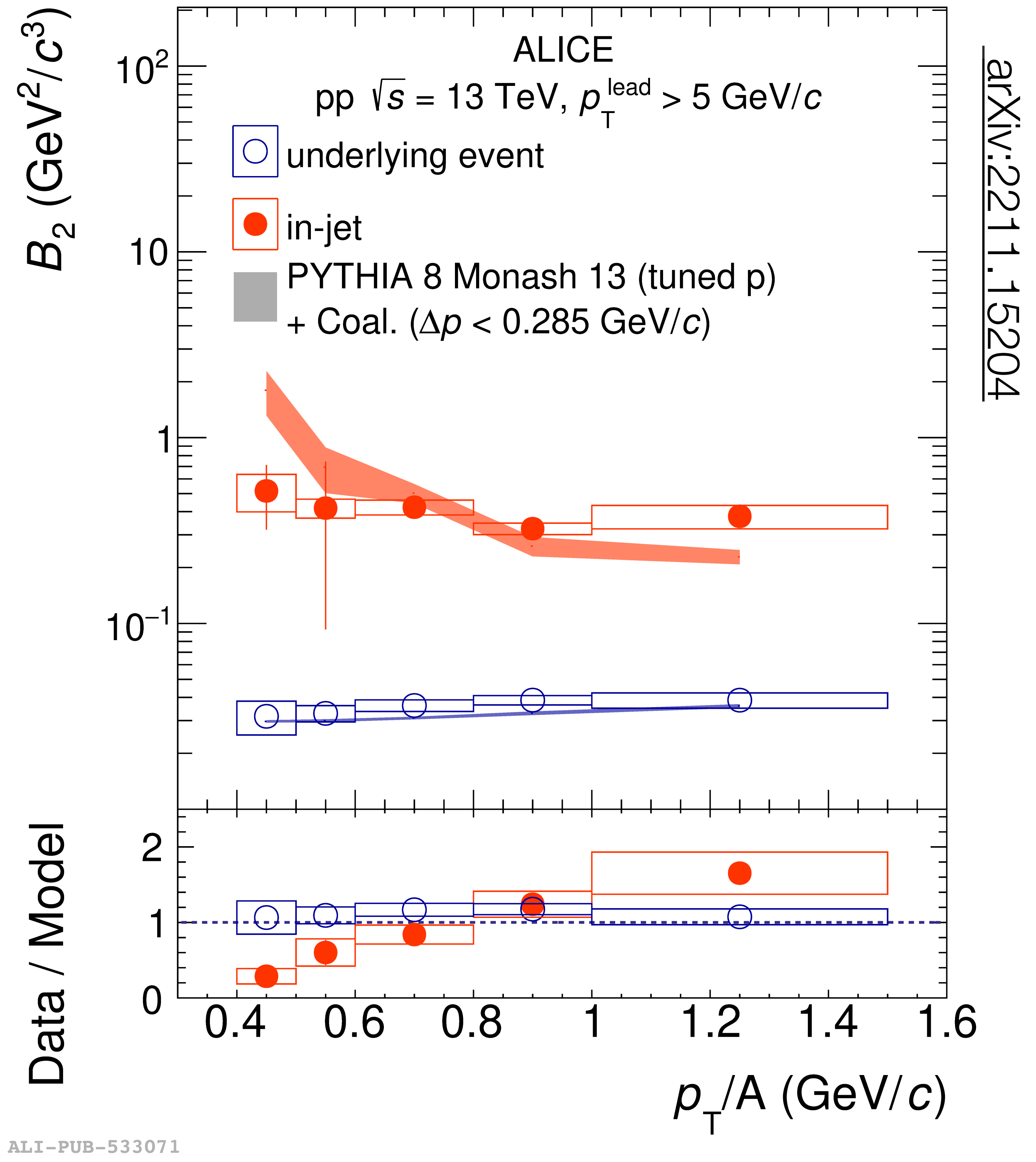

Deuteron production in jets: increase of rate due to higher local density in line with coalescence model expectation

- New results in pp, p-Pb collisions as a function of multiplicity
  - Smooth trend as a function of multiplicity
  - Data more in line with coalescence model

Hadron interactions: 3-particle correlations

arXiv:2303.13448

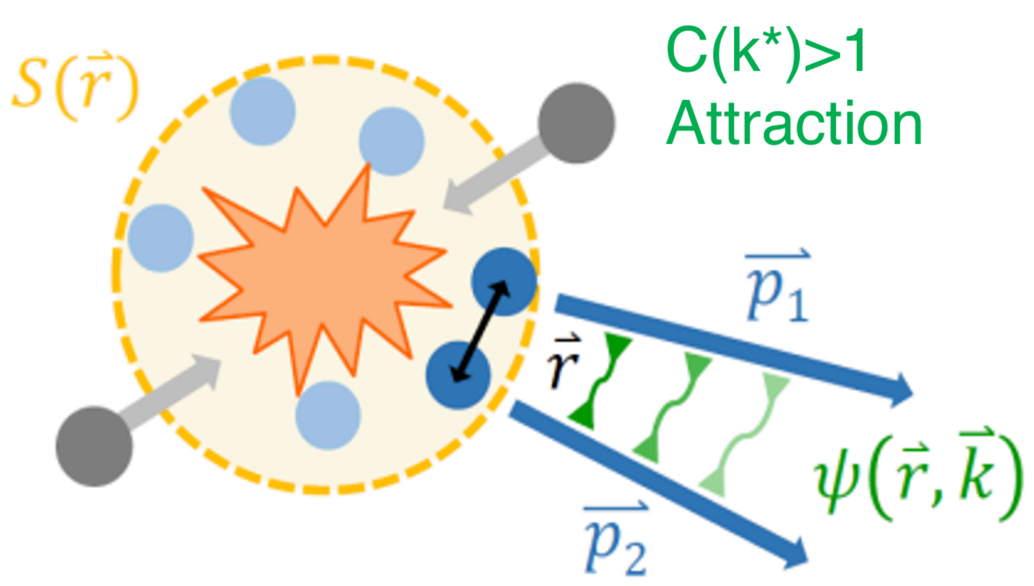

ppK⁻ correlations

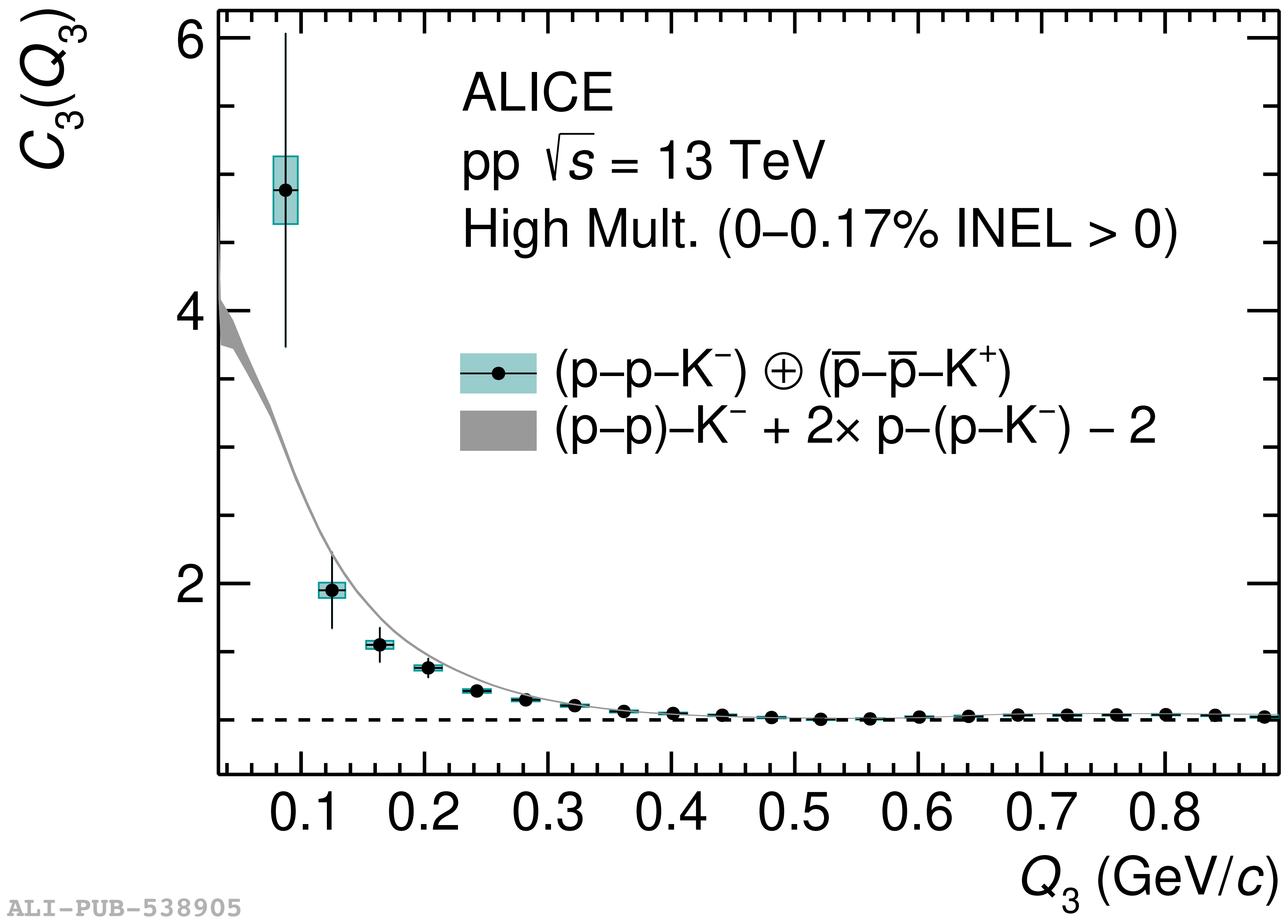

ppK⁺ correlations

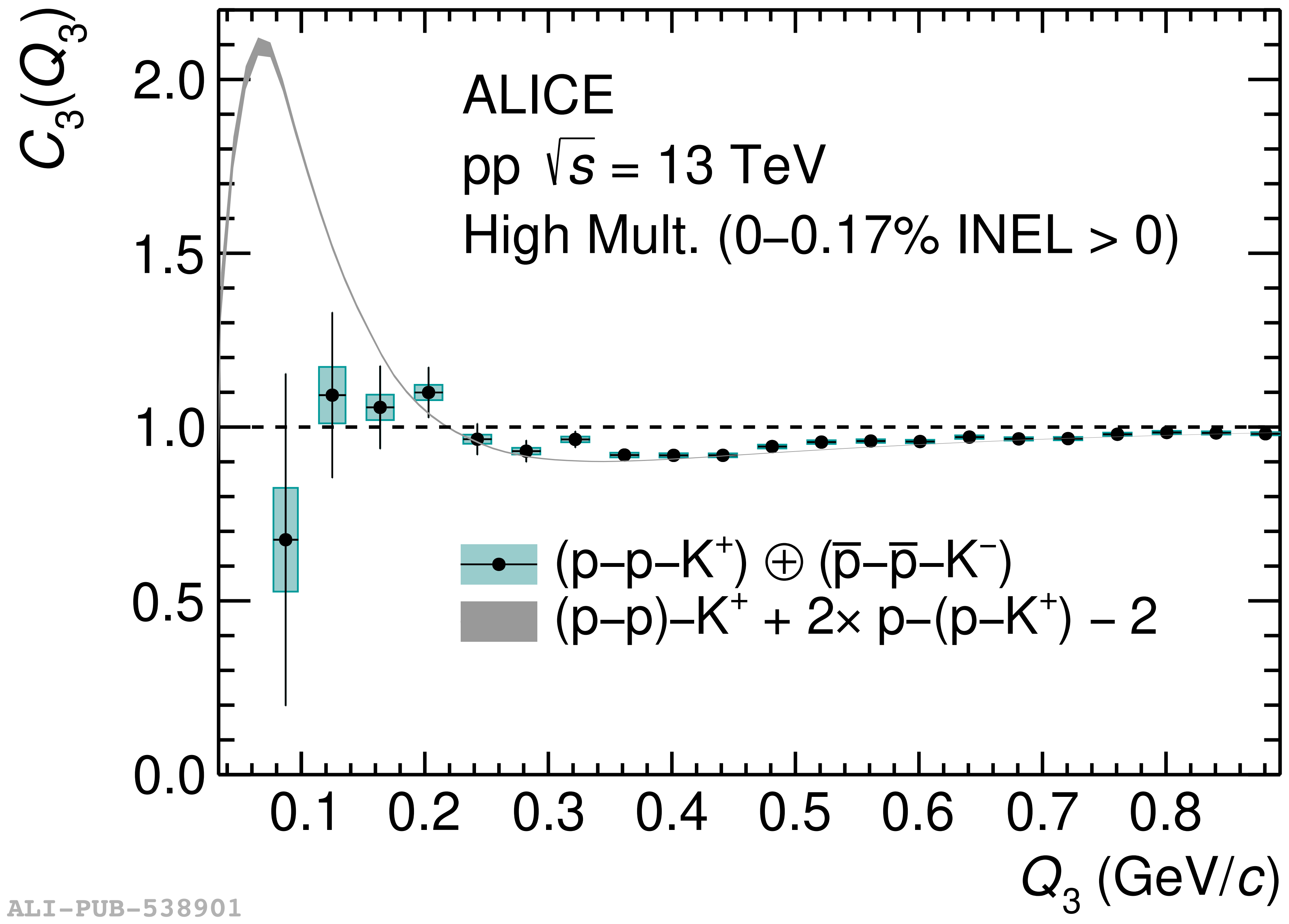

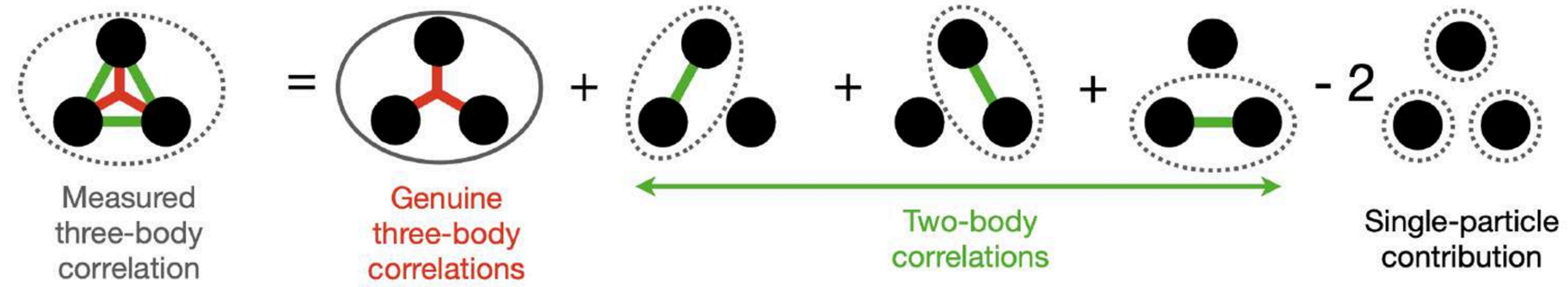

- Use correlations of pairs with similar momentum to measure potential
- First direct study of 3-body potential ppK
- No evidence of true 3-body force; 2-body interactions fully explain correlation signal

Melting and regeneration of charmonia: $\psi(2S)$ vs J/ψ

arXiv:2210.08893

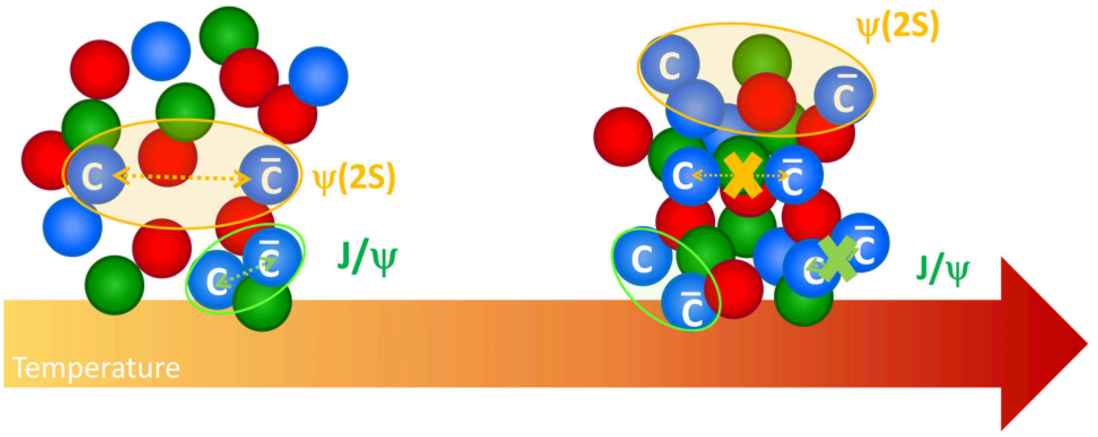

Different $c\bar{c}$ bound states:

$\psi(2S)$ and J/ψ

different binding energies, sizes

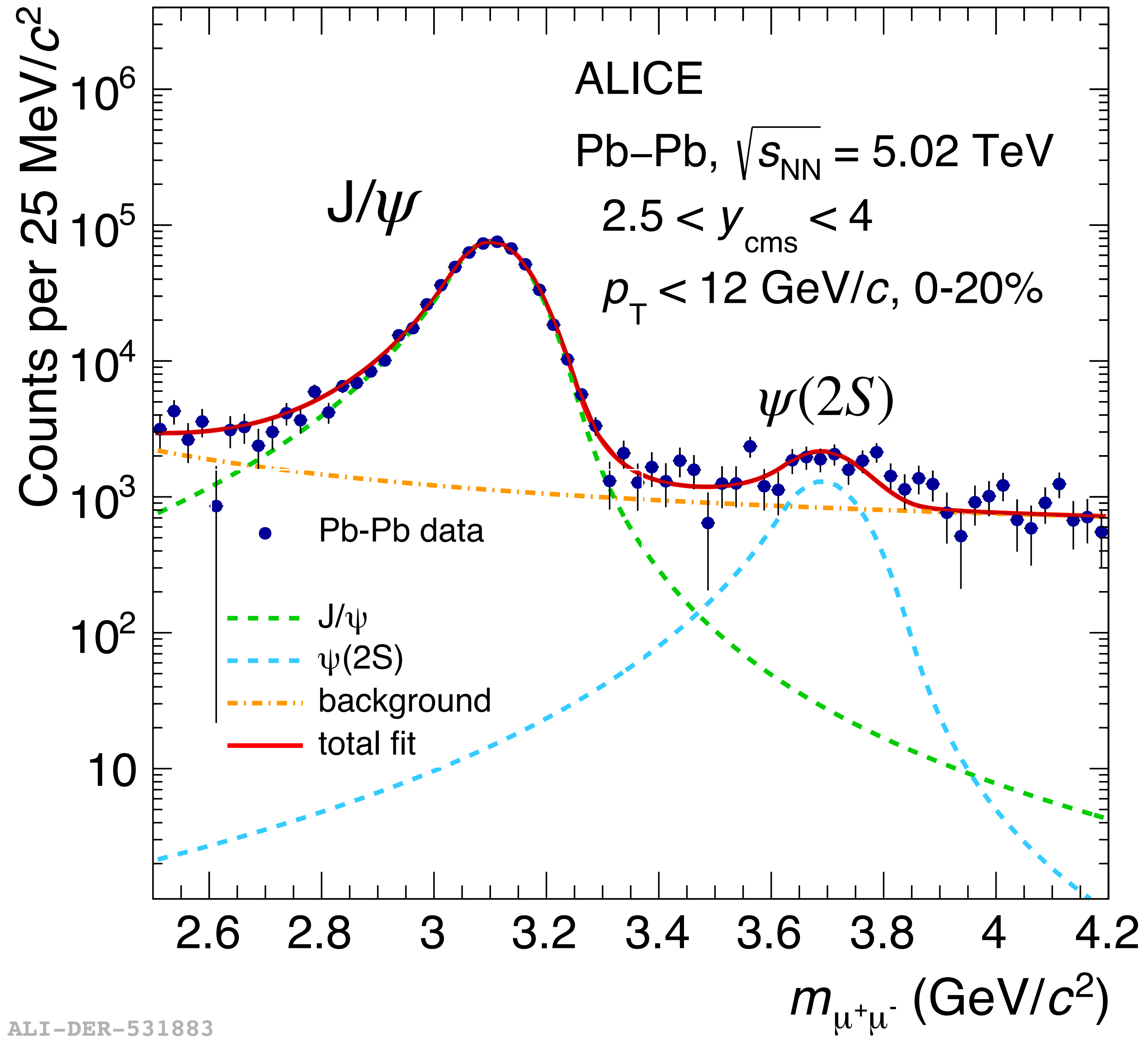

Nuclear modification factor vs p_T

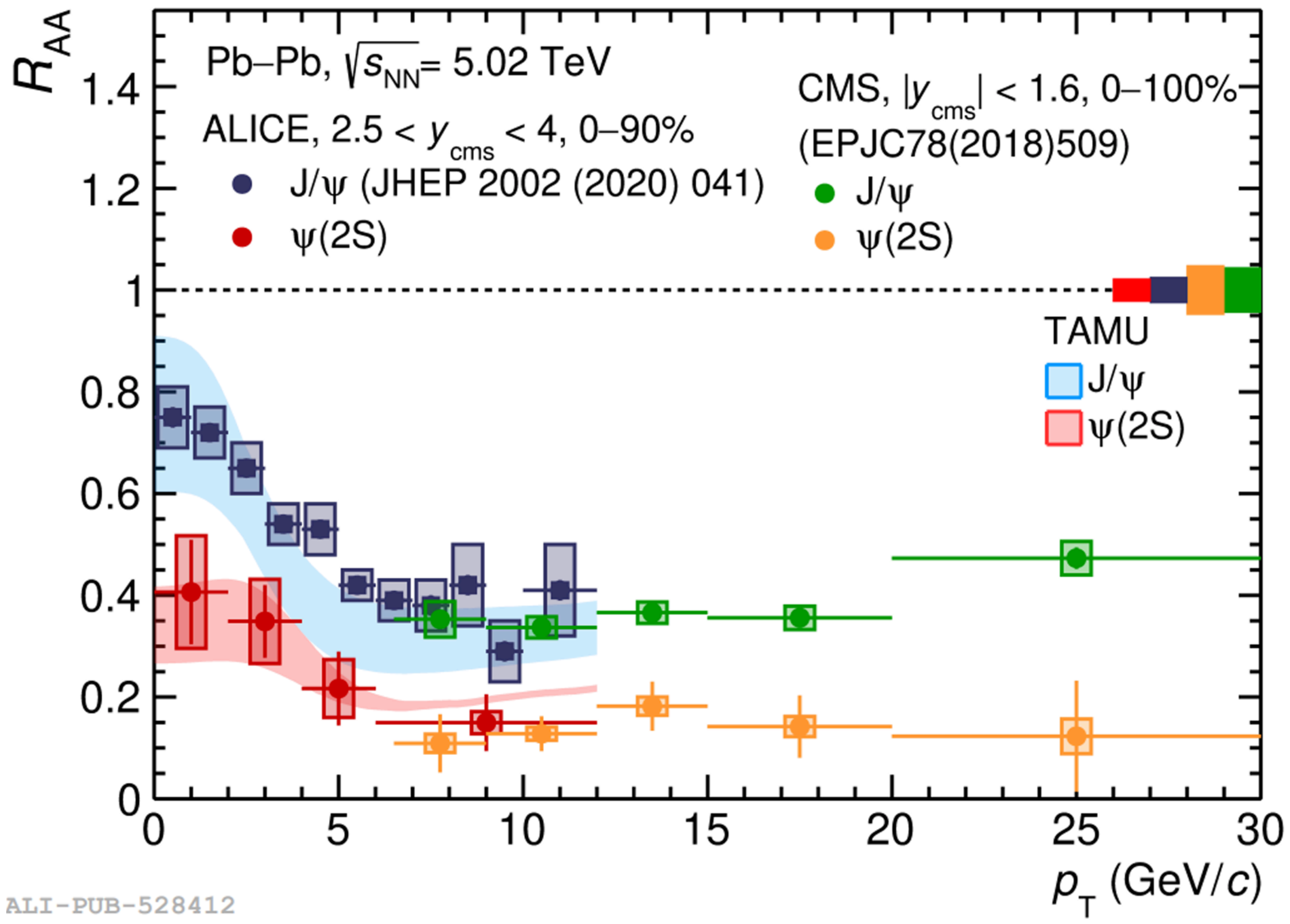

$$R_{AA} = \frac{dN/dp_T|_{AA}}{\langle N_{coll}\rangle\, dN/dp_T|_{pp}}$$

- High p_T: stronger suppression of $\psi(2S)$— lower melting temperature
- Low p_T: R_{AA} increases — regeneration similar to J/ψ

ALICE upgrade plans for LS3 and LS4

LS3 upgrades

Forward Calorimeter

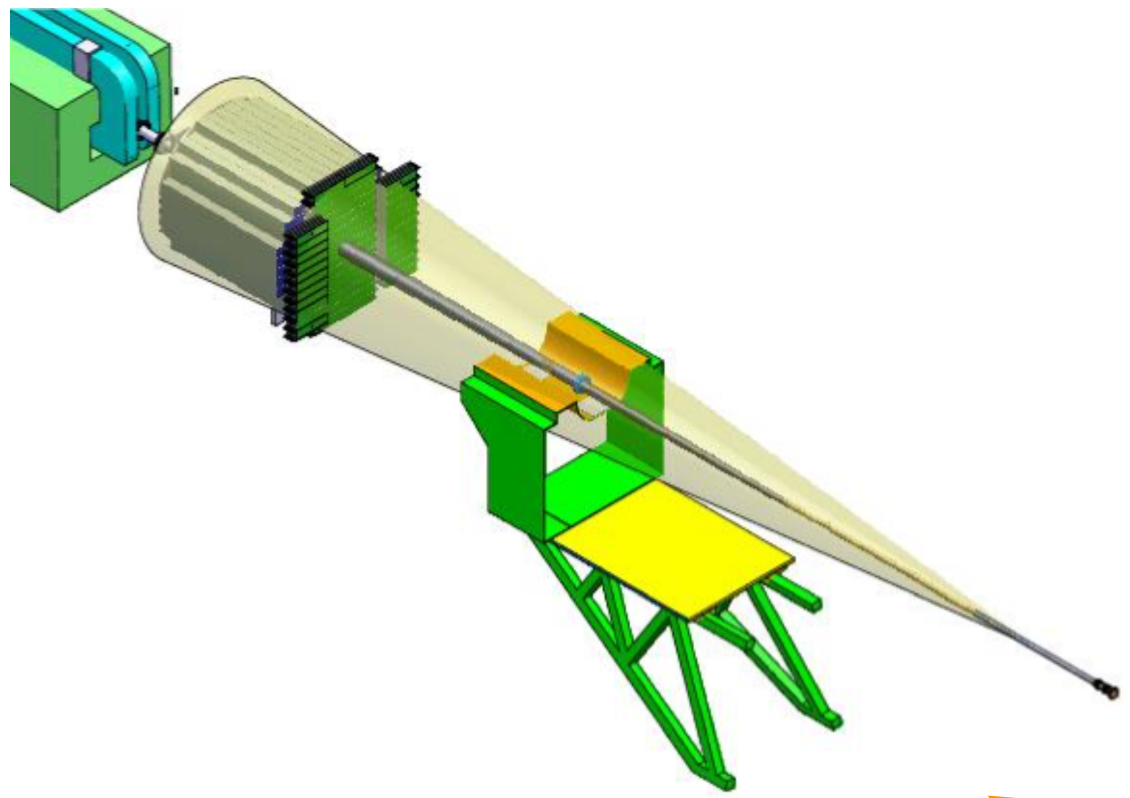

FoCal LoI:
CERN-LHCC-2020-009

ITS 3

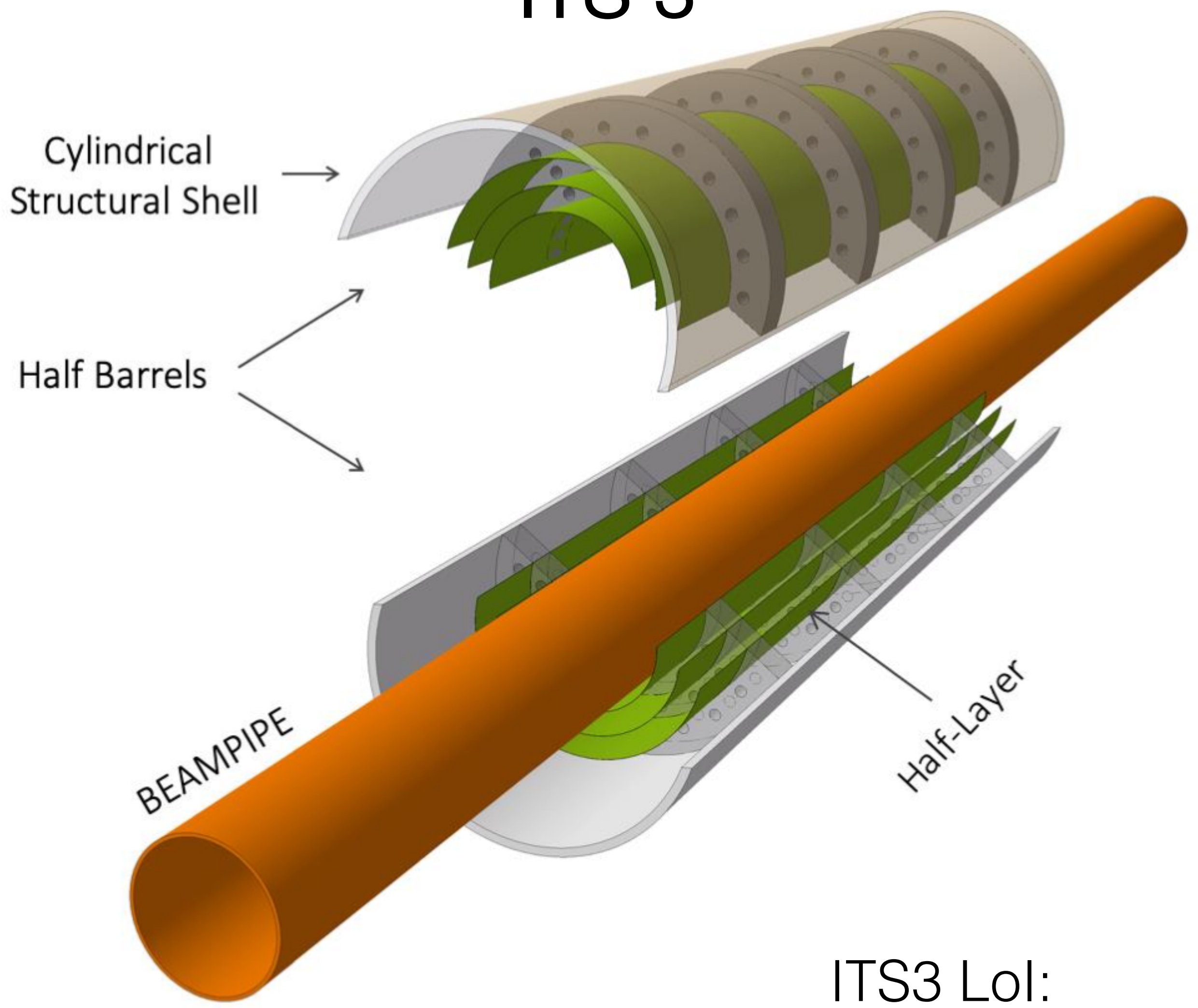

ITS3 LoI:
CERN-LHCC-2019-018

ALICE 3: LS4

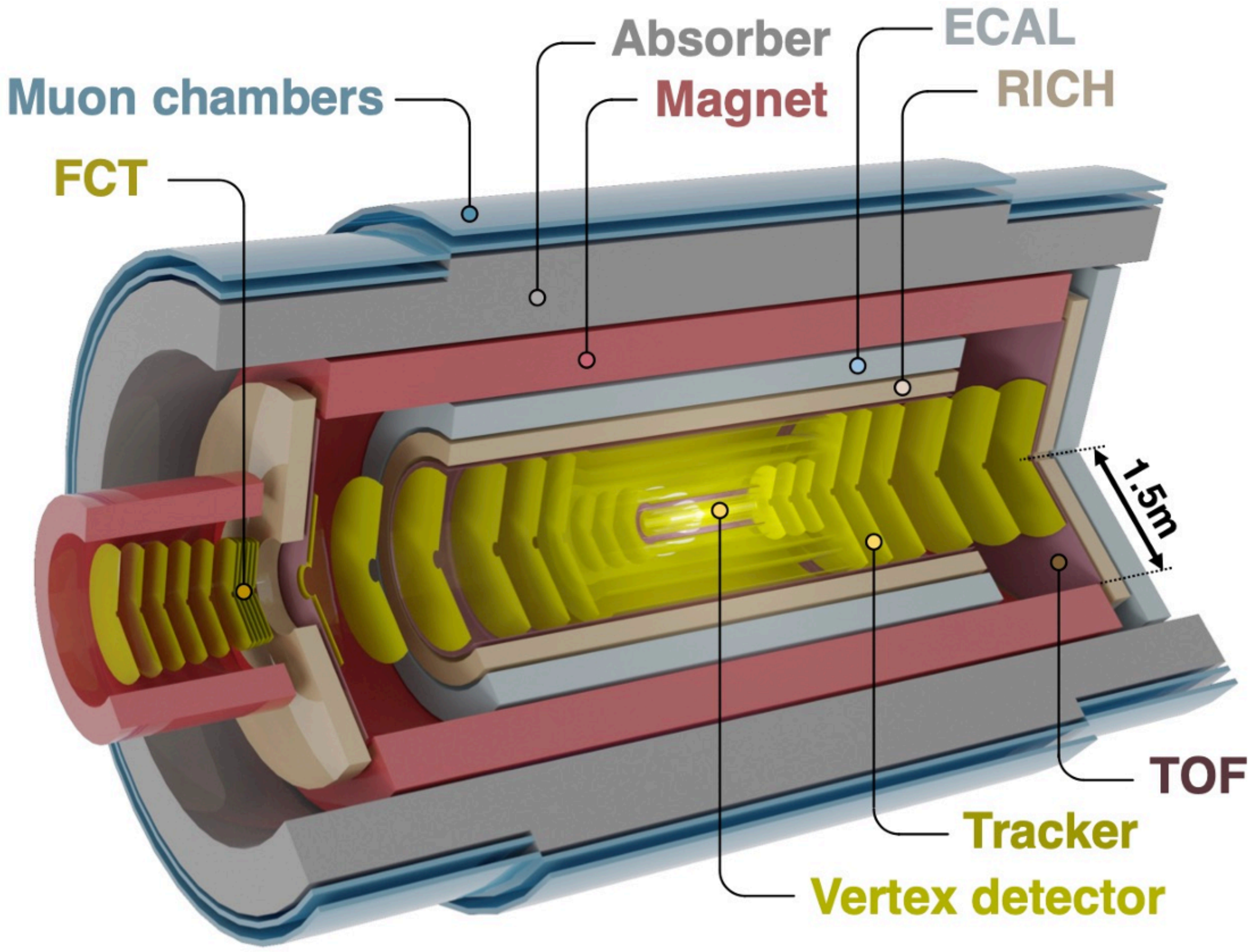

ALICE 3 LoI:
CERN-LHCC-2022-009

Detector development: silicon pixel sensors

High-energy physics experiments bring together disciplines:
- detector development
- electronics
- computing
- cooling
- mechanics
- super-conducting magnet technology

Upgraded inner tracking system

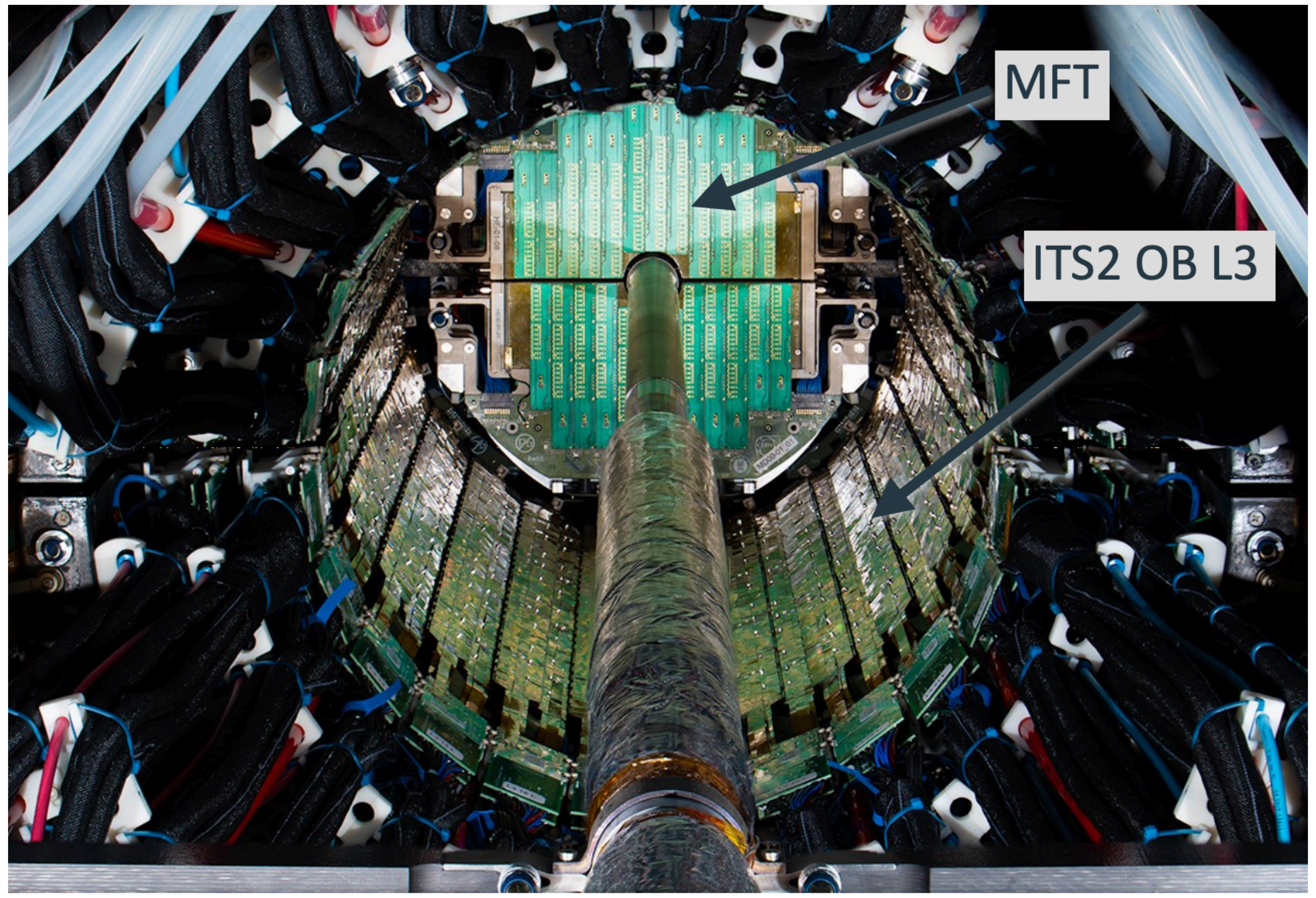

Detector development: silicon pixel sensors

High-energy physics experiments bring together disciplines:
- detector development
- electronics
- computing
- cooling
- mechanics
- super-conducting magnet technology

Upgraded inner tracking system

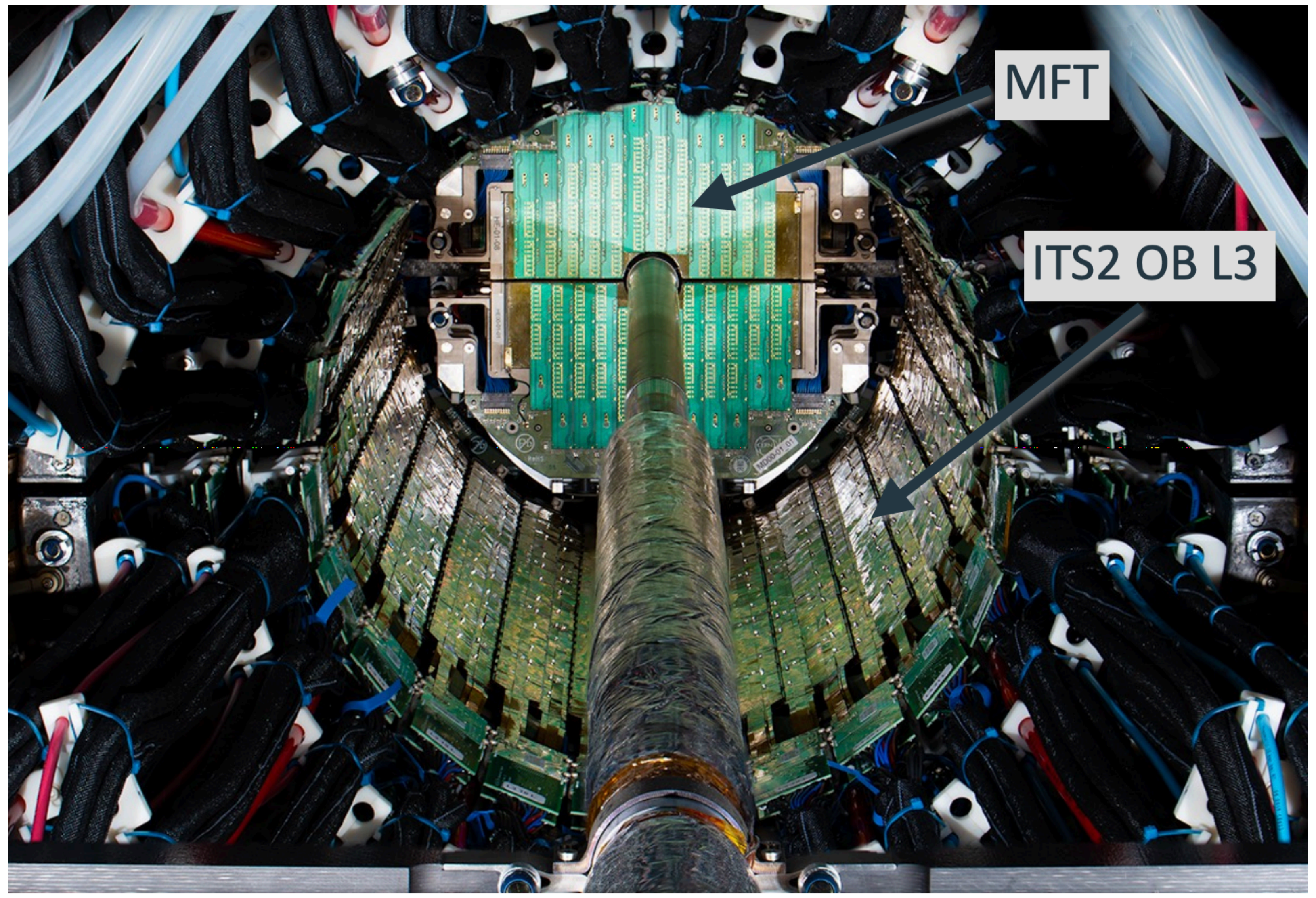

ALICE has spearheaded the development and adoptation of monolithic active pixel sensors

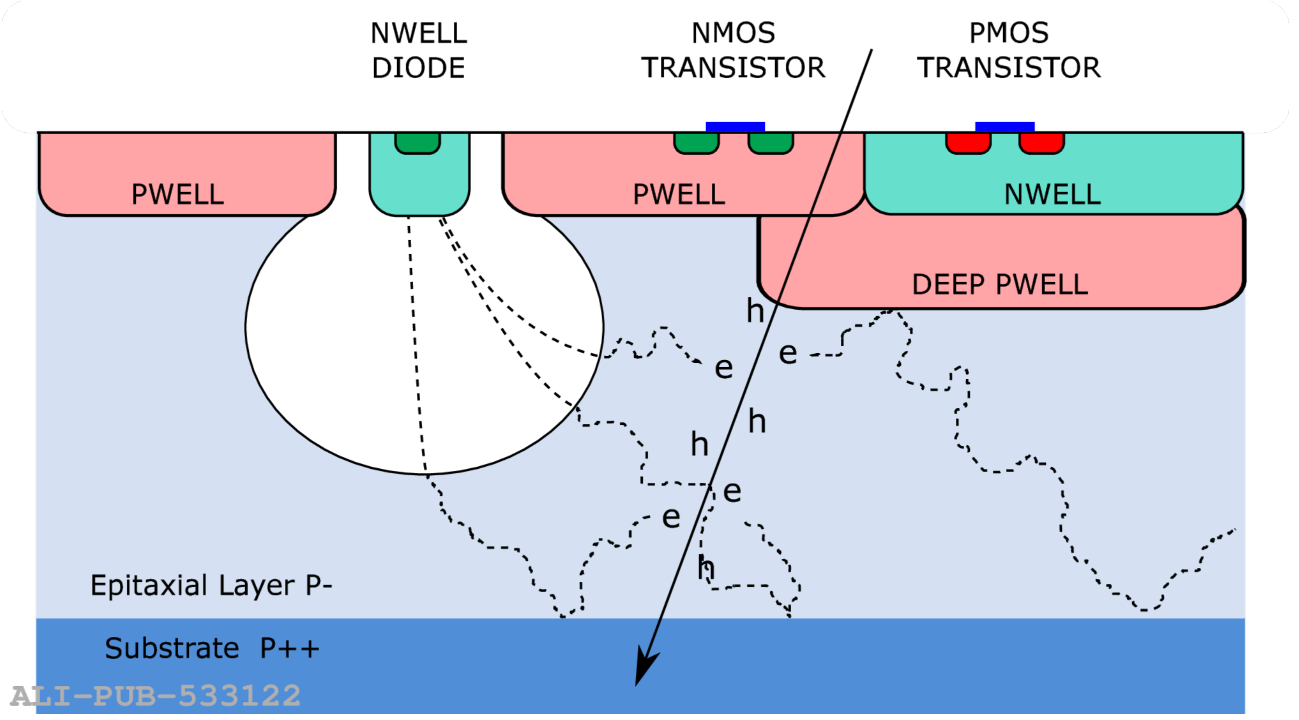

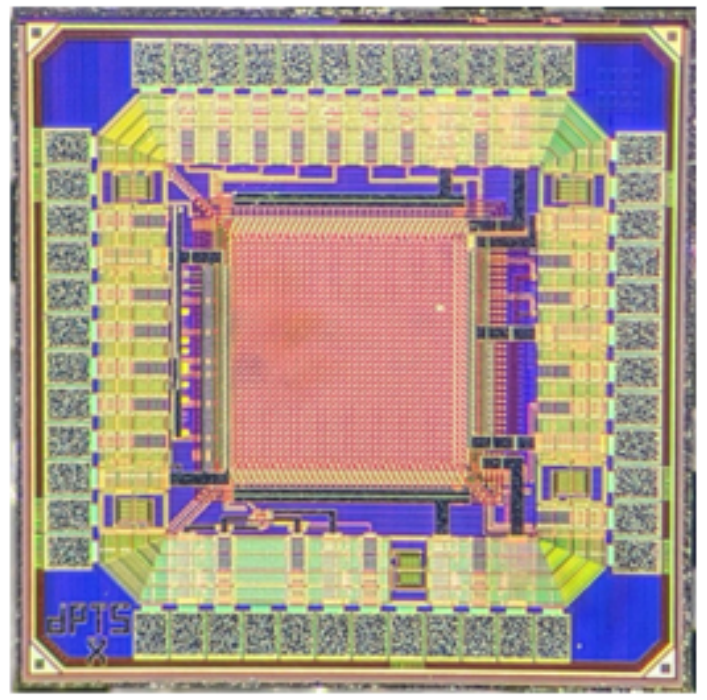

DPTS test paper arXiv:2212.08621

Detector development: silicon pixel sensors

Upgraded inner tracking system

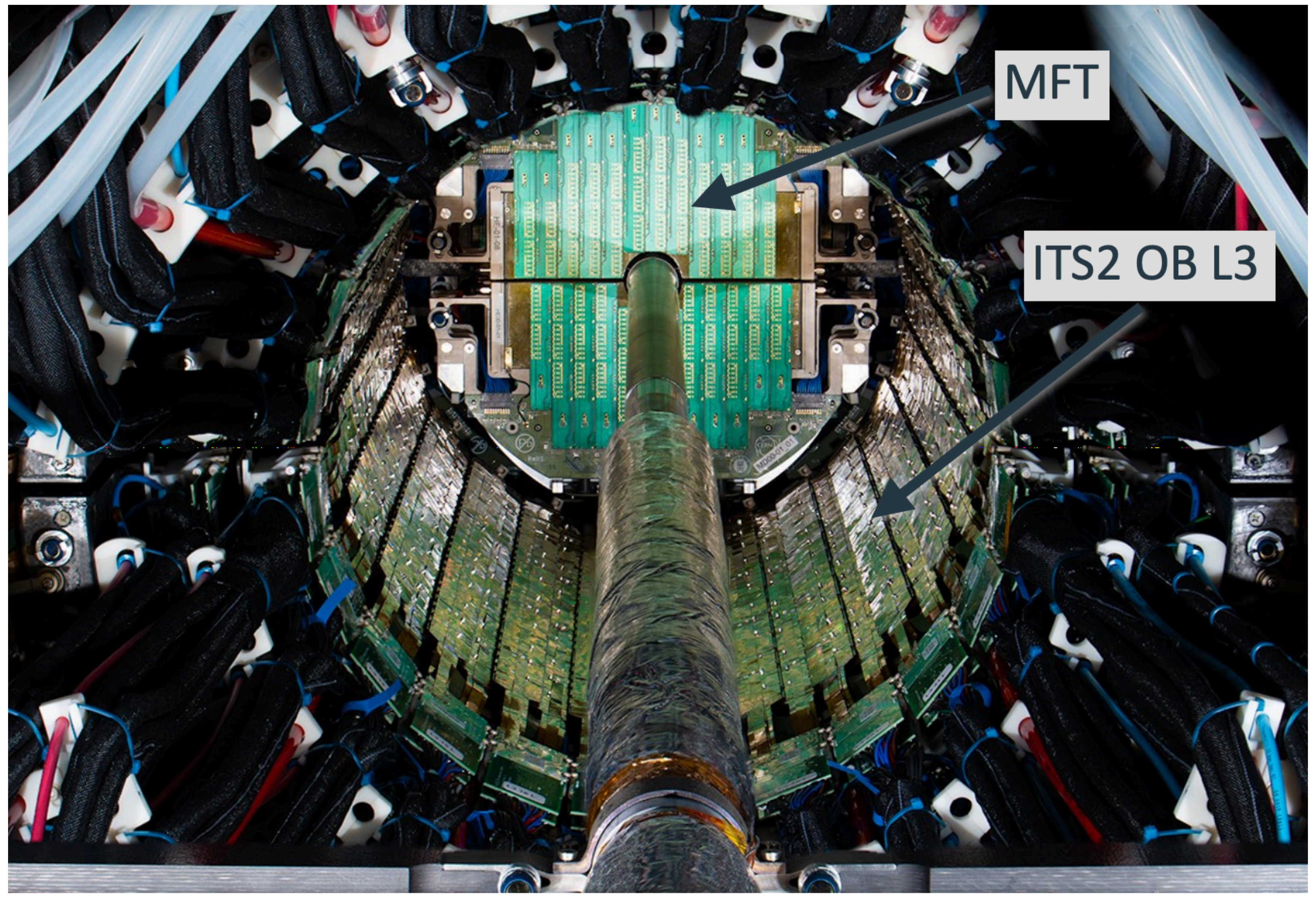

High-energy physics experiments bring together disciplines:
- detector development
- electronics
- computing
- cooling
- mechanics
- super-conducting magnet technology

ALICE has spearheaded the development and adoptation of monolithic active pixel sensors

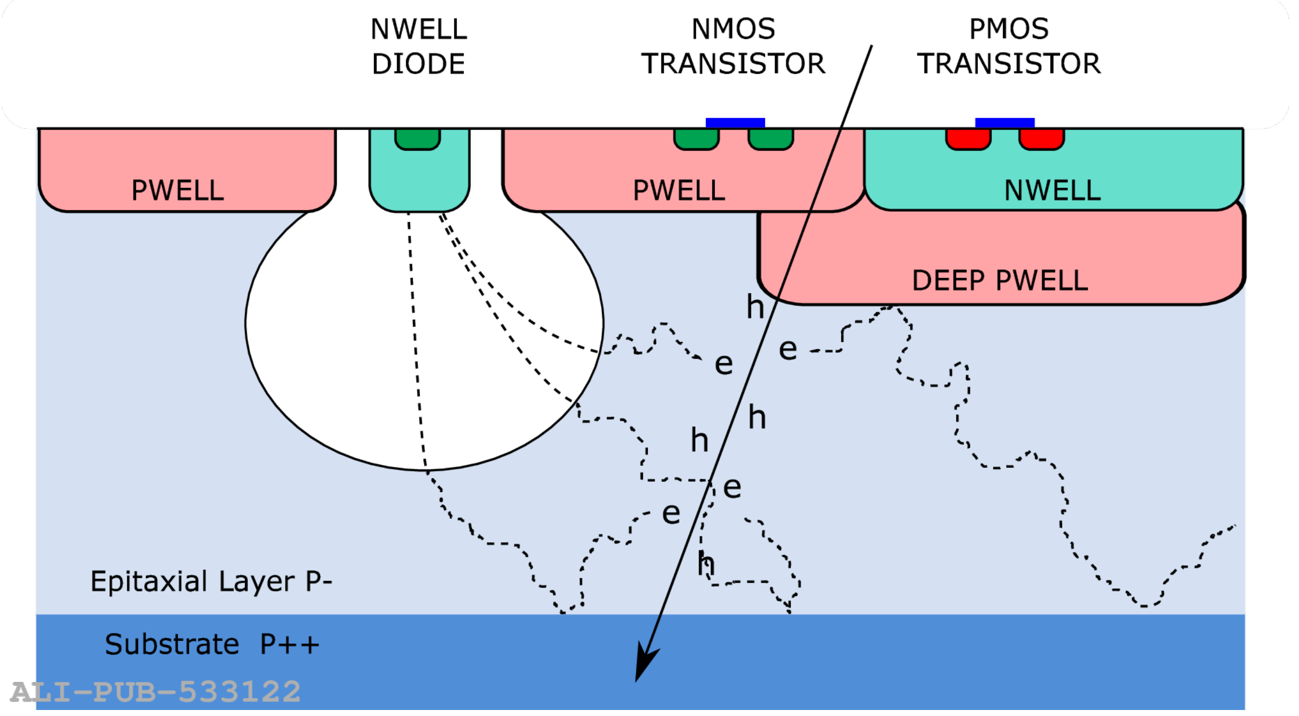

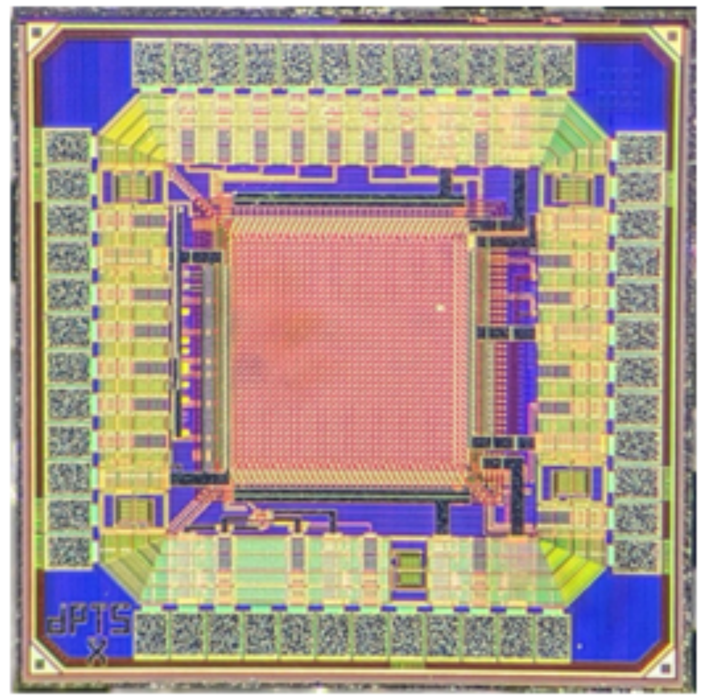

DPTS test paper arXiv:2212.08621

ITS3 upgrade

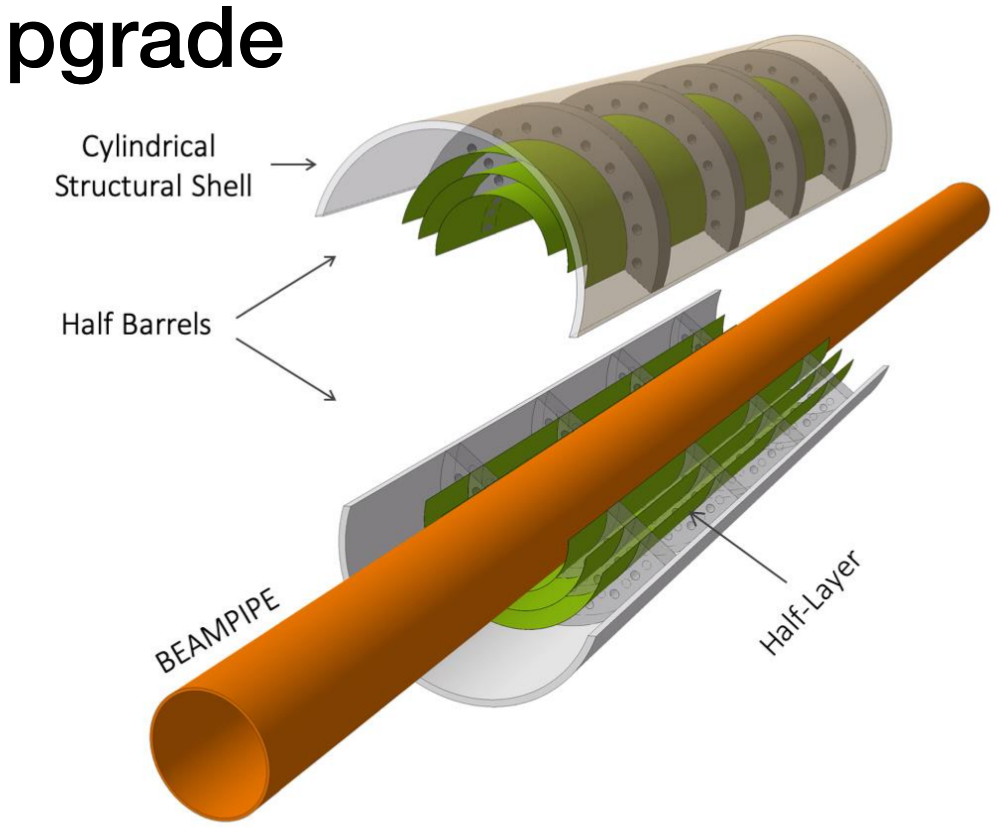

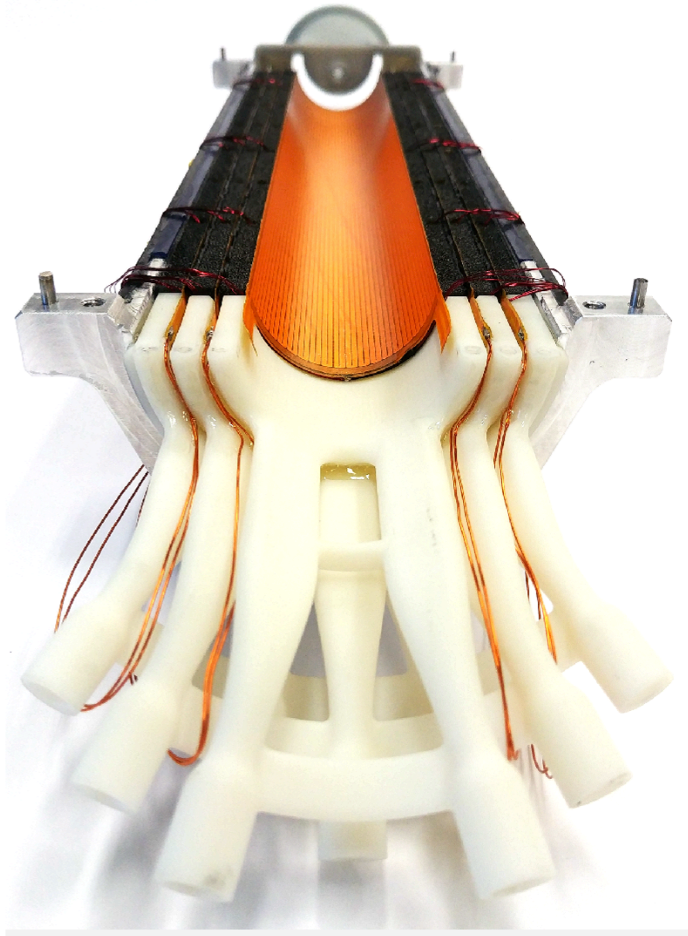

Ultralight inner layers: improved pointing resolution

Multi-charm baryon detection

New technique: strangeness tracking

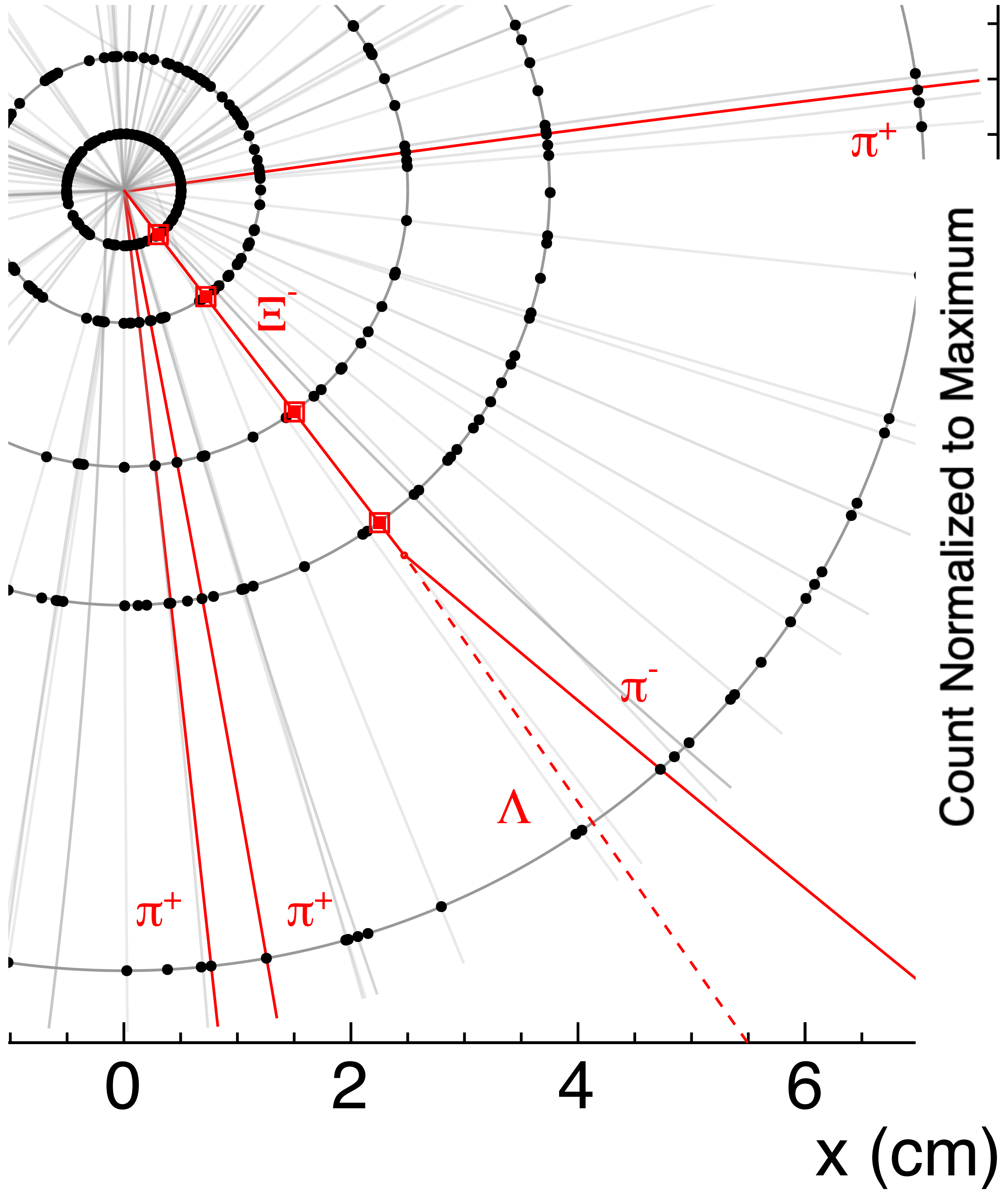

Impact parameter of Ξ

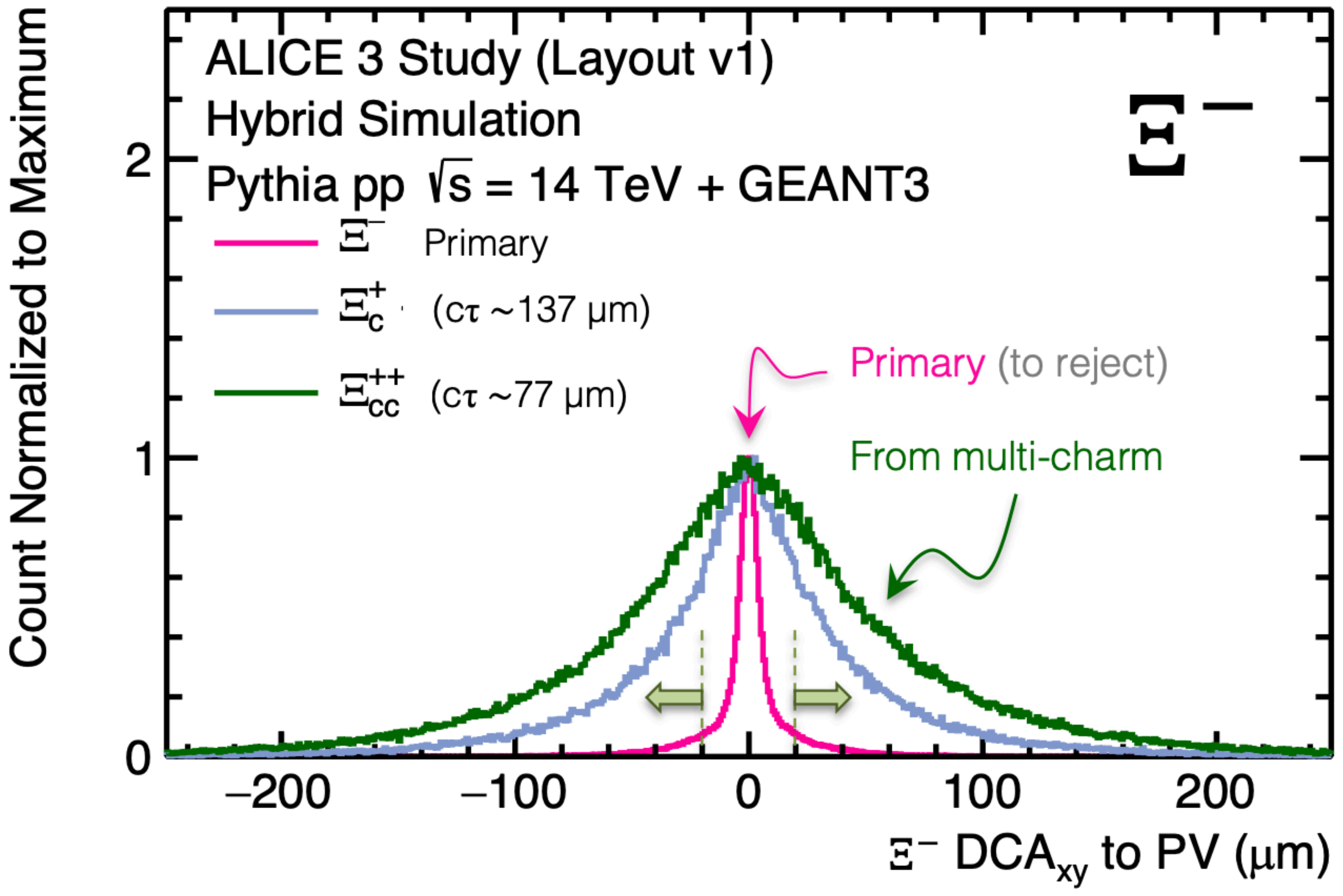

baryon provides high selectivity

$$\Xi_{cc}^{++} \rightarrow \Xi_{c}^{+} + \pi^{+} \qquad \Xi_{c}^{+} \rightarrow \Xi^{-} + 2\pi^{+}$$

Multi-charm baryon detection

New technique: strangeness tracking

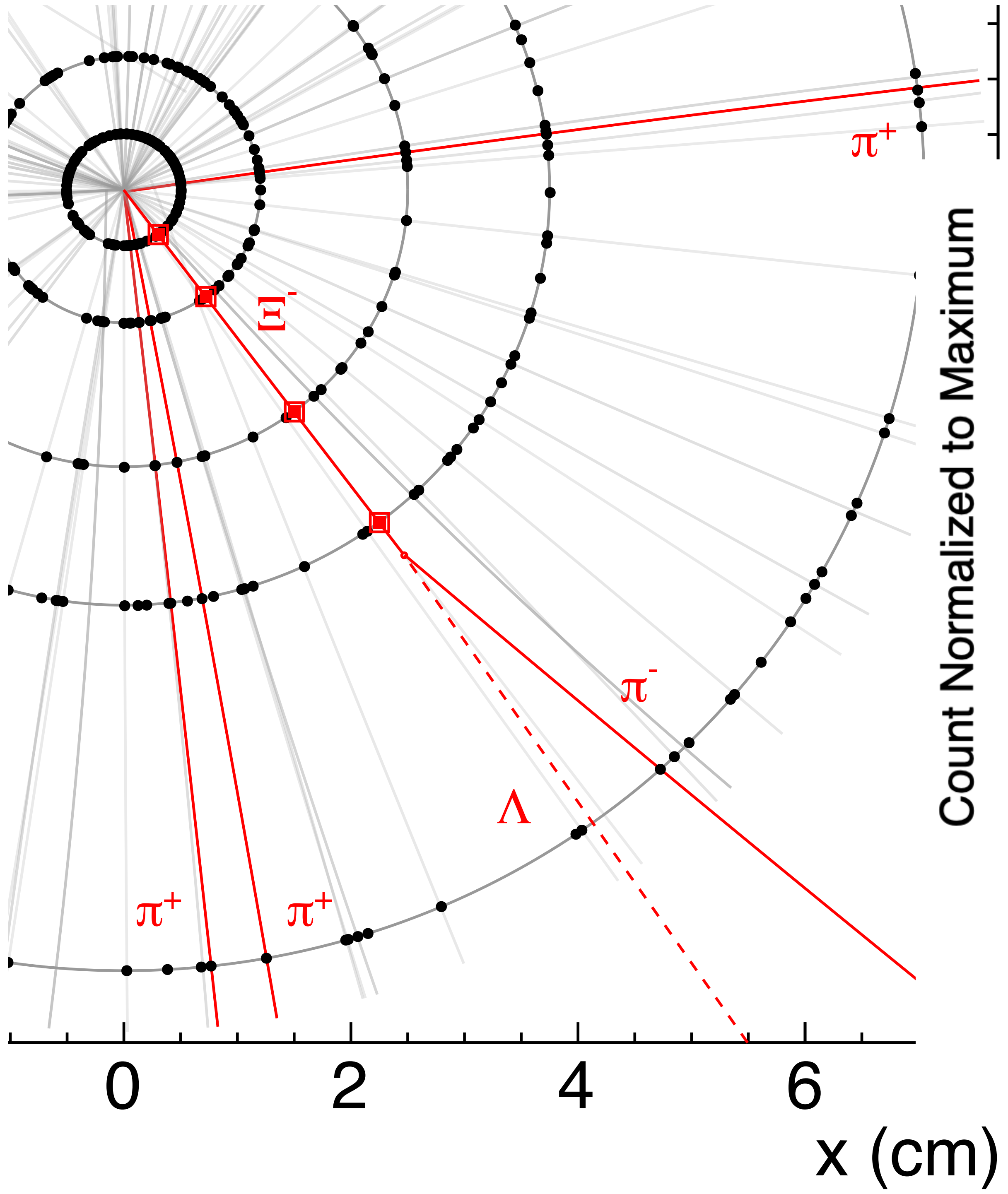

Impact parameter of Ξ

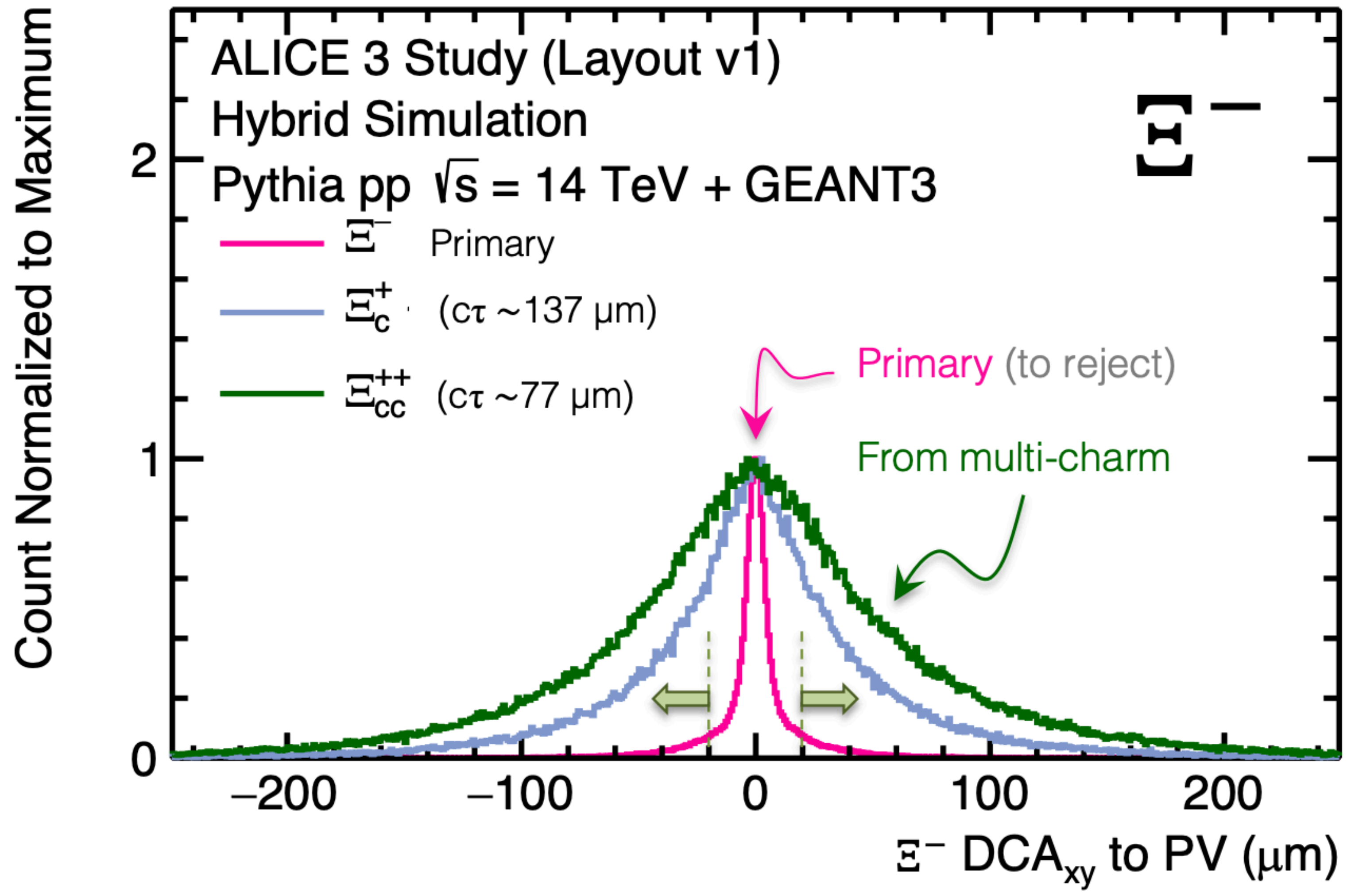

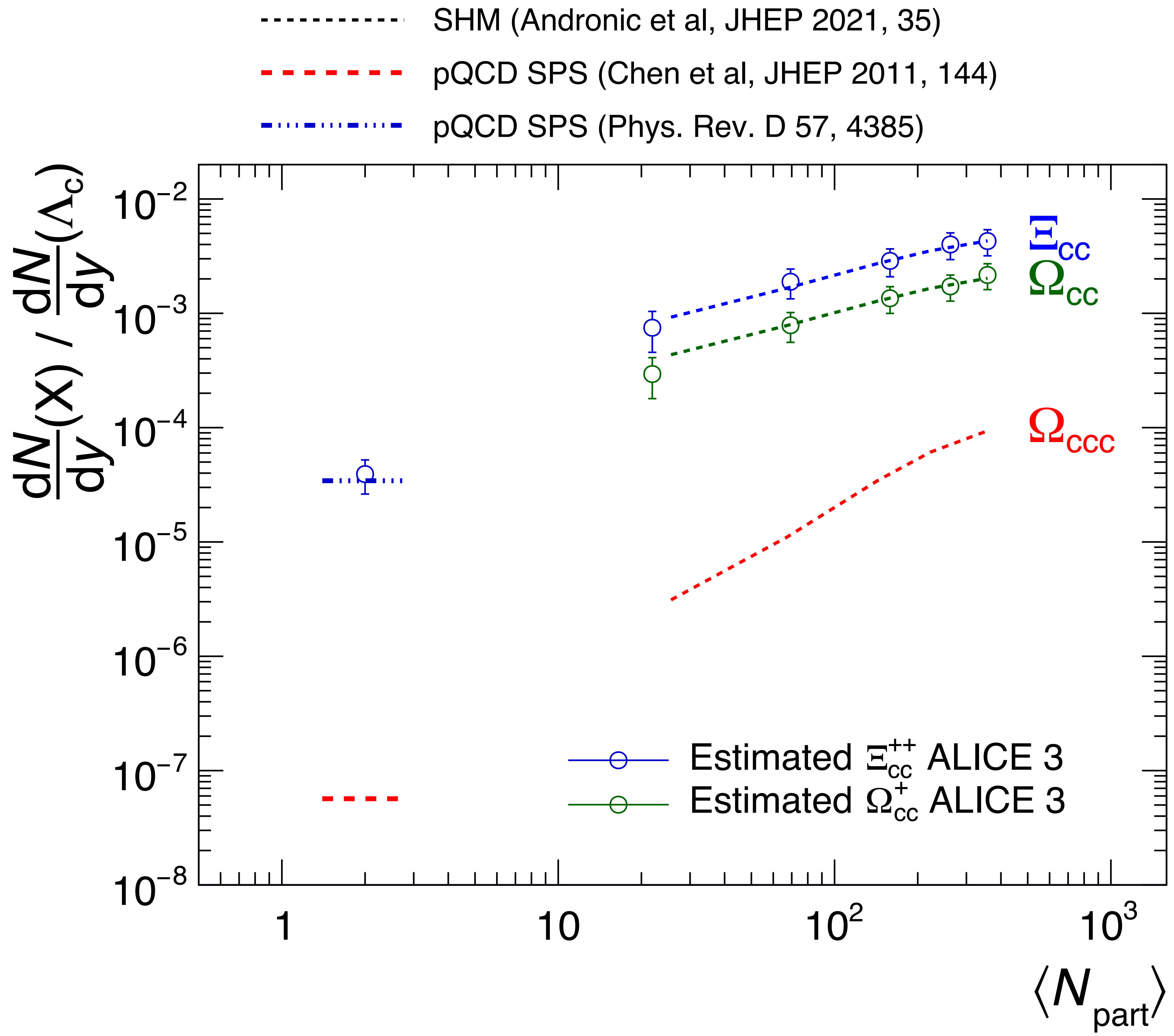

baryon provides high selectivity

$$\Xi_{cc}^{++} \rightarrow \Xi_c^{+} + \pi^{+} \qquad \Xi_c^{+} \rightarrow \Xi^{-} + 2\pi^{+}$$

Large enhancements: unique sensitivity to thermalisation and hadronisation dynamics

Unique access in Pb-Pb collisions with ALICE 3

Probing the gluon density in a hadron collider

Direct photon production

Incoming partons:
quark and gluon

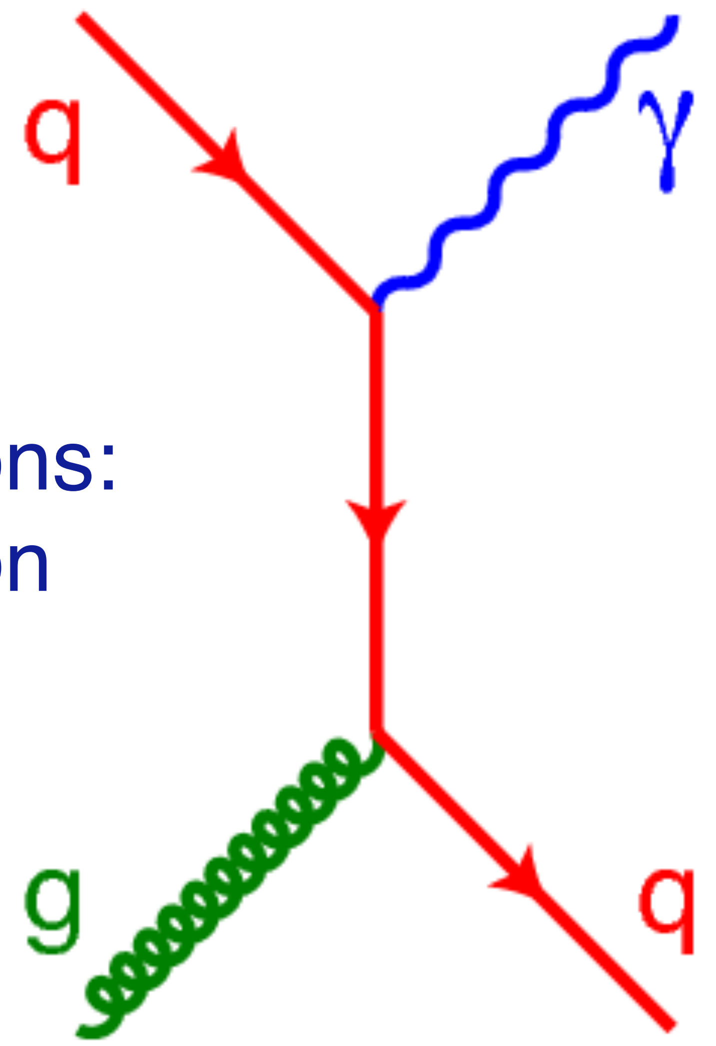

direct-γ, Compton (LO)

Sensitive to **gluons at LO**

Photon momentum directly related to incoming partons

Charm production

Incoming partons:
2 gluons

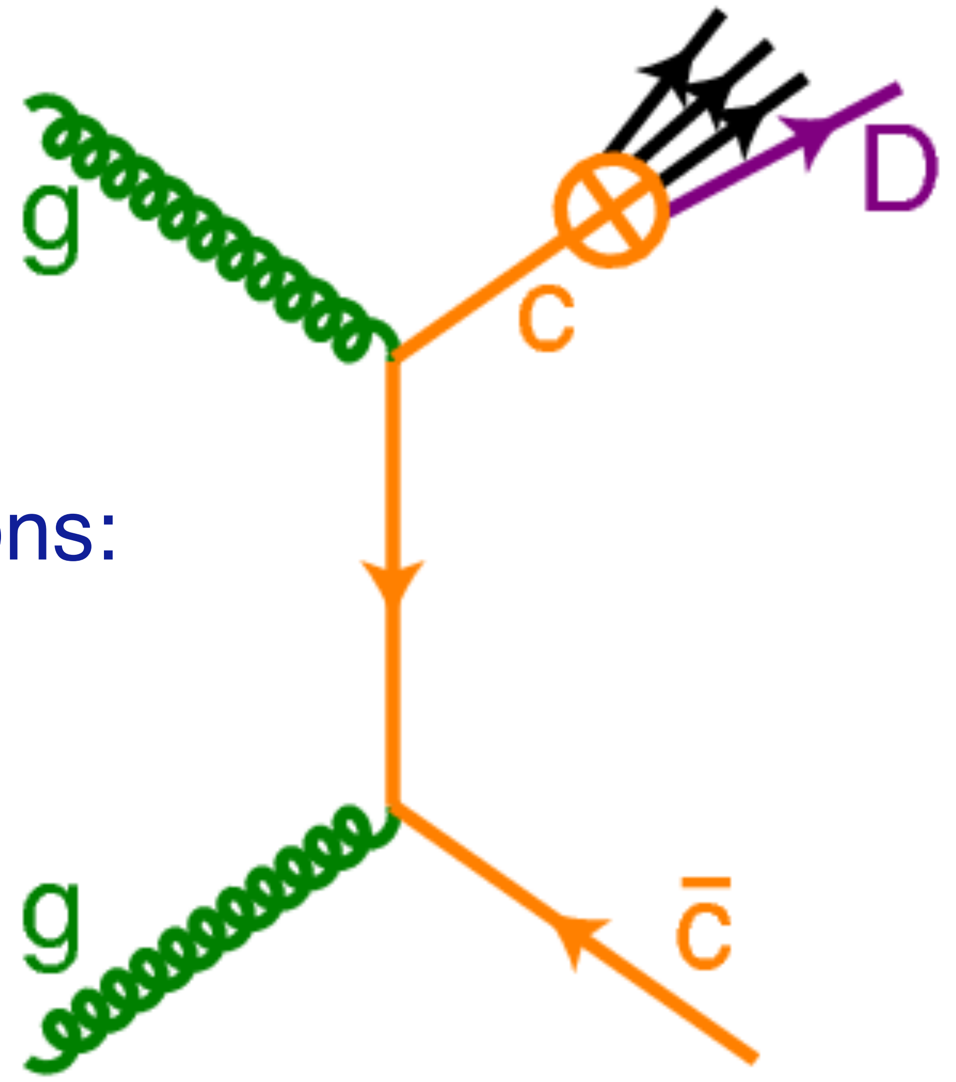

Heavy hadron:

also directly sensitive but fragmentation reduces kinematic constraint

More processes contribute, e.g. gluon splitting

Forward photons with FoCal

Signal photon fraction

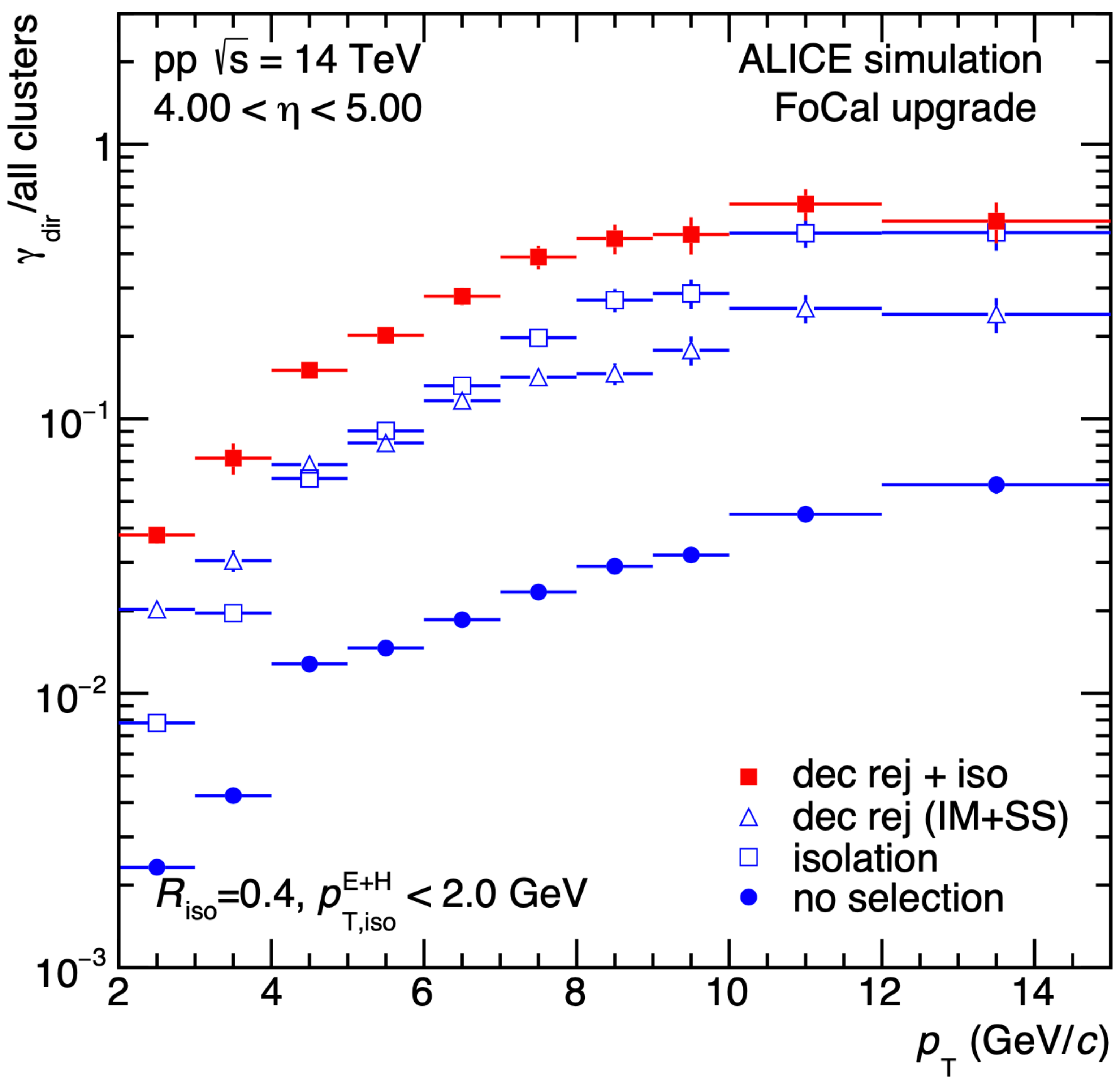

High granularity to reject decay background

Projected photon uncertainties

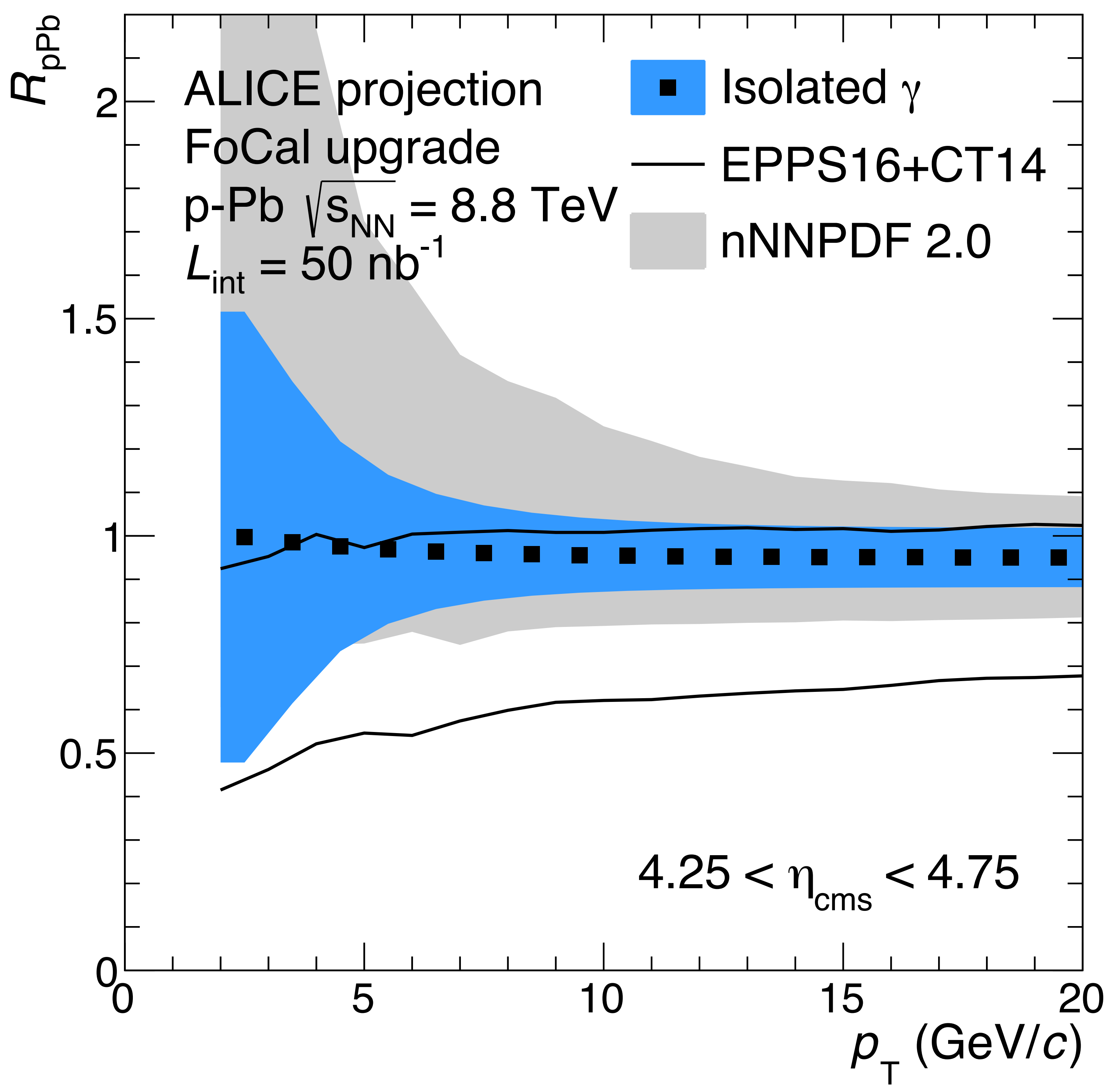

High precision direct photon measurement down to low p_T

Projected PDF uncertainties

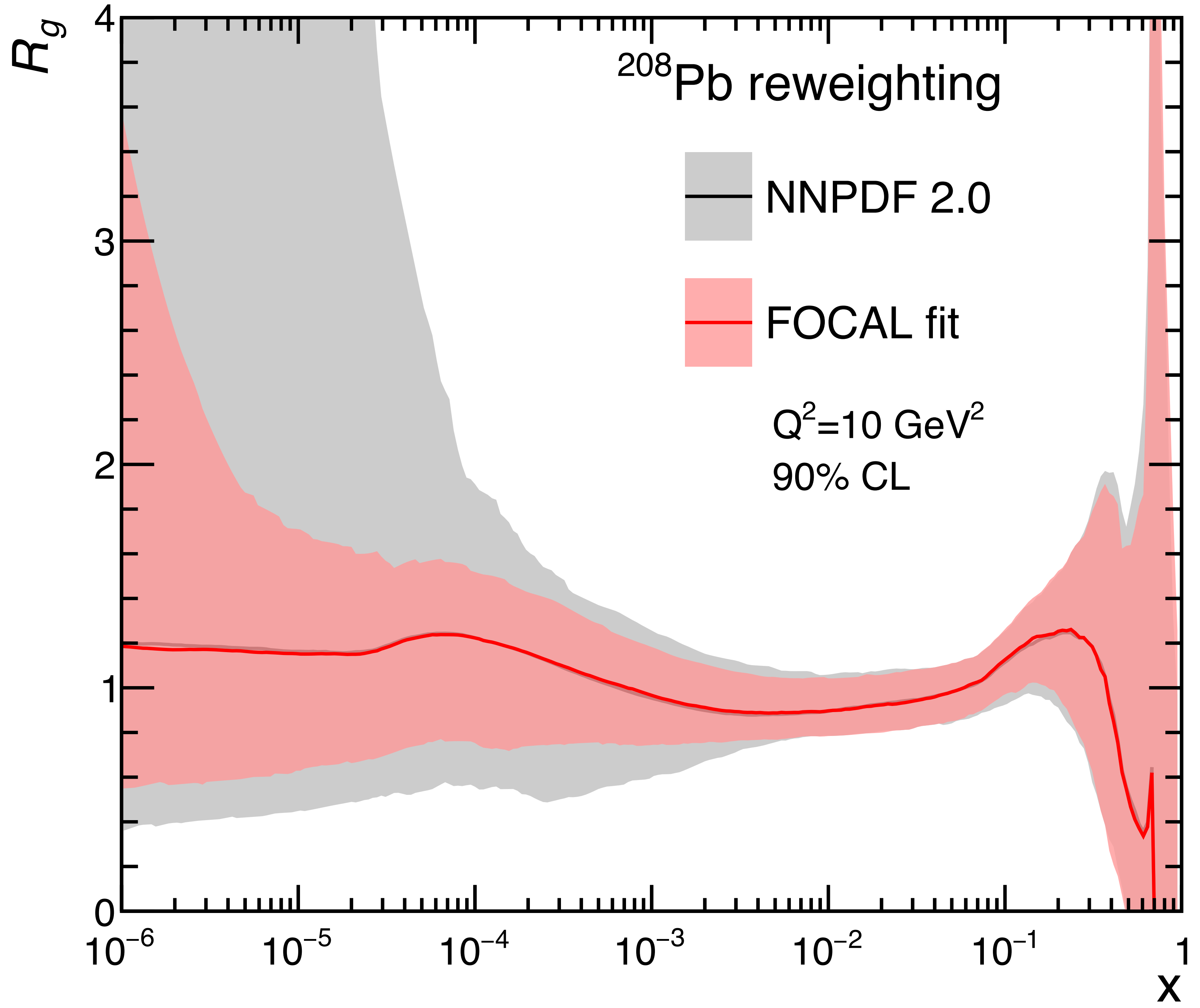

Constrain gluon density in nuclei over a broad range: $x \sim 10^{-5} - 10^{-2}$ at small Q^2

Elliptic flow of quarkonia

J/ψ v_2

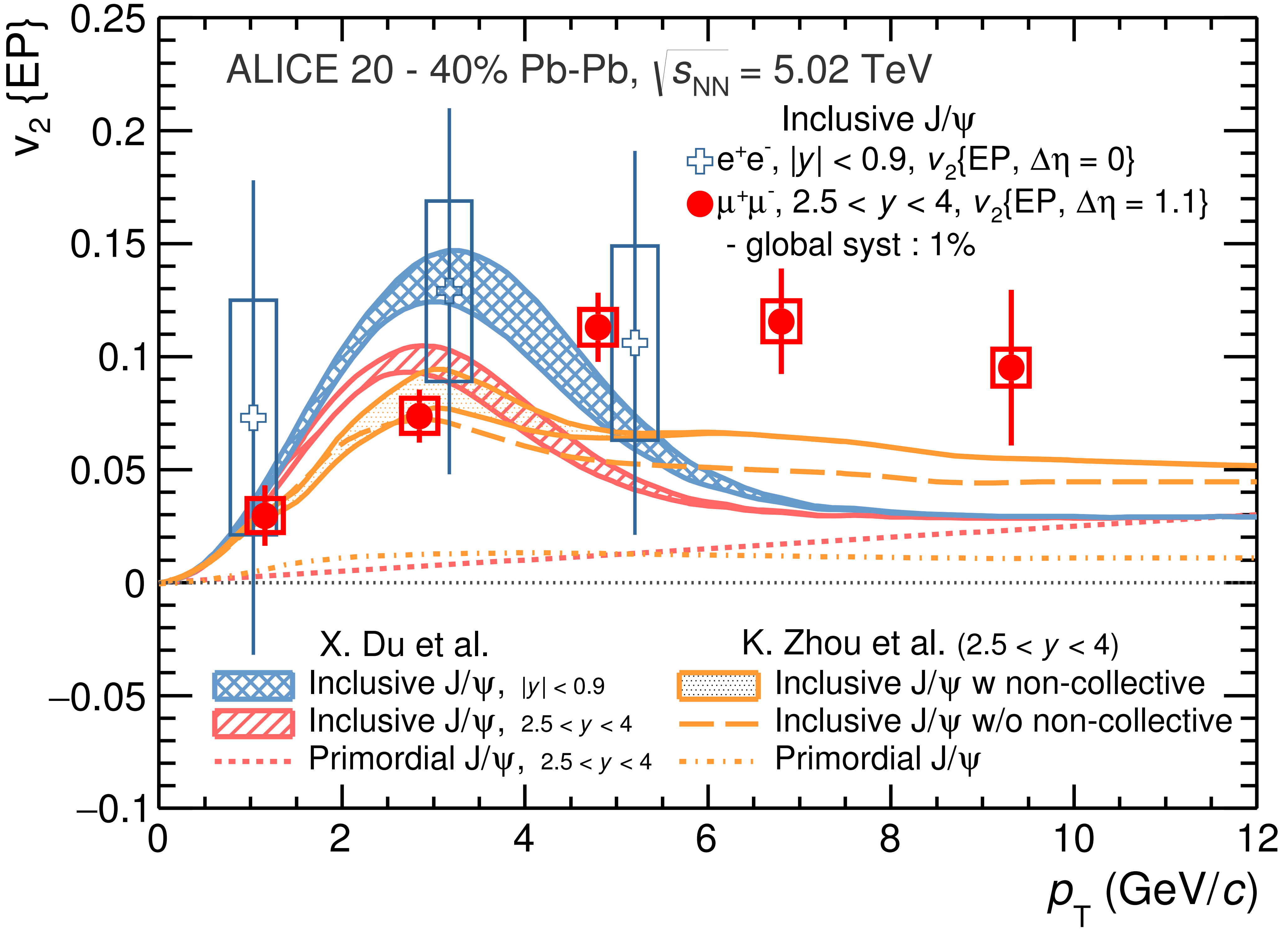

PRL 119, 242301

J/ψ v_2: new model calculation

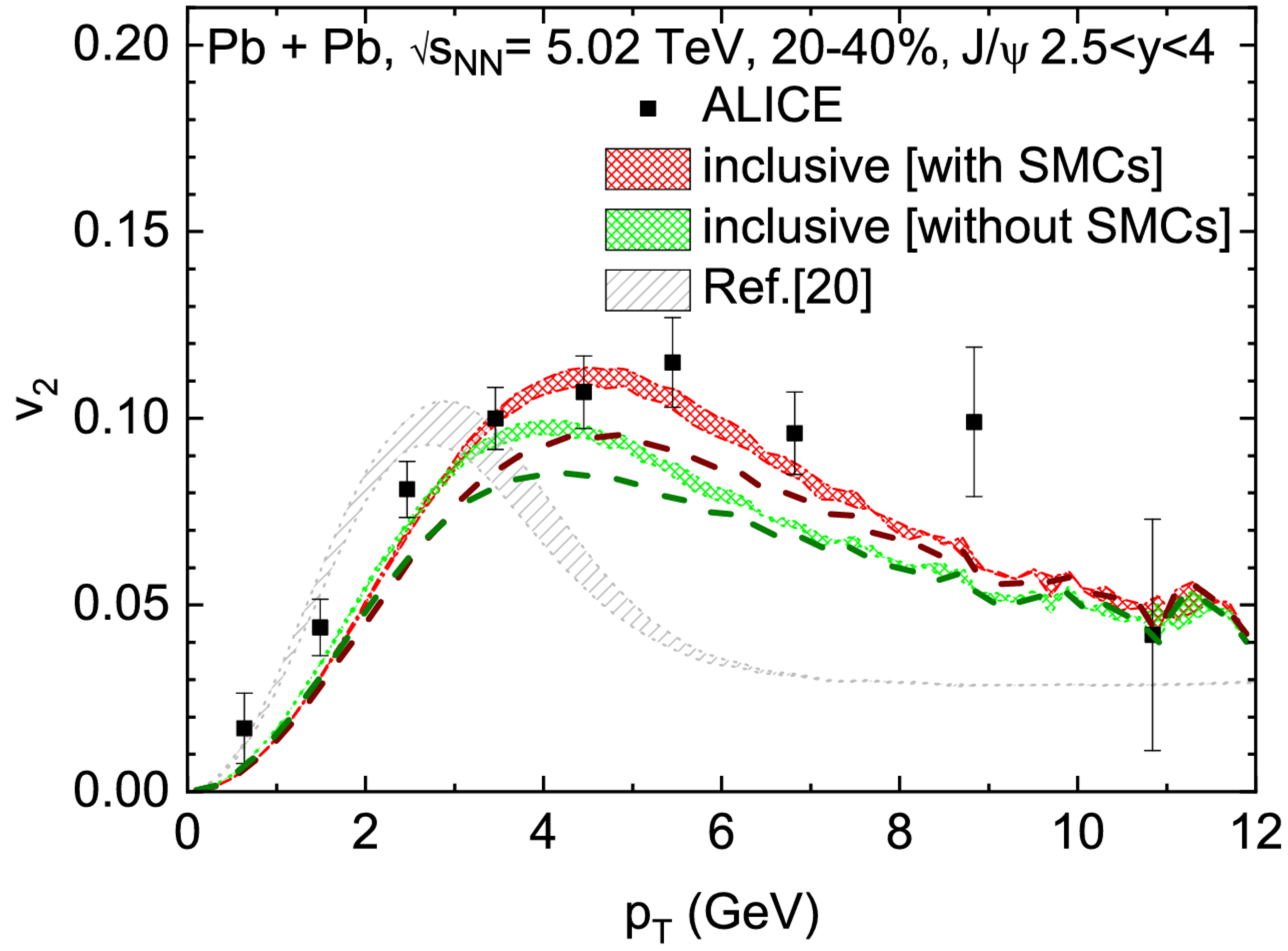

Min He and Ralf Rapp, PRL 128 (2022) 16, 162301

J/ψ melting is not directional; expect no or very little v_2

Recombination sensitive to v_2 of QGP

—> Expect non-zero v_2 at low p_T

Updated model: v_2 extends to larger p_T

ALICE

Interactions of beauty quarks with the QGP: v_2

Prompt and non-prompt (from B decay) D^0 v_2

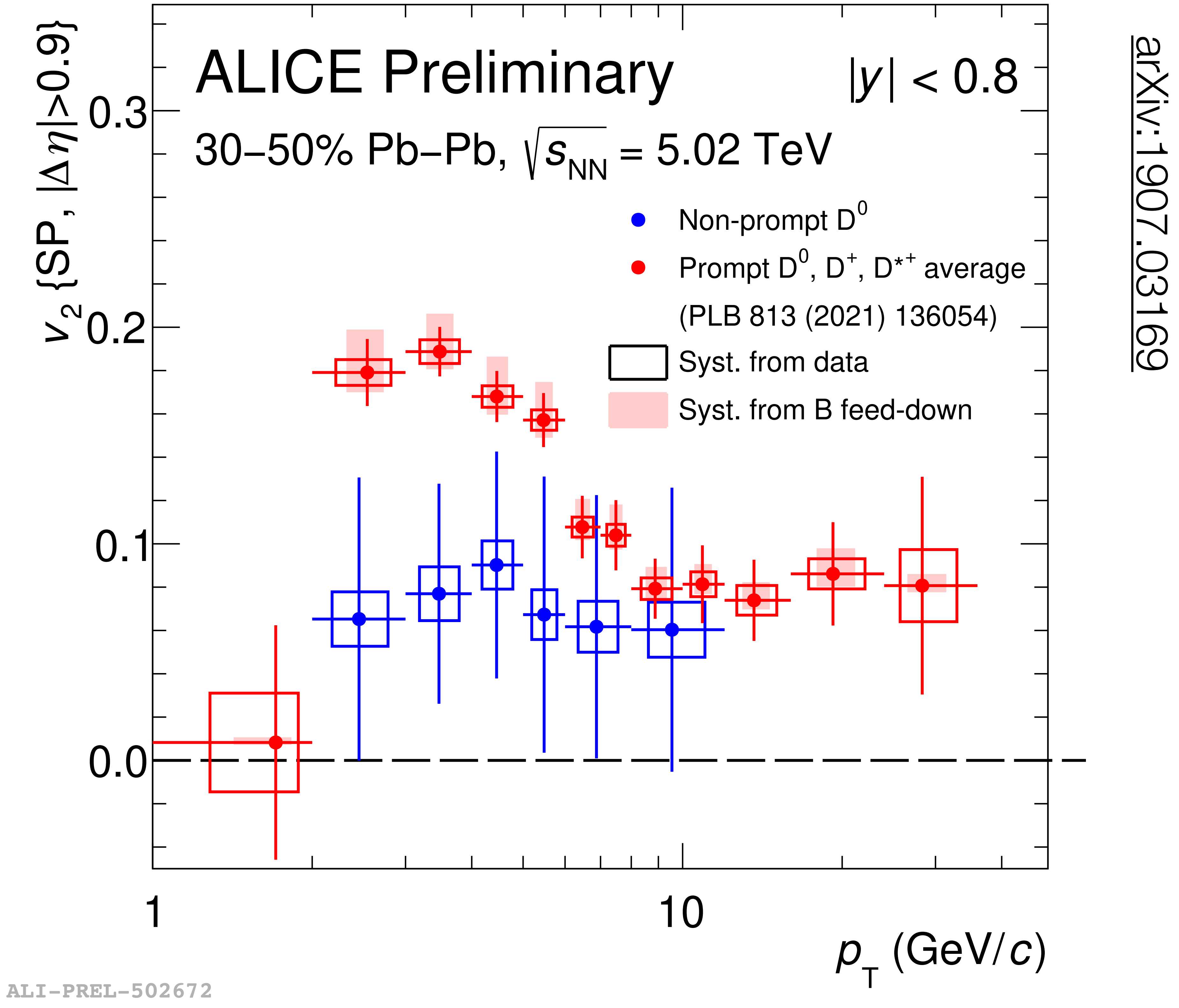

Open HF: smaller v_2 for beauty than charm

J/ψ and Υ v_2

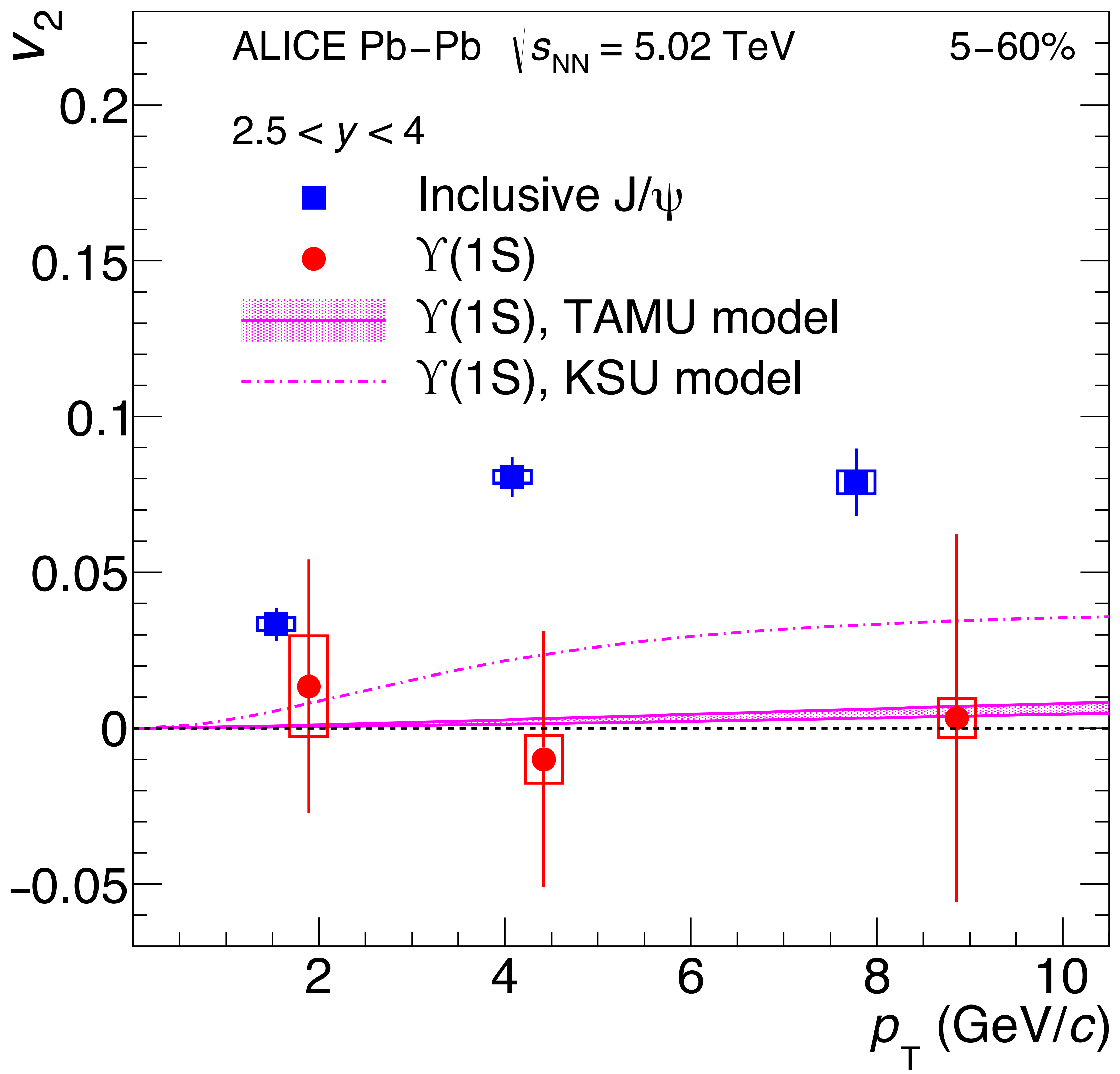

Hidden HF: no beauty v_2 ?

Suggests smaller interaction cross sections for beauty than charm — longer thermalisation time

Interactions of beauty quarks with the QGP: v_2

Prompt and non-prompt (from B decay) D^0 v_2

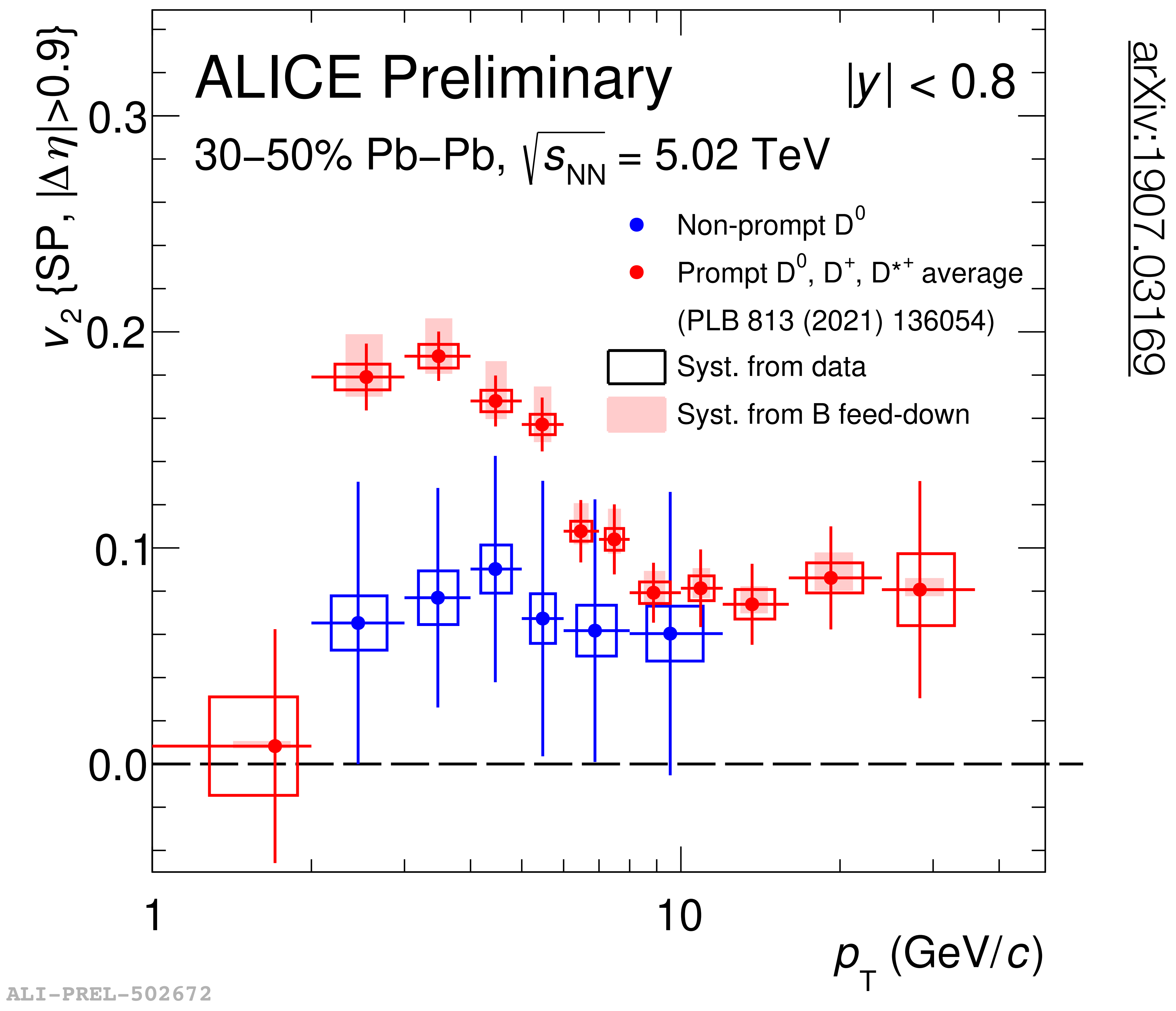

J/ψ and ϒ v_2

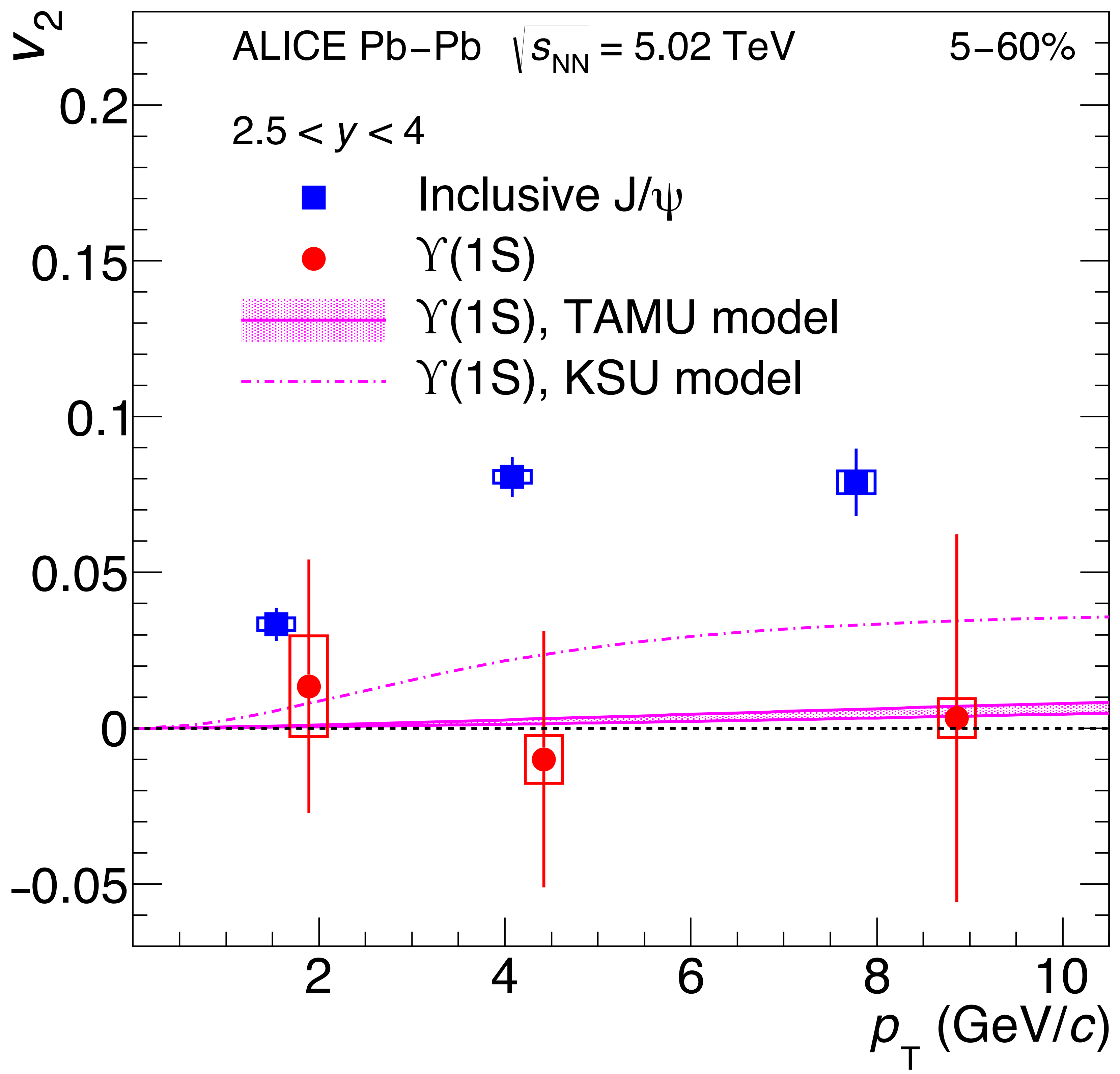

Open HF: smaller v_2 for beauty than charm

Hidden HF: no beauty v_2 ?

Suggests smaller interaction cross sections for beauty than charm — longer thermalisation time

Light quark v_2 may contribute to open beauty v_2, via recombination

Uncertainties large — improve precision to conclude

Probing the QGP with jets at LHC

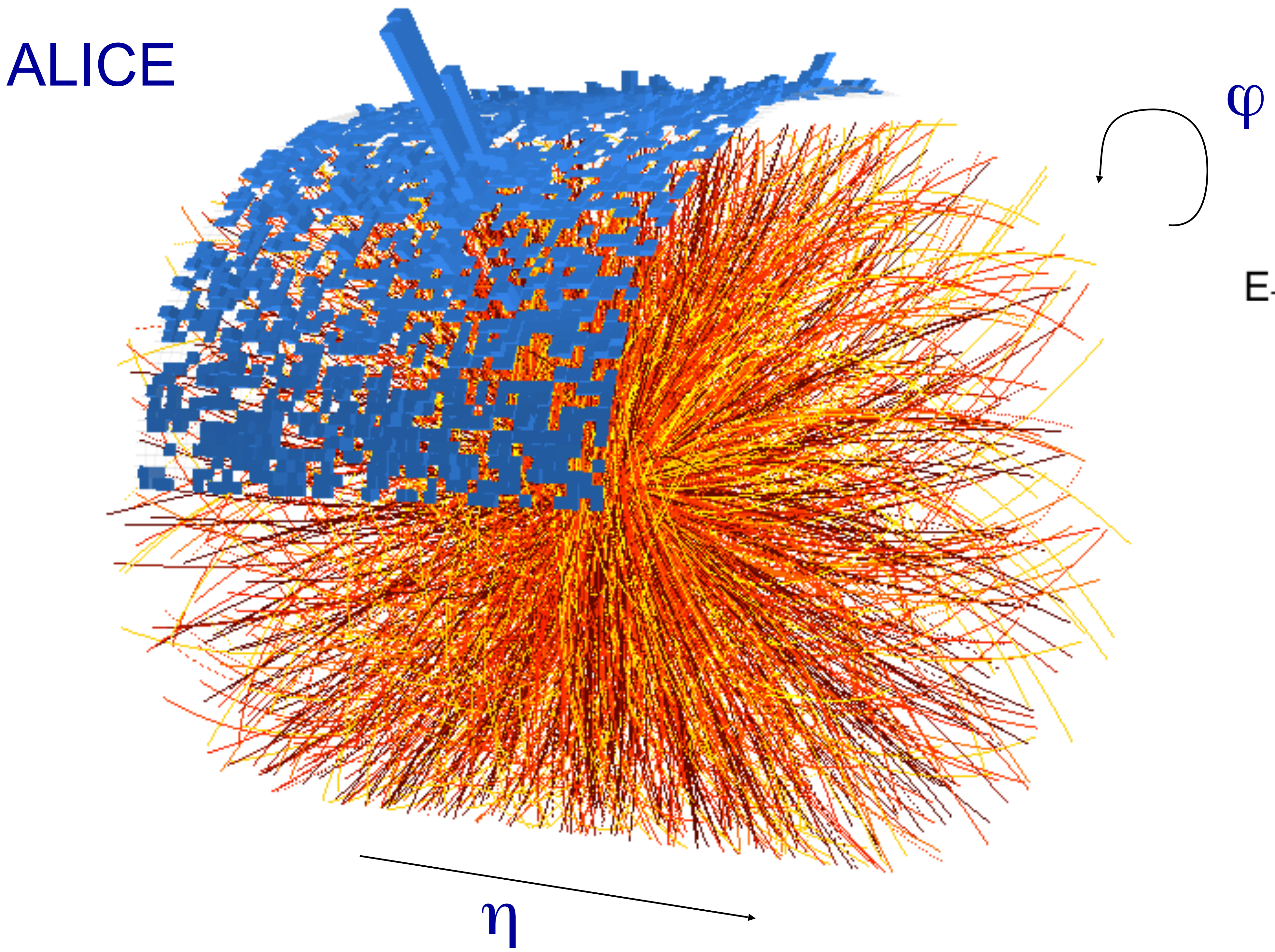

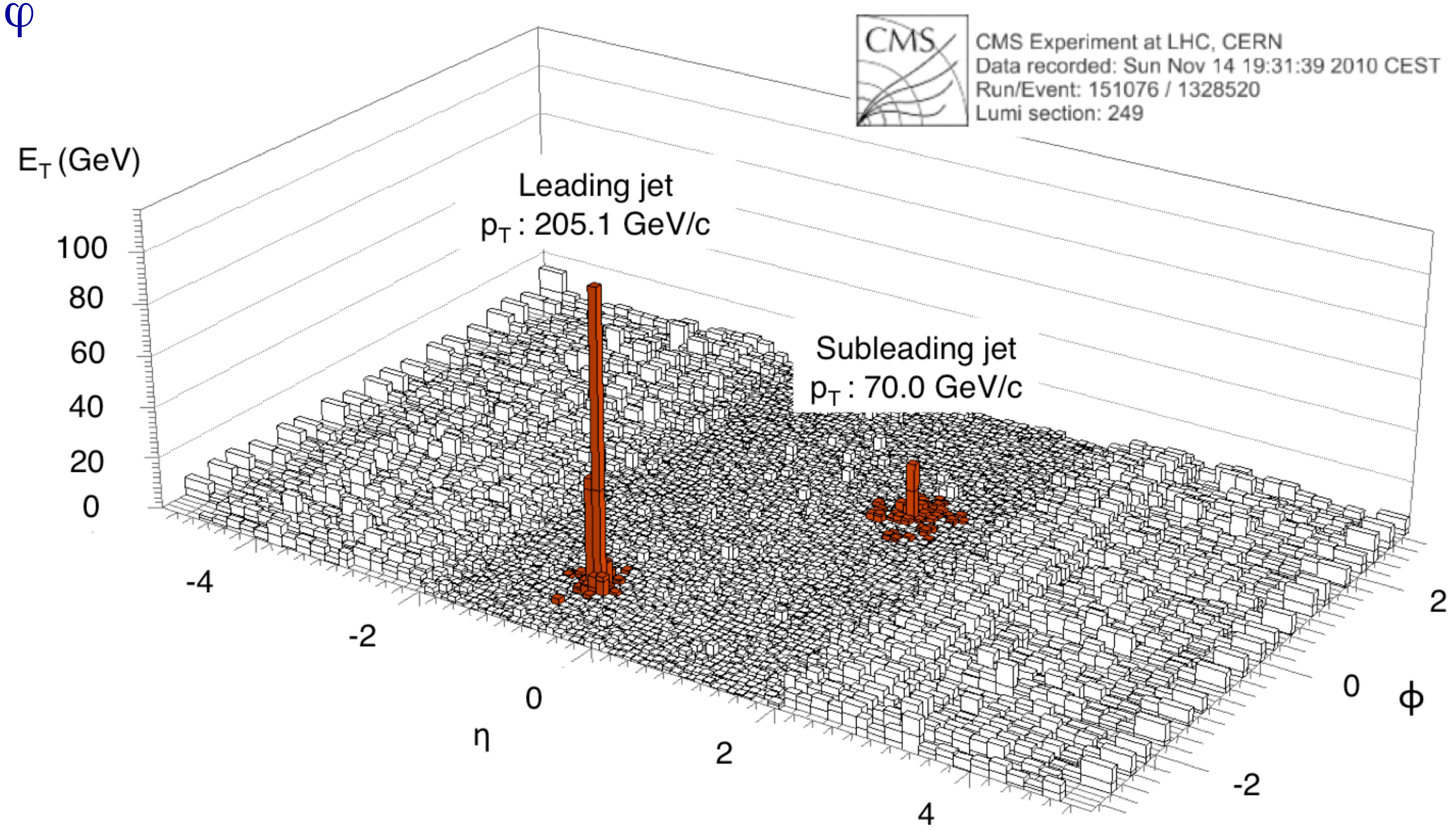

Very clear signals at high p_T: jets stand out above uncorrelated 'soft' background

Interactions with QGP: energy loss, high-p_T suppression

Energy loss: di-jet asymmetry

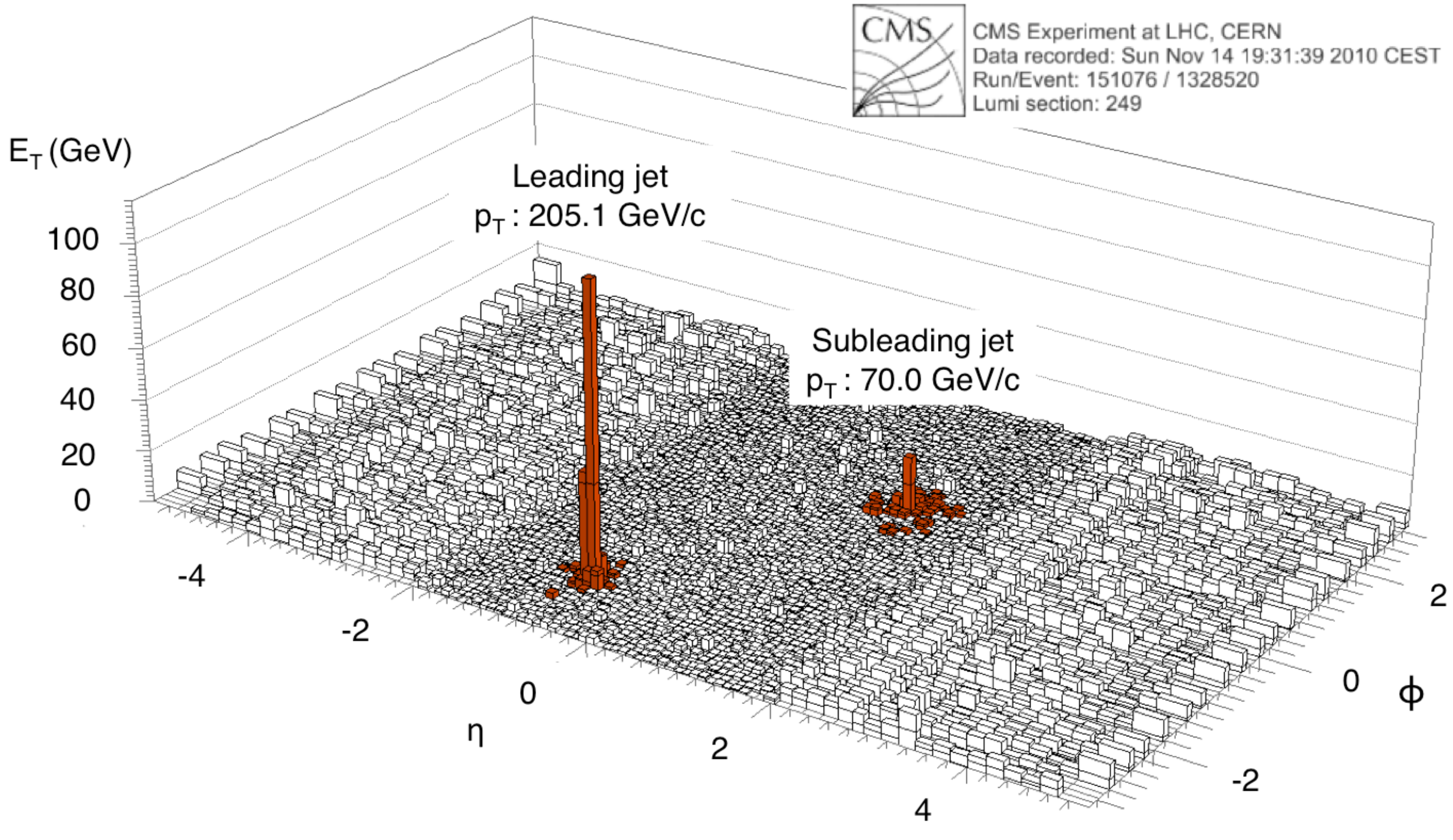

Single event: p_T not balanced!

Energy fraction of second jet

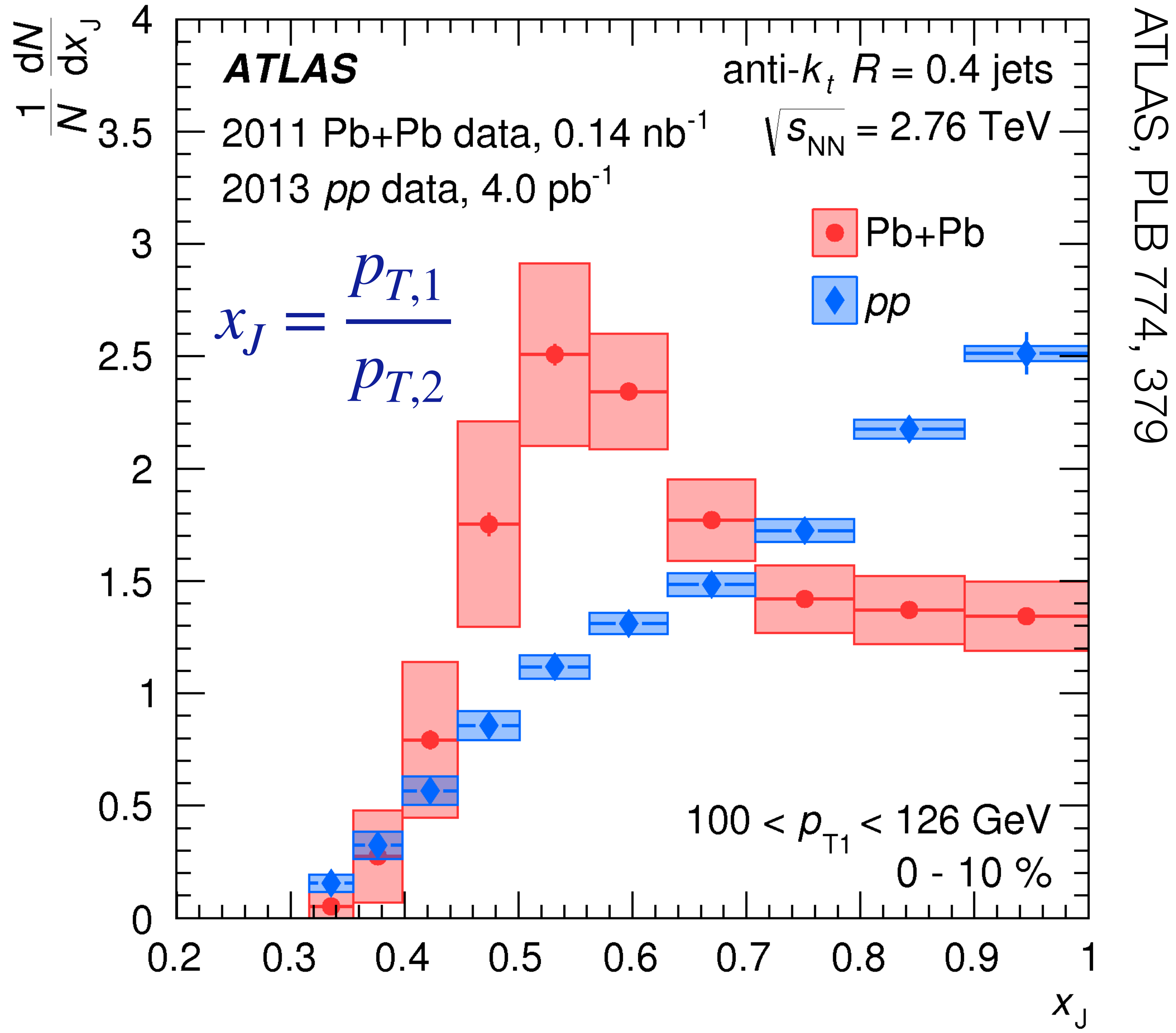

$$x_J = \frac{p_{T,1}}{p_{T,2}}$$

pp: peak at 1 — balanced jets
PbPb: shift towards lower values

Di-jet energy imbalance: jets lose energy as they propagate through the plasma

Experimental challenge: large combinatorial background in Pb-Pb

Haake and Loizides, PRC99, 064904

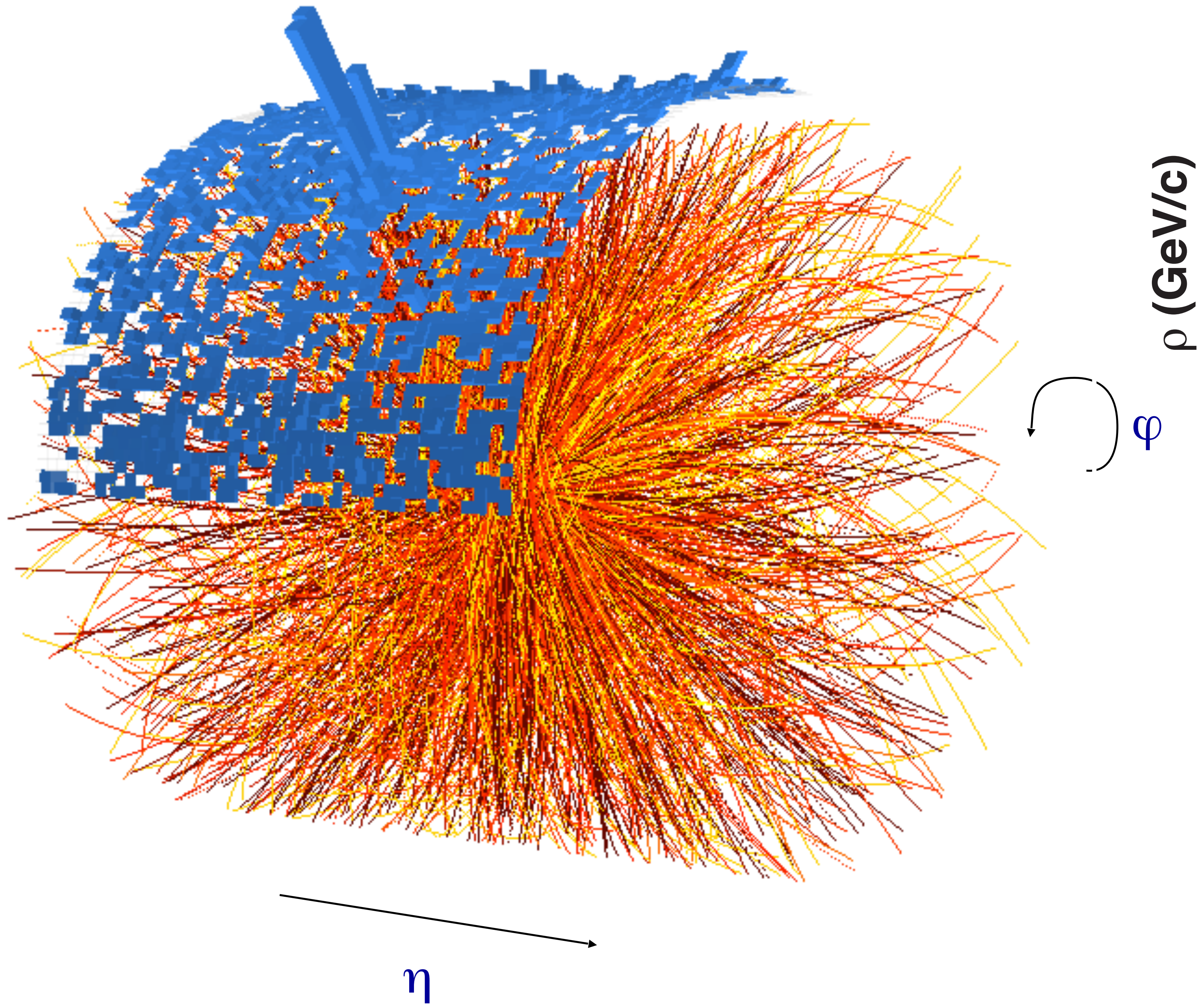

JHEP 03 (2012) 053

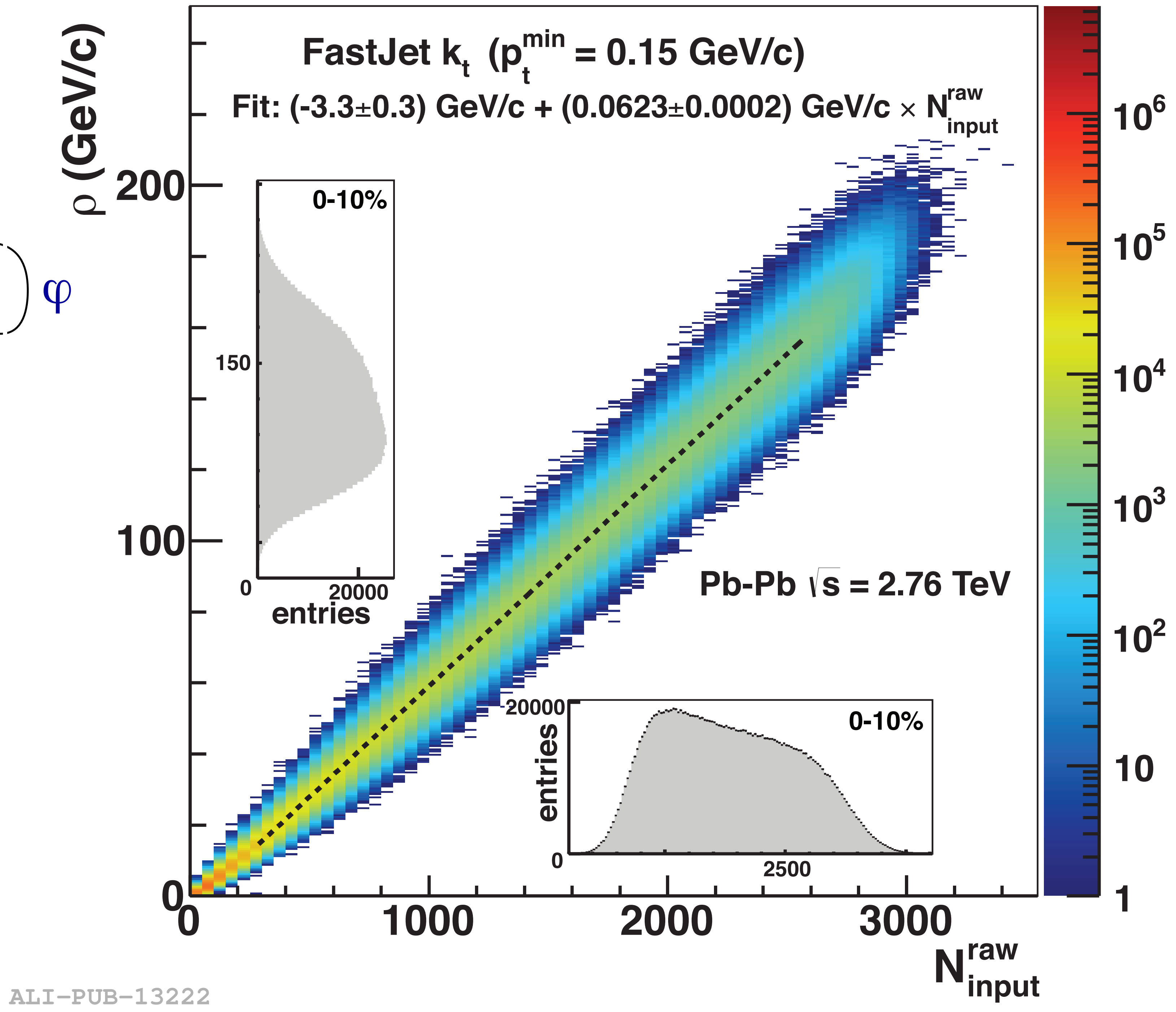

Machine-learning technique

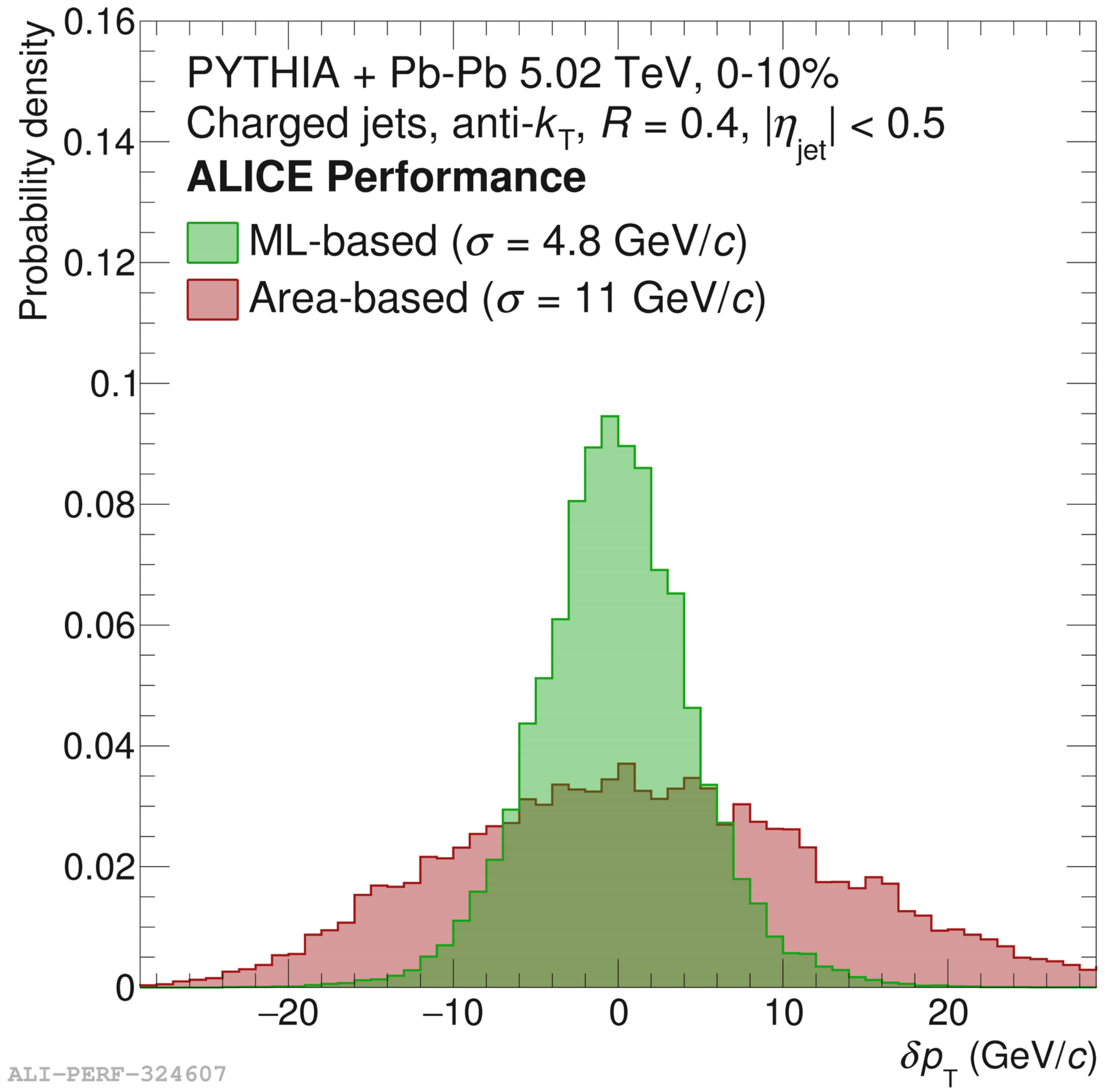

Standard technique: measure background E_T density outside jet 'Area based'

Background subtraction refined based on e.g. leading particle p_T
Reduces fluctuations

Residual fluctuations due to finite number statistics

Allows to measure jets with larger R, lower p_T

Jet-radius dependence of energy loss in Pb-Pb collisions

ALICE, arXiv:2303.00592

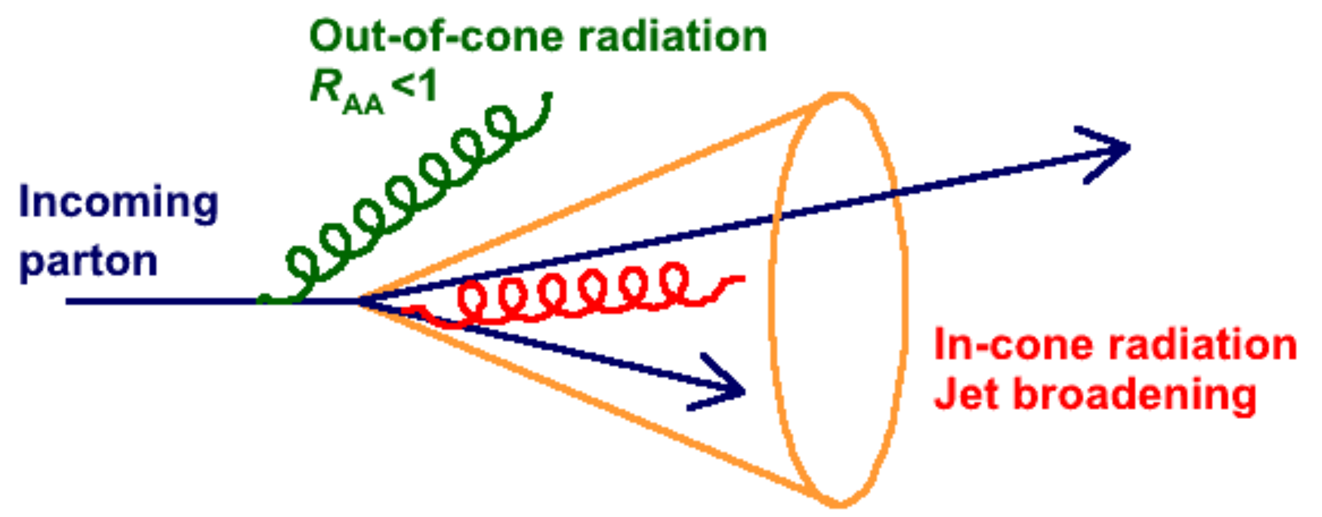

Quantify in- and out-of-cone radiation by measuring jet quenching vs cone radius

Nuclear modification factor

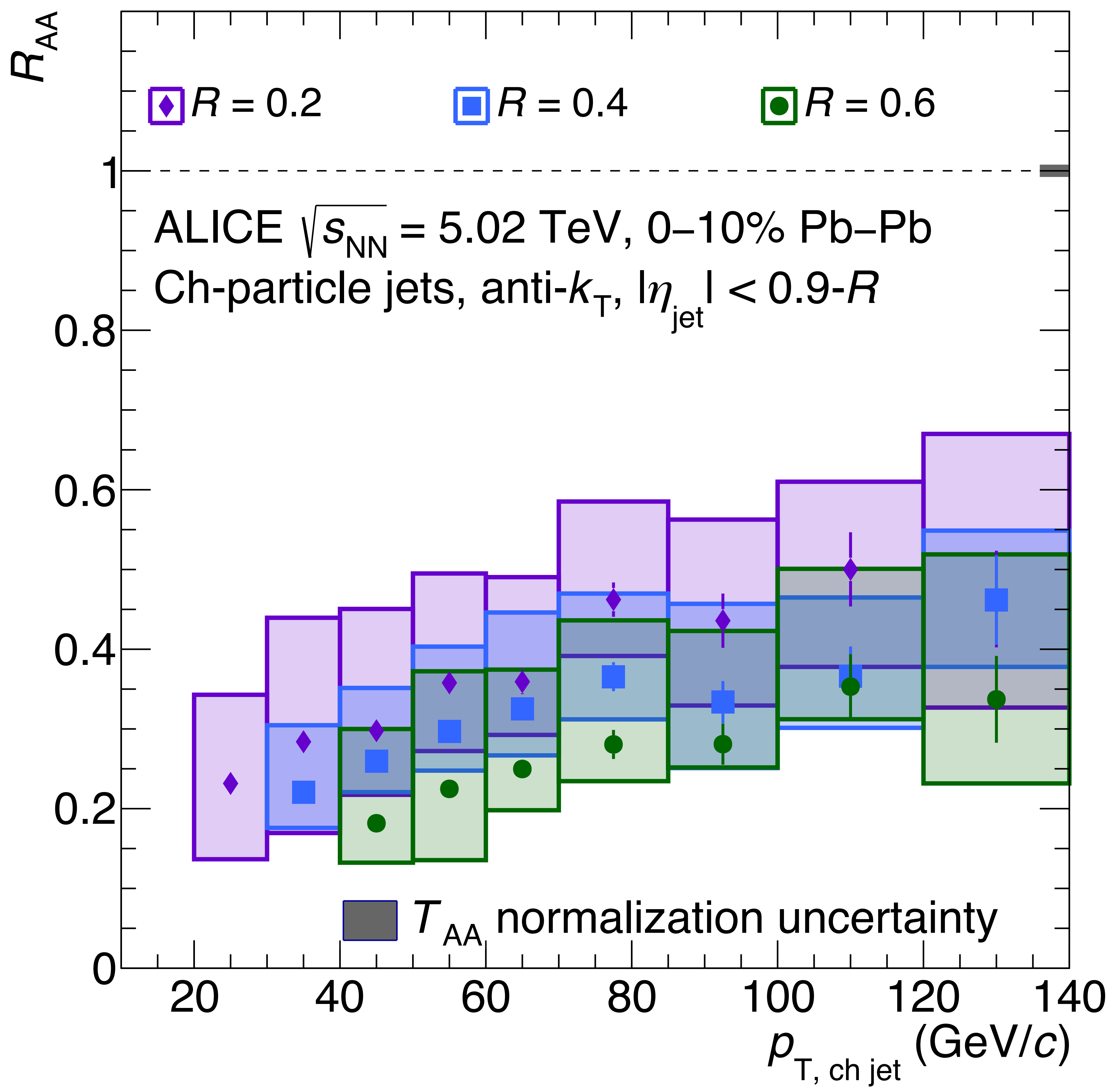

R-dependence: ratio R=0.6/R=0.2

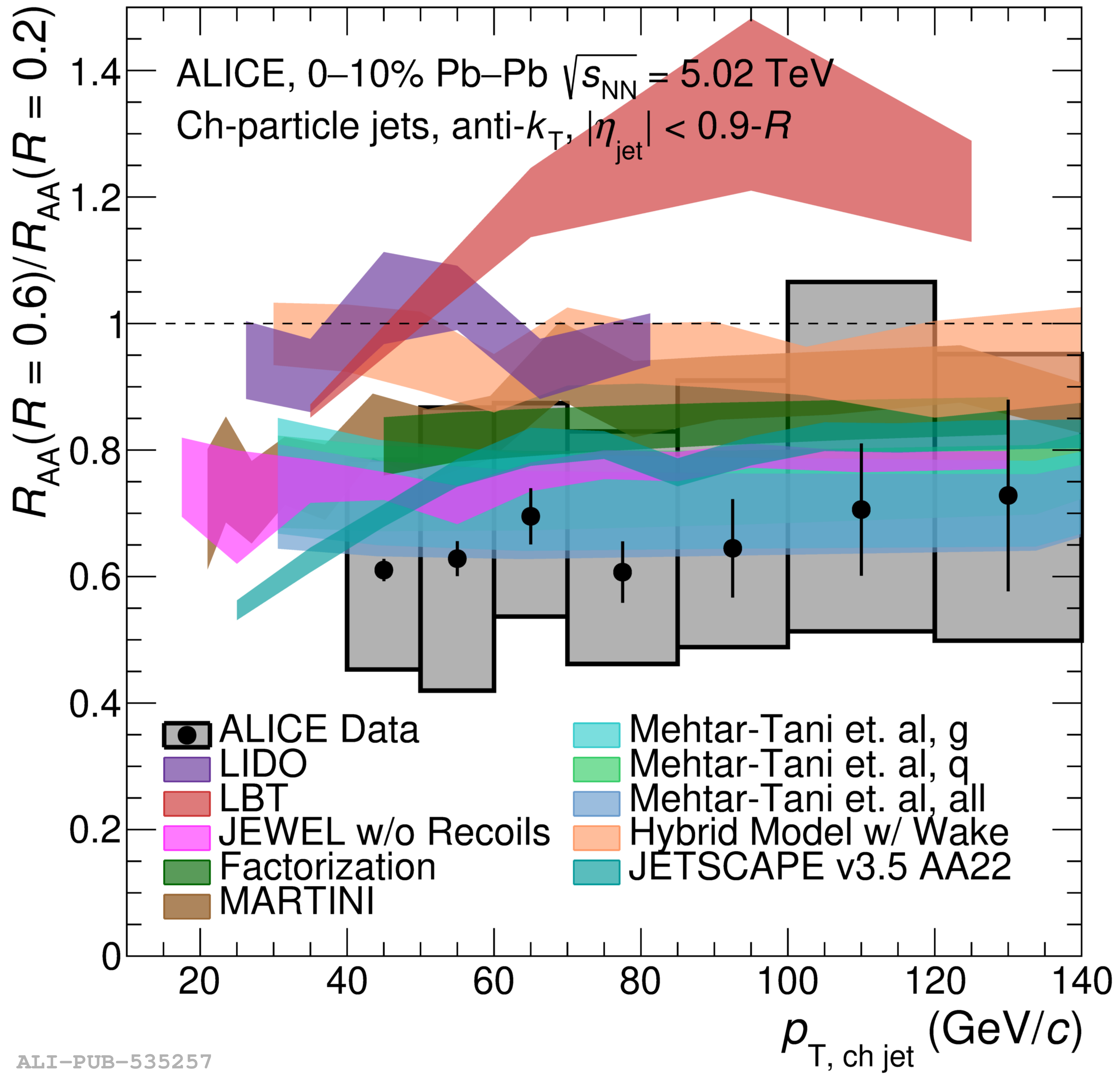

- Machine-learning based background subtraction enables jet measurements with R up to 0.6 at p_T ~ 50 GeV
- Jet suppression increase with increasing R: wider jets lose more energy

Flow-like effects in pp and Pb-Pb: long range correlations

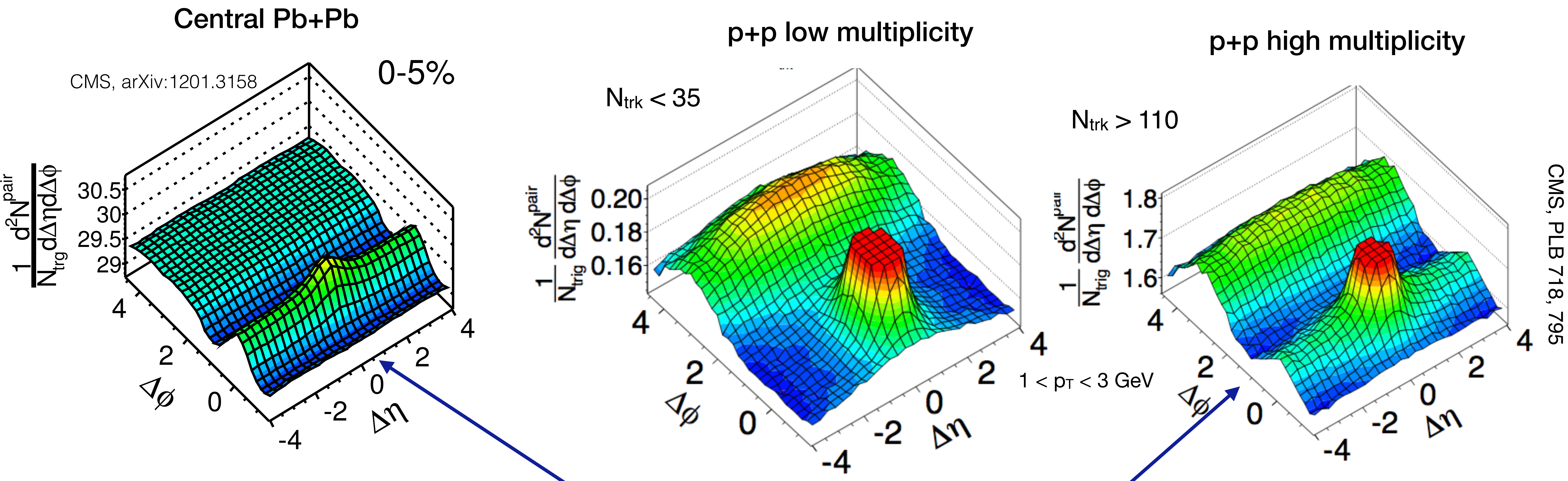

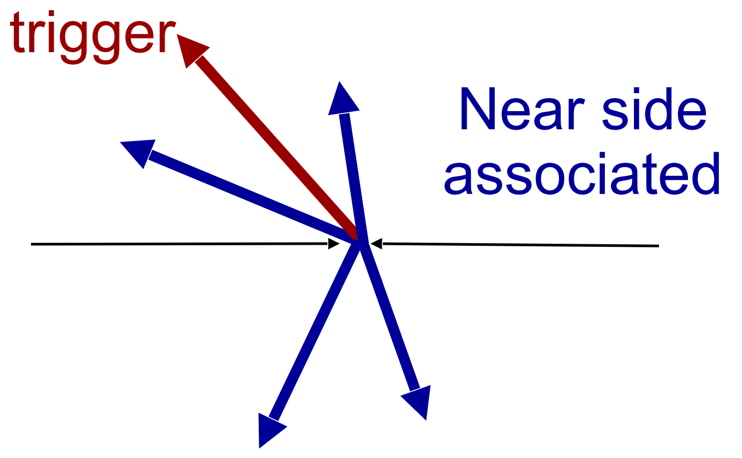

Near-side long range correlation: indicates early time origin

Flow-like effects in pp and Pb-Pb: long range correlations

Central Pb+Pb

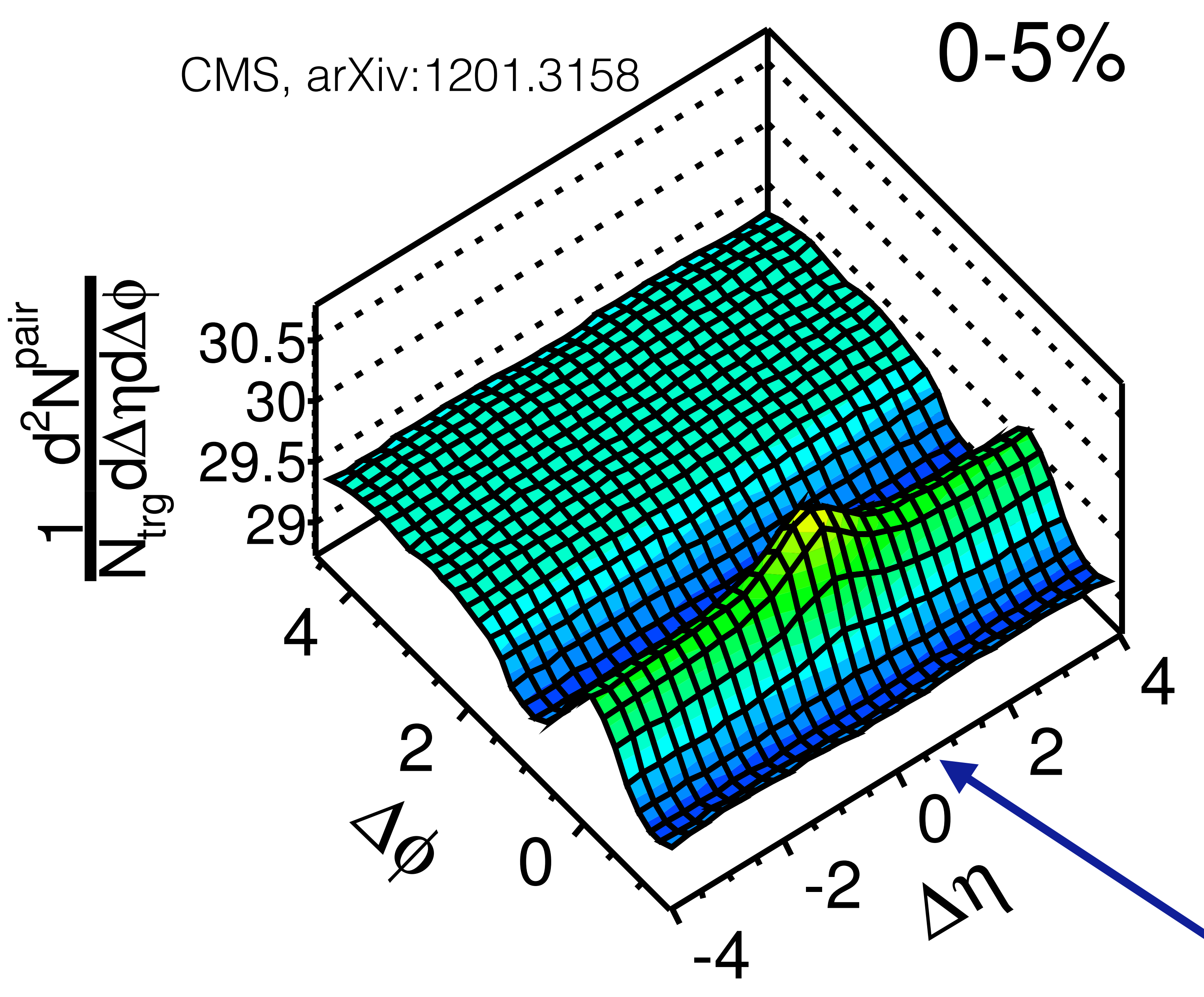

p+p low multiplicity

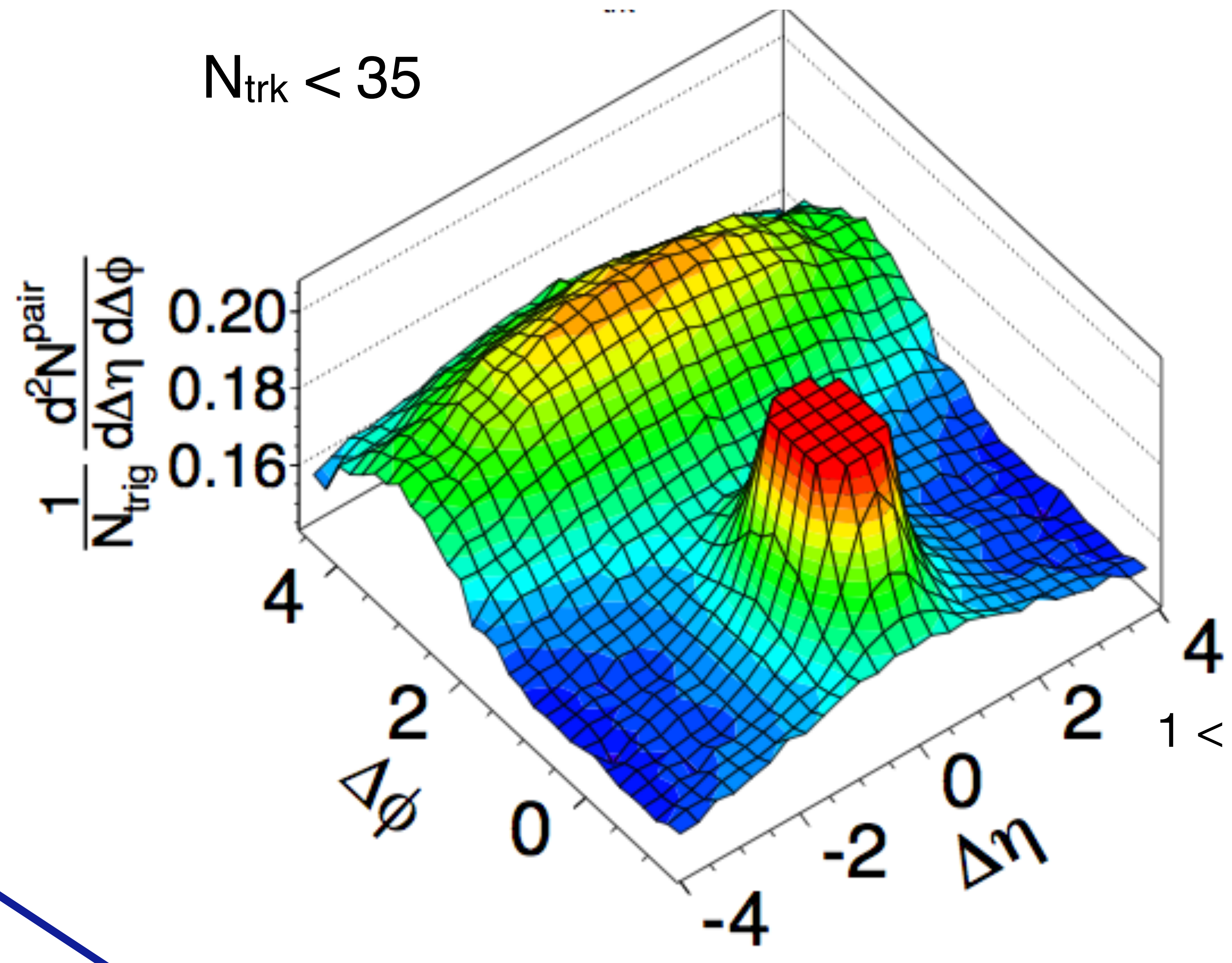

$1 < p_T < 3$ GeV

p+p high multiplicity

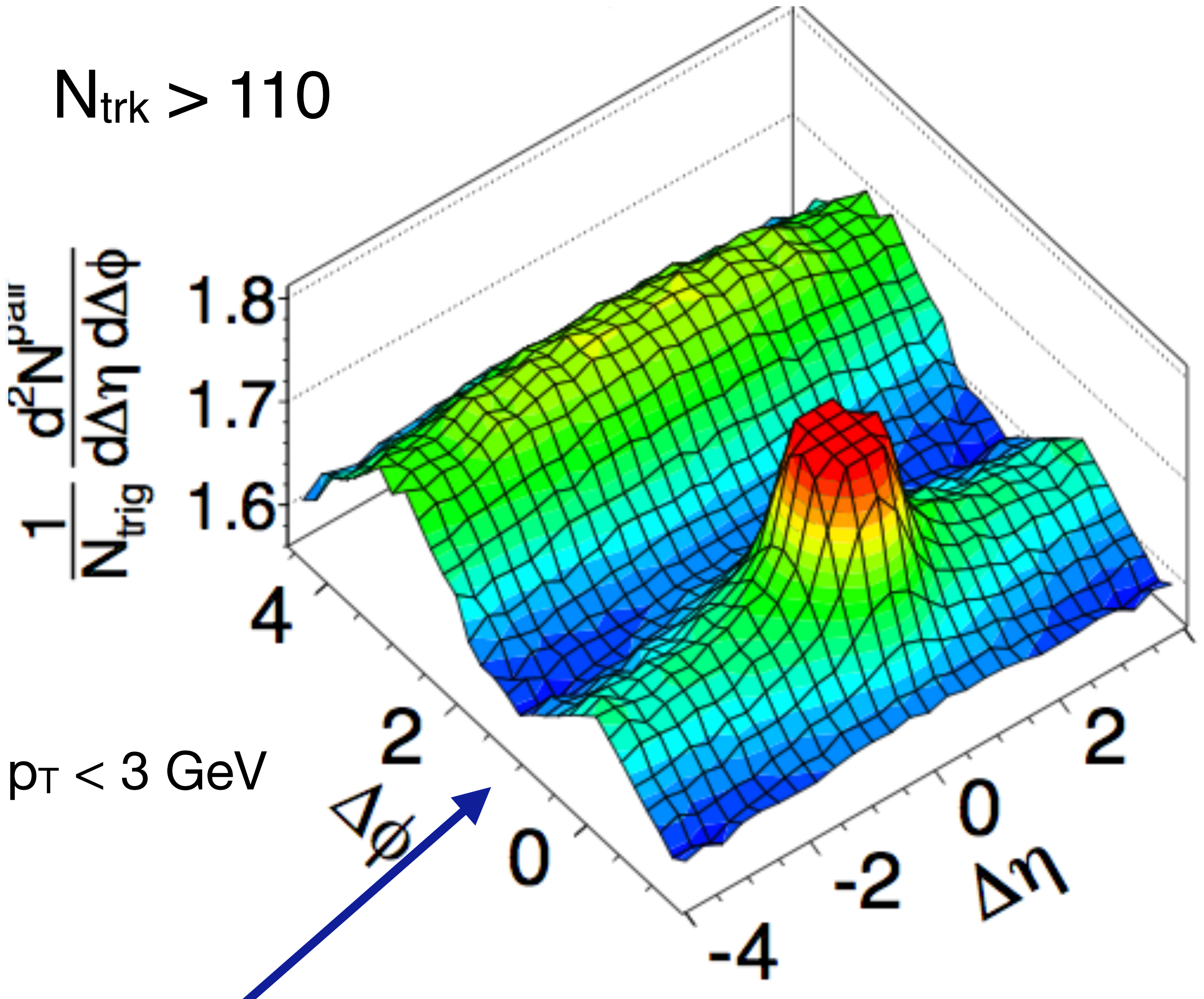

CMS, PLB 718, 795

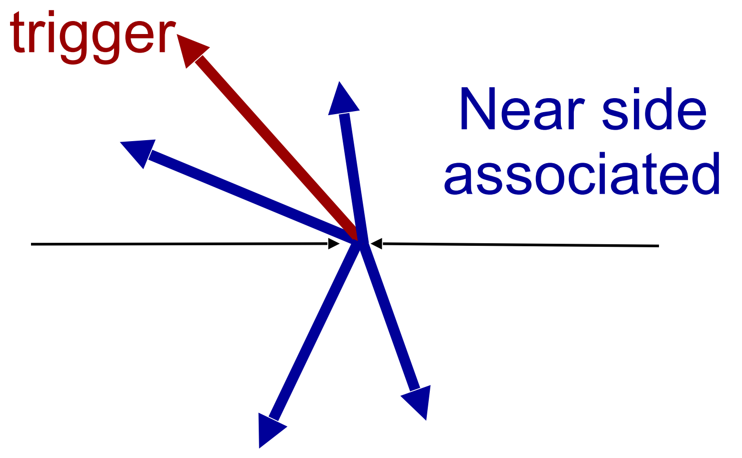

Near-side long range correlation: indicates early time origin
Seen in high-multiplicity pp and p+Pb events

Elliptic flow in p-Pb

Pb-Pb: elliptic flow v_2

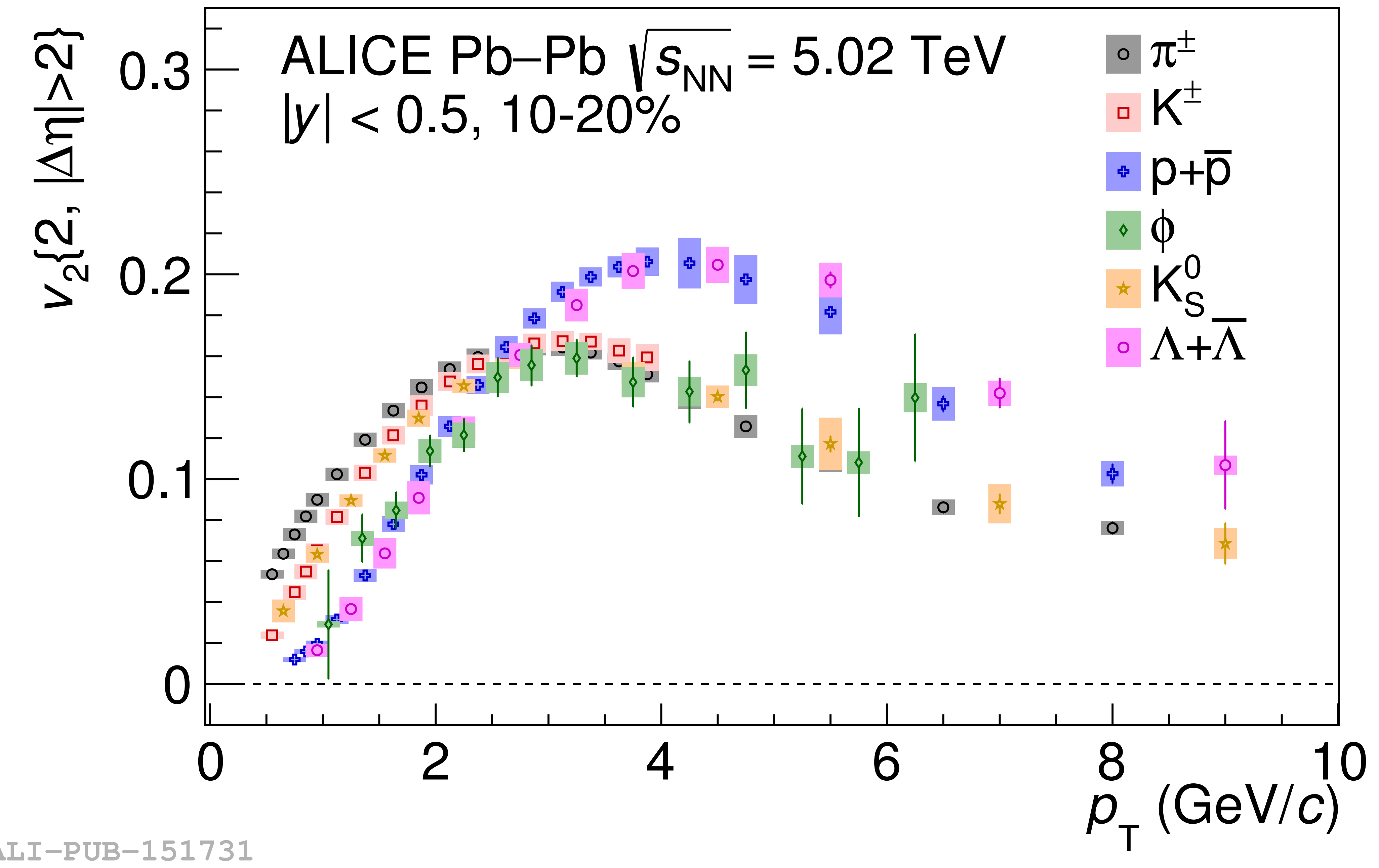

p-Pb: v_2 from two-particle correlations

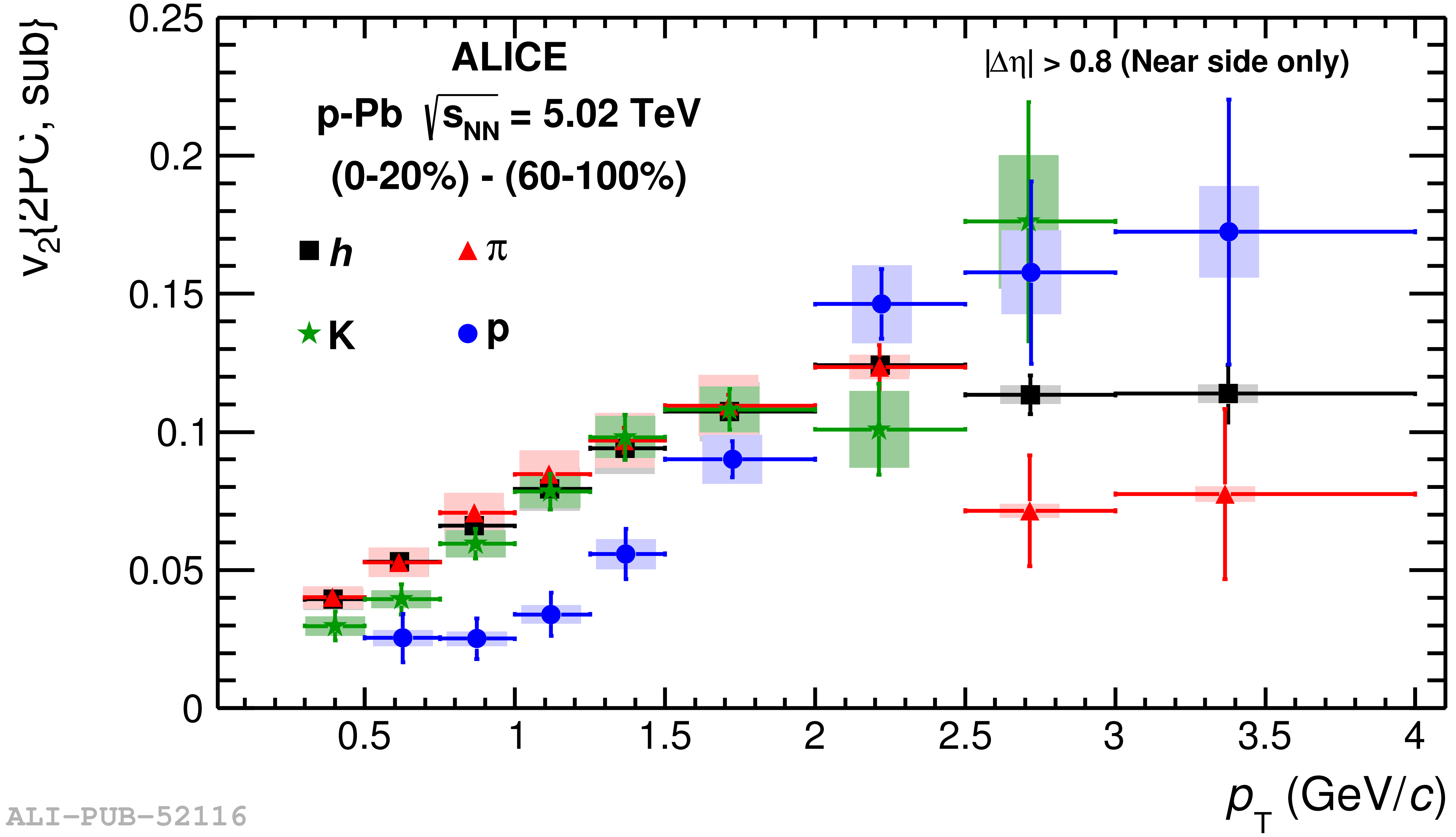

Mass-dependence of v_2 measures flow velocity

Similar 'mass ordering' observed for v_2 from two-particle correlations in p+Pb

Is this pressure driven?

Flow effects in small systems

Many aspects of the observed ridge have
a natural explanation in hydrodynamics:

- Long range correlation
- 2- and 3-fold symmetries
- Dependence on initial geometry
- Many-particle correlations
- Particle mass dependence

Why would the system behave as a fluid?
Is there enough time, volume to thermalise?

- Hydrodynamisation (isotropisation) of a dense gluon system?
- Partonic/hadronic rescattering?
- How many scatterings/what density is needed to approximate fluid behaviour?

Limits on hydrodynamic behaviour

Naive expectation: need at least a few collisions for each parton to reach thermal equilibrium and apply hydrodynamic

1) System size: $R > \lambda$

Would not expect azimuthal asymmetries in pp and p-Pb

Heiselberg and Levy, nucl-th/9812034,
W Lin et al,

2) Thermalisation time: $\tau > \dfrac{\lambda}{v}$

Fits to data: thermalisation times $\tau \approx$ 0.1-1 fm/c

pQCD calculation:
$\tau \gtrsim$ 6.9 fm/c

Baier et al, PLB 502, 51, PLB 539, 46

Limits on hydrodynamic behaviour

ALICE

Naive expectation: need at least a few collisions for each parton to reach thermal equilibrium and apply hydrodynamic

1) System size: $R > \lambda$

Would not expect azimuthal asymmetries in pp and p-Pb

Turns out to be too strict: asymmetries also generated in kinetic with $R < \lambda$

Density tomography

Heiselberg and Levy, nucl-th/9812034,
W Lin et al,

2) Thermalisation time: $\tau > \dfrac{\lambda}{v}$

Fits to data: thermalisation times $\tau \approx$ 0.1-1 fm/c

pQCD calculation:
$\tau \gtrsim$ 6.9 fm/c

Baier et al, PLB 502, 51, PLB 539, 46

Limits on hydrodynamic behaviour

Naive expectation: need at least a few collisions for each parton to reach thermal equilibrium and apply hydrodynamic

1) System size: $R > \lambda$

Would not expect azimuthal asymmetries in pp and p-Pb

Turns out to be too strict: asymmetries also generated in kinetic with $R < \lambda$

Density tomography

Heiselberg and Levy, nucl-th/9812034,
W Lin et al,

2) Thermalisation time: $\tau > \dfrac{\lambda}{v}$

Fits to data: thermalisation times $\tau \approx$ 0.1-1 fm/c

pQCD calculation:

$\tau \gtrsim$ 6.9 fm/c

Baier et al, PLB 502, 51, PLB 539, 46

Turns out to be too strict: (viscous) hydro describes non-thermal systems, see next slide

Naive expectations can be ‘bypassed’ in nature?

Limits on hydrodynamic behaviour

Naive expectation: need at least a few collisions for each parton to reach thermal equilibrium and apply hydrodynamic

1) System size: $R > \lambda$

Would not expect a… mmetries in pp and p-Pb

Turns out to b… symmetries also generated in kinetic with $R < \lambda$

Density tom…

Heiselberg and Levy, nucl-th/9812034,
W Lin et al,

Closely related, since v ≈ c = 1

2) Ther… e: $\tau > \dfrac{\lambda}{v}$

Fits to data: thermalisation times $\tau \approx$ 0.1-1 fm/c

pQCD calculation:
$\tau \gtrsim$ 6.9 fm/c

Baier et al, PLB 502, 51, PLB 539, 46

Turns out to be too strict: (viscous) hydro describes non-thermal systems, see next slide

Naive expectations can be 'bypassed' in nature?

Hydrodynamic behaviour in non-thermalised system

$p_L/p_T = 1$ isotropy; condition for thermalisation

Non-equilibrium expansion in AdS/CFT kinetic theory

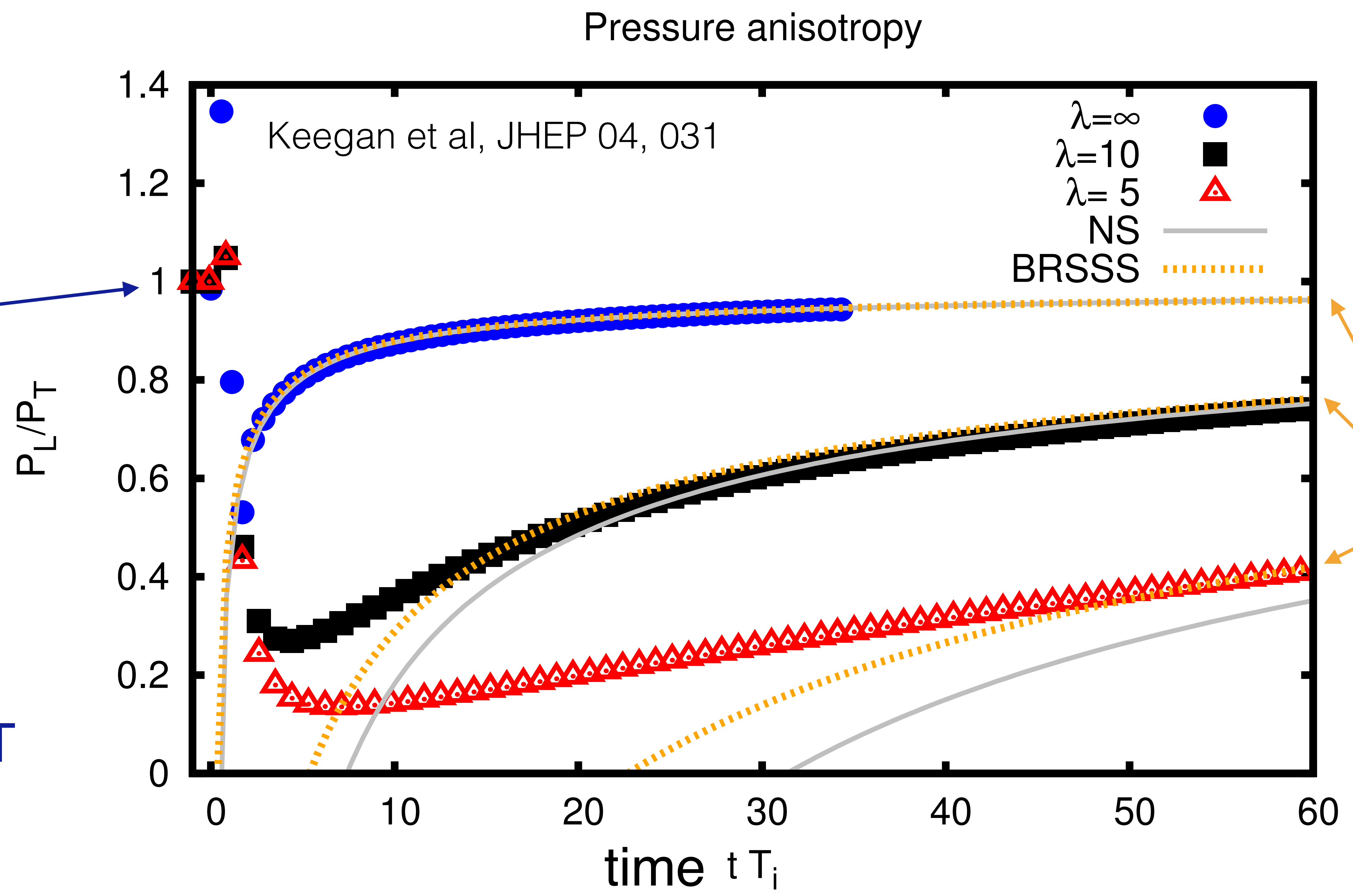

Lines: viscous hydro

Emerging understanding:

Hydrodynamical description valid before thermalisation/isotropisation

Estimate of smallest (possible) system size with fluid behaviour: $r \approx 0.15$ fm

Weller, Romatschke, EPJC 77, 21